

BULKY METAL COMPLEXES AS MODEL NANOSCALE CATALYSTS

by

CYRIL YOUNG

A dissertation Submitted in the fulfillment of the requirements for the degree of

PHILOSOPHIAE SCIENTAE

in the

DEPARTMENT OF CHEMISTRY

FACULTY OF SCIENCE

at the

UNIVERSITY OF THE FREE STATE

SUPERVISOR: PROF. ANDREAS ROODT

CO-SUPERVISOR: PROF. BEN BEZUIDENHOUDT

NOVEMBER 2012

Acknowledgements

I wish to express my gratitude:

To my heavenly Father for the talents and capabilities He has bestowed on me and the opportunity to use them to explore his wonderful creation. For giving me the determination to continue in times when the challenges were many and the outcomes few.

Prof Andreas Roodt, who has mentored me for the duration of studies, thank you for your support and enthusiasm. You have played a critical role in the development of chemistry ability and it has been a privilege to have you as a mentor.

Prof BCB Bezuidenhoudt, thank you for your help and input throughout the years. Your insights and opinions changed the way I approach much of the chemistry that I do today.

The UFS inorganic group: Thank you all especially Theuns, Bradley Marietjie, and Ilana for your help, insight and friendship.

To my parents Elsabe' and Peter John Young; thank you for the sacrifices you have made to provide me with the opportunity to further my education. This could not have been possible without your love, support and understanding. Even though times were tough you still drove me to succeed and achieve to the highest degree.

To my brother P.J. and my sister Dina for your friendship and advice.

Lastly to my wife Marna, very few people truly understand the frustration of constantly trying and failing while hoping for those moments when great discoveries are made. You shared every frustrating moment and together we discovered each other; Perhaps this was the greatest and most exciting discovery I have made to date.

Table of Contents

Table of Contents	i
Abbreviations and Symbols	vii
Summary	viii
Opsomming	ix
General Background and Aim	1
1.1 Introduction	1
1.2 Brief Overview of Catalysis	1
1.3 Heterogeneous <i>versus</i> Homogeneous Catalysis	2
1.4 Heterogeneous Catalyst Problems and Developments	3
1.5 Aim of this Study	4
Literature Review of Heterogeneous Catalysis and Synthetic Protocols	6
2.1 Introduction	6
2.2 The Importance of Catalysis	6
2.3 Heterogeneous Catalyst Dispersion	9
2.3.1 Impregnation	10
2.3.2 Co-Precipitation	10
2.3.3 Ion-Exchange	10
2.3.4 Chemical Vapour Deposition	11
2.3.5 Grafting	11
2.4 Metal Organic Frameworks and Coordination Ligands as Dispersion Spacers or Heterogeneous Catalysts	13
2.4.1 Polymer-Supported Metal Phosphine Complexes	13
2.4.2 Single-Atom Active Sites and Monolayers from Metal Organic Frameworks	14
2.5 Construction of Planar Bridging Ligands with Multiple Coordination Sites	18
2.6 1,4,5,8-Naphthalenetetracarboxylic Dianhydride Derivatives	19
2.6.1 The Functionalization of 1,4,5,8-Naphthalenetetracarboxylic Dianhydride (NTCDA)	20
2.7 Pyromellitic Diamide Derivatives	24
2.7.1 The Functionalization of Pyromellitic Diamide	25
2.8 1,10-Phenanthroline	27
2.8.1 Chemical Properties	28
2.9 The Functionalization of 1,10-Phenanthroline	29

Table of Contents

2.9.1	2,9-Disubstituted 1,10-Phenanthroline Derivatives	30
2.9.2	5-Mono or 5,6-Disubstituted 1,10-Phenanthroline Derivatives	32
2.9.3	Oxidative Substitution Reactions of 1,10-Phenanthroline	33
2.10	Construction of Multidentate Schiff Base Bridging Ligands	35
2.10.1	Mechanism and Synthetic Procedure	35
2.10.2	Planar Multi-Nuclear Schiff Base Ligands	36
2.10.3	1,10-Phenanthroline-5,6-diamine Bridged Species	44
2.11	Heck coupling	47
2.11.1	Mechanistic Aspects of the Heck Coupling Reactions	48
2.12	Bidentate and Nitrogen Donor Ligands as Heck Catalysts	54
2.12.1	Palladium (II) 1,10-Phenanthroline Type Ligands as Heck Catalysts	56
Planar Diamide Building Blocks		58
3.1	Introduction	58
3.2	Chemicals and Apparatus	61
3.3	Organic Bridging Ligands	61
3.3.1	4,5,9,10-Tetrabromo-naphtho-isochromene-1,3,6,8-tetraone	61
3.3.2	4,7,11,14-Tetrabromoanthra[2,1,9-def:6,5,10-d'e'f']diisochromene-1,3,8,10(3aH,10aH)-tetraone	62
3.3.3	4,5,6,7,11,12,13,14-Octabromoanthra[2,1,9-def:6,5,10-d'e'f']diisochromene-1,3,8,10(3aH,10aH)-tetraone	62
3.3.4	2,7-Diallyl-4,5,9,10-tetrakis(allylamino)benzo[lmn][3,8]phenanthroline-1,3,6,8(2H,7H)-tetraone	63
3.3.5	2,6-Dihydroxypyrrolo[3,4-f]isoindole-1,3,5,7(2H,6H)-tetraone (pyro-hydroxylamine)	63
3.3.6	1,3,5,7-Tetraoxo-5,7-dihydropyrrolo[3,4-f]isoindole-2,6(1H,3H)-dicarboxamide (pyro-urea)	64
3.3.7	2,7-Dihydroxybenzo[lmn][3,8]phenanthroline-1,3,6,8(2H,7H)-tetraone (naph-hydroxylamine)	64
3.3.8	1,3,6,8-tetraoxo-6,8-dihydrobenzo[lmn][3,8]phenanthroline-2,7(1H,3H)-dicarboxamide (naph-urea)	65
3.3.9	7-Bis(6-aminopyridin-2-yl)benzo[lmn][3,8]phenanthroline-1,3,6,8(2H,7H)-tetraone	65
3.3.10	<i>N,N'</i> -Bis(2-pyridyl)naphthalene-3,4:7,8-di-carboximide (dpbpt)	66
3.3.11	2,6-di(pyrimidin-2-yl)pyrrolo[3,4-f]isoindole-1,3,5,7(2H,6H)-tetraone (pyro-pyrimidine)	66
3.4	Bridged Metal Complexes	67
3.4.1	[Pd(OAc) ₂ (pyro-hydroxylamine)]	67

Table of Contents

3.4.2	[Pd ₂ (OAc) ₄ (pyro-hydroxylamine)]	67
3.4.3	[Pd(OAc) ₂ (naph-hydroxylamine)]	68
3.4.4	[Pd(OAc) ₂ (pyro-urea)]	68
3.4.5	[Pd ₂ (OAc) ₄ (pyro-urea)]	68
3.4.6	[Pd ₄ (OAc) ₈ (pyro-urea)]	68
3.4.7	[Pd(OAc) ₂ (pyro-pyrimidine)]	69
3.4.8	[Pd ₂ (OAc) ₄ (pyro-pyrimidine)]	69
3.4.9	[Pd ₄ (OAc) _x (pyro-pyrimidine)]	69
3.5	Discussion	70
1,10-Phenanthroline Based Synthons		74
4.1	Introduction	74
4.2	Chemicals and Apparatus	78
4.3	Synthesis of Organic Ligands	78
4.3.1	1,10-Phenanthroline- 5,6-dione (phendione)	78
4.3.2	1,10-Phen-5,6-diol	79
4.3.3	5-Nitro-1,10-phenanthroline	79
4.3.4	5-Amino-6-nitro-1,10-phenanthroline	80
4.3.5	1,10-Phenanthroline-5,6-diamine	80
4.3.6	4,5-Diazafluoren-9-one (Dafone)	81
4.3.7	Diquinoxalino[2,3-a:2',3'-c]phenazine	81
4.3.8	Pyrazino[2,3-f][1,10]phenanthroline-2,3-dicarbonitrile	82
4.3.9	Tetrapyrido[3,2-a:2',3'-c:3'',2''-h:2''',3'''-j]phenazine	82
4.3.10	9,11,20,22-Tetraazatetrapyrido[3,2-a:2'3'-c:3'',2''-l:2''', 3'''-n]pentacene (tatpp)	83
4.4	Synthesis of Metal-ligand Complexes	84
4.4.1	Dichlorido-(2,2'-bipyridine)-palladium(II)	84
4.4.2	Dichlorido-1,10-phenanthroline-palladium(II)	84
4.4.3	Dichlorido-(1,10-phendione)-palladium(II)	84
4.4.4	Dichlorido-(5-nitro-1,10-phenthroline)-palladium(II)	84
4.4.5	6-amino-5-nitro-1,10-phenthroline-dichlorido-palladium(II)	85
4.4.6	6-amino-5-nitro-1,10-phenthroline-dichlorido-palladium(II)	85
4.4.7	Dichlorido-(μ ₂ -5,6-diamino-1,10-phenthroline)-palladium(II)	85
4.4.8	Tetrachlorido-(μ ₂ -2,2'-Bipyrimidine)-palladium(II) ⁵	86
4.4.9	Dichlorido-(2,2'-Bipyridine)-platinum(II)	86

Table of Contents

4.4.10	Diacetonitrile-bis-dichlorido-palladium(II) ⁶	86
4.4.11	Bis-(5-diazafluoren-9-one)-dichlorido-palladium(II) ⁵	86
4.5	Discussion	87
4.5.1	Synthetic Challenges	87
4.5.2	Solubility	88
4.5.3	Characterisation	89
	Single Crystal X-Ray Study of Selected Model Ligands	90
5.1	Introduction	90
5.2	Experimental	91
5.3	Organic Bridging Ligands	92
5.3.1	1,6,7,12,13,18-Hexaazatrinaphthylene octa-chloroform solvate (heprazine) (I)	93
5.3.2	Benzo[1,2-c:4,5-c']dipyrrole-1,3,5,7(2H,6H)-tetrone, 2,6-dihydroxy-dihydrate (<i>N,N'</i> -dihydroxypyromellitic diimide)(II)	98
5.3.3	<i>N,N'</i> -Bis(2-pyridyl)naphthalene-3,4:7,8-di-carboximide (dpbpt) (III)	101
5.3.4	2-Amino-4,6-dichloropyrimidine, acetic acid solvate	105
5.3.5	Comparison of Organic Ligands	110
5.4	Conclusions	120
	Crystallographic Study of Platinum(II) and Palladium(II) Complexes	121
6.1	Introduction	121
6.2	Crystallographic Study of Selected Metal Complexes	122
6.2.1	Crystal structure of <i>cis</i> -[Pd(C ₁₂ H ₈ N ₄ O ₂)Cl ₂].2DMSO (I)	123
6.2.2	Crystal structure of <i>cis</i> -[Pt(C ₁₂ H ₈ N ₄ O ₂)Cl ₂].2DMSO (II)	128
6.2.3	Comparison of Crystal Structures	132
6.3	Conclusions	136
	Catalytic Evaluation of Palladium and Bridged Palladium Complexes	137
7.1	Introduction	137
7.2	Experimental Section	138
7.2.1	Typical Procedure for the Heck Coupling Reactions	139
7.2.2	Results and Discussion	140
7.3	Conclusions	152
	Critical Evaluation of the Study	153
8.1	Introduction	153
8.2	Scientific Relevance of the Results Obtained	153

Table of Contents

8.2.1	Diamide Type Building Blocks	153
8.2.2	1,10-Phenanthroline Based Bridging Ligands	154
8.2.3	Catalytic Evaluation of Phenanthroline and Diamide Ligands	155
8.3	Future Research	155
Appendix A		

Abbreviations and Symbols

Symbol / Abbreviation	Meaning
Z	Number of molecules in a unit cell
Å	Ångstrong
NMR	Nuclear Magnetic Resonance spectroscopy
KMR	Kern Magnetische Resonance spektroskopie
ppm	(Unit of chemical shift) parts per million
IR	Infrared spectroscopy
ν	Stretching frequency on IR
MO	Molecular orbital
π	Pi
σ	Sigma
α	Alpha
β	Betha
γ	Gamma
λ	Wavelength
θ	Sigma
$^{\circ}$	Degrees
$^{\circ}\text{C}$	Degrees Celcius
cm	Centimetre
g	Gram
M	(mol/L)
mg	Milli gram
h	Planck's constant
k_B	Boltzman's constant
T or temp.	Temperature
UV	Ultraviolet region in light spectrum
Vis	Visible region in light spectrum
KOH	Potassium Hydroxide
CO	Carbon monoxide
DMF	Dimethylformaldehyde
PVA	Polyvinyl acetate
MOF	Metal Organic Framework
ATR	Attenuated Total Reflectance
GC	Gas Chromatography
SEM	Scanning Electron Microscope
NaH	Sodium Hydride
K	Kelvin
Bpym	2,2-Bipyrimidine
PPh_3	Triphenylphosphine
DMSO	Dimethylsulfoxide
Daf	4,5-diazafluoren-9-one
THF	Tetrahydrofuran
LUMO	Lowest unoccupied molecular orbital
PTCDA	perylene-tetracarboxylic Dianhydride
NTCDA	1,4,5,8-Naphthalenetetracarboxylic Dianhydride
MS	Mass spectroscopy
GDP	Gross domestic product
GNP	Gross national product
MLCT	Metal-to-ligand charge transfer

Summary

The lifestyle of modern society has created a massive demand for various chemicals such as fuels, chlorine-free refrigerants, high-strength polymers, stain-resistant fibres, cancer treatment drugs and thousands of other products. The demand for these compounds can only be met through the use of catalysts. Heterogeneous catalysis has become a fundamental part of the industrial scale production of these chemicals. Although heterogeneous catalysis is better suited for these processes than its homogeneous counterpart, some of the systems are plagued by poor distribution of the active metal species throughout the support.

The aim of this study was to investigate the feasibility of synthesising robust, planar, bridging ligands that could act as spacers between active metal species in the deposition of active catalysts onto heterogeneous supports. By choosing different building blocks, for the simple Schiff base reaction, the distance and proximity between active metal species could theoretically be controlled for a desired application. 1,10-Phenanthroline and diamide type ligands (Figure 1) were identified as possible candidates for this application

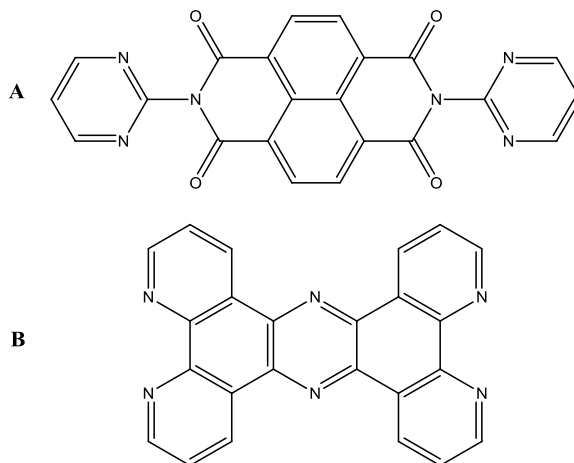


Figure 1: Different ligand systems identified as possible dispersion spacers. (A) represents the diamide type ligands and (B) the 1,10-phenanthroline ligands.

The aim of this study was pursued by the identification and synthesis of building blocks such as 5,6-diamino-1,10-phenanthroline and 1,10-phenanthroline-5,6-dione which could act as bridging ligands and could be used to construct larger bridging systems. The bridging ligands

and building blocks were coordinated to square planar metal centres such as platinum and palladium. This would enhance the possibility of creating a single layer network on the surface of the support. The ligands and complexes were characterised using solid state techniques and single crystal X-Ray Diffractometry to investigate the planarity of these species and the coordination mode to some of the diamide type complexes that have not found many applications in this field.

The Heck coupling was identified as a standard reaction which could be utilised to test the catalytic properties of the palladium species. The catalytic activity of a range of diamide and 1,10-phenanthroline type ligands was evaluated after the optimisation of the Heck coupling. It was found that reducing the electron density on the five and six position of the phenanthroline ring drastically enhances the catalytic capabilities of these compounds. The diamide type complexes and larger bridging ligands showed less promising results.

Key terms:

Platinum

Palladium

Crystal structure

Supports

Metal organic frameworks

Heck coupling

Catalysts

Dispersion

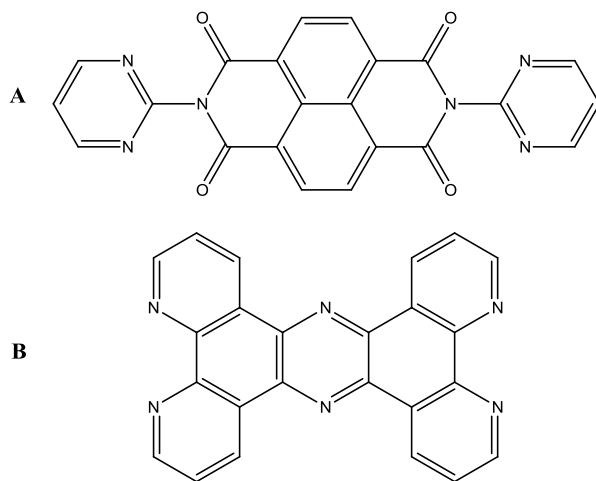
Bridging ligands

Schiff Base

Opsomming

Die lewenstyl van die moderne samelewing het 'n massiewe aanvraag na verskeie chemikalieë soos brandstof, chloor-vrye verkoelingsmiddels, hoë-sterkte polimere, vlekbestande materiaal, dwelms vir die behandeling van kanker en duisende ander produkte geskep. Die aanvraag na hierdie verbindings kan net nagekom word deur die gebruik van katalisators. Heterogene katalise is 'n fundamentele deel van die industriële skaal produksie van hierdie chemikalieë. Alhoewel heterogene katalise beter geskik is vir hierdie prosesse as homogene katalise, is 'n paar van die stelsels geteister deur swak verspreiding van die aktiewe metaalspesie dwarsdeur die steunraamwerke.

Die doel van hierdie studie was om 'n ondersoek in te stel na die haalbaarheid van die sintetisering van sterk, planêre, bruggende ligande wat die afstand tussen aktiewe metaal spesies op die heterogene steunraamwerke te kan beheer. Deurdat die keuse van die verskillende boustene vir die eenvoudige Schiff-basis reaksie te wissel, kan die afstand en nabyheid tussen aktiewe metaal spesies teoreties vir 'n gewenste kompleks beheer word.



Figuur 1: Verskillende ligand-stelsels geïdentifiseer as 'n moontlike verspreiding ligande. (A) verteenwoordig die diamied tipe ligande en (B) die 1,10-fenantrolien ligande.

Die doel van hierdie studie is bewerkstellig deur die identifisering en sintese van die boustene soos 5,6-diamino-1,10-fenantrolien en 1,10-fenantrolien -5,6-dioon wat kan optree as

oorbruggingsligande en gebruik kan word om groter oorbruggingsligande te bou. Die oorbruggingsligande en boublokke is gekoördineer aan vierkantig planêre metale soos platinum en palladium. Dit sal verder die moontlikheid van 'n enkellaag netwerk op die oppervlak van die steunraamwerke steun. Hierdie ligande en komplekse is gekarakteriseer deur gebruik te maak van vaste toestand tegnieke. Enkelkristal X-straaldiffraktometrie was gebruik om die planêriteit van hierdie spesies en die koördineringsmotief van sommige van die diamide tipe komplekse, wat nie baie toepassings vind in hierdie veld nie, te ondersoek.

Die Heckkoppeling is geïdentifiseer as 'n standaard reaksie wat gebruik kan word om die katalitiese eienskappe van die palladium spesie te toets. Die katalitiese aktiwiteit van 'n reeks diamide en 1,10- fenantrolien tipe ligande is geëvalueer na die optimisering van die Heck koppeling. Daar is bevind dat die vermindering van die elektron digtheid op die vyf en ses posisie van die fenantrolien ring die katalitiese funksies van hierdie verbindings drasties verhoog. Die diamide en groter bruggingsligand tipe komplekse het minder belowende resultate getoon.

Sleuteltermes:

Platinum

Palladium

Kristalstruktuur

Ondersteun

Metal organiese raamwerke

Heck koppeling

Kataliste

Dispersie

Bruggingligande

Schiff Base

1

GENERAL BACKGROUND AND AIM

1.1 Introduction

As it stands today, the human population is in the region of seven billion and growing at a massive rate of roughly 70 million people per year.¹ Although these numbers are alarmingly large, it cannot compare to the thirty two billion litres of oil which is consumed per annum by the human race.² It is only logical to realise that this sort of consumption cannot be sustained forever. This has become evident as the world's most used fossil fuel also stimulates wars within countries and between nations. New strategies and new inventions to reduce this are now needed more than ever. As scientists it has become our responsibility to develop and explore solutions to the current problems. The greatest contribution of the chemical society throughout the existence of the human race could perhaps be the discovery and development of catalysts. Catalysis will not magically solve all the energy needs of human civilisation, but it provides an excellent place to start.

1.2 Brief Overview of Catalysis

A catalyst is a chemical substance that reduces the activation energy required by a process, without being consumed by the process itself.³ The working of metals as catalysts within certain processes was observed as far back as the early 1800's, although a decisive explanation for this process was only later formulated by Ostwald.⁴

¹ Worldometers; real time world statistics (world population) [Online] (Updated 22 November 2012), Available at: <http://www.worldometers.info/world-population/>, [accessed 22 November 2012]

² British Petroleum (statistical review) [Online] (Updated 22 November 2012), Available at: <http://www.bp.com/sectionbodycopy.do?categoryId=7500&contentId=7068481>, [accessed 22 November 2012]

³ A. J. B. Robertson, *Platinum Metals Review* **1975**, *19*, 42–47.

⁴ M. W. Roberts, *Catalysis Letters*, **2000**, *67*, 1–4.

At the start of the 19th century, once catalytic systems were better understood, industrial scale reactions started exploiting the benefits of catalysis. This led to the large scale production of hydrochloric acid through the Deacon process.⁵ These developments served as a stepping stone to the development of catalytic processes for the production of sulfuric acid and ammonia in the early twentieth century. The industrial scale production of these chemicals was exploited by the mining industry and was used throughout the Second World War in the manufacturing of explosives.⁶

Today catalysts are used worldwide for the production of an enormous array of compounds. They play a vital role in the economy of most of the developed nations. Many of the catalysts are dominated by platinum group metals, although lately, the majority of the transition metal series are used in some processes. Catalysts have become one of the major artillery in the fight towards green chemistry, which serves to drastically reduce energy consumption of industrial manufacturing and limit the production of toxic waste substances as far as possible.⁷ Catalysis, in the broad sense, utilises homo or heterogeneous concepts. Although homogeneous catalysts do find industrial applications in processes like the Monsanto and Cativa⁸ processes, the bulk of the industrial catalytic sector is based on heterogeneous processes.

1.3 Heterogeneous *versus* Homogeneous Catalysis

Heterogeneous catalysis is largely favoured in industrial scale applications and the major reasons for this are related to poor performance of homogeneous catalysts with regards to separation, cost, energy requirements and contamination of products. Although homogeneous catalysts do show better specificity, controllability and reproducibility than their heterogeneous counterparts, it is difficult to separate the catalyst from products. This makes the processes energy intensive, which leads to higher costs.⁹ Heterogeneous catalysts are generally more robust, have better thermal stability and can handle moisture and oxygen better than homogeneous catalysts.

⁵ Chem. Ind., 21 January **2002**, 22–23

⁶ R. Van Santen, *Catalysis: an integrated approach*; 2nd ed.; Elsevier: Amsterdam; New York, **1999**

⁷ P.T. Anastas, J.C. Warner, *Green Chemistry: theory and practice*; Oxford University Press; **1998**.

⁸ P. W. N. M. Van Leeuwen, *Homogeneous catalysis : understanding the art*, Kluwer Academic Publishers, Dordrecht; Boston, **2004**.

⁹ S. Bhaduri, *Homogeneous catalysis mechanisms and industrial applications*; Wiley: New York, **2000**.

Even though heterogeneous catalyst particles are lost due to leaching and sintering, no plating occurs, which leads to less catalyst deactivation. In recent years, the role of the support in heterogeneous catalysis has added another dimension to catalytic processes that were previously characterised by poor tunability. The manipulation of the immediate environment of catalytic particles is starting to provide scientists with the ability to use otherwise unstable and unusable systems in ways that were previously not possible.¹⁰ Consequently, investigations to control particles on a nanoscale have become extremely popular.¹¹ These investigations seek to find possible solutions to some of the major problems such as dispersion in heterogeneous catalysis.

1.4 Heterogeneous Catalyst Problems and Developments

One of the major advantages of heterogeneous catalysis is the ease of separation of the products from the catalysts. Although these products are typically comprised of a mixture of different compounds, each compound, once separated finds some sort of application. Operating temperatures can be high when using heterogeneous systems, as the catalysts tend to be more robust. Catalysis within a heterogeneous system occurs on the surface of the active metal particles. Logically, the greater the number of metal particles, the greater the reactivity of the catalyst will be. However, the size of the particles can play a vital role in the success of the process. The size of the metal species varies between 1–20 nm and the performance in terms of activity and selectivity of various catalyst species has been directly linked to the size and dispersion of these metal species. A large number of techniques have been developed to characterise these moieties.¹² Unfortunately, there are two major stumbling blocks encountered in the synthesis of heterogeneous catalysts; the first being the inability to accurately and controllably deposit the active metal species uniformly across the surface of the support, and secondly to prevent these particles from agglomerating under the harsh operating environments. Various techniques such as impregnation, grafting, co-precipitation, ion-exchange and chemical vapour deposition have been developed to try and minimise some of the challenges regarding catalyst dispersion. Each of these processes have distinct advantages and applications are found

¹⁰ F. Hartley, *Supported metal complexes: a new generation of catalysts*; Kluwer Academic Publishers: Dordrecht; Boston; Hingham MA U.S.A., **1985**

¹¹ M. J. Pitkethly, *Nanotoday* **2003**, 36-42.

¹² *Comprehensive coordination chemistry: from biology to nanotechnology*; Pergamon: Amsterdam, **2002**, vol. 1.







in numerous arenas. A single process that addresses all the different problems of dispersion has unfortunately not yet been developed. Another range of compounds namely, metal organic frameworks (MOFs) have started finding application in the dispersion of catalysts or as heterogeneous supports. The majority of these MOFs can be tuned significantly to create different particle and pores sizes.¹³ These two and three-dimensional frameworks have also added a further dimension to heterogeneous catalysis since the ability to tune catalysts is introduced. These types of systems can also be used for heterogenisation of homogeneous catalytic systems. This process involves attaching the active homogeneous catalyst to supports, using linking molecules or a metal organic framework.

1.5 Aim of this Study

The problems with regards to heterogeneous catalysis and catalyst dispersion have already been highlighted. As a result, the void in procedures that have the ability to controllably deposit active metal species onto supports cannot be ignored. There are various ways in which this can be achieved. One particular area that has received limited attention is the construction of a network or monolayer of active species that can be deposited onto a support. In doing so, catalysis can effectively take place at a single metal atom. This can be achieved by making use of planar bridging ligands, combined with square planar metal centres such as platinum and palladium. Another approach that can also be simultaneously pursued is the control of particle size of conglomerates. In theory, by placing a number of metallic atoms in the close vicinity of each other on a support, once conglomeration occurs, the sintered particle size could be determined by limiting the number of metal particles in that area. This can be achieved by investigating planar bridging compounds that coordinate to a number of metal species. In the synthesis of heterogeneous catalysts, the final catalyst is calcined. This involves heating the catalyst to high temperatures, in a reducing environment, to remove ligands and reduce the metal to the active species. The removal of ligands and precursors also contributes to the sintering process. By constructing robust bridging ligands that can withstand higher temperatures, ligands that remain present can continue preventing agglomeration. In order to investigate the validity of creating this network of bridged metal species, it was decided to identify and synthesise planar

¹³ H. Kajiro, A. Kondo, K. Kaneko, and H. Kanoh, *International Journal of Molecular Sciences*, **2010**, *11*, 3803–3845.

bridging ligands that could be used for this purpose. Keeping these factors in mind, the following aims were set for this study:

-  Identify and synthesise synthons such as 1,10-phenanthroline and other planar diamide backbones that can be used to construct planar organic systems which can in turn be exploited as bridging ligands.
-  Use these synthons to synthesise bridging ligands that can theoretically be used to control the positioning of the metal atoms on heterogeneous supports.
-  Use the synthons to vary the distances between coordination sites on the planar bridging ligands.
-  Coordinate square planar metals such as platinum and palladium to the synthons and bridging ligands.
-  Fully characterise the ligands and metal complexes, using single crystal X-Ray crystallography, IR, ^1H NMR and ^{13}C NMR, to obtain insight into the possible interactions between metal centres and to investigate the planarity of the complexes and ligands.
-  Develop a standard catalytic reaction to test the catalytic activity of the bridging compounds before and after depositing the catalyst onto a support.

2 LITERATURE REVIEW OF HETEROGENEOUS CATALYSIS AND SYNTHETIC PROTOCOLS

2.1 Introduction

Embedded in the DNA of the human race lies a multitude of characteristics, some good and some bad, but the majority of the ‘normal’ qualities determine the way the human civilisation functions. A small investigation into everyday life reveals that money and speed lie at the epitome of human existence. Fast expensive cars, shortcuts to the perfect abs, cooking a family meal in 15 minutes, get-rich-quick schemes and faster computer systems are just a few of the daily messages that people all over the world encounter.

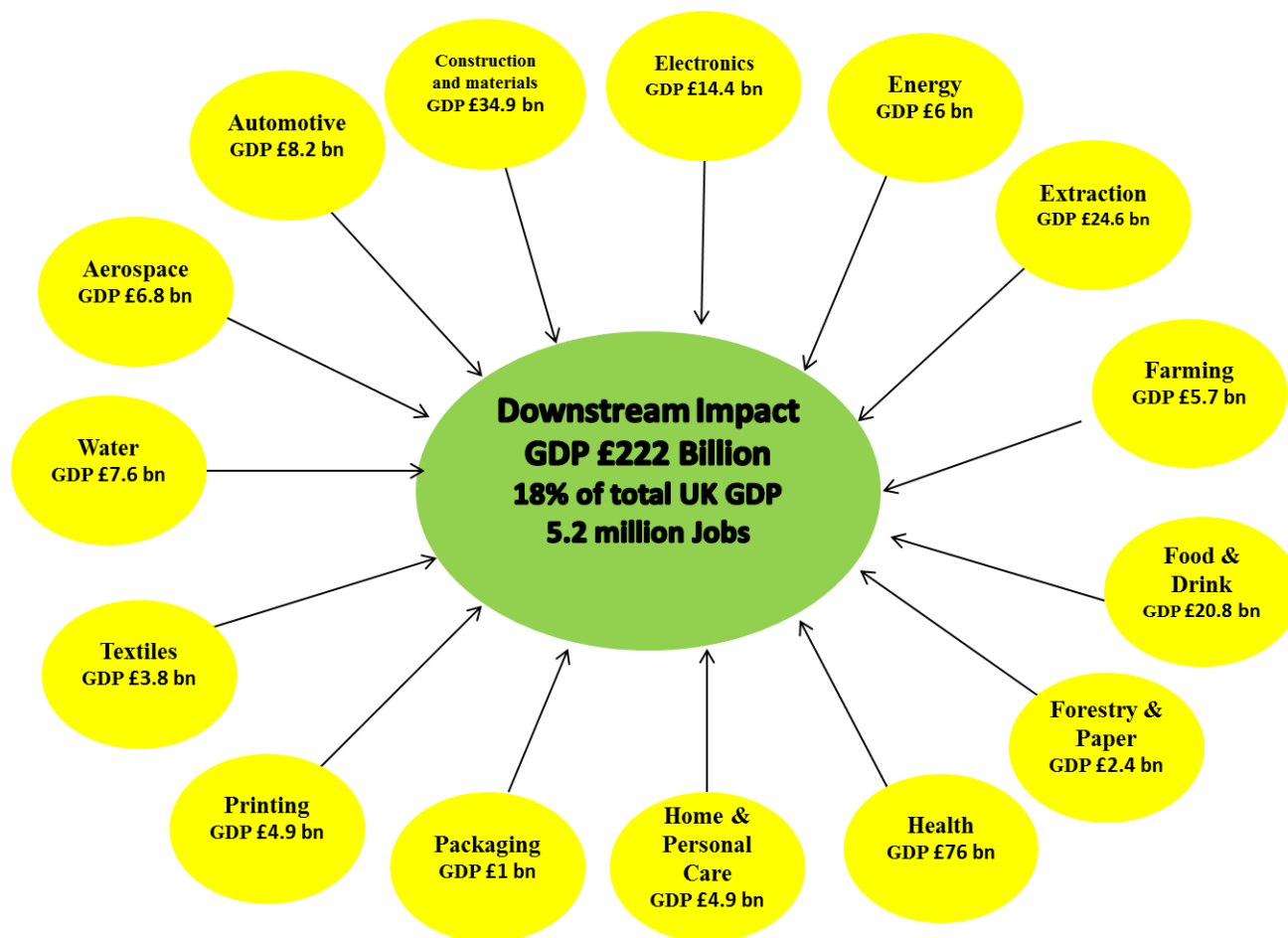
It is then only logical to see that in the world of chemistry nothing is different; a constant drive to perform reactions faster and more cost-effective, while still generating the most profit exists among most chemical researchers. Recently these drivers are followed or preceded by words such as ‘green chemistry’, ‘environmental impact’ and ‘sustainability’. The reason for this is simple: the human race and its constant drive for ‘bigger’, ‘better’ and ‘faster’ have scorned mother nature. She has heard and responded in the form of natural disasters occurring all over the globe. In the following paragraphs, the importance of catalysis and the most recent developments in heterogeneous catalysis, which is the most commonly used to produce chemicals on an industrial scale today, will be discussed.

2.2 The Importance of Catalysis

The lifestyle of modern society has created a massive demand for various chemicals such as fuels, chlorine-free refrigerants, high-strength polymers, stain-resistant fibres, cancer treatment drugs and thousands of other products. The demand for these compounds can only be met through the use of catalysts.¹ As a result, catalytic processes that are used in the production of fine chemicals, have become the corner stone of modern day society. Recent studies have

¹ A. T. Bell, *Science*, **2003**, 299, 1688–1691.

indicated a catalytic process is involved in more than a third of the gross national products (GNP) in the United States.² Similar trends are seen in the UK. A study conducted by Oxford economics concluded that the chemical industry constitutes 21 % of the United Kingdom's gross domestic product (GDP) and provides job opportunities for more than six million people.³ Scheme 2.1 shows all the sectors in which chemistry plays a vital role in the UK's GDP.



Scheme 2.1: The economic contribution of industries using chemistry to the UK's GDP.³

² Chem. Ind., 21 January 2002, 22–23.

³ Royal Society of Chemistry Website. 2012. (Updated September 2010) Available at: <http://www.rsc.org/ScienceAndTechnology/Policy/Documents/ecobenchem.asp> [Accessed 17 September 2012]

From the statistics above, it is clear to see that chemistry plays a fundamental role in the functioning of the world's leading economic powers. It is therefore not surprising that research and development in chemistry have become vital to economic growth. There is no question that catalysis is an important tool that is used in the manufacturing of thousands of compounds. However, there are two other factors that need to be addressed, namely; the impact of chemical processes on the earth and the sustainability of this production. Various regulations have been put in place to govern the production of substances which are detrimental to the environment; still these regulations do not encourage the invention of new processes. This led to the introduction of the term 'green chemistry' which is defined as 'the design, development and implementation of chemical products and processes to reduce or eliminate the use and generation of substances hazardous to human health and the environment.'⁴ Green chemistry considers the entire life-cycle of a chemical process. It is seen as an opportunity for innovation and also challenges scientists to use energy and matter in a way that increases performance but guards the well-being of the environment and human health. Since the adoption of the green chemistry approach, massive strides have been made in the reduction of hazardous waste production and pollution prevention. It is estimated that in the 10 years in which the Presidential Green Chemistry Challenge Award programme has been running in the United States, three billion pounds of hazardous substances were never used or generated.⁵ Many of the strides that have been taken in these achievements have been through the effective design and use of catalysts. Catalysts have been described as one of the fundamental pillars of green chemistry.⁶ The use of catalysis has furthered green chemistry by lowering energy requirements, using catalytic *versus* stoichiometric amounts of materials, increasing selectivity and decreasing the use of processing and separation agents. Heterogeneous catalysis, in particular, provides benefits such as ease of separation of product and catalyst, which eliminates the need for separation through distillation or extraction.⁶ Although many catalysts have contributed to the chemical industry, there are still many improvements that can be made in the processes used today. There are still many challenges in a lot of the catalytic processes including creating better selectivities, more active

⁴ P.T. Anastas, J.C. Warner, *Green Chemistry: theory and practice*. Oxford: Oxford University Press; 1998.

⁵ J. B. Manley, P. T. Anastas, and B. W. Cue, *Journal of Cleaner Production*, **2008**, 16, 743–750.

⁶ P. T. Anastas, M. M. Kirchhoff, and T. C. Williamson, *Applied Catalysis A: General*, **2001**, 221, 3–13.

and stable catalysts, milder process conditions and reducing coking.⁷ In order to solve some of these problems, it is critical to design new catalysts which could also introduce the possibility of creating novel manufacturing processes. Although there are many challenges with regards to the development and improvement of catalysts, the numbers of possible solutions are vast, with an equally large amount of research being performed in chemistry around the world. In order to prevent the pitfall of being a ‘jack of all trades and a master of none’, this research project sought to investigate possible solutions to one of the major problems within heterogeneous catalysis, namely dispersion.

2.3 Heterogeneous Catalyst Dispersion

The majority of industrial catalysts consist of a high surface area support with an active metal species deposited onto it. The size of the metal species varies between 1 nm and 20 nm. The performance in terms of activity and selectivity of various catalyst species has been directly linked to the size and dispersion of these metal species with a large number of techniques developed to characterise these moieties.⁸ The supported metal catalysts are among the most important industrial catalysts. Most of the deposition routes for industrial catalysts are well known, efficient and most importantly economical. These techniques include impregnation and ion-exchange using the metal salt; although a large amount of other techniques have also been developed. The deposition process is usually followed by calcination and reduction to yield the final catalyst. Unfortunately, these processes typically produce high non-uniform materials.⁹ These non-uniform materials result in the formation of multiple products, side reactions and prevent correlations between catalyst structure and performances from being made. In the following paragraphs a short explanation of the most commonly used techniques and the associated advantages and disadvantages will be given. Realistically, there are too many different techniques such as sol-gel, spray drying, sputtering, fusion, photo-deposition, hydrothermal synthesis and zeolites, to discuss in this context. The idea is to illustrate the difficulties with regards to some of the most common strategies.

⁷ P. R. Courty and A. Chauvel, *Catalysis Today*, **1996**, 29, 3–15.

⁸ *Comprehensive coordination chemistry : from biology to nanotechnology*, Pergamon, Amsterdam, 2002, vol. 1.

⁹ J. R. Regalbuto, *Handbook of catalyst preparation*, Taylor & Francis, Boca Raton, **2007**.

2.3.1 Impregnation

Impregnation, also known as incipient wetness, is the term assigned to the process whereby a dissolved precursor is added to a high surface area support. The active metal precursor which can be neutral, positive or negative is dissolved in an aqueous or organic medium and added to a support that can be amorphous, crystalline or a metal oxide.⁹ Surface interactions do not play a big role in the loading process, since the driving force for pore filling is capillary pressure. Impregnation is simple and easy to perform and is mostly used with metal oxide supports which have made the process favourable for application in industrial scale projects. However, this process is plagued by little or no uniform distribution of catalytic species. These are not the only problems that are present and here mention is made of a few of these problems that are encountered with this technique: leaching,¹⁰ crystallisation of active precursors due to solvent evaporation and unfavourable charge balancing between support and surface precursors.

2.3.2 Co-Precipitation

Co-precipitation follows a different route to accomplish catalyst dispersion and deposition. A solid is precipitated from a solution containing precursors of the support and surface oxides. A precipitation agent, change in pH or saturation is responsible for starting this process. After precipitation, the solid is filtered and excess ions are washed away to yield a co-precipitated binary framework that is more spatially distributed than a strictly supported metal oxide. This particular method creates the opportunity for better support-active metal species interactions. However, some of the active particles are included in the substructure which ultimately reduces the activity of the final catalyst. This process also operates under the assumption that the precursor has similar solubilities which is often not the case.⁹

2.3.3 Ion-Exchange

Ion-exchange or equilibrium adsorption involves placing a porous support in an excess solution of surface oxide precursors for long periods. The distribution of the particles is controlled by the concentration gradient and electrostatic interactions. Another major difference is the fact that the

¹⁰ D. C. Sherrington, A. P. Kybett, and Royal Society of Chemistry (Great Britain), *International Symposium on Supported Reagents and Catalysts in Chemistry*, Royal Society of Chemistry, Cambridge, **2001**.

oxide support bears a charge, which then attracts the active catalytic species with an opposite charge. There are hydroxyl groups at the surface of the support which can be manipulated by means of pH to form the desired charge. This technique typically produces catalysts that show better dispersion than impregnation, but they show poorer distribution throughout the pores compared to the co-precipitation process.⁹ This is probably caused by the evaporation of the fluid. Other problems encountered with ion exchange processes include the use of harsh acidic conditions and the inability to determine the degree of loading.

2.3.4 Chemical Vapour Deposition

Chemical vapour deposition is a process whereby a thin film is deposited onto a support through chemical reactions of the constituents in the gas phase. This process can be distinguished from other processes, such as evaporation and sputtering, due to the fact that a chemical reaction occurs. Typically, this process is carried out at temperatures around 1000 °C, with pressures that vary according to the different demands. These two parameters play a vital role in the success of the deposition process.¹¹ Although this technique has excellent monolayer forming abilities, there are still some drawbacks. This process requires specialised equipment and operates under the assumption that the catalysts can withstand high temperatures.

2.3.5 Grafting

Grafting is a catalyst dispersion technique that uses functional group interactions to attach the active species to the support. Coordination metal complexes, such as metal halides and organometallics, are attached to the surface *via* oxo or hydroxyl groups. This step is preceded by thermal treatment of the support to remove physisorbed water that can hinder the process. In some cases, precursor ligands that are first added to the support are washed from the catalyst once the active catalyst is covalently attached to the support. These covalent bonds anchor the active metal species in such a way as to prevent sintering and agglomeration during the thermal treatment of the catalyst. Essentially, this process provides better distribution of the active catalytic species than the other methods that have been discussed.⁹ Unfortunately catalyst loading is determined by the surface hydroxyl density and the ability of all the hydroxyl groups

¹¹ Y. Xu and X.-T. Yan, *Chemical vapour deposition an integrated engineering design for advanced materials*, Springer, London, **2010**.

to react with the metal species. This process is essentially the most suited to the chemical aspects of this project. Although the ligands were not specifically designed for this process, many of the ligands can be constructed to have covalent interactions with either the hydroxyl or oxo groups or the actual metal species used in the metal oxide supports. Heprazine, which is discussed in Paragraph 2.10.2.1 coordinates well with the titanium species.¹² This can be exploited as a central core that attaches to the active metal species and can then be attached to the support. This concept is illustrated in Figure 2.1, where the grey circles display the active metal species and the semi-circles display ligands to which these metals are coordinated. If the titanium atoms within the support are not available for coordination to the spacer ligand, the oxo species and covalent interactions can be exploited for the grafting process.

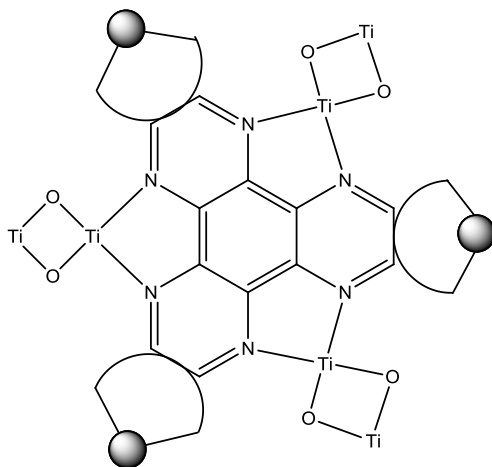


Figure 2.1: Proposed heprazine backbone used as spacer ligand for grafting attachment to heterogeneous supports. The grey circles designate the active species while the semi-circle is the spacer ligand to which the metal species is coordinated.

Although this method of catalyst dispersion is just a theoretical assumption, it does provide a legitimate area to investigate. Although there is minimal literature available focusing on this specific application of spacer ligands, there has been a thrust towards heterogeneous systems that make use of metal organic frameworks which are essentially very complex spacer ligands. It must be mentioned though, that in some of the proposed systems, the frameworks act as the support itself rather than the spacer which ensures optimal dispersion.

¹² I. M. Piglosiewicz, R. Beckhaus, G. Wittstock, W. Saak, and D. Haase, *Inorganic Chemistry*, **2007**, 46, 7610–7620.

2.4 Metal organic Frameworks and Coordination Ligands as Dispersion Spacers or Heterogeneous Catalysts

Metal organic frameworks (MOFs) have recently become a hot topic due to the fact that these unique structures have tuneable diversity and a number of different functions.¹³ MOFs have been used in the construction of two and three-dimensional coordination polymers, that have found application in catalysis and have desirable adsorption and desorption properties. In short, these compounds can be selectively designed to perform the required task and by simply selecting from the vast amount of linking ligands and counterions, a seemingly endless number of possibilities exist with these compounds. Unique characteristics such as host-guest interactions, structural flexibility and multi-metal systems can also provide a further dimension to heterogeneous catalysis. In order to create a better understanding of these and other compounds a number of examples are discussed in short.

2.4.1 Polymer-Supported Metal Phosphine Complexes

A wealth of transition metal phosphine complexes have been investigated. These complexes have found applications in catalysis and synthetic organic transformations for more than a decade.¹⁴ Phosphines play a critical role in the success of many homogenous catalysts as the multitude of electronic and steric properties of phosphines provide the necessary tools to tune catalysts to specific needs. It is therefore not surprising that attempts to integrate these phosphines into heterogeneous supports have been made since the early 1980's. The integration of phosphine ligands such as PPh_2 into heterogeneous supports is achieved through the reaction between a functionalized polymer, such as bromopoly-styrene or Merrifield's resin with a derivative of the preferred phosphine.¹⁵ Once the phosphine has been linked to the support, the desired catalytic metal species is anchored to the support by a substitution reaction. There are many different phosphines and supports that are used for these processes and range from simple PPh_2 systems to large macro-molecules that are used to link the phosphine to the support. Two of the more elaborate catalysts are shown in Figure 2.2. Ultimately the great tunability of linking

¹³ H. Kajiro, A. Kondo, K. Kaneko, and H. Kanoh, *International Journal of Molecular Sciences*, **2010**, *11*, 3803–3845.

¹⁴ N. E. Leadbeater and M. Marco, *Chemical Reviews*, **2002**, *102*, 3217–3274.

¹⁵ M. J. Farrall, J. M. Fréchet, *J. Org. Chem.* **1976**, *41*, 3877–3882.

spacers, steric properties and electronic environments give this methodology for creating heterogeneous catalysts tremendous potential. Systems using palladium, ruthenium, copper, cobalt, rhodium and platinum in catalytic processes such as hydroformylation, hydrogenation, isomerisation and many other catalytic systems have been developed.¹⁴

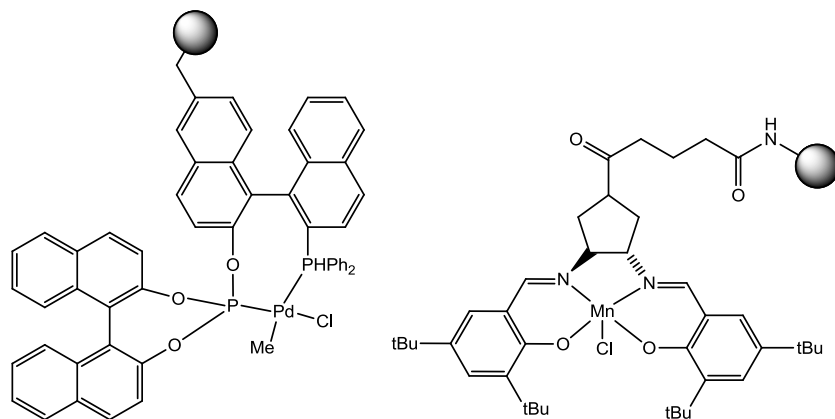


Figure 2.2: Different linking molecules used to create environments favourable for specific heterogeneous catalysis. The support is represented by the grey circles.¹⁴

As illustrated in Figure 2.2, the selective design of ligand systems that are used to link metal species to supports, is a viable methodology to combine the specificity of homogeneous catalysis with the ease of separation of a heterogeneous catalyst. Furthermore, this anchoring process can provide a solution to leaching and poor dispersion. It is however important to understand that due to the complexity of these compounds, a large amount of research is needed in the ligand design process. Characterisation and understanding of these catalysts is not simple and often require very specialised equipment and conditions.

2.4.2 Single-Atom Active Sites and Monolayers from Metal Organic Frameworks

In Paragraph 2.4.1 the advantages of the heterogenisation of homogeneous catalytic systems have been highlighted. The majority of the systems that have been developed utilise mesoporous silica as support. However, as previously mentioned, there are some limitations with regards to the characterisation of these compounds. In the quest to obtain a better understanding of heterogeneous catalysts, various techniques such as single crystal X-ray diffraction and NMR, which are mostly used in fine structure determination at an atomic level, have been incorporated

into this venture. Unfortunately these techniques perform best when using crystalline materials, a property that many of the silicas do not have. More recently metal organic frameworks have come to fore.¹⁶ MOFs are new age porous materials with a wealth of different possibilities and novel catalytic systems using these compounds are being developed at a rapid rate. By combining a multitude of spacer ligands, MOFs of different chemical compositions can be constructed with pre-determined topology and pore sizes. Functional groups, such as amines, can be incorporated into the substructure as required by specific catalysts and pore sizes can be regulated (see Figure 2.3).

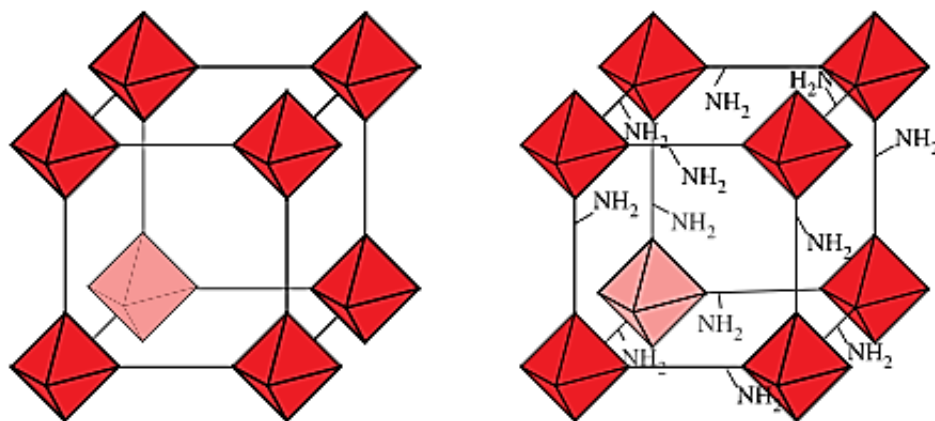


Figure 2.3: Representation of a three-dimensional metal organic framework before and after the incorporation of amines into the metal organic framework which can function as anchoring points or coordination sites for active metal species.¹⁶

Typically, there are two different approaches which can be followed in the synthesis of MOF based catalysts. The direct approach involves systematically building the active catalytic species into the system as part of the framework. The other approach, known as post synthesis modification, is where the active catalyst is attached to the functional groups by making use of ion-exchange, grafting or impregnation.¹⁷ The systematic, controllable coordinative construction of these compounds ensures that functional groups are uniformly dispersed throughout the material. This can ultimately ensure dispersion to the degree that catalytic processes effectively take place at a single-atom site. Single site heterogeneous catalysts will eventually become the optimum catalysts, as these systems combine the specificity of homogeneous catalysis with the

¹⁶ M. Ranocchiari, C. Lothschütz, D. Grolmund, and J. A. van Bokhoven, *Proceedings of the Royal Society A: Mathematical, Physical and Engineering Sciences*, **2012**, 468, 1985–1999.

¹⁷ V. Dal Santo, F. Liguori, C. Pirovano, and M. Guidotti, *Molecules*, **2010**, 15, 3829–3856.

ease of separation, recovery and recyclability of heterogeneous catalysis. These particular catalysts are still in the development phase and there are still many possibilities that need to be investigated and exploited. Different technologies and capabilities are being developed in nano-architecture. This means that processes which were not possible ten years ago can now be performed.¹⁸ By making use of all the general properties of compounds, it becomes possible to design bridging compounds that determine the distance between metal centres. These bridging compounds can also play an active role in the catalysis, such as charge transfer and oxidation/reduction functions. Most of the theory discussed with regards to MOFs in this section pertains to their use as either bulk material or the actual support that is used for catalysis. There is however another approach which involves growing MOFs in thin films on surfaces.^{19,20,21} Crystalline functionalised self-assembled monolayers can effectively be grown on polar surfaces by utilising a micro-contact printing technique. Not only can the crystalline metal organic framework be grown onto the surfaces, but the orientation of these crystals can also be controlled²² (see Figure 2.4).

¹⁸ V. Dal Santo, M. Guidotti, R. Psaro, L. Marchese, F. Carniato, and C. Bisio, *Proceedings of the Royal Society A: Mathematical, Physical and Engineering Sciences*, **2012**, 468, 1904–1926.

¹⁹ S. Hermes, F. Schröder, R. Chelmoski, C. Wöll, and R. A. Fischer, *Journal of the American Chemical Society*, **2005**, 127, 13744–13745.

²⁰ O. Shekhah, H. Wang, S. Kowarik, F. Schreiber, M. Paulus, M. Tolan, C. Sternemann, F. Evers, D. Zacher, R. A. Fischer, and C. Wöll, *Journal of the American Chemical Society*, **2007**, 129, 15118–15119.

²¹ D. Zacher, A. Baunemann, S. Hermes, and R. A. Fischer, *Journal of Materials Chemistry*, **2007**, 17, 2785.

²² K. Szelagowska-Kunstman, P. Cyganik, M. Goryl, D. Zacher, Z. Puterova, R. A. Fischer, and M. Szymonski, *Journal of the American Chemical Society*, **2008**, 130, 14446–14447.

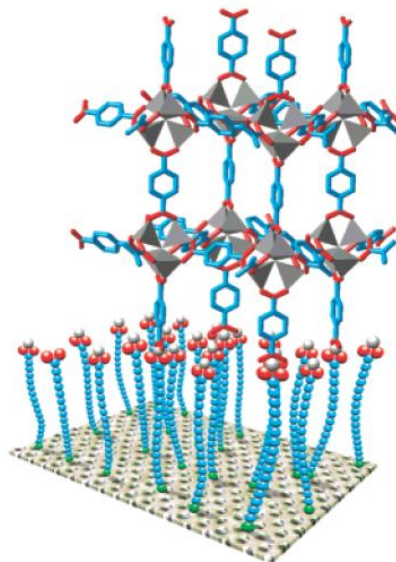


Figure 2.4: Simplified model for the growth of metal organic frameworks on surfaces.¹⁹ The grey triangles show the active metal species and the blue and red show the spacer/linking ligands.

In Figure 2.4 the metal organic frameworks that are attached to the surfaces consist of a three-dimensional framework which can be exploited in terms of catalyst design. However, this methodology could also be applied to two-dimensional compounds that are essentially not metal organic frameworks but planar bridged moieties. By rationally designing planar bridging ligands and combining these compounds with metal centres, a two-dimensional ‘net’ can be constructed which in turn can be attached to surfaces in a similar monolayer fashion. In this manner, the surface of supports can be covered with a single layer of active metal species. By performing this sort of deposition, it might not necessarily be the optimal system, as many of the tuning capabilities of these metal systems will be lost when investigating solely planar systems. This approach could also suffer due to the fact that planar ligands with essentially no catalytic function in homogeneous systems need to be used in order to achieve this dispersion. However, single site heterogeneous catalysis is not the only desired form of active metal species. In some systems, clusters or metal nanoparticles are required for the catalytic process to function.¹ Most of the catalytic dispersion methods that are discussed in Paragraph 1.4 are followed by a high temperature calcination step which is responsible for some of the coagulation problems encountered in heterogeneous catalysts. By using the aforementioned two-dimensional bridging ligands, a certain number of active metal species can be placed in close proximity of each other

and therefore the size of the nanoparticles can be controlled to a certain degree. This concept is illustrated in Figure 2.5.

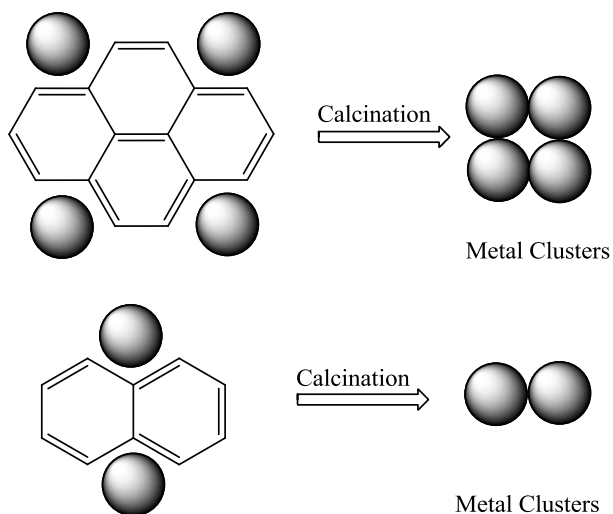


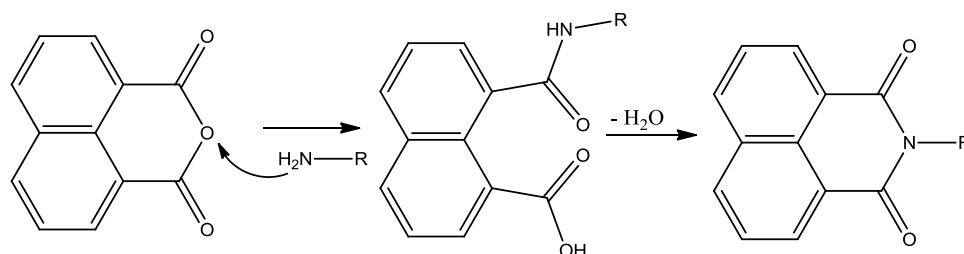
Figure 2.5: Proposed schematic method for the control of particle size in calcination of heterogeneous catalysts to form metal clusters.

2.5 Construction of Planar Bridging Ligands with Multiple Coordination Sites

In order to pursue the possibility of using planar bridging ligands as monolayers on heterogeneous supports, two different pathways were followed. In the first instance, planar ligands that can coordinate bidentate fashion to two or four metal species were constructed. By manipulating these ligands, a charge could also be introduced into the system. This concept is discussed in more detail from Paragraph 2.6. The second approach involved functionalising 1,10-phenanthroline ligands, of which the coordination chemistry is well known, in such a way that these ligands could be linked to a central core to create a bridging ligand. By using the different cores, ligands that can accommodate two, three and four metal centres can be constructed. The different aspects of these ligands are discussed from Paragraph 2.8 onwards. It is important to note that the coordination of multiple metal species was not the only criteria used when these compounds were chosen as possible spacer ligands. Cost, charge transfer properties, robustness and the ability to attach to heterogeneous supports were also taken into account.

2.6 1,4,5,8-Naphthalenetetracarboxylic Dianhydride Derivatives

The title compound consists of two centrally fused benzene rings with two pentanedioic anhydride units attached on opposite ends. This combination yields a planar organic molecule that exhibits some interesting properties. The resulting compound is robust and has high mechanical strength and modulus, good film-forming ability and superior chemical resistance.²³ This compound and its derivatives also display excellent electronic charge transfer properties²⁴ which can be exploited for charge transfer between metal species involved in the catalysis process. The pentanedioic anhydride units can also be functionalised in a fairly simple manner by performing a nucleophilic dehydration reaction (see Scheme 2.2). It is important to note that all these properties are accompanied by a degree of insolubility, which poses a major problem with regards to characterisation and further investigations into the mechanistic workings of these compounds.



Scheme 2.2: Nucleophilic dehydration reaction with pentanedioic anhydride and nitrogen derivatives.

In the following paragraphs, the properties and application of 1,4,5,8-naphthalenetetracarboxylic dianhydride and its derivatives will be discussed. This will shed some insight regarding the possible uses of these compounds as bridging ligands in heterogeneous catalysis.

²³ Y. Yin, *High Performance Polymers*, **2006**, 18, 617–635.

²⁴ K. Yuney and H. Icil, *European Polymer Journal*, **2007**, 43, 2308–2320.

2.6.1 The Functionalization of 1,4,5,8-Naphthalenetetracarboxylic Dianhydride (NTCDA)

The title compound (NTCDA) is the basic backbone used in the construction of various ligands which will be discussed in the following paragraphs. Essentially, this molecule does not have the ability to coordinate to active metal species such as palladium and platinum. However, it is important to indicate the properties which led to its identification as a possible dispersion spacer. NTCDA has found applications in n-channel organic transistor materials²⁵ and has been used as a spacer in heterostructures.²⁶ Laquindanum *et al.*²⁵ reported that the NTCDA molecule contains an accessible LUMO for electron injection with electron mobilities up to $3 \times 10^{-3} \text{ cm}^2 \text{ V}^{-1} \text{ s}^{-1}$. This is a clear indication that the electronic properties can be exploited in potential bridging complexes.

Another structural property of NTCDA which can be of potential use is its ability to form long-range ordered films on single crystalline metal substrates such as the monolayer which was reported by Zirotto *et al.*²⁷ The monolayer of NTCDA which was deposited onto an Ag(III) surface, displayed a new narrow peak in the excitation spectra near the Fermi level. This provides further evidence of the electronic capabilities of these systems. NTCDA can function as an organic semi-conductor with good crystallinity and has been extensively studied for use in molecular electric devices.²⁸ Lithium ions can be inserted into the C₆ rings and the insolubility and robustness of the ligand can be exploited for Li-ion batteries. One NTCDA molecule can accommodate approximately eighteen lithium ions. The above application gives a clear indication of the qualities that can be exploited for application in heterogeneous catalysis. Further functionalization of NTCDA provides further even more possibilities and capabilities for this ligand system.

²⁵ J. G. Laquindanum, H. E. Katz, A. Dodabalapur, and A. J. Lovinger, *Journal of the American Chemical Society*, **1996**, *118*, 11331–11332.

²⁶ F. F. So, S. R. Forrest, Y. Q. Shi, and W. H. Steier, *Applied Physics Letters*, **1990**, *56*, 674.

²⁷ J. Zirotto, S. Hame, M. Kochler, A. Bendounan, A. Schöll, and F. Reinert, *Physical Review B*, **2012**, 85.

²⁸ X. Han, G. Qing, J. Sun, and T. Sun, *Angewandte Chemie International Edition*, **2012**, *51*, 5147–5151.

In order to transform the NTCDA backbone into a ligand with coordinating abilities, various approaches were followed. The first approach was to perform a dehydration reaction with 2-aminopyridine, 2,6-diaminopyridine and various other pyridine and pyrimidine variations. This could create a planar molecule with two (pyridine) to four (pyrimidine) coordinating sites (see Figure 2.6).

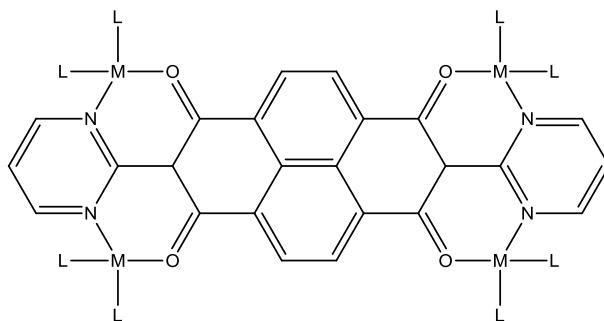


Figure 2.6: Proposed bridging mode for NTCDA derivatives indicating the four coordination cavities when using 2-aminopyrimidine.

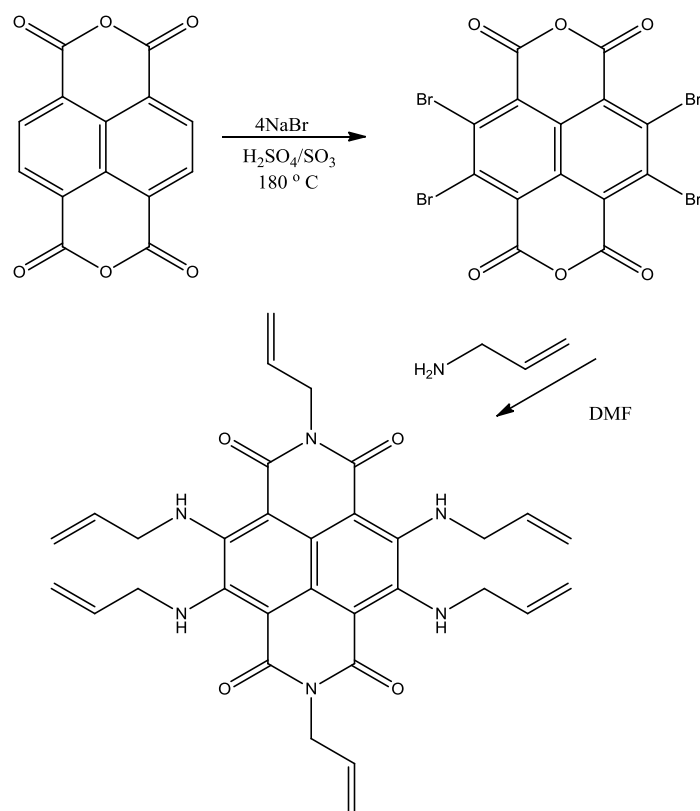
The synthesis of the 2-aminopyridine compound is reported in Paragraph 3.4 and the crystal structure is discussed in Paragraph 5.3.3. It consists of the NTCDA backbone combined with 2-aminopyridine molecules on both ends of the backbone. This compound and the 4-pyridine variations were reported by Trivedi *et al.*²⁹ who investigated a range of these compounds as possible colorimetric indicator array moieties, that could be used to discriminate between positional isomers of aromatic organic molecules. The ability of these compounds to act as charge transfer compounds when mixed with organic molecules in the solid state was investigated and exploited to discern between different isomers with the naked eye. It was found that these compounds have a π -electron acceptor ability, which suggests that as a whole the molecule is electron deficient. This could lead to it being a very hard ligand rather than the softer variation which is needed to employ this ligand using square planar centres such as platinum and palladium.

Ideally, the introduction of electron rich functional groups on the benzene rings would make the ligands softer, however this also creates synthetical challenges. Bell and co-workers³⁰

²⁹ D. R. Trivedi, Y. Fujiki, N. Fujita, S. Shinkai, and K. Sada, *Chemistry - An Asian Journal*, **2009**, 4, 254–261.

³⁰ T. D. M. Bell, S. Yap, C. H. Jani, S. V. Bhosale, J. Hofkens, F. C. De Schryver, S. J. Langford, and K. P. Ghiggino, *Chemistry - An Asian Journal*, **2009**, 4, 1542–1550.

investigated the selective bromination of the NTCDA backbone using oleum and NaBr at 180° C. The bromination was followed by a reaction with allylamines, which yielded compounds depicted in Scheme 2.3. The longer allyl chains increased the electron density of these compounds to such an extent that photophysical properties were observed. Similar reactions were performed by Krüger *et al.*³¹ who employed polythiophenes rather than the allylamines for the substitution reactions. The diamide oxygens were replaced in the ring by fluorinated carbon chains which created a charge transfer compound with applications in polymer electronics. The addition of a fluorinated carbon chain on the central diamide oxygen also gives NTCDA n-type semi-conductor properties with processing versatility type functionality as reported by Jones.³²



Scheme 2.3: The bromination of NTCDA followed by the amination using allylamine.

³¹ H. Krüger, S. Janietz, D. Sainova, D. Dobрева, N. Koch, and A. Vollmer, *Advanced Functional Materials*, **2007**, 17, 3715–3723.

³² B. A. Jones, M. J. Ahrens, M.-H. Yoon, A. Facchetti, T. J. Marks, and M. R. Wasielewski, *Angewandte Chemie International Edition*, **2004**, 43, 6363–6366.

The addition of the bromine atoms to NTCDA greatly improves the solubility of the compound in common organic solvents. However, the increased electron density requires a much stronger nucleophile for the subsequent amination and dehydration. As a result, the reaction proceeds well with the electron rich allylamine. This cannot however be said for the aminopyridine variation. One could argue that the bromination can follow the synthesis of the proposed bridging ligands (Figure 2.6) but these ligands cannot handle the harsh reaction conditions of this process. As a result, the brominated variation of the proposed bridging ligand could not be synthesised. This is detrimental to the coordination of soft metal species to these molecules.

Another approach that can be followed is to introduce a charge on the ligand to facilitate its coordination to charged metal species. A simple way that this can be achieved is to combine NTCDA with hydroxyl amine. This automatically provides an OH group which can be deprotonated before its coordination to the metal species. The synthesis and characterisation of this compound is given in Paragraph 3.3.7. In order to ensure that the resulting compound will be able to accommodate a metal species, compounds with similar coordination modes were investigated. Evidence for the proposed compounds is found in the palladium and copper complexes reported by Xu *et al.*³³ and Kovalchukova *et al.*³⁴ respectively (see Figure 2.7).

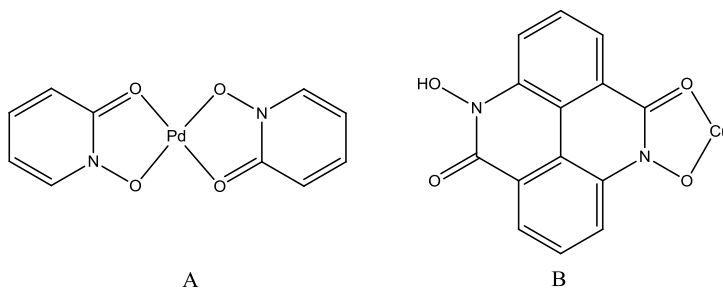


Figure 2.7: Palladium and copper complexes with O-N-C-O coordination mode reported by Xu *et al.*³³ (A) and Kavalchukova *et al.*³⁴ (B) respectively.

³³ L. Xu, Y.-Z. Li, X.-T. Chen, and X.-X. Ji, *Acta Crystallographica Section E Structure Reports Online*, **2004**, 60, m769–m770.

³⁴ O. V. Kovalchukova *et al.*, *Russian Journal of Inorganic Chemistry*, **2010**, 55, 709–713.

2.7 Pyromelletic Diamide Derivatives

Pyromelletic diamide consists of a central benzene ring with two acetic anhydride units attached on opposite ends to the benzene ring. This creates a molecule that has similar features to that of the NTCDA counterpart. However, there are some key differences which are indicated in the following paragraphs. The first major difference is the five membered diamide ring in comparison to the six membered ring in NTCDA and results in some structural changes with regards to the terminal oxygen components. These angles play key roles in the bite angle which is formed in complex formation. A comparison of the distances between potential coordinating atoms between the NTCDA crystal structure reported in Paragraph 5.3.3 and a similar compound reported by Miao *et al.*³⁵ (Figure 2.8) shows that this change translates into a 0.36 Å larger gap. The larger gap could facilitate the coordination of these compounds to larger metal centres.

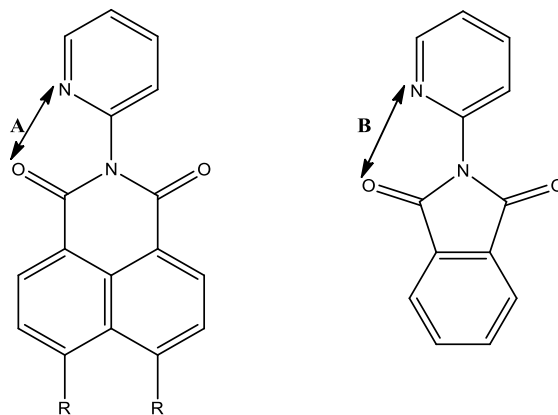


Figure 2.8: Graphical illustration of the change in bonding angles at the coordination site through the manipulation of the backbone moiety by utilising a six membered ring (A) vs the five membered (B) counterpart.

Another major difference between NTCDA and pyromelletic diamide is found in the solubility of the compounds. The latter shows better solubility in solvents like THF and methanol, which cannot be said for NTCDA which is only soluble in hot DMF and DMSO. As a result, these compounds could be used to gain more insight into the coordinating capabilities of the proposed bridging compounds and facilitate characterisation of metal species.

³⁵ Miao, F. M.; Wang, J. L.; Miao, X. S. *Acta Crystallographica Section C Crystal Structure Communications* **1995**, *51*, 712-713.

2.7.1 The Functionalization of Pyromelletic Diamide

The similarities between pyromelletic diamide and NTCDA have already been discussed, and as a result both molecules can be functionalized to form bridging ligands in a similar fashion. In this section the functionalization and application of the resulting compounds will be discussed. The possibility of coordinating these ligands to active metal species will also be explored.

The dehydration of the pyromelletic backbone with 2-aminopyridine and 2-aminopyrimidine derivatives is the most basic way to transform the non-coordinating backbone into a bridging ligand. This can be achieved quite easily, although the basicity of the attacking nucleophile does play a role in the ease of synthesis. Similar compounds have been reported and a variety of applications were found. Trivedi *et al.*²⁹ investigated a range of these compounds along with the NTCDA counterparts as possible colorimetric indicator array moieties. Other derivatives were found to have significant biological activity.^{36,37} Hassanzadeh *et al.*³⁸ found that the mono substituted derivatives show anxiolytic properties.

Although interesting, these reported compounds do not give much insight into the properties that could be exploited in order to create the desired spacer ligands. Although the pyromelletic backbone has not been investigated to a great extent, various 2-phthalimidopyrimidine derivatives have been investigated as possible spacers for supramolecular structures³⁹ (see Figure 2.9). Although Rodríguez *et al.*³⁹ did not investigate the coordination of these compounds to metal centres they did evaluate the supramolecular aggregation, which showed that substantial π - π stacking was found within the packing of these compounds. Unfortunately this phenomenon leads to solubility problems.

³⁶ A. Shoji, M. Kuwahara, H. Ozaki, and H. Sawai, *Journal of the American Chemical Society*, **2007**, *129*, 1456–1464.

³⁷ D. Rennison, S. Bova, M. Cavalli, F. Ricchelli, A. Zulian, B. Hopkins, and M. A. Brimble, *Bioorganic & Medicinal Chemistry*, **2007**, *15*, 2963–2974.

³⁸ F. Hassanzadeh, M. Rabbani, and G. A. khodarahmi, *Research in Pharmaceutical Sciences*, **2007**, *2*, 35–41.

³⁹ R. Rodríguez, M. Nogueras, J. Cobo, J. N. Low, and C. Glidewell, *Acta Crystallographica Section C Crystal Structure Communications*, **2008**, *64*, o392–o394.

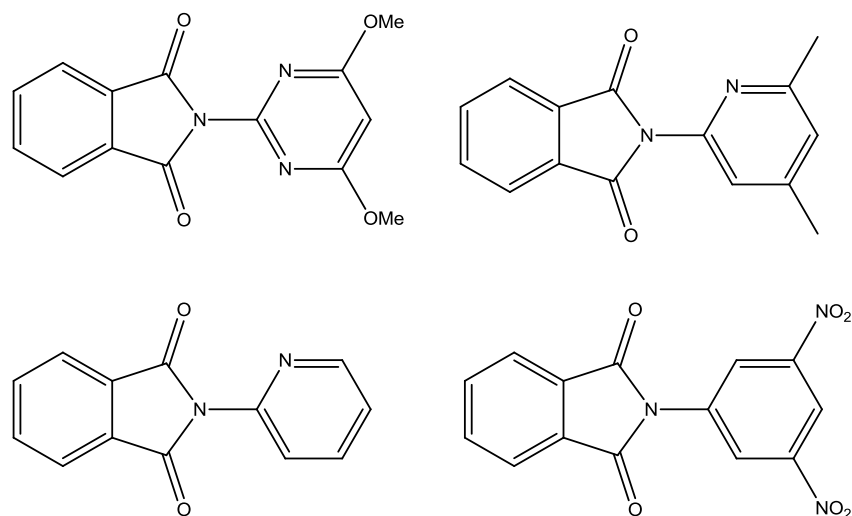


Figure 2.9: Structures investigated by Rodríguez *et al.*³⁹ as possible supramolecular bridging spacers.

Neels and co-workers⁴⁰ investigated the 2-amino-2-pyridine, 2-amino-4-pyridine and 2-amino-2-chloro-4-pyridine variations of pyromellitic diamide as possible supramolecular spacers. The investigations using powder and single crystal X-ray diffraction revealed that compounds form one dimensional ribbons which are linked by C-H \cdots Cl interactions to form a two-dimensional layer-like structure (see Figure 2.10).

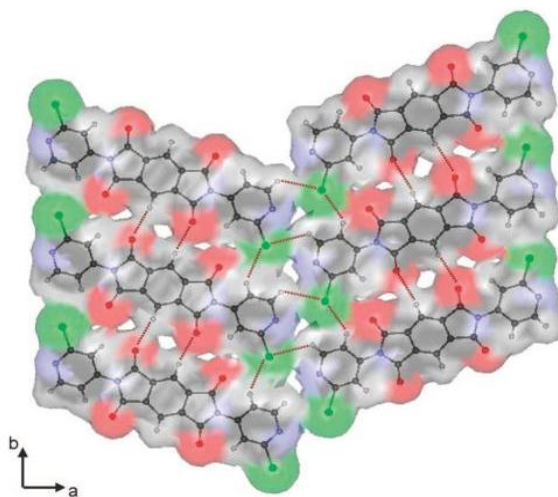


Figure 2.10: Two-dimensional layer like structure of pyromellitic 2-amino-2-chloro-4-pyridine diamide reported by Neels *et al.*⁴⁰ The green areas indicate the position of the chlorine atoms and the red areas the oxygen atoms.

⁴⁰ A. Neels, D. G. Mantero, and H. Stoeckli-Evans, *Crystal Growth & Design*, **2008**, 8, 1147–1153.

This provides evidence that these compounds can be used to form monolayers on heterogeneous supports. However, this is dependent on the ability of these compounds to coordinate to metal species that play an active role in catalysis.

2.8 1,10-Phenanthroline

1,10-Phenanthroline (Phen) was first discovered in the early twentieth century along with 2,2'-bipyridine. Phen is a planar, hydrophobic, electron poor heteroaromatic molecule with two nitrogen atoms, which makes the ligand perfect for cation binding. These structural features determine its coordination ability towards metal ions. The coordination chemistry of phen and 2,2'-bipyridine was investigated and produced important information on the coordinating properties of the transition metals series.⁸ Blau and Gerdiessen published the first synthetic routes to the synthesis of the phen ligand. In 1931, the colorimetric indicating capability of phen was discovered and led to its use as an indicator for many transition metals. Phen has been synthesised by various synthetic routes, but to date the best-known procedure for its preparation is the use of sequential Skraup or Dobner–Miller condensations, with isolation of the 8-aminoquinoline intermediate. This then reacts with glycerol or acrolein in the presence of sulphuric or phosphoric acid and arsenic pentoxide.^{41,42,43,44,45} Due to the usefulness of 1,10-phenanthroline as an indicator, Smith⁴¹, Case⁴⁶ and Schilt⁴⁷ also developed a wealth of synthetic routes for the synthesis of phen derivatives.

⁴¹ F. Richter and G. F. Smith, *J. Am. Chem. Soc.*, **1944**, 66, 396–398.

⁴² R. Antkowiak and W. Z. Antkowiak, *Tetrahedron Letters*, **1997**, 38, 1857–1858.

⁴³ S. Gladiali, L. Pinna, G. Delogu, S. De Martin, G. Zassinovich, and G. Mestroni, *Tetrahedron: Asymmetry*, **1990**, 1, 635–648.

⁴⁴ C. R. Smith, *J. Am. Chem. Soc.*, **1930**, 52, 397–403.

⁴⁵ S. Toyota, C. R. Woods, M. Benaglia, and J. S. Siegel, *Tetrahedron Letters*, **1998**, 39, 2697–2700.

⁴⁶ F. H. Case, *J. Org. Chem.*, **1951**, 16, 941–945.

⁴⁷ A. A. Schilt, *Analytical Applications of 1,10-Phenanthroline and Related Compounds*, Pergamon Press, New York, **1969**.

2.8.1 Chemical Properties

Phen is a weak base in an aqueous solution with a protonation constant of 4.95 log units.^{48,49} Its basicity is considerably lower than aliphatic diamines, such as ethylenediamine, with a value of 10.65 and 8.04 log units for the successive addition of acidic protons.⁵⁰ This is due to the electron-poor characteristics of the heteroaromatic rings that lower the σ -donor ability of the nitrogen atoms.⁵¹ Irrespective of the above-mentioned anomaly, phen easily coordinates to transition metal cations. Octahedral complexes of the type $[\text{M}(\text{phen})(\text{H}_2\text{O})_4]^{2+}$, $[\text{M}(\text{phen})_2(\text{H}_2\text{O})_2]^{2+}$ and $[\text{M}(\text{phen})_3]^{2+}$ are easily synthesised with the first-row transition metal cations in an aqueous medium. The formation constants of the $[\text{M}(\text{phen})]^{2+}$ type complexes, follows the Irving-Williams sequence, spanning in log units from 4.13 for $[\text{Mn}(\text{phen})]^{2+}$ to 9.25 for $[\text{Cu}(\text{phen})]^{2+}$.⁴⁹ Due to the low σ -donor ability of the heteroaromatic nitrogen atoms, it would be expected that the metal complexes of the ethylene diamine counterpart will be more stable than the phen complexes. However, the opposite of the above statement is found as phen shows a higher entropic stabilisation effect than ethylene diamine. This can be attributed to the hydrophobic nature of phen, which causes larger desolvation of the metal cations upon complex formation.^{48,49} Phen also has the ability to act as a π -acceptor which compensates for the poor σ -donor ability of the nitrogen atoms. As a result, phen can form strong coordination bonds with most of the first row transition metals.

Another feature of the phen ligand is a low energy π -orbital, that is responsible for strong metal-to-ligand charge-transfer. As a result of this, absorption bands in the visible spectrum and red-shifted fluorescent emissions are observed.^{52,53} By making use of the planarity, rigidity and hydrophobicity of phen and its derivatives, their metal complexes have various uses such as being intercalating or groove binding agents for DNA and RNA.⁵⁴

⁴⁸ G. Anderegg, *Helvetica Chimica Acta*, **1963**, 46, 2397–2410.

⁴⁹ G. Anderegg, *Helvetica Chimica Acta*, **1963**, 46, 2813–2822.

⁵⁰ P. Paoletti, *Pure and Applied Chemistry*, **1984**, 56, 491–522.

⁵¹ S. Ashcroft, *Thermochemistry of transition metal complexes*, Academic Press, London, **1970**.

⁵² A. Juris, V. Balzani, F. Barigelli, S. Campagna, P. Belser, and A. von Zelewsky, *Coordination Chemistry Reviews*, **1988**, 84, 85–277.

⁵³ N. Armaroli, *Chemical Society Reviews*, **2001**, 30, 113–124.

⁵⁴ A. Sigel, *Probing of nucleic acids by metal ion complexes of small molecules*, Marcel Dekker, New York, **1996**.

It is clear that phen has unique characteristics which could have a number of applications. Thus, it has been actively studied since the seventies for its catalytic, redox, photochemical and photophysical properties.^{52,55,56} More recently, phen derivatives have been used as building units for the assembly of luminescent materials and photoswitchable molecular devices.^{57,58} In the last two decades, functionalised phen derivatives have also been used for molecular self-assembly. Structures such as catenanes, rotaxanes and knots were all designed from the knowledge imparted by the coordinating properties of phen.⁵⁹

2.9 The Functionalization of 1,10-Phenanthroline

In this paragraph, the functionalization on various carbons in the phen ring will be discussed. This will show all the different possibilities for the construction of planar bridging ligands and multidentate ligands. The numbering scheme used for phen is shown in Figure 2.11. It is important to note that there are a vast number of possible ligand variations and realistically not all of them can be discussed here. Only a short background will be given and more focus will be placed on the ligands relevant to this study.

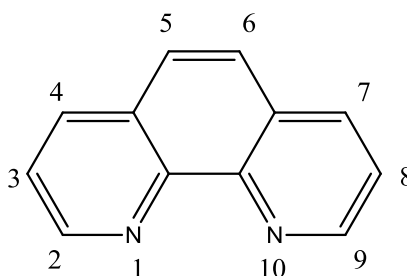


Figure 2.11: Numbering scheme used for 1,10-phenanthroline.

⁵⁵ D. V. Scaltrito, D. W. Thompson, J. A. O'Callaghan, and G. J. Meyer, *Coordination Chemistry Reviews*, **2000**, 208, 243–266.

⁵⁶ A. Lavie-Cambot, M. Cantuel, Y. Leydet, G. Jonusauskas, D. M. Bassani, and N. D. McClenaghan, *Coordination Chemistry Reviews*, **2008**, 252, 2572–2584.

⁵⁷ Z. N. Chen, Y. Fan, and J. Ni, *Dalton Transactions*, **2008**, 573.

⁵⁸ V. Balzani, A. Credi, and M. Venturi, *Molecular devices and machines concepts and perspectives for the nanoworld*, Wiley-VCH, Weinheim, **2008**.

⁵⁹ J.P. Sauvage and C. Dietrich-Buchecker, *Molecular catenanes, rotaxanes, and knots : a journey through the world of molecular topology*, Wiley-VCH, Weinheim; New York, **1999**.

2.9.1 2,9-Disubstituted 1,10-Phenanthroline Derivatives

The preparation of phen derivatives bearing substituents at position two and nine can be prepared by making use of the Friedländer condensation method. In this classic reaction, an aminoaldehyde is condensed with an enolizable ketone, that results in the loss of water. This versatile method has recently been applied by Thummel and co-workers for the construction of a large selection of symmetrical phen-based bridging ligands (Figure 2.12).^{60,61,62,63}

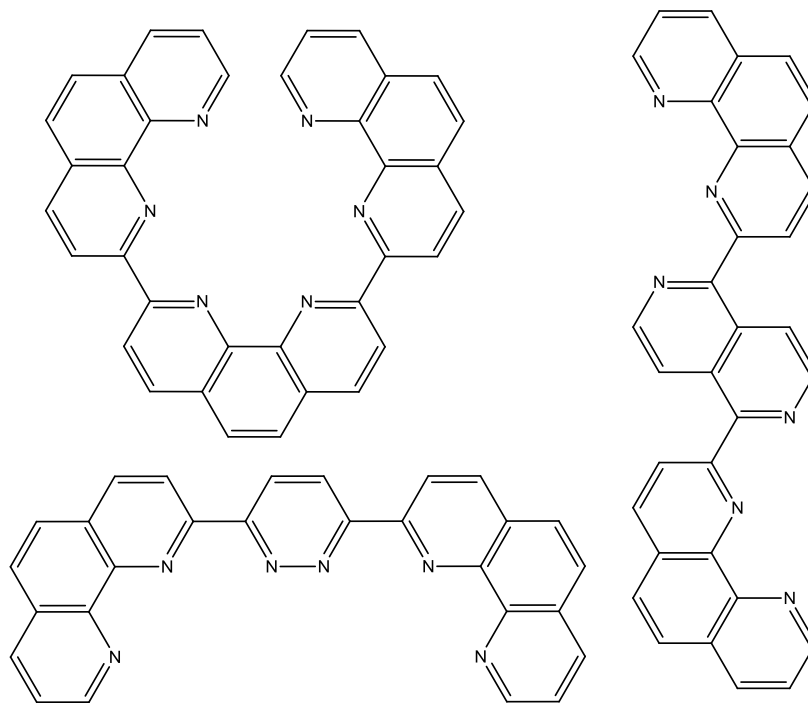


Figure 2.12: Multi-dentate ligands synthesised by Thummel and co-workers.^{61,62}

⁶⁰ E. C. Riesgo, X. Jin, and R. P. Thummel, *The Journal of Organic Chemistry*, **1996**, *61*, 3017–3022.

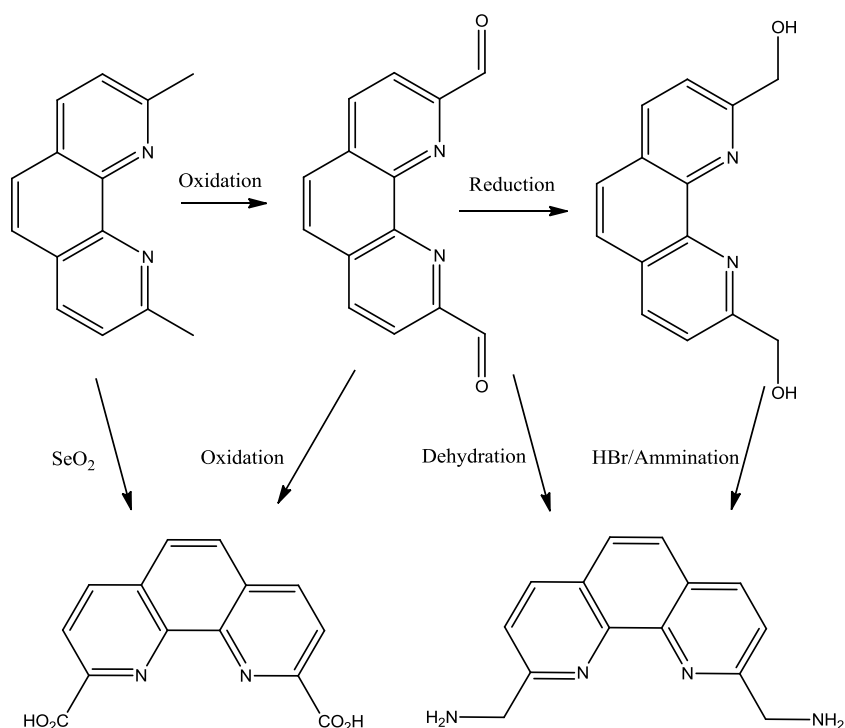
⁶¹ R. Zong, D. Wang, R. Hammitt, and R. P. Thummel, *The Journal of Organic Chemistry*, **2006**, *71*, 167–175.

⁶² A. Juris, L. Prodi, A. Harriman, R. Ziessel, M. Hissler, A. El-ghayoury, F. Wu, E. C. Riesgo, and R. P. Thummel, *Inorganic Chemistry*, **2000**, *39*, 3590–3598.

⁶³ T. Bark and R. P. Thummel, *Inorganic Chemistry*, **2005**, *44*, 8733–8739.

Various metals can coordinate with these ligands and there are a variety of properties that can be tuned to attain the desired effect. Distances between metal centres, as well as specific electrical environments, can be chosen to obtain preferred electrochemical properties. The conjugated π -aromaticity that is present on these moieties also allows for metal-metal interaction, which is ideal for electron transfer properties.^{63,64,65}

Another approach to alter position two and nine on phen, is to make use of 2,9-dimethyl-1,10-phenanthroline. It can easily be oxidised by selenium dioxide, which affords the dialdehyde that can further be oxidised to the diacid or reduced to the diol. To obtain the diamine, the bisoxime is prepared and dehydrated to the nitrile, which is then reduced to the diamine (Scheme 2.4).⁶⁶



Scheme 2.4: Schematic representation of the potential conversion of 2,9-dimethyl-1,10-phenanthroline to various derivatives based on the 1,10-phenanthroline template.

⁶⁴ L. Chouai, F. Wu, Y. Jang, and R. P. Thummel, *European Journal of Inorganic Chemistry*, **2003**, 2774–2782.

⁶⁵ D. Brown, R. Zong, and R. P. Thummel, *European Journal of Inorganic Chemistry*, **2004**, 3269–3272.

⁶⁶ P. G. Sammes and G. Yahiolu, *Chemical Society Reviews*, **1994**, 23, 327–334.

It has been shown that position two and nine on the phen ligand can be successfully altered with various methods. Although, this does pose a legitimate route to follow for the synthesis of planar bridging ligands for the purpose of this study, alteration of the less favoured positions five and six was pursued.

2.9.2 5-Mono or 5,6-Disubstituted 1,10-Phenanthroline Derivatives

The phen derivatives with substituents on position five and six, have been slightly less explored than the two and nine substituted counterparts. One reason for this is the fact that the five and six substituted moieties have less scope to act as multidentate ligands. Nevertheless, techniques were developed to introduce functionalized groups on these two positions. Figure 2.13 illustrates some of the possible ligands that can be synthesised when functionalizing position five and six on the phen ring.⁴⁰ From Figure 2.13 one is able to see that ligand 1, 4 and 6 already have the capacity to act as bridging ligands. Also, in the case of ligand 4 and 6, there are two significantly different bonding sights. The nitrogen atoms in the heteroaromatic rings are considerably softer than the oxygen atoms on the other side of the molecule. This immediately introduces the possibility of creating multiple metal centre species in a more controlled manner.

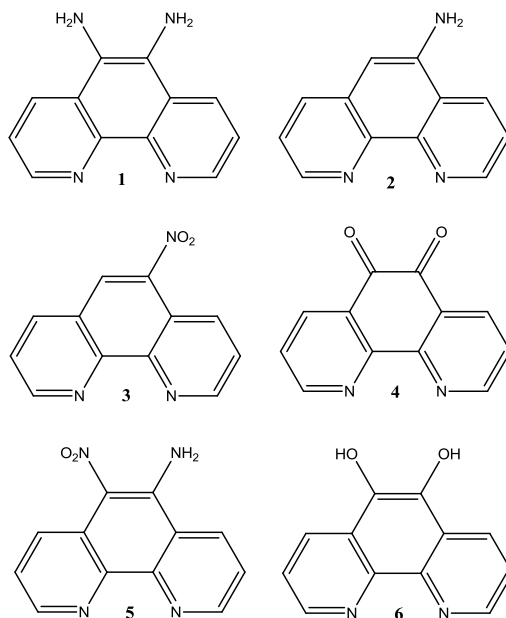


Figure 2.13: Possible modifications on position five and six of 1,10-phenanthroline.²

Various catalytic systems such as the Wacker oxidation make use of two metal species with varying oxidation states and electron transfer between two different metal ions. Consequently, the possibility of introducing these ‘joined’ metal species can be seen as an exciting prospect. It is important to note that this is in fact easier said than done, since remarkable challenges were found not only in the synthesis of these ligands, but also in the isolation of a single dual metal species.

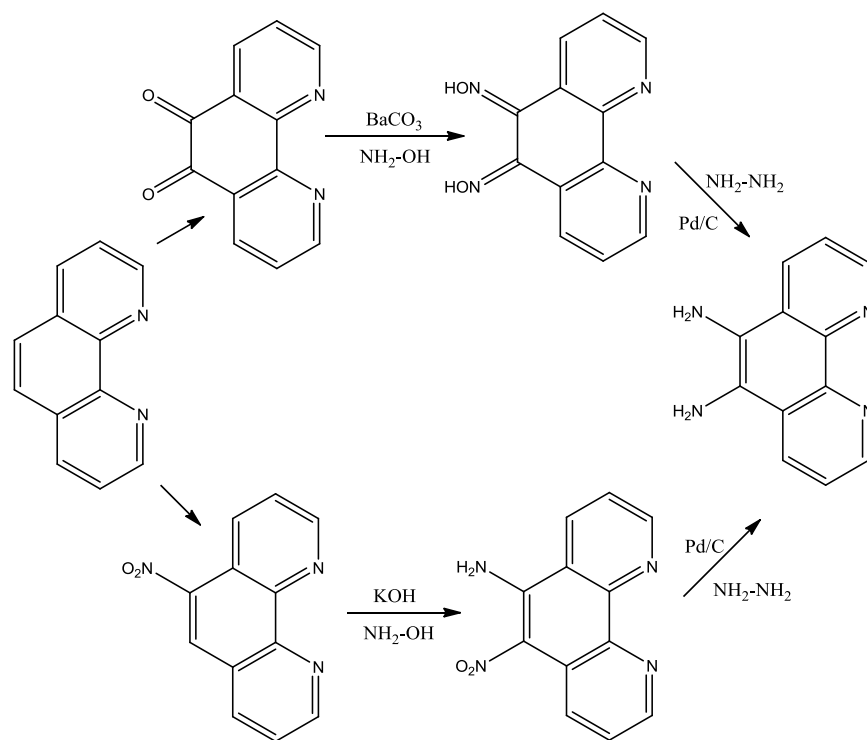
2.9.3 Oxidative Substitution Reactions of 1,10-Phenanthroline

All the ligands that are shown in Figure 2.13 were synthesised using strong initial oxidative conditions. The dione (4) is typically prepared by making use of KBr, using a mixture of nitric and sulphuric acid.^{67,68} Similarly the 5-nitro species (3) makes use of nitric and sulfuric acid at 170 °C without the presence of bromine.⁶⁹ The diamine (1) can be obtained by the two different routes shown in Scheme 2.5. The first involves conversion of the dione to the dioxime using hydroxyl amine in a basic medium. The dioxime is then hydrogenated using palladium on carbon and hydrazine. Although this route seems fairly basic, some challenges were encountered when performing this reaction.

⁶⁷ A. Torres, D. . Maloney, D. Tate, Y. Saad, and F. . MacDonnell, *Inorganica Chimica Acta*, **1999**, 293, 37–43.

⁶⁸ R. D. Gillard and R. E. E. Hill, *Journal of the Chemical Society, Dalton Transactions*, **1974**, 1217–1236.

⁶⁹ F. H. Westheimer, E. Segel, and R. Schramm, *Journal of the American Chemical Society*, **1947**, 69, 773–785.



Scheme 2.5: Possible synthetic routes for the synthesis of 5,6-phendiamine starting from 1,10-phenanthroline.

The dioxime molecule is insoluble, difficult to characterise and the yields are typically poor. The hydrogenation is effective and no real trials have been encountered in this regard. The second pathway involves making the 5-nitro species which can then be reacted with hydroxylamine to give 6-nitro-1,10-phenanthroline-5-amine (5) in Figure 2.13. This species can be hydrogenated to give the diamine. The second reaction sequence is typically less favoured than the first that leads to an overall poor conversion of the starting material. It is important to note that experimentally it was found that the best path to follow is in fact *via* the 6-nitro-1,10-phenanthroline-5-amine intermediate, even though the oxime route seems like the optimum procedure to use. By successfully synthesising the ligands displayed in Figure 2.13 a wealth of chemistry can be performed. The properties of the bridging ligands can be investigated and these molecules can be used as synthons in the construction of other bridging entities. One way in which this can be achieved is by using Schiff base reactions.

2.10 Construction of Multidentate Schiff Base Bridging Ligands

Schiff base ligands have played an important role in the development of coordination chemistry.⁴⁰ These ligands form stable coordination compounds with transition metals and display remarkable versatility and stability. Consequently, these ligands have been used to construct a large number of macrocyclic moieties,⁷⁰ which is further aided by the large number of available ketones and amines. Countless combinations of ligands with various shapes, sizes, electronic, spectroscopic and steric properties can be constructed using a simple nucleophilic condensation reaction. The Schiff base ligands also find application in different disciplines, which include bioinorganic chemistry, catalysis and magnetochemistry.^{70,71,72}

In the following paragraphs, some general information regarding Schiff bases and its reaction mechanism will be discussed. Furthermore, some insight will be given into the possible bridging ligands which were identified as good candidates for this study.

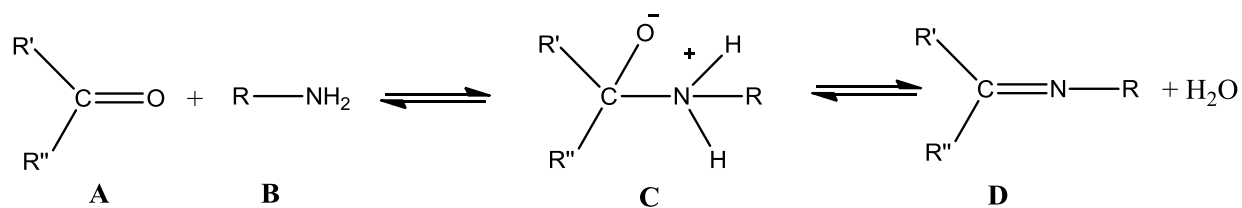
2.10.1 Mechanism and Synthetic Procedure

As previously mentioned, Schiff base ligands are quite easily synthesised (Scheme 2.6). The common reaction scheme involves the reaction of a carbonyl group (A) and a primary amine (B) in an ethanol solution. This gives a carbinolamine (C) intermediate, that loses water to produce the desired Schiff base (D). Due to the reversibility of the reaction, it is necessary to remove water from the reaction mixture. This is attained by making use of refluxing conditions or using the Dean Stark reaction conditions which involves azeotropic distillation with benzene.

⁷⁰ P. Guerriero, S. Tarnburini, and P. A. Vigato, *Coordination Chemistry Reviews*, **1995**, 139, 17–243.

⁷¹ P. Guerriero, S. Tamburini, P. A. Vigato, U. Russo, and C. Benelli, *Inorganica Chimica Acta*, **1993**, 213, 279–287.

⁷² H. Ōkawa, H. Furutachi, and D. E. Fenton, *Coordination Chemistry Reviews*, **1998**, 174, 51–75.



Scheme 2.6: Mechanism of the general Schiff base synthesis via aldol condensation.⁴⁰

This reaction proceeds spontaneously when using aliphatic amines; however, when using other primary amines, acids can be used as an effective catalyst to activate the carbonyl group. Although many of the Schiff bases do show stability, some tend to decompose. Template synthesis has become a very successful way to overcome this problem. It usually involves the above mentioned reaction scheme in the presence of metal cations such as Ba(II), lanthanoids or Pb(I). This methodology is frequently used for the synthesis of macrocyclic Schiff base complexes.^{69,71}

2.10.2 Planar Multi-Nuclear Schiff Base Ligands

As a result of the versatility of the Schiff base ligands, a range of ligands with various bonding modes and denticity have been constructed. Furthermore, these ligands have different N, O, S and P donor atoms. There are too many ligands available to discuss in this project. It is also important to note that a large amount of Schiff base ligands are constructed solely to coordinate to a single metal centre in various ways. In this study the aim was to link ligands with known bonding modes, in such a way that the resulting planar ligand could house multiple metal centres. These planar bridging ligands could then also act as spacers in heterogeneous catalyst deposition. Consequently, only a small number of relevant ligand systems will be shown.

Insight into the various 1,10-phenanthroline derivatives which were synthesised as synthons for this particular purpose have already been given in Paragraph 2.9.2. It is important however, to give a general indication of the available building blocks and how combinations of these building blocks are to be used. These building blocks are given in Figure 2.14.

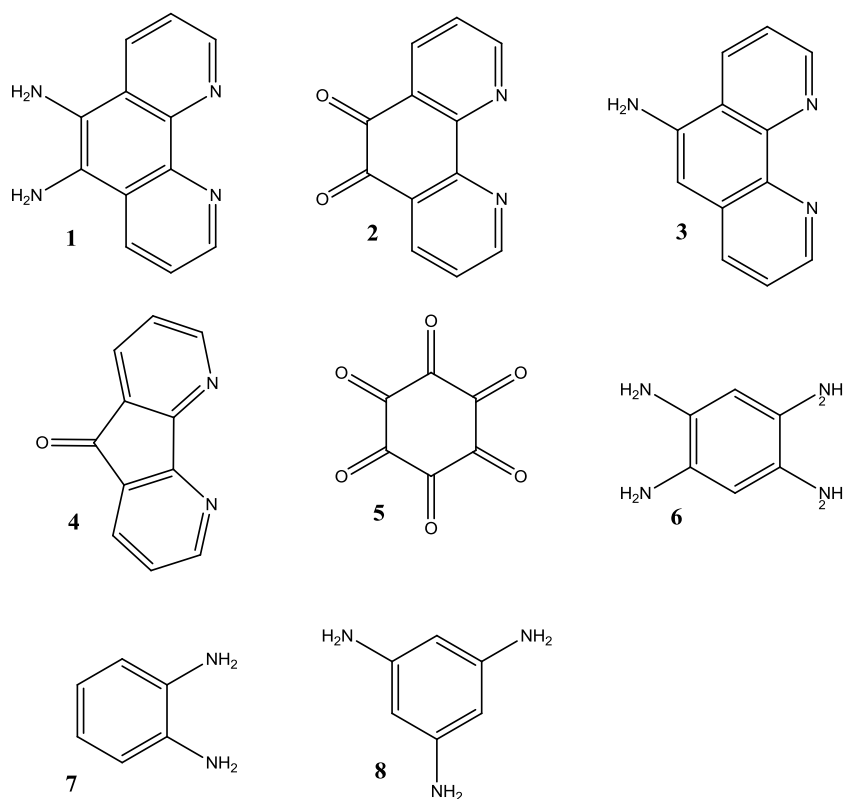


Figure 2.14: Building blocks for the construction of 1,10-phenanthroline based bridging ligands.

From Figure 2.14, ligands 1, 2, 3, 4 and 8 were synthesised whereas the rest were purchased from Sigma-Aldrich. The synthesis of these ligands is discussed in Chapter 4. It is also important to note that immense difficulties were encountered in the synthesis of ligands 1 and 4. Due to time constraints, only some of the many possible combinations were shown.

2.10.2.1 Diquinoxalino[2,3-a:2',3'-c]phenazine (heprazine)

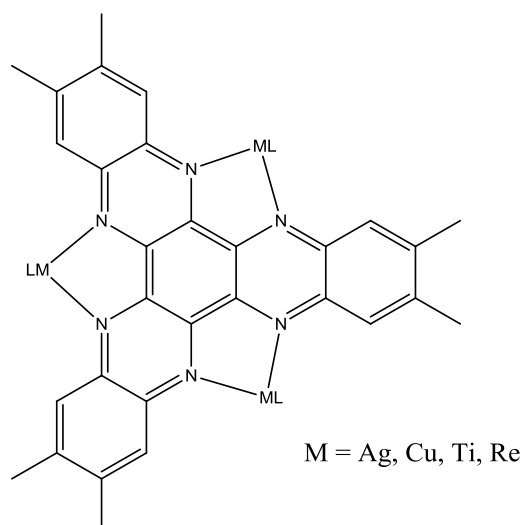
Diquinoxalino[2,3-a:2',3'-c]phenazine (heprazine) can be constructed by combining synthon 5 and 7. This creates a bridging ligand which can house three metal centres as shown in Scheme 2.7. Various bridged metal species such as copper⁷³, titanium⁷⁴, rhenium⁷⁵ and silver⁷⁶

⁷³ S. J. Lind, T. J. Walsh, A. G. Blackman, M. I. J. Polson, G. I. S. Irwin, and K. C. Gordon, *The Journal of Physical Chemistry A*, **2009**, *113*, 3566–3575.

⁷⁴ I. M. Piglosiewicz, R. Beckhaus, W. Saak, and D. Haase, *Journal of the American Chemical Society*, **2005**, *127*, 14190–14191.

⁷⁵ M. G. Fraser, C. A. Clark, R. Horvath, S. J. Lind, A. G. Blackman, X. Z. Sun, M. W. George, and K. C. Gordon, *Inorganic Chemistry*, **2011**, *50*, 6093–6106

have been reported for the methylated counterpart. Multi-metal center complexes have also been synthesised by Catalano *et al.*⁷⁷ who combined palladium and rhenium using the methylated heprazine.



Scheme 2.7: Heprazine as bridging ligand between different metal centers.

There are some disadvantages to utilising heprazine as a bridging ligand when using soft metals such as palladium and rhenium. The coordination of one metal centre like palladium, alters the electronic and physical properties of the ligand. This is probably due to the lack of electron donating abilities of the nitrogen atoms. This lack of electron donating ability also accounts for the majority of methylated reported species as the methyl groups act as electron donating species. The alteration of these properties makes the coordination of the next incoming metal species more difficult, that seriously inhibits this ligands usefulness. This phenomenon is shown in Figure 2.15.

⁷⁶ X.-H. Bu, K. Tanaka, M. Shionoya, K. Biradha, T. Yamaguchi, M. Nishimura, and T. Ito, *Chemical Communications*, **2000**, 1953–1954.

⁷⁷ V. J. Catalano, W. E. Larson, M. M. Olmstead, and H. B. Gray, *Inorganic Chemistry*, **1994**, 33, 4502–4509.

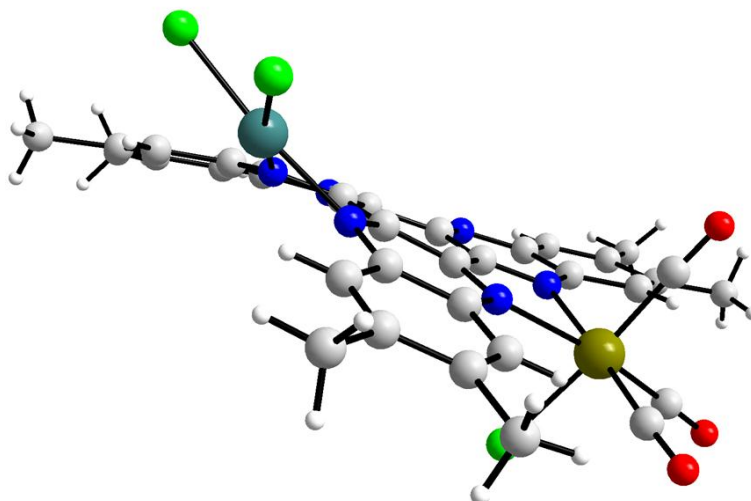


Figure 2.15: Crystal structure of distorted palladium and iron bridged species.⁷⁸ The green atom indicates the iron metal center and the turquoise atom the palladium center.

Although this distortion, where the metal centre lies out of the plane of the contorted ligand, can be attributed to an electronic origin, the hexaazatriphenylene backbone does not display the same phenomena when coordinated to iron⁷⁸ and ruthenium⁷⁹ which suggests that a steric parameter is also present.

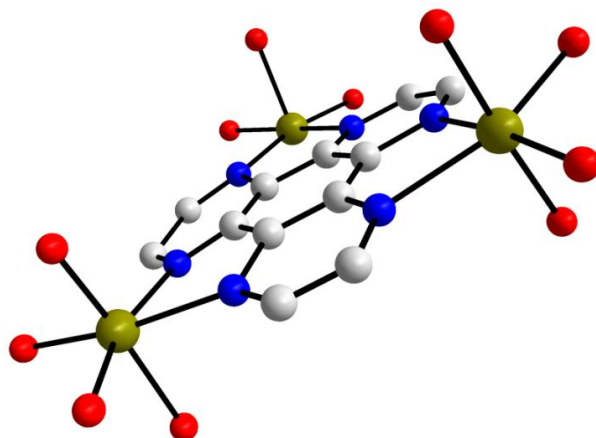


Figure 2.16: Less-distorted hexaazatriphenylene bridging three iron centres.⁷⁹ The iron centers are indicated by the green atoms.

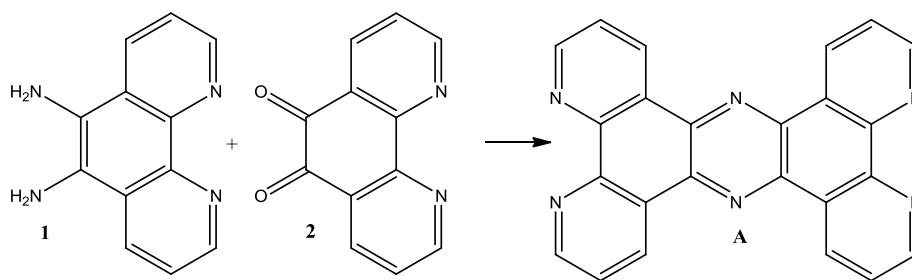
⁷⁸ M. Shatruk, A. Chouai, A. V. Prosvirin, and K. R. Dunbar, *Dalton Transactions*, **2005**, 1897–1902.

⁷⁹ J.M. Herrera, S. J. A. Pope, A. J. H. M. Meijer, T. L. Easun, H. Adams, W. Z. Alsindi, X.-Z. Sun, M. W. George, S. Faulkner, and M. D. Ward, *Journal of the American Chemical Society*, **2007**, 129, 11491–11504.

Heprazine was successfully synthesised and crystallised but regrettably no square planar metal species such as palladium, platinum and rhodium could be isolated. As a result, no further investigations into the bridging capabilities of heprazine were conducted.

2.10.2.2 Tetra-pyrido[3,2-a:2',3'-c:3'',2''-h,3''-j]phenazine (tpphz)

As previously stated ligands 1 and 2 can not only be used as bridging ligands, but are also very useful when combined with some of the other displayed compounds in Figure 2.14. By reacting compound 1 and 2 with each other the following ligand can be obtained.



Scheme 2.8: Schiff base type ligand obtained by condensing 1,10-phenylenediamine with 1,10-phenanthroline.

The synthesis of tetra-pyrido[3,2-a:2',3'-c:3'',2''-h,3''-j]phenazine (tpphz) is accomplished fairly easily as indicated by Scheme 2.8. Tpphz was previously synthesised by Bolger *et al.* and used successfully to link ruthenium and osmium metal centres.⁸⁰ However, difficulties surrounding the formation of multiple products were encountered. In order to circumvent this problem, the metal species were added to phenanthroline ligands before the above procedure was performed, which drastically increased the formation of the desired species. It is also important to note that due to the planar nature of these ligands, various solubility problems were encountered.⁸⁰ In addition, tpphz is a fully aromatic moiety, creating the possibility of charge transfer between metal centres. This and the photophysical properties of mono- and dinuclear ruthenium complexes have been investigated.⁸¹ Chiorboli and co-workers found a direct link between metal centres when looking at the photophysically active, lowest metal-to-ligand charge transfer (MLCT) transitions from the d orbitals of the metal to the π orbitals of tpphz. It was shown that

⁸⁰ J. Bolger, A. Gourdon, E. Ishow, and J. P. Launay, *Inorganic Chemistry*, **1996**, 35, 2937–2944.

⁸¹ C. Chiorboli, C. A. Bignozzi, F. Scandola, E. Ishow, A. Gourdon, and J.-P. Launay, *Inorganic Chemistry*, **1999**, 38, 2402–2410.

in mononuclear complexes, MLCT excited-state energies were very sensitive to interactions at the free bipyridine end of the tpphz ligand, such as metalation and protonation. When investigating the dinuclear complexes, it was found that the electronic ground state behaves as a valence-localised, supramolecular system, while a considerable amount of inter-component electronic coupling is shown by the MLCT excited-state. Heterodinuclear complexes of ruthenium and osmium showed fast ($k > 10^9 \text{ s}^{-1}$) energy and electron transfer processes taking place across the bridging ligand.⁸¹

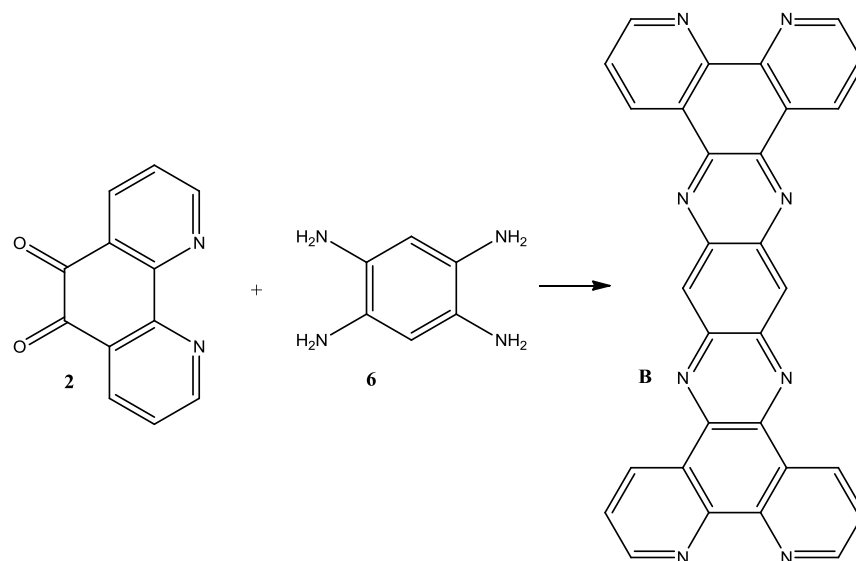
From the above evidence, the tpphz ligand clearly has enormous potential to act as a charge transfer bridging ligand as well as a spacer for possible mono-layer deposition on solid supports. The Wacker oxidation was identified as a useful reaction to evaluate this as it involves the transfer of electrons between Pd(0) and Cu(II). The results of these catalytic evaluations are discussed in Chapter 6.

2.10.2.3 9,11,20,22-Tetraazatetrapyrido[3,2-a:2'3'-c:3'',2''-l:2''',3'''-n]pentacene

9,11,20,22-Tetraazatetrapyrido[3,2-a:2'3'-c:3'',2''-l:2''',3'''-n]pentacene (tatpp) is another ligand that can be constructed using the building blocks that were chosen for this study (Scheme 2.9). Mahn-Jong Kim *et al.*⁸² reported the synthesis of tatpp and its quinoline counterpart (Scheme 2.10). Both ligands were successfully used to bridge ruthenium and osmium centers. Extensive research has been done linking these metals, as they play an important role in the development of multi-component (supramolecular) artificial systems for photochemical energy conversion.⁸³

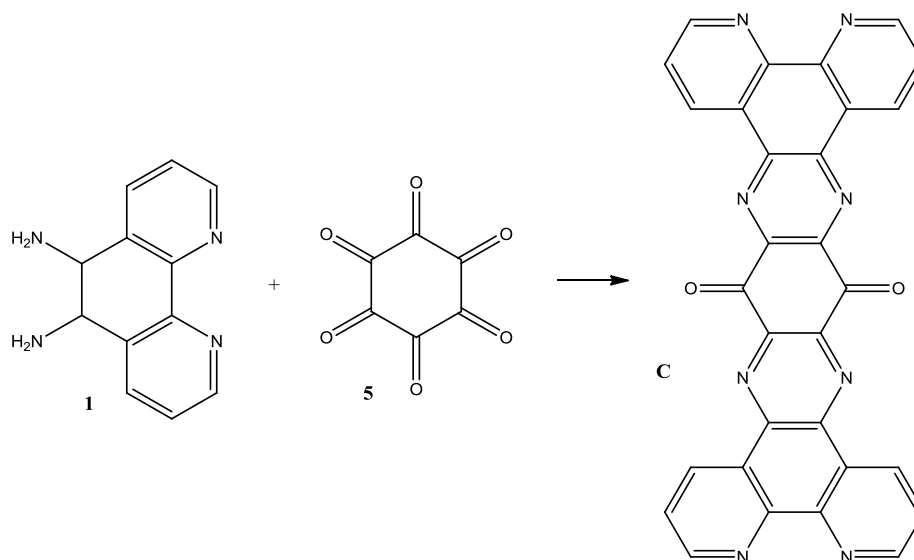
⁸² M.J. Kim, R. Konduri, H. Ye, F. M. MacDonnell, F. Puntoriero, S. Serroni, S. Campagna, T. Holder, G. Kinsel, and K. Rajeshwar, *Inorganic Chemistry*, **2002**, 41, 2471–2476.

⁸³ A. Hagfeldt and M. Graetzel, *Chemical Reviews*, **1995**, 95, 49–68.



Scheme 2.9: Schiff base synthesis of tatpp from phendione using benzene tetra-amine.

Photochemical studies have indicated that although there is definite ‘communication’ between metals on opposite ends of the ligand, the interaction is very small. This can be attributed to the large number of electrons present in the bridging sub-units. These sub-units of electrons found on the ligand tend to absorb many of the metal oxidation states rather than allow for the transfer of electrons from one end to the other end of the complex.⁴

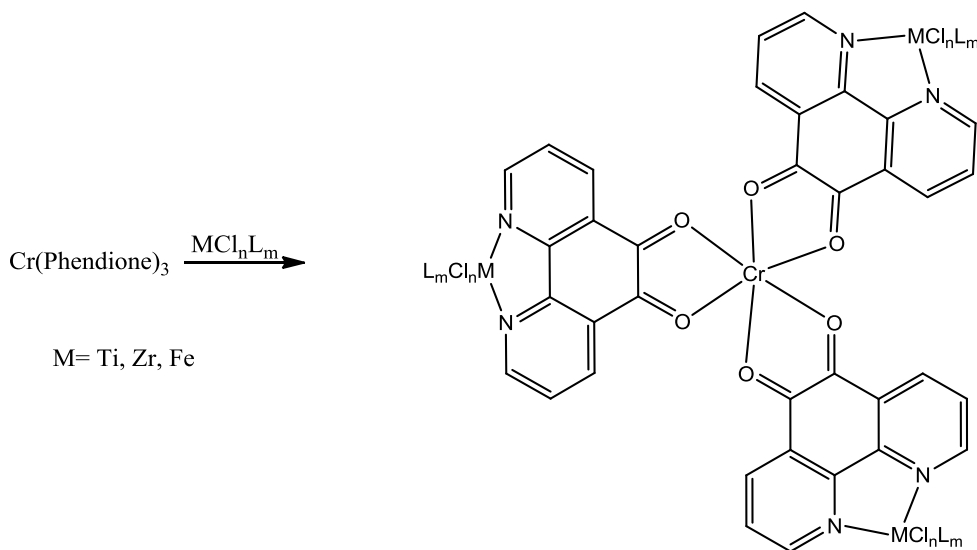


Scheme 2.10: Synthesis of dipyrido[3',2':5,6;2'',3'':7,8]quinoxalino[2,3-i]dipyrido[3,2-a:2',3'-c]phenazine-10,21(9aH,21aH)-dione from phendiamine and cyclohexane-1,2,3,4,5,6-hexaone.

The research conducted on these two ligands gave valuable insight into the limit of the distance between two metal centres for charge transfer across a bridging ligand. For this reason, the general size of tatpp was chosen as the outer size limit for the construction of bridging ligands. Due to the planarity of these systems, characterisation of desired products was an exceptionally challenging problem. Time constraints on this study resulted in minimum attention being given to these two ligands.

2.10.2.4 1,10-Phenanthroline-5,6-dione/diol Bridged Metal Species

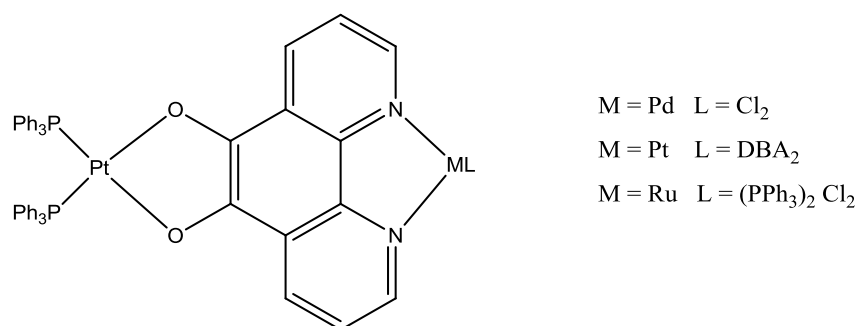
1,10-Phenanthroline-5,6-dione (phendione) is quite easily synthesised and the molecule contains two distinct coordination sites. The environment at these two sites can be seen as a quinonoid and di-iminic. The quinonoid side has redox capabilities while the di-iminic end acts as a Lewis base. These properties can be exploited in the synthesis of multi-metal species, as certain metals have an affinity for these different environments. Systems that make use of this anomaly have been reported by Calucci *et al.*⁸⁴ who introduced the methodology for using chromium as a central atom to which the quinonoid end of the molecule coordinates. Scheme 2.11 shows how various metals such as titanium, iron and zirconium are coordinated to the diiminic side to form bridged species.



Scheme 2.11: Phendione bridging various metal species.⁸⁴

⁸⁴ L. Calucci, G. Pampaloni, C. Pinzino, A. Prescimone, *Inorganica Chimica Acta*, **2006**, 359, 3911–3920.

Although the chromium complex indicates the bridging capability of phendione, predominantly octahedral coordinating metal species were used. Interestingly, square planar bridged metal species have also been synthesised using phendione. The bridged species reported by Fox *et al.*⁸⁵ are shown in Scheme 2.12. Platinum was bridged with itself, palladium and ruthenium. This however was achieved by first reducing the neutral phendione to the diol which can be deprotonated to form a 2- charged ligand. It is important to note that although the metals were bridged, considerable attention was given to creating the correct electronic environment on the metal centres in order to tailor their affinity for the O, O' and N, N' environments. This is made easier by the presence of a charge on the bridging ligand.



Scheme 2.12: Square planar bridged phendione complexes.⁸⁵

Similarly, ruthenium and osmium have been linked using the diol species.⁸⁶ In these particular systems the bridging ligand played a pivotal role in the redox reactions taking place at the metal centres. This further provides evidence that these bridging ligands can find application in catalytic reactions where metal species interchange oxidation states throughout the cycle. Furthermore, species that aid in the recycling of the active catalyst can be attached to one end of these ligands.

2.10.3 1,10-Phenanthroline-5,6-diamine Bridged Species

1,10-Phenanthroline-5,6-diamine (phendiamine) also has application as a simple bridging ligand similar to phendione, however there are far fewer instances found in literature. This is probably due to phendiamine not being readily available, as well as its challenging synthetic procedures.

⁸⁵ G. A., S. Bhattacharya, C. G. Pierpont, *Inorganic Chemistry*, **1991**, 30, 2895–2899.

⁸⁶ A. D. Shukla, A. Das, *Polyhedron*, **2000**, 19, 2605–2611.

In the case of phendiamine, the diamine part of the molecule is often functionalized into a tetradentate ligand. These types of ligands have been used by Comba *et al.*⁸⁷ to bridge various metal species such as copper, palladium and ruthenium. A typical complex is shown in Figure 2.17.

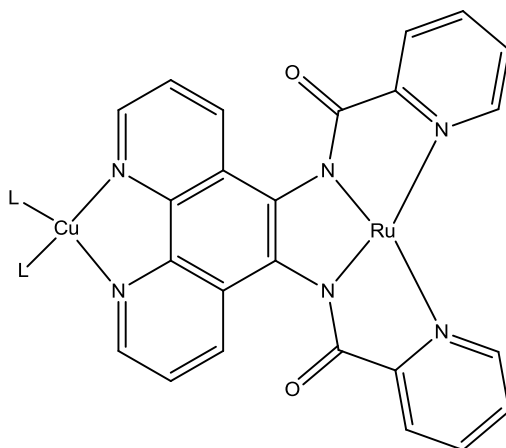


Figure 2.17: Phendiamine derivatives used as bridging ligand.⁸⁷

Simpler complexes using just phendiamine have been developed where ruthenium metal centres are bridged.^{88,89} The electrochemistry of these compounds was also investigated, and indicated that charge transfer can occur *via* these bridging ligands. From the information provided it is clearly possible to use these ligands for the intended purposes of this project. Unfortunately, this is not a simple system and specific tailoring is needed when designing these bridged complexes.

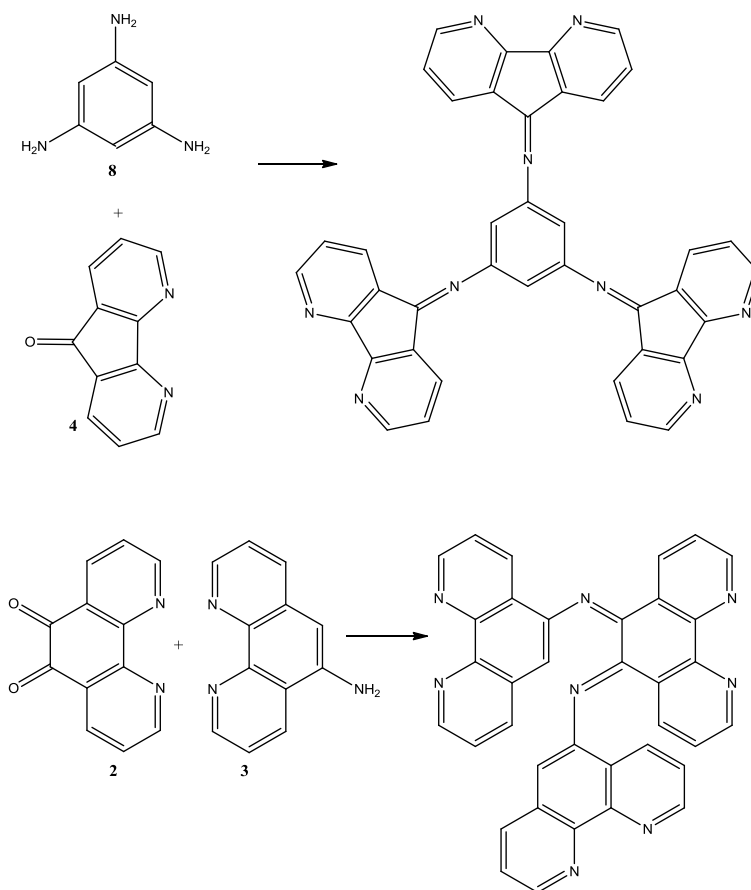
2.10.3.1 Further Possible Synthon Combinations

Although a number of known bridging ligands and complexes have been shown in the previous paragraphs there are few combinations that have not previously been explored. Some insight into the possible structures are given with only the structures of the compounds of interest shown in Scheme 2.13.

⁸⁷ P. Comba, R. Krämer, A. Mokhir, K. Naing, and E. Schatz, *European Journal of Inorganic Chemistry*, **2006**, 4442–4448.

⁸⁸ S. Ghumaan, B. Sarkar, S. Patra, J. van Slageren, J. Fiedler, W. Kaim, and G. K. Lahiri, *Inorganic Chemistry*, **2005**, *44*, 3210–3214.

⁸⁹ N. C. Fletcher, T. C. Robinson, A. Behrendt, J. C. Jeffery, Z. R. Reeves, and M. D. Ward, *Journal of the Chemical Society, Dalton Transactions*, **1999**, 2999–3006.



Scheme 2.13: Possible synthon combinations for bridging ligands.

Although these bridging ligands appear to be exciting new species, the actual synthesis of these compounds is far more intricate than it initially seems. Attempts to synthesise these compounds were made, however the time spent on these reactions was kept to a minimum. Finally, upon the successful synthesis of these synthons and bridging ligands, the catalytic properties of these compounds will be investigated before and after it is deposited onto a support, using a standard reaction such as the Heck coupling.

2.11 Heck Coupling

The selective aerobic oxidation of organic molecules has become a fundamental part of modern chemistry. One way in which these transformations can be achieved is through the use of the Heck coupling reaction. The discovery of the palladium catalysed arylation of an alkene with an organic halide by Heck⁹⁰ and Mizoroki⁹¹ in the early 1970's led to the development of a versatile process that is used in the academic and industrial environment. The Heck reaction exploits the ability of Pd(0) to form aryl or vinyl bonds through the oxidative addition of the subsequent halide. Palladium is a versatile transition metal used for both oxidative and non-oxidative transformations.^{92,93} Although palladium is by far the most effective metal for these types of reactions, there is one major drawback: in most of the homogeneous systems the catalyst becomes inactive due the formation of the bulk metal.⁹⁴ In order to circumvent this problem large amounts of research have been performed in order to develop soft ligands that can stabilise the Pd(0) center and significant ligand effects have been observed for some catalytic systems. Unfortunately, most of these effects have only been witnessed in non-oxidative conditions and most ligands decompose rapidly which leads to poor turnovers.⁹⁴ The formation of bulk palladium metal also leads to the contamination of the final products with trace amounts of the metal. This is typically unwanted in industrial applications such as the pharmaceutical industry. Some advances include the extraction of trace amounts of palladium by making use of strong coordinating compounds⁹⁵ or by making use of solid supports⁹⁶. This further supports the notion that the heterogenisation of the Heck coupling reaction does hold considerable advantages. Although there are some drawbacks to using the Heck coupling reaction, the benefits far outweigh the problems and as a result there are a considerable number of applications for this process. It is important to note that the reaction performed to test the catalytic activity of

⁹⁰ R. F. Heck, J. P. Nolley, *Journal of Organic Chemistry*, **1972**, 37, 2320.

⁹¹ T. Mizoroki, K. Mori, A. Ozaki, *Bulletin of the Chemical Society of Japan*, **1971**, 44, 581.

⁹² P.M. Henry, *Palladium catalyzed oxidation of Hydrocarbons*, **1980**, Kluwer, Boston.

⁹³ J. Tsuji, *Palladium Reagents and Catalyst*, **1995**, Wiley, New York.

⁹⁴ S. S. Stahl, *Angewandte Chemie International Edition* **2004**, 43, 3400–3420.

⁹⁵ G. W. Kabalka, R. M. Pagni, C. M. Hair, *Organic Letters*, **1999**, 1, 1423.

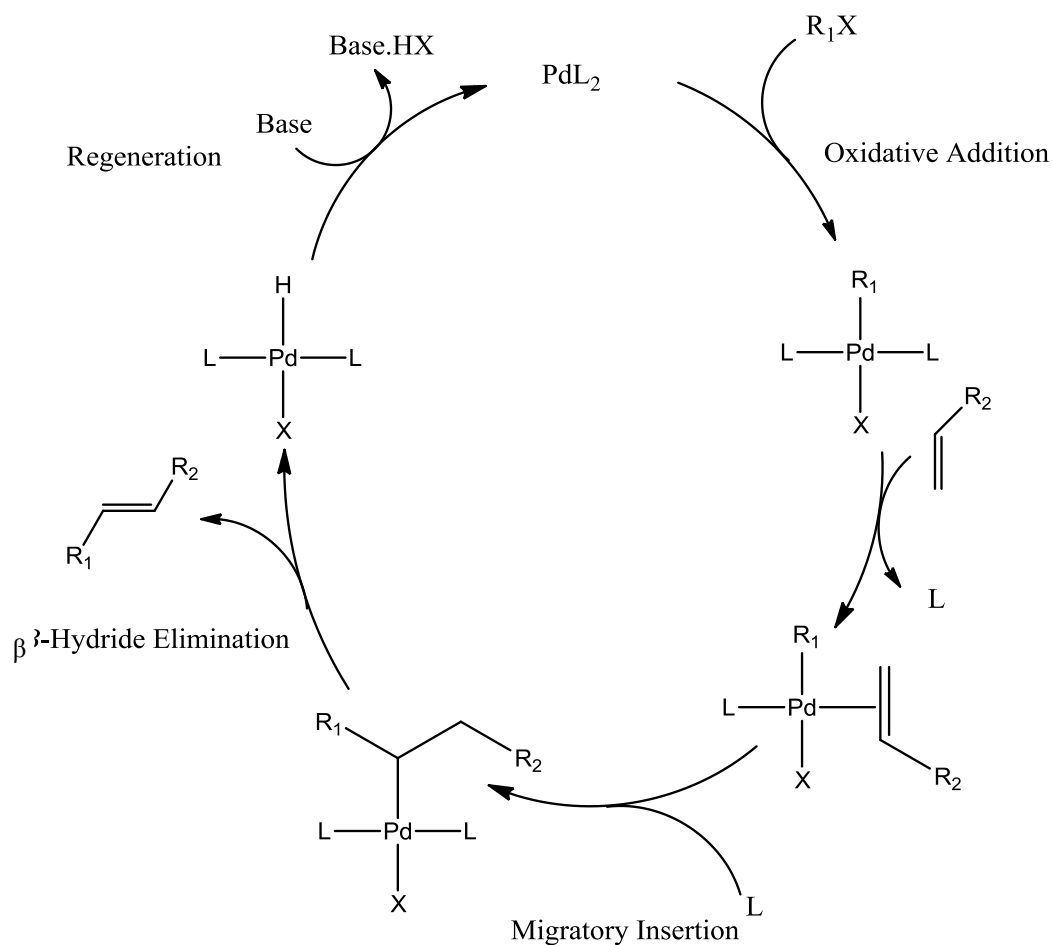
⁹⁶ C. P. Mehnert, J. Y. Ying, D. W. Weaver, *Journal of the American Chemical Society*, **1998**, 120, 12289.

bridging ligands and precursors was not the classical Heck reaction. Instead of using an aryl halide, phenyl boronic acid was used. The mechanistic aspects remained the same and the general Heck mechanism is therefore discussed.

2.11.1 Mechanistic Aspects of the Heck Coupling Reactions

Not only has a massive amount of research been performed on the development of catalysts for the Heck coupling reaction, but a large number of investigations have also been conducted into the understanding of the mechanism for the reaction. To date, the general accepted mechanism for the reaction is considered well known and understood and is presented in Scheme 2.14.⁹⁷

⁹⁷ R. F. Heck, *Organic Reactions*, **1982**, 27, 345.



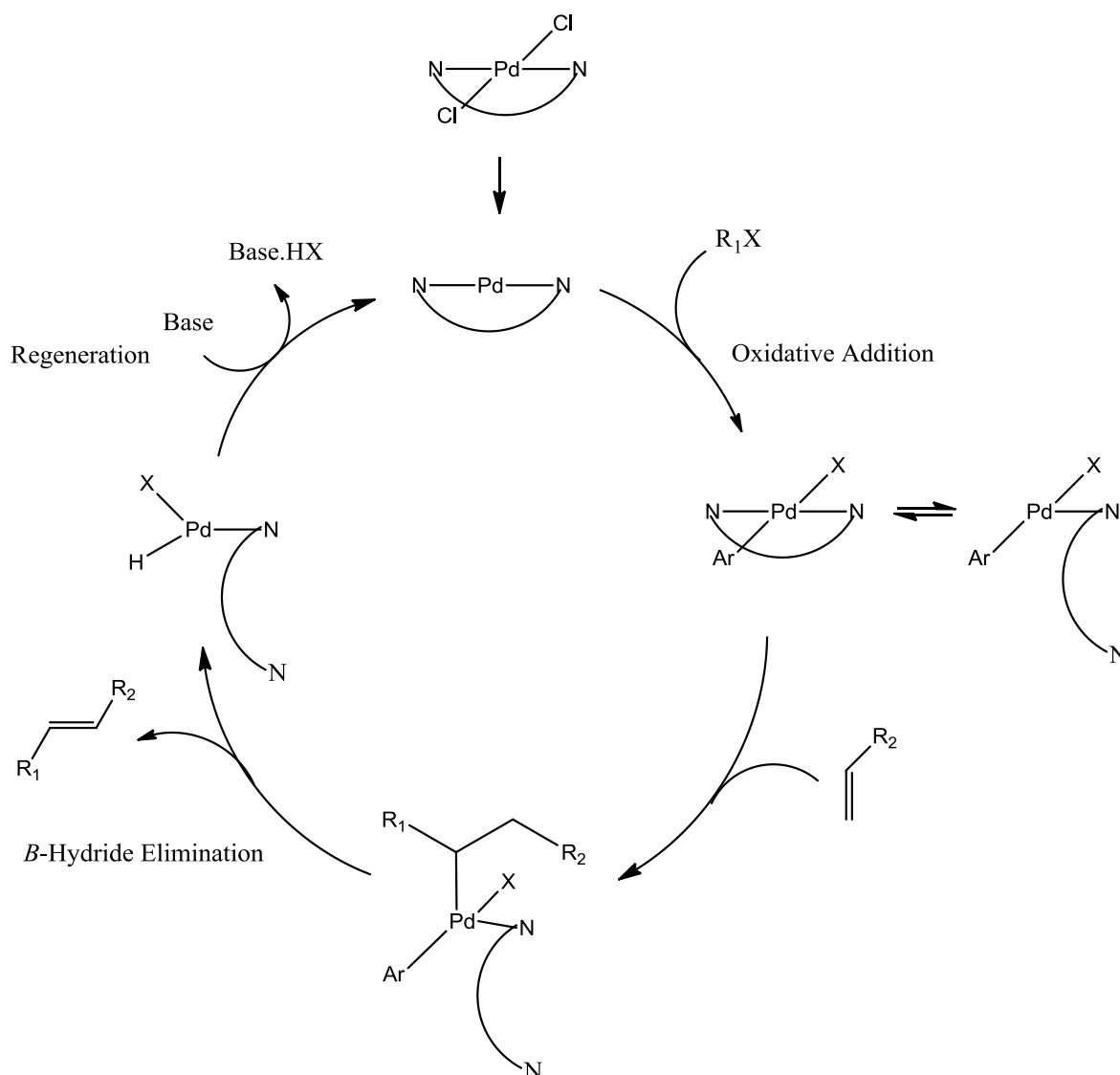
Scheme 2.14 Mechanism of the Heck coupling reaction ($\text{R}_1 = \text{Ar}$ or vinyl; $\text{R}_2 = \text{OMe}$; $\text{L} = \text{PPh}_3$; $\text{X} = \text{I}, \text{Br}$).⁹⁷

In this mechanism a $\text{Pd}(0)$ species is required and is usually generated *in situ* from the $\text{Pd}(\text{II})$ precursor. This is followed by the oxidative addition step where the palladium inserts itself into the aryl halide bond. In the next step, palladium forms a π bond with the alkene, while one of the ligands is replaced. The free ligand is re-coordinated to the metal species in the migratory insertion step, where the alkene and olefin are joined to yield the desired coupled molecule. The new alkene is eliminated by β -hydride elimination to yield the palladium hydride species. The regeneration of the starting catalytic complex is facilitated by the presence of a base. Although the mechanism depicted is widely accepted, there still remains some doubt regarding some of the mechanistic aspects that are not completely clarified. Significant doubt exists with regards to the formation of the PdL_2 species at the start of the mechanism. As a result, many investigations are still being performed in order to obtain irrefutable evidence of the proposed mechanism. Many of the studies are performed under milder temperatures to prevent the formation of side products

which exist at higher temperatures.⁹⁷ The mechanism proposed in Scheme 2.14 initially only featured monodentate coordinating ligands but recently Kawano *et al.*⁹⁸ proposed a different mechanism that features a bidentate ligand (see Scheme 2.15).

This mechanism proposes that the initial palladium complex is first reduced to form the required Pd(0) metal species which is stabilised by the bidentate ligand. This species can then undergo oxidative addition in a similar fashion to the traditional mechanism (Scheme 2.14). The subsequent coordination of the palladium species to the alkene results in one of the bidentate donor ligands dissociating before the product is released through β -hydride elimination. Reports⁹⁸ suggest that the potential of any bidentate ligands used as stabilising ligands are determined by their ability to dissociate from the ligand before the elimination step. The rest of the mechanism is the same as for the monodentate system.

⁹⁸ T. Kawano, T. Shinomaru, I. Ueda, *Organic Letters*, **2002**, 4, 2545–2547.



Scheme 2.15: Mechanism for the Heck process using a bidentate ligand proposed by Kawano *et al.*⁹⁸

It is generally accepted that a detailed explanation of any one system is not completely known and that the mechanism for any one catalyst can be different from the next. The type of catalyst, substrate and reaction conditions also contribute to the complexity and presence of any single mechanism. Fortunately, the proposed mechanism acts as an excellent starting point for a hypothesis on any ligand system. Although the mechanistic details of the Heck coupling play a vital role in the success of a catalytic system, there are other factors such as ligand and base effects that also need to be considered.

2.11.1.1 Base Effect on the Heck Reaction with Boronic Acids and Olefins

The importance of bases within palladium coupling reactions is clear when evaluating the Miyaura-Suzuki reaction.⁹⁹ The transmetallation of organoboron compounds *via* the formation of organoborate salts is facilitated by the presence of a base within these reactions. The initial aryl halides that were used in the classical Heck reaction have since been replaced by arylboronic acids. The same process will apply for the reactions investigated in this study. Although the presence of a base can facilitate the transmetallation process, there is one major disadvantage; when using reactive borate salts in the presence of bases, the formation of the homo-coupled product is seen. This can be avoided by using non-reactive borate salts or avoiding bases completely, although this could dramatically decrease the reactivity of the system.¹⁰⁰ In the absence of bases there can be a dramatic decrease of reactivity as previously mentioned, but this loss of activity can be circumvented by the use of solvents such as dimethyl acetamide and dimethyl formamide.

The use of a specific palladium salt as a starting material can also have a significant influence on the reaction time. In the system to be utilised here, investigations have revealed, in concurrence with our results, that palladium(II) chloride systems generally give very poor yields.¹⁰⁰ The reason for the observation of this phenomena can possibly be traced back to the transmetallation step, where the phenyl ring is transferred from the boron to the palladium species. It would seem that oxo species coordinated to the palladium are better at coordinating to the boron species prior to the transmetallation step. In the presence of a base, the possibility that the oxo species is deprotonated prior to this process is enhanced. This cannot occur for the chloride species. Interestingly, systems using Pd(PPh₃)₄ ligands have found that the homo-coupled product is formed as the major product rather than the desired trans-coupled species.¹⁰¹ Although the use of different bases could provide an interesting study, it was decided to keep the base constant throughout the catalysis range. 4-Methylmorpholine has earlier been identified as an effective base for Heck type reactions¹⁰² and therefore was chosen as a suitable base for this study.

⁹⁹ N. Miyaura, A. Suzuki, *Chemical Reviews*, **1995**, 95, 2457–2483.

¹⁰⁰ K. S. Yoo, C. H. Yoon, K. W. Jung, *Journal of the American Chemical Society*, **2006**, 128, 16384–16393.

¹⁰¹ Yoshida, H.; Yamaro, Y.; Ohshita, J.; Kunai, A. *Tetrahedron Letters*, **2003**, 44, 1541–1544.

¹⁰² Hsu, Chien-Ming, Li, Chih-Bin, Sun, Chia-Hsing, *Journal of the Chinese Chemical Society*, **2009**, 56, 873–880.

2.11.1.2 The Effects of Ligands on the Cross Coupling of Boron Compounds and Olefins

As mentioned in Paragraph 2.11 the presence of a ligand that can stabilise the Pd(0) that is formed through the oxidative addition step within the Heck coupling, is vital to the process. Previously phosphine,¹⁰³ N-heterocyclic carbene, NHC pincer¹⁰⁴ and palladacycle¹⁰⁵ type systems have been developed and investigated substantially. Although these systems all have the typical pros and cons, only the relevant bidentate nitrogen ligands will be discussed in the next paragraph. It is however important to illustrate the general trends that have been identified for ligands used in the Heck process.

The characteristic formation of phosphine oxides within oxidative environments for most of the phosphine systems that have been investigated are one of the major drawbacks to the conventional system. Essentially, nitrogen based ligands can perform the same function as the phosphine compounds, however not all nitrogen based systems are active. It is generally accepted that when using bidentate ligands the *cis* configuration is favoured, as it results in a more effective migratory insertion step.¹⁰⁶ By considering these factors, it can be concluded that Pd-nitrogen chelating strength, the coordination angle and the steric environment should be considered in the design process. The effects of bite angles on the Heck process has been investigated by Elsevier¹⁰⁷ by making use of the dafone ligand that is also investigated in this study. Instead of observing a classical bidentate coordination mode, a bimetallic species was identified (see Figure 2.18). Even so, in some cases, the bimetallic species still proceeded to give the desired cross-couple product in excellent yields. Another important aspect to take notice of is the formation of the homo-coupled product that is observed when using N,N,N',N'-tertramethylpropylamine and diphenylphosphonopropane as ligands.¹⁰⁷ Ultimately the use and effectiveness of nitrogen donor ligands cannot be ignored.

¹⁰³ A. M. Trzeciak, J. J. Ziółkowski, *Coordination Chemistry Reviews*, **2005**, 249, 2308–2322.

¹⁰⁴ M. Ohff; A. Ohff; M. E. van der Boom, D. Milstein, *Journal of the American Chemical Society*, **1998**, 120, 3273–3273.

¹⁰⁵ W. A. Herrmann, V. P. Böhm, C.P. Reisinger, *Journal of Organometallic Chemistry*, **1999**, 576, 23–41.

¹⁰⁶ M. Portnoy; Y. Ben-David; I. Rouso, D. Milstein, *Organometallics*, **1994**, 13, 3465–3479.

¹⁰⁷ C. J. Elsevier, *Coordination Chemistry Reviews*, **1999**, 185-186, 809–822

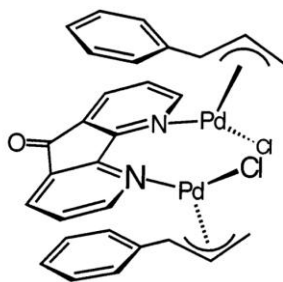


Figure 2.18: Di-metallic 4,5-diazofluorenone catalytic species identified within the Heck coupling process by Elsevier.¹⁰⁷

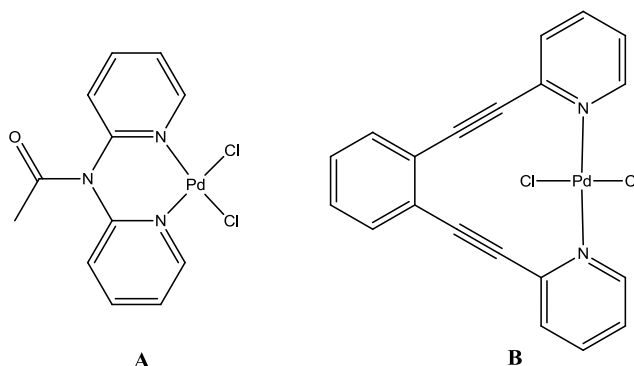
2.12 Bidentate and Nitrogen Donor Ligands as Heck Catalysts

The mechanistic workings of the Heck coupling have just been discussed but in this section some of the problems and possible solutions will be shown. One of the major drawbacks of the process in question is the precipitation of the bulk metal which is essentially inert. One of the ways this process can be prevented, or at least minimised, is through the use of bidentate amine ligands that generally result in the formation of only the cross-coupled product.¹⁰⁰ Developing the optimal conditions for the reactions of these systems typically involves choosing the correct base, starting materials and reaction temperatures. It is also important to note that nitrogen based stabilising ligand systems are only becoming more popular recently.

Although many of the phosphine and pincer ligand systems that have previously been mentioned did display substantial promise, investigations by Bushmeiser *et al.*¹⁰⁸ (A) and Kawano *et al.* (B), showed that nitrogen donor ligands also possess the necessary qualities needed to successfully stabilise palladium for Heck coupling reactions (see Scheme 2.16). Typically the nitrogen based ligands are stable and can be effectively tuned in terms of steric and electronic transformations. Although the bis(pyrimid-2-yl)amine (A) ligand did show considerable potential with Heck coupling reactions using bromo and chloro aryls, the reactions were typically performed at higher temperatures (150 °C) for 72 hours which is not ideal. The 1,2-bis(2-pyridylethynyl)benzene type ligands (B) were used to perform Heck couplings at much milder

¹⁰⁸ M. R. Buchmeiser, T. Schareina, R. Kempe, K. Wurst, *Journal of Organometallic Chemistry*, **2001**, 634, 39–46.

conditions (100 °C) and showed promising conversions after 17 hours for the iodated aryl halides, however the bromo and chloro variations took much longer.



Scheme 2.16: Nitrogen base ligands reported by Bushmeiser *et al.*¹⁰⁸ (A) and Kawano *et al.*⁹⁸ (B) used for Heck coupling.

Although the illustrated examples are very effective at completing the classical Heck coupling, another type of Heck coupling known as oxidative Heck coupling has received considerable attention as of late. This has been driven by the need for halide free systems and a large number of publications have been reported in the pursuit of this venture.^{109,110,111} These systems typically make use of transmetalation which involves the transfer of an aryl group from one metal to another, palladium in the case of Heck coupling. A number of different substrates have been investigated¹¹² but the most effective, least toxic, cheapest and readily available was found in the arylboronic acids.¹¹³ Another major advantage of the aryl boronic systems is the ability of molecular oxygen to act as the sole oxidant which eliminates the need for copper based compounds. The copper based systems tend to generate toxic heavy metal waste that is detrimental to the environment, however, one could argue that molecular oxygen is difficult to handle and scale up due to its explosive nature with organic compounds. Ideally a system that uses atmospheric air would be the best suited for safe operation and minimal environmental damage.

¹⁰⁹ J. P. Parrish, Y. C. Jung, S. I. Shin, K. W. Jung, *The Journal of Organic Chemistry*, **2002**, 67, 7127–7130.

¹¹⁰ K. Matoba, S. Motofusa, C. Sik Cho, K. Ohe, S. Uemura, *Journal of Organometallic Chemistry*, **1999**, 574, 3–10.

¹¹¹ A. Inoue, H. Shinokubo, K. Oshima, *Journal of the American Chemical Society*, **2003**, 125, 1484–1485.

¹¹² R. F. Heck, *Journal of the American Chemical Society*, **1969**, 91, 6707–6714.

¹¹³ P. A. Enquist, J. Lindh, P. Nilsson, M. Larhed, *Green Chemistry*, **2006**, 8, 338.

2.12.1 Palladium (II) 1,10-Phenanthroline Type Ligands as Heck Catalysts

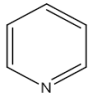
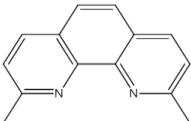
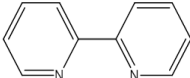
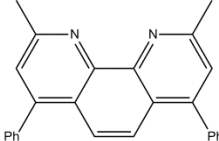
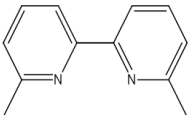
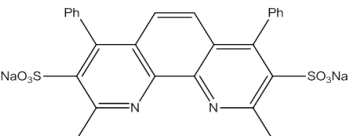
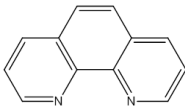
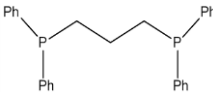
Very few Heck systems that do not require heating have been reported,¹¹³ but a system utilising 2,9-dimethyl-1,10-phenanthroline with aryl triflates operating at 40 ° C has been reported by Andappan.¹¹⁴ Yields of more than 95 % were obtained using oxygen as the sole oxidant. Although the mechanistic aspects of the phenanthroline ligands, with regards to the Heck coupling, have not been fully elucidated¹¹⁵ it has been found that phenanthroline type ligands facilitate palladium dioxygen interactions. If this phenomena can be exploited, the possibility exists that the Pd(0)/Pd(II) redox cycling can be performed at room temperature.¹¹⁶ The coupling of butyl acrylate to various boronic acids using 1,10-phenanthroline and 2,2-bipyridine type ligands was investigated by Enquist.¹¹³ The reported yields and the investigated ligands are presented in Table 2.1. From the table, one can deduce firstly that the phenanthroline and bipyridine ligands are crucial to the success of the oxidative Heck coupling as indicated by the pyridine ligands' poor performance. Although many of the reactions did take considerable time to complete, it should be taken into account that these reactions were performed at room temperature. Secondly the 2,9-dimethyl-1,10-phenanthroline showed enormous potential giving yields of 94 % within one hour. From this, one can deduce that the electronic configuration of the phen type ligands is essential in determining the effectiveness of the catalysts. This is confirmed by the poor performance of the 2,9-dimethyl-4,7-diphenyl-1,10-phenanthroline ligand.

¹¹⁴ M. M. S. Andappan, P. Nilsson, H. von Schenck, M. Larhed, *The Journal of Organic Chemistry*, **2004**, 69, 5212–5218.

¹¹⁵ J. M. Keith, R. J. Nielsen, J. Oxgaard, W. A. Goddard, *Journal of the American Chemical Society*, **2005**, 127, 13172–13179.

¹¹⁶ G. T Brink, I. Arends, R. A. Sheldon, *Science*, **2000**, 287, 1636–1639.

Table 2.1: Comparison of ligands, time and % yield reported by Enquist.¹¹³

Ligand	Time/hrs	Yield	Ligand	Time/hrs	Yield
	144	0		1	94
	12	73		72	35
	15	75		8	87
	48	39		12	77

Reactions condition: Open vessel charged with p-tolyboronic acid (2.0 mmol), n-butyl acrylate (1.0 mmol), N-methylmorpholine (2.0 mmol), Pd(OAc)₂ 0.02 mmol, ligand (0.048 mmol) with rapid stirring.

3 PLANAR DIAMIDE BUILDING BLOCKS

3.1 Introduction

Due to the massive amount of available pyridine-, pyrimidine-, phenanthroline type ligands and other building blocks for larger ligand systems, a vast number of possible bridging ligands can be constructed. Furthermore, the properties of the linking species can be adjusted and tuned as required for specific purposes. There are some properties that are of specific interest for this project which include; charge transfer between linked mono or bimetallic metal species, mechanical strength, relatively low cost and good monolayer forming abilities. As a result, the ligand backbones were chosen in such a way that multiple metal species can be accommodated and that a conjugated electronic environment could be created between linked metal centres. The addition of more specific properties of bridging ligands is not always possible because of the difficulty of synthesising the desired compounds. In order to minimise the search amongst the vast number of possibilities, pyromellitic (A), naphthalenetetracarboxylic (NTCDA) (B) and perylenetetracarboxylic dianhydride (PTCDA) (C) backbones were identified as possible planar moieties, with a conjugated electronic configuration, which could provide the desired bridging ligand characteristics (see Figure 3.1).

The differences in size between the different compounds also determine the distance between metal centres. The possible functionalization and properties of these compounds have been discussed in Paragraph 2.6 and Paragraph 2.7. It is important to note, that although some reactions were performed with the PTCDA backbone, the majority of the work focused on the pyromellitic and NTCDA backbones due to solubility problems with the former.

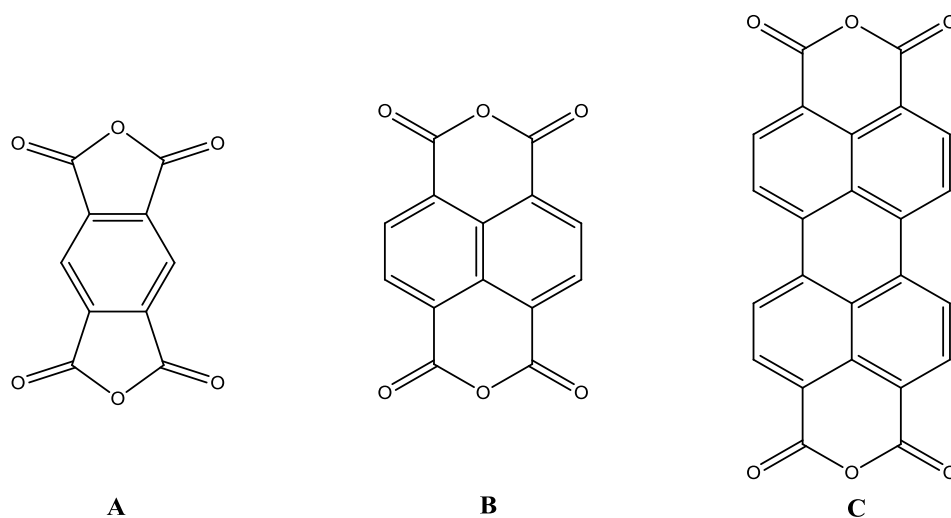
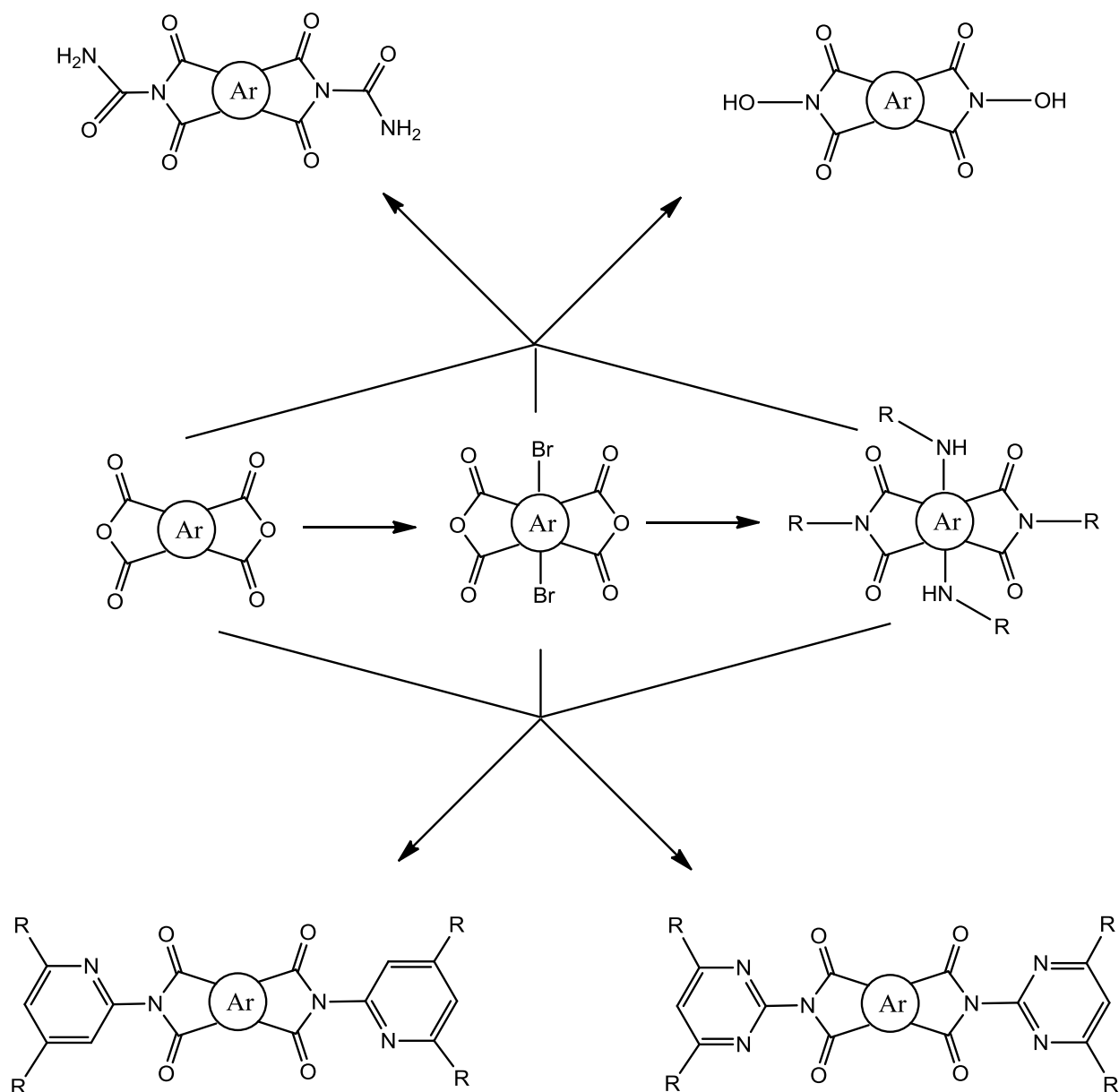


Figure 3.1: Graphical illustration of the pyromellitic(A), naphthalene and (B) perylene (C) backbones.

The general reaction scheme that was followed in the synthesis of these potential bridging ligands is shown in Scheme 3.1. As previously mentioned, there are two possible pathways that can be followed in the design of these bridging ligands. The one pathway involves functionalising the various backbones to accommodate a charge on the ligand, which can then facilitate the coordination of charged metal species such as palladium and platinum. The top half of Scheme 3.1 shows the strategies used to create bridging ligands that can accommodate two or four metal centres. The second approach involves the introduction of pyridine- and pyrimidine ligands on the terminal rings to create ligands that, once again, can accommodate two and four metal centres, although the coordination mode will be purely non-ionic. The R-groups on the pyridine/pyrimidine rings can also be used to control the electron density of the coordinating nitrogen atoms. The central part of the scheme indicates the bromination of these compounds, which was performed to increase the solubility of these species. The bromine atoms can also be aminated to form bridging type compounds. Unfortunately, the bromination process also has a number of drawbacks. The loss of protons destroys the ability to characterise the resulting complexes using NMR techniques, and the bromine atoms alter the electronic environment of the ligands in such a way that the condensation reactions do not yield the desired compounds.



Scheme 3.1: Systematic functionalization of various backbones used in the construction of potential bridging ligands (Ar = pyromellitic and naphthalene).

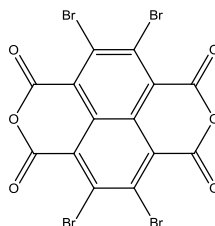
The resulting ligands were reacted with palladium acetate, palladium chloride and Zeise's salt to investigate the coordinating capabilities of these ligands. The catalytic properties of the subsequent palladium complexes will be discussed in Chapter 7.

3.2 Chemicals and Apparatus

All reagents utilised for the synthesis of compounds were of analytical grade and were purchased from Sigma-Aldrich, South Africa. Reagents were used as received without further purification. All experiments were performed in air unless otherwise stated. Infrared spectra of the complexes were recorded on a Bruker Tensor 27 Standard System ATR spectrophotometer with a laser range of $4000 - 370 \text{ cm}^{-1}$. Data was collected at ambient temperatures in the air and reported in cm^{-1} . The ^1H NMR data was obtained from a Bruker 300 MHz spectrometer using the mentioned deuterated solvent. ^{13}C NMR data was obtained from a Bruker 600 MHz. All chemical shifts (δ) are reported in ppm using ^1H -TMS as an internal standard. Coupling constants (J) are reported in Hertz. The powder products that were collected from the reported synthetic procedures were air dried with mild heating. The yields reported for products were reported under the assumption that all solvents were removed in the drying process. The crystal structures obtained are discussed in Chapter 5 and Chapter 6.

3.3 Organic Bridging Ligands

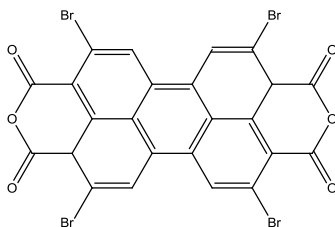
3.3.1 4,5,9,10-Tetrabromo-naphtho-isochromene-1,3,6,8-tetraone



The title compound was synthesised according to the published procedure.¹ Naphthalene-1,4,5,8-tetracarboxylic acid dianhydride (1.0 g, 3.75×10^{-3} mol), sodium bromide (1.7 g, 16.6×10^{-3} mol) and fuming sulphuric acid (25 ml) were introduced into a reactor and heated to 180°C for six hours. The reaction mixture was added to ice water and filtered. The product was obtained as a yellow powder. Yield: 1.6 g, 74 %. ^1H NMR (300 MHz, DMSO): no proton signal was observed. ^{13}C NMR (150 MHz, DMSO): 159.92 (s), 137.49 (s), 132.18 (s), 125.09 (s). IR (ATR): 1778 ($\nu_{\text{C-O}}$).

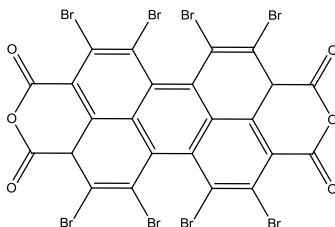
¹ T. D. M. Bell, S. Yap, C. H. Jani, S. V. Bhosale, J. Hofkens, F. C. De Schryver, S. J. Langford, and K. P. Ghiggino, *Chemistry - An Asian Journal*, **2009**, 4, 1542–1550.

3.3.2 4,7,11,14-Tetrabromoanthra[2,1,9-def:6,5,10-d'e'f']diisochromene-1,3,8,10(3aH,10aH)-tetraone



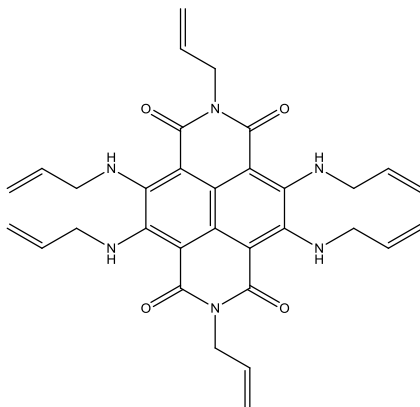
The title compound was synthesised by modifying the published procedure¹. Perylenetetracarboxylic anhydride (1.0 g, 2.5×10^{-3} mol), sodium bromide (1.16 g, 12.0×10^{-3} mol) and fuming sulphuric acid (25 ml) were added to a reactor and heated to 180 °C for six hours. The reaction mixture was added to ice water and filtered. The product was obtained as a dark red powder. Yield: 1.0 g, 56 %. ¹H NMR (300 MHz, DMSO): 7.17 (s, 1H). ¹³C NMR (150 MHz, DMSO): 157.55 (s), 134.67 (s), 133.99 (s), 131.58 (s), 129.21 (s), 128.76 (s), 120.32 (s). IR (ATR): 1772 ($\nu_{C=O}$) 1736.43 ($\nu_{C=O}$).

3.3.3 4,5,6,7,11,12,13,14-Octabromoanthra[2,1,9-def:6,5,10-d'e'f']diisochromene-1,3,8,10(3aH,10aH)-tetraone



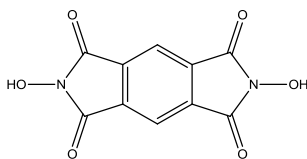
The title compound was synthesised by modifying the published procedure¹. Perylenetetracarboxylic anhydride (1.0 g, 2.5×10^{-3} mol), sodium bromide (2.4 g, 24.0×10^{-3} mol) and fuming sulphuric acid (25 ml) were placed in a reactor and heated to 180 °C for six hours. The reaction mixture was added to ice water and filtered. The product was obtained as a reddish purple powder. Yield: 2.1 g, 83 %. ¹H NMR (300 MHz, DMSO): no proton signal was observed. ¹³C NMR (150 MHz, DMSO): 156.76 (s), 134.09 (s), 133.20 (s), 131.58 (s), 128.58 (s), 127.87(s), 120.68 (s). IR (ATR): 1780 ($\nu_{C=O}$).

3.3.4 2,7-Diallyl-4,5,9,10-tetrakis(allylamino)benzo [lmn][3,8]phenanthroline-1,3,6,8(2H,7H)-tetraone



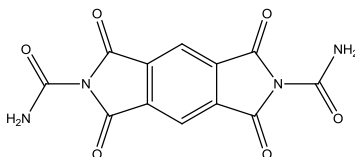
The title compound was synthesised according to the published procedure. Tetrabromonaphthalene-1,4,5,8-tetracarboxylic acid dianhydride (0.20 g, 3.45×10^{-4} mol) was dissolved in DMF. To this allylamine (2 ml, excess) was added. The solution was stirred overnight. The addition of excess water resulted in a dark brown powder which was filtered and washed with diethyl ether. Yield: 0.087 g, 44 %. ^1H NMR (300 MHz, DMSO): δ 5.93 (dd, $J = 16.6, 11.1, 5.2$ Hz, 6H), 5.38 – 5.05 (m, 12H), 4.08 (d, 4H), 3.45 (d, $J = 5.8$ Hz, 8H). IR (ATR): 1795 ($\nu_{\text{C=O}}$).

3.3.5 2,6-Dihydroxypyrrolo[3,4-f]isoindole-1,3,5,7(2H,6H)-tetraone (pyro-hydroxylamine)



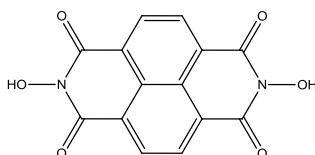
Pyromellitic anhydride (0.50 g, 2.29×10^{-3} mol) and hydroxylamine (0.160 g, 4.6×10^{-3} mol) were refluxed in acetic acid for three hours and allowed to cool down. The turbid solution was filtered and washed with a small amount of water. Light yellow crystals suitable for X-Ray diffraction were afforded after being left in the fume hood for one day. The crystal structure of the above compound is discussed in Paragraph 5.3.2. Yield: 0.32 g, 56 %. ^1H NMR (300 MHz, DMSO): 11.18 (s, 2H), 8.16 (s, 2H). ^{13}C NMR (150 MHz, DMSO): 162.97 (s), 134.69 (s), 117.45 (s). IR (ATR): 2719 ($\nu_{\text{O-H}}$), 1707 ($\nu_{\text{C=O}}$).

3.3.6 1,3,5,7-Tetraoxo-5,7-dihydropyrrolo[3,4-f]isoindole-2,6(1H,3H)-dicarboxamide (pyro-urea)



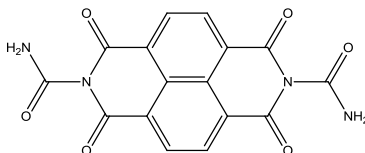
Pyromelletic anhydride (0.50 g, 2.29×10^{-3} mol) and urea (0.285 g, 4.75×10^{-3} mol) were ground together with a mortar and pestle. THF (50 ml) was added to the mixture and the solution was placed in a sonic bath for thirty minutes and thereafter refluxed for thirty minutes. The white powder was filtered and washed with diethyl ether. Yield: 0.357 g, 51 %. ^1H NMR (300 MHz, DMSO): 8.14 (s, 2H), 5.7 (s, 2H). ^{13}C NMR (150 MHz, DMSO): 167.87 (s), 160.26 (s), 135.10 (s), 129.04 (s). IR (ATR): 3462 ($\nu_{\text{N-H}}$), 1688 ($\nu_{\text{C=O}}$), 1617 ($\nu_{\text{C=O}}$), 1253 ($\nu_{\text{C-N}}$).

3.3.7 2,7-Dihydroxybenzo[lmn][3,8]phenanthroline-1,3,6,8(2H,7H)-tetraone (naph-hydroxylamine)



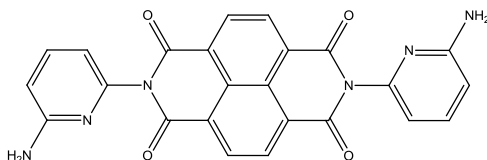
The title compound was prepared according to a published procedure. Naphthalene-1,4,5,8-tetracarboxylic acid dianhydride (0.50 g, 1.87×10^{-3} mol), hydroxylamine (0.272 g, 3.74×10^{-3} mol) and sodium carbonate were added to water and was refluxed for three hours. The solution was filtered and redissolved in water and the pH adjusted to pH 2 using a 1 M HCl solution. The resulting pale yellow precipitate was filtered and washed with cold water. Yield: 0.21 g, 37 %. ^1H NMR (300 MHz, DMSO): δ 11.04 (s, 2H), 8.69 (s, 4H). ^{13}C NMR (150 MHz, DMSO): 160.55 (s), 131.11 (s), 127.35 (s), 125.79.

3.3.8 1,3,6,8-Tetraoxo-6,8-dihydrobenzo[lmn][3,8]phenanthroline-2,7(1H,3H)-dicarboxamide (naph-urea)



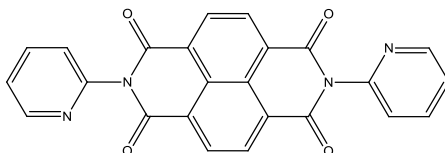
The title compound was prepared by dissolving naphthalene-1,4,5,8-tetracarboxylic acid dianhydride (0.50 g, 1.87×10^{-3} mol) in hot DMF and urea (2.0 g, 1×10^{-3} mol) was added to it. The solution was stirred at 110 °C for twelve hours. An off-white precipitate was filtered off upon cooling and washed with diethyl ether. Yield: 0.325 g, 50 %. ^{13}C NMR (150 MHz, DMSO): 163.48 (s), 160.22 (s), 132.24 (s), 128.24 (s), 124.24 (s). IR (ATR): 3074 ($\nu_{\text{N-H}}$), 1678 ($\nu_{\text{C-O}}$), 1266 ($\nu_{\text{C-N}}$).

3.3.9 7-Bis(6-aminopyridin-2-yl)benzo[lmn][3,8]phenanthroline-1,3,6,8(2H,7H)-tetraone



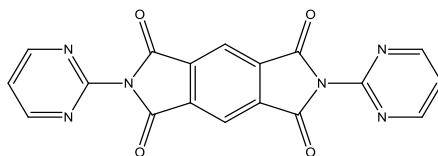
The title compound was prepared by reacting naphthalene-1,4,5,8-tetracarboxylic acid dianhydride (0.50 g, 1.87×10^{-3} mol) with 2,6-diaminopyridine (0.410 g, 3.7×10^{-3} mol) in DMSO at 145 °C for twenty four hours. A golden-yellow powder was obtained. Yield: 0.157 g, 18 %. ^1H NMR (600 MHz, DMSO): δ 8.72 (s, 4H), 7.65 – 7.55 (m, 2H), 6.66 (d, $J = 7.1$ Hz, 2H), 6.56 (d, $J = 8.3$ Hz, 2H), 6.21 (s, 4H). ^{13}C NMR (150 MHz, DMSO): 162.96 (s), 160.80 (s), 147.68 (s), 139.39 (s), 131.00 (s), 127.30 (s), 127.25 (s), 111.36 (s), 108.70 (s). IR (ATR): 3349. ($\nu_{\text{N-H}}$), 1703 ($\nu_{\text{C-O}}$), 1468 ($\nu_{\text{C-N}}$).

3.3.10 *N,N'*-Bis(2-pyridyl)naphthalene-3,4:7,8-di-carboximide (dpbpt)



The title compound was prepared by reacting naphthalene-1,4,5,8-tetracarboxylic (0.50 g, 1.87×10^{-3} mol) with 2-aminopyridine (0.410 g, 3.7×10^{-3} mol) in DMSO at 145 °C for twenty four hours. A pale white powder was obtained. Crystals were grown from DMSO in the fume hood. The crystal structure is discussed in Paragraph 5.3.3. Yield 0.325 g, 41 %. ^1H NMR (600 MHz, DMSO): 8.75 (s, 4H), 8.69 (dd, $J = 4.9, 1.2$ Hz, 2H), 8.10 (td, $J = 7.7, 1.9$ Hz, 2H), 7.66 (d, $J = 7.8$ Hz, 2H), 7.60 (ddd, $J = 7.5, 4.9, 0.9$ Hz, 2H). ^{13}C NMR (150 MHz, DMSO): 163.22 (s), 150.01 (s), 149.61(s), 139.43 (s), 131.13 (s), 127.40 (s), 127.32 (s), 125.03 (s), 124.86 (s). IR (ATR): 1713 ($\nu_{\text{C-O}}$), 1251 ($\nu_{\text{C-N}}$), 751 ($\nu_{\text{Ar-H}}$).

3.3.11 2,6-Di(pyrimidin-2-yl)pyrrolo[3,4-f]isoindole-1,3,5,7(2H,6H)-tetraone (pyro-pyrimidine)



Pyromellitic anhydride (0.50 g, 2.3×10^{-3} mol) and 2-aminopyrimidine (0.48 g, 4.5×10^{-3} mol) were stirred in THF for four hours and then heated to 70 °C for thirty minutes. Excess acetone was added to afford a white powder after filtration. Yield: 0.41 g, 60 %. ^1H NMR (300 MHz, MeOD): 8.30 (d, $J = 4.9$ Hz, 2H), 8.14 (s, 1H), 6.69 (t, $J = 4.9$ Hz, 1H). ^{13}C NMR (150 MHz, DMSO): 167.81 (s), 163.31 (s), 158.39 (s), 135.19(s), 129.57 (s), 110.55(s). IR (ATR): 1669 ($\nu_{\text{C-O}}$), 1494 ($\nu_{\text{C-N}}$), 857 ($\nu_{\text{Ar-H}}$).

3.4 Bridged Metal Complexes

The coordination of palladium chloride or palladium acetate to various bidentate ligands such as 2,2'-bipyridine occurs very quickly. The addition of the metal precursor to the ligand is usually followed by the rapid formation of a yellow precipitate. Most of the organic bridging ligands that have been synthesised in the previous paragraphs have some solubility problems without having any metal species coordinated to it. This problem is enhanced when these compounds are coordinated to palladium acetate, although the same yellow precipitate is observed upon the addition of the metal to the ligand. The resulting precipitate, however, is extremely insoluble in most organic solvents. As a result, the characterisation of these compounds becomes a problem. Poor NMR spectrums were obtained and gave some indication as to what product formed. Other techniques such as MS and elemental analysis were performed to try and determine how many palladium species coordinate to these compounds. Although the characterisation of these compounds is poor, the observed reaction conditions and characterisation of these compounds are reported in the following paragraphs. An 'x' is used to designate the number of palladium species that are coordinated.

3.4.1 [Pd(OAc)₂(pyro-hydroxylamine)]

Pd(OAc)₂ (0.020 g, 8.9×10^{-5} mol) was dissolved in DMF (2 ml). To this pyro-hydroxylamine (0.022 g, 8.9×10^{-5} mol) was added and slightly heated to 60 °C. This resulted in the formation of a dark ruby red solution. The solvent was evaporated to produce a red powder. Yield: 0.019 g, 45 %. IR (KBr): 3455 ($\nu_{\text{O-H}}$), 1778 ($\nu_{\text{C-O}}$), 1694 ($\nu_{\text{C-O}}$), 1582 ($\nu_{\text{C-O}}$), 1394 ($\nu_{\text{C-N}}$).

3.4.2 [Pd₂(OAc)₄(pyro-hydroxylamine)]

Pd(OAc)₂ (0.020 g, 8.9×10^{-5} mol) was dissolved in DMF (2 ml). To this pyro-hydroxylamine (0.011 g, 4.45×10^{-5} mol) was added and slightly heated to 60 °C. This resulted in the formation of a ruby red solution. The solvent was evaporated to produce a dark red powder. Yield: 0.017 g, 54 %. IR (KBr): 3442 ($\nu_{\text{O-H}}$), 1780 ($\nu_{\text{C-O}}$), 1697 ($\nu_{\text{C-O}}$), 1402 ($\nu_{\text{C-N}}$).

3.4.3 [Pd(OAc)₂(naph-hydroxylamine)]

Pd(OAc)₂ (0.020 g, 8.9×10^{-5} mol) was dissolved in DMF (2 ml). To this naph-hydroxylamine (0.0260 g, 8.9×10^{-5} mol) was added and slightly heated to 60 °C. This resulted in the formation of a ruby red solution. Yield: 0.031 g, 65 %. IR (KBr): 3389 ($\nu_{\text{N-H}}$), 1601 ($\nu_{\text{C=O}}$), 1694 ($\nu_{\text{C=O}}$), 1582 ($\nu_{\text{C=O}}$), 1394 ($\nu_{\text{C-N}}$).

3.4.4 [Pd(OAc)₂(pyro-urea)]

Pd(OAc)₂ (0.020 g, 8.9×10^{-5} mol) was dissolved in DMF (2 ml). To this solution, pyro-urea (0.0270 g, 8.9×10^{-5} mol) was added and slightly heated to 60 °C. This resulted in the formation of a yellow precipitate. The yellow precipitate was filtered and dried. Yield: 0.041g, 87 %. ¹H NMR (600 MHz, DMSO): 7.90 (s, 2H), 7.25 – 6.84 (m, 2H), 1.89 (d, $J = 107.3$ Hz, 1H). IR (KBr): 3389 ($\nu_{\text{N-H}}$), 1610 ($\nu_{\text{C=O}}$), 1474 ($\nu_{\text{C=O}}$), 1355 ($\nu_{\text{C-N}}$).

3.4.5 [Pd₂(OAc)₄(pyro-urea)]

Pd(OAc)₂ (0.020 g, 8.9×10^{-5} mol) was dissolved in DMF (2 ml). To this solution, pyro-urea (0.0130 g, 4.45×10^{-5} mol) was added and slightly heated to 60 °C. This resulted in the formation of a yellow-orange precipitate. The yellow-orange precipitate was filtered and dried. Yield: 0.024 g, 73 %. ¹H NMR (600 MHz, DMSO): 7.86 (s, 2H), 7.18 – 6.64 (m, 2H), 1.76 (s, 3H). IR (KBr): 3432 ($\nu_{\text{N-H}}$), 1614 ($\nu_{\text{C=O}}$), 1364 ($\nu_{\text{C-N}}$).

3.4.6 [Pd₄(OAc)₈(pyro-urea)]

Pd(OAc)₂ (0.020 g, 8.9×10^{-5} mol) was dissolved in DMF (2 ml). To this solution, pyro-urea (0.007 g, 2.23×10^{-5} mol) was added and slightly heated to 60 °C. This resulted in the formation of an orange precipitate. The orange precipitate was filtered and dried. Yield: 0.013 g, 48%. IR (KBr): 3448 ($\nu_{\text{N-H}}$), 1576 ($\nu_{\text{C=O}}$), 1370 ($\nu_{\text{C-N}}$).

3.4.7 [Pd(OAc)₂(pyro-pyrimidine)]

Pd(OAc)₂ (0.020 g, 8.9×10^{-5} mol) was dissolved in DMF (2 ml). To this solution, pyro-pyrimidine (0.0330 g, 8.9×10^{-5} mol) was added and slightly heated to 60 °C. This resulted in the formation of a light yellow precipitate. The light yellow precipitate was filtered and dried. Yield: 0.048 g, 90 %. ¹H NMR (600 MHz, DMSO): δ 8.84 – 8.09 (m, 7H), 7.88 (d, $J = 21.4$ Hz, 8H), 6.74 (d, $J = 124.6$ Hz, 1H), 2.00 – 1.61 (m, 2H). IR (ATR): 1580 (ν_{C-O}), 1362 (ν_{C-N}), 803 (ν_{Ar-H}).

3.4.8 [Pd₂(OAc)₄(pyro-pyrimidine)]

Pd(OAc)₂ (0.020 g, 8.9×10^{-5} mol) was dissolved in DMF (2 ml). To this solution, pyro-pyrimidine (0.0165 g, 4.45×10^{-5} mol) was added and slightly heated to 60 °C. This resulted in the formation of a yellow precipitate. The yellow precipitate was filtered and dried. Yield: 0.020 g, 77 %. ¹H NMR (300 MHz, DMSO): 9.10 (d, $J = 4.8$ Hz, 2H), 8.50 (s, 1H), 8.21 (d, $J = 4.8$ Hz, 2H), 7.75 (t, 1H, $J = 4.8$ Hz), 6.58 (m, 2H), 6.54 (t, 1H), 1.77 (m, 6H). IR (ATR): 1559 (ν_{C-O}), 1361 (ν_{C-N}), 758 (ν_{Ar-H}).

3.4.9 [Pd₄(OAc)_x(pyro-pyrimidine)]

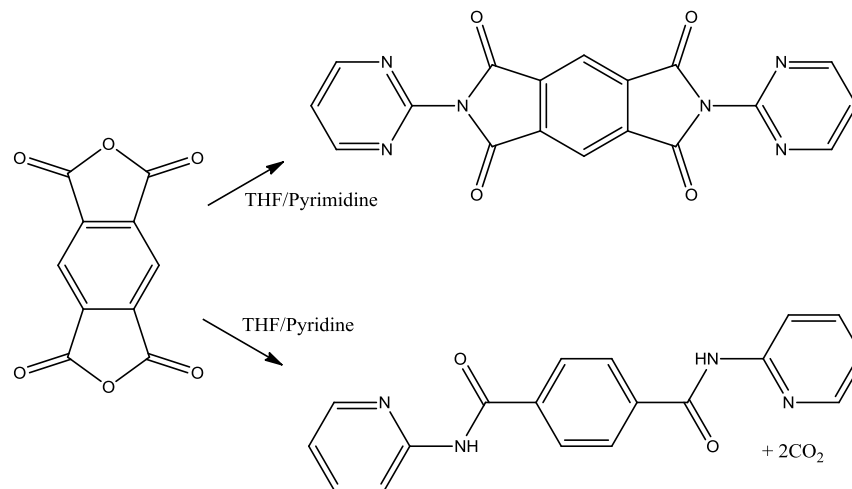
Pd(OAc)₂ (0.020 g, 8.9×10^{-5} mol) was dissolved in methanol (25 ml). To this solution, pyro-pyrimidine (0.0080 g, 2.23×10^{-5} mol) was added and slightly heated to 60 °C. This resulted in the formation of a light yellow powder that was filtered and dried. Yield: 0.018 g, 64 %. ¹H NMR (300 MHz, DMSO): 8.31 (s, 6H), 7.84 (d, $J = 14.9$ Hz, 2H), 6.71 (s, 1H), 1.75 (d, $J = 17.4$ Hz, 4H). IR (ATR): 1593 (ν_{C-O}), 1365 (ν_{C-N}), 818 (ν_{Ar-H}).

3.5 Discussion

The bromination of the NTCDA and PTCDA backbones was attempted as they are the more insoluble species. Although the bromination is carried out under harsh conditions, the resulting compounds do have improved solubility. Bell *et al.*¹ developed the methodology to selectively brominate these compounds with a selected number of bromine atoms. As previously mentioned, there are some drawbacks to the bromination process. These compounds are already difficult to characterise and the introduction of bromine results in the loss of protons from which valuable NMR information is obtained. The electronic environment of these bromine species also differs from the backbone in such a way that the nucleophilic addition reactions that proceed without problems when using NTCDA are difficult to perform after the bromination of the ligands. The bromine species also tend to be less stable than the starting backbones and do decompose over time. The PTCDA backbone was also brominated in a similar fashion, but the same problems were encountered when trying to further functionalise the compounds. The large molecular mass of the bromine atoms also creates problems when attempting to utilise MS for characterisation purposes. The only successful reactions that were performed with these brominated compounds were the amination reaction using allylamine. The double bond in this compound increases the nucleophilicity of the nitrogen species in such a way that the reaction is able to proceed in DMF. There were further problems with the tetraallylamine substituted species, and although the complete aminated product could be isolated the yields were poor. This could be due to multiple product formation as well as side reactions.

Due to the poor range of results obtained for the brominated species, further attention was not paid to these compounds and subsequently was not reported. In-depth reaction tailoring could probably reduce some of these problems and due to the increased solubility the brominated backbones could be used to investigate the mechanism of metal bonding further if proper characterisation methods could be developed. The majority of reactions performed for this part of the project were done using the pyromellitic and NTCDA backbones, which showed some very interesting differences in reactivities. When using the pyromellitic dianhydride the bipyrimidine type bridging ligands could be isolated quite easily under the correct reaction conditions, although it was much harder to obtain the pyridine species. The reactions were

performed under the same conditions but very different results were obtained. An NMR investigation indicated the following reaction mechanism (see Scheme 3.2).



Scheme 3.2: Different products obtained when reacting pyromellitic anhydride with pyridine and pyrimidine under the same reaction conditions.

This phenomenon is probably caused by the difference in basicity of the pyridine and pyrimidine ligands, as shown by the differences in pK_a values which were 5.6 and 1.24 respectively. Similar problems were encountered when using the methoxy- and chloro- substituted pyrimidines. Reactions were also performed in acidic mediums to try and minimise this effect but the isolation of the desired compounds remained challenging. The opposite was found when looking at the NTCDA backbone. The pyridine and pyrimidine reactions were performed under identical reaction conditions but gave different results. The pyridine compounds of the NTCDA backbone could be isolated; however, none of the pyrimidine analogues could be obtained. It was concluded that the solvent, acidic or basic environment and the electron donor capabilities of the substituents on the pyridine/pyrimidine rings play a vital role in the nucleophilicity, reactivity and synthesis of these compounds.

Although different challenges were encountered with the synthesis of the potential bridging systems, some interesting ligands, which have the geometric ability to coordinate to two or four metal species, were successfully synthesised and characterised. The coordination of various metal species to similar compounds has already been discussed, even though the particular coordination mode to the selected metal species has been investigated to a lesser extent than other bidentate systems. Based on this information, one would expect these ligands to form the

desired bridging complexes fairly easily. However, significant challenges were encountered with characterisation of compounds that were formed.

As mentioned in Paragraph 3.4, the reactions performed using the bridging ligands and palladium behaved in a similar fashion as well known ligands, such as 2,2-bipyridine and 1,10-phenanthroline, when evaluated visually. Unfortunately visual observations may provide an indication that a reaction is happening but gives very little conclusive and scientific proof that the observed reaction was successful. Varied mol amounts were added to the ligands which resulted in different coloured precipitates; this suggests that there could be a different number of palladium species coordinated in each case. It could also be argued that the different ligand concentrations could also account for the colour changes.

The most valuable tool in the characterisation of these compounds was ultimately NMR. Due to the fact that the compounds are symmetrical before the coordination of metal species, the coordination of one metal ion to the ligand would destroy this symmetry and a shift in NMR peaks would reflect this process. The coordination of two or four metal ions would restore the symmetry, and by simply applying the shielding/de-shielding principle one should be able to distinguish whether two or four metal species are coordinated by these ligands.

One factor that was not taken into account in the design of these dianhydride bridging compounds was the HSAB theory. When coordinating these ligands to a soft palladium moiety, the ligands act as a base which donates electron density to the acidic metal species. Due to the conjugated nature of the bridging ligands, the coordination of the first metal to the ligand, affects the electronic characteristics of the rest of the molecule and also the basicity of the next coordinating atom. Essentially, the coordinating sites for metal species on the synthesised ligands could lie far enough apart to prevent the coordination of the second and third metal ion. However, there is a third anomaly that also affects the coordination ability of the next incoming metal species, namely solubility. As mentioned before, the resulting precipitates from the coordination of metals species to these ligands, excluding the hydroxylamine functionalities, are extremely insoluble which suggests that further coordination is prevented by coordination of the first metal species which then subsequently yields insoluble complexes. The NMR peaks observed for the pyro-pyrimidine species strongly suggests that a single palladium centre is coordinated to the ligand. The only solvents that can be used to keep these compounds in a 'semi'-soluble state are DMF and DMSO, which are extremely basic. This creates further

problems as these basic solvents can compete with ligands i.e. the metal species are stabilised by these solvents in such a way that it is not able to coordinate further to the bridging ligands, which are obviously present in a much lower concentrations.

As a result of the above-mentioned factors, the positive characterisation of a bridged complex could not be achieved successfully. The compounds that were obtained were analysed by NMR and MS, but none of these techniques were sufficient enough to identify the desired compounds unequivocally. The major reason is simply the solubility and large molar mass of the compounds. Bridged complexes using almost identical compounds have been reported^{2,3,4} which strongly suggests that these ligands have the capability to be used as bridging spacers within heterogeneous catalysis. Unfortunately within the time frame of this PhD project, the desired compounds could not be characterised completely. Due to the problems that were encountered with regards to the coordination of the desired metal species, it was undertaken to modify ligands like 1,10-phenanthroline, of which the coordination is well understood, in such a manner to link the ligands together to form bridging spacers that could accommodate more than one metal centre.

² P. Venugopal, V. Ravinder, and P. Lingaiah, *Journal of Chemical Sciences*, **1992**, 104, 1–8.

³ O. V. Kovalchukova, O. A. Tsegel'nik, P. V. Strashnov, B. E. Zaitsev, S. B. Strashnova, O. V. Volyanski, and K. E. Kobrakov, *Russian Journal of Inorganic Chemistry*, **2010**, 55, 709–713.

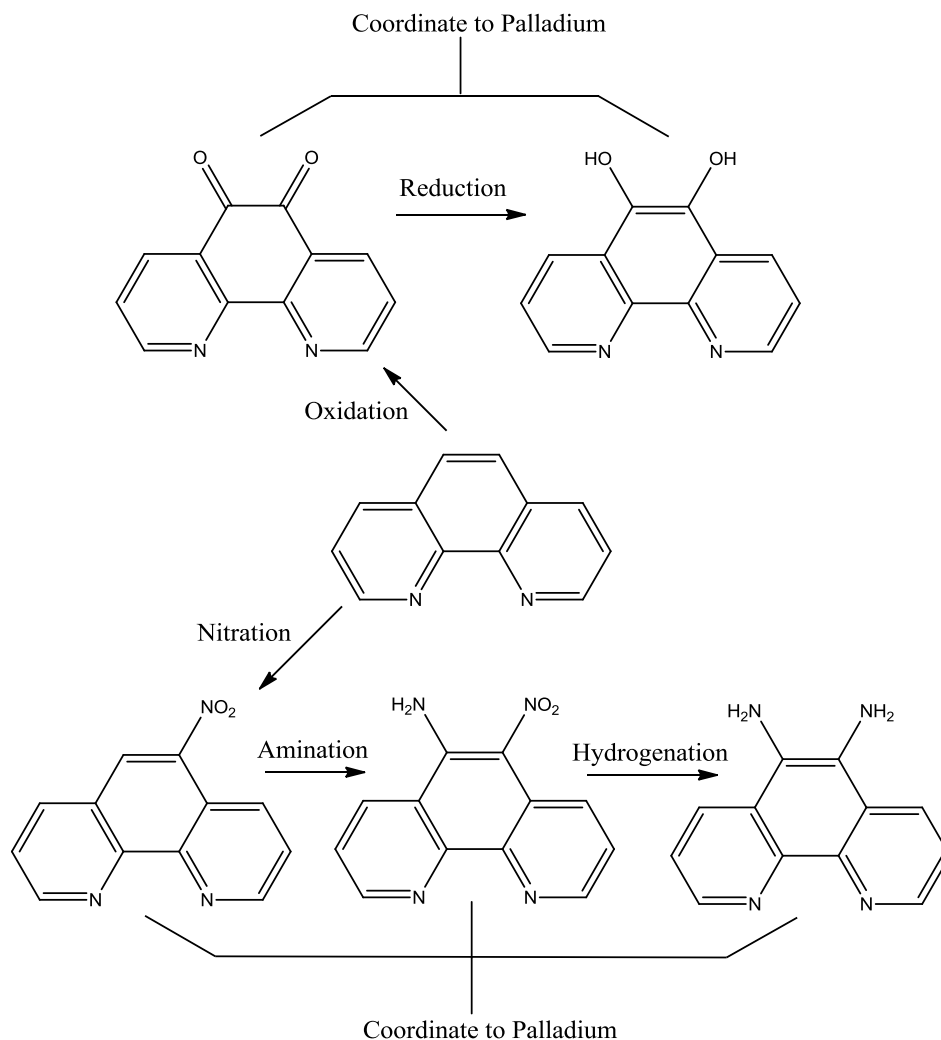
⁴ L. Xu, Y.-Z. Li, X.-T. Chen, and X.-X. Ji, *Acta Crystallographica Section E Structure Reports Online*, **2004**, 60, m769–m770.

4

**1,10-PHENANTHROLINE
BASED SYNTHONS****4.1 Introduction**

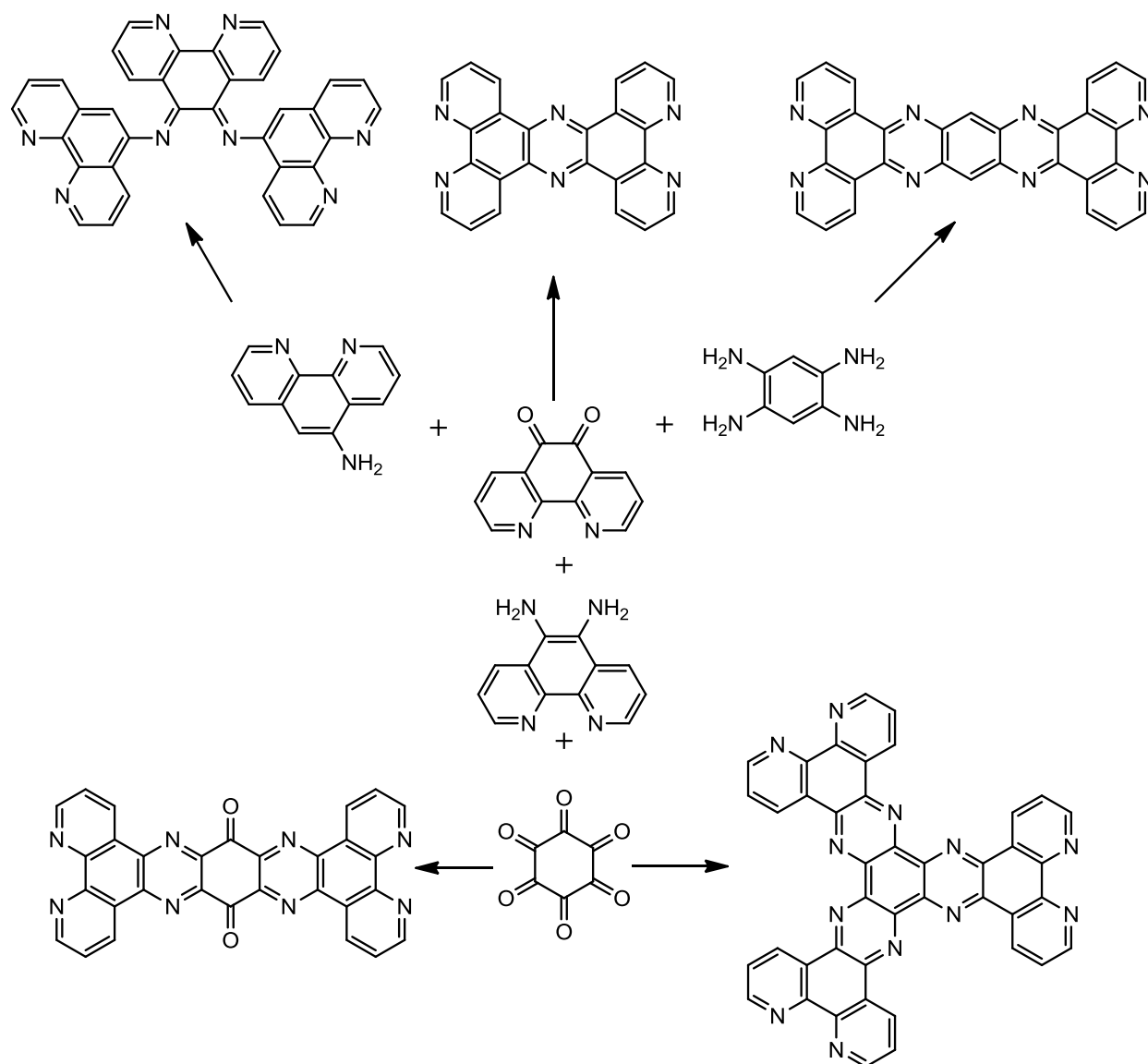
In Chapter 3 the design and synthesis of potential planar bridging ligands that can accommodate one to four metal centres were discussed and synthesised. However, the majority of these ligands assumed a rather unknown diamide coordination mode and although previous compounds of this nature had been reported, the isolation of these species remained difficult. As a result of complexities, lack of characterisation of the palladium complexes and the poor solubility of the diamide backbone, it was therefore decided to design planar bridging ligands using 1,10-phenanthroline (phen) based ligand structures.

The coordination mode and chemistry of phen have been extensively studied for most of the transition metal series. By constructing these bridging ligands using the available building blocks that were discussed in Chapter 2, in theory one would be able to synthesise a fairly general bridging ligand that could accommodate a range of metal centres. Other compounds like 4,5-diazafluoren-9-one (dafone), 2,2'-bipyrimidine and 5-amino-1,10-phenanthroline were also incorporated to investigate the coordination of metals in bridged structures and as synthons for ligand construction. Other ligands that have a similar structure as phen were synthesised, although the coordination ability of the ligands towards metal centres such as platinum and palladium were limited. Essentially, three different pathways were followed as a guideline towards the synthesis of the desired compounds. First, phen was functionalised in such a manner that it could act as a synthon for larger bridging ligands and also act as a bridging ligand without further modifications. The synthetic routes to bridging synthons and palladium complexes that were followed are presented in Scheme 4.1. The oxo and amine functionalizations both create different coordinating environments that can in principle be exploited in the synthesis of multiple metal centre compounds.



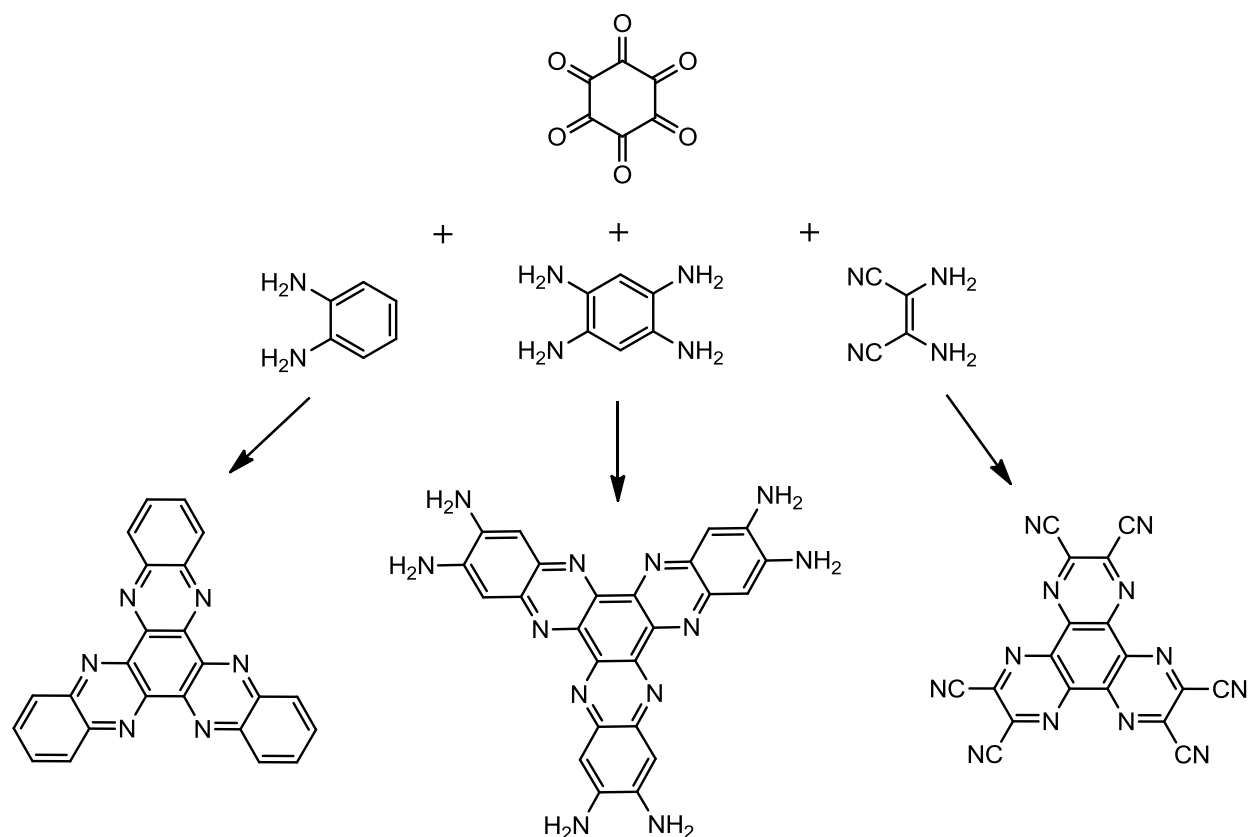
Scheme 4.1: Synthetic pathway followed for the synthesis of bridging synthons and the coordination to palladium centres based on the phen framework.

The successful synthesis of the 5,6-diamine-1,10-phenanthroline (phendiamine) and 5,6-diketone-1,10-phenanthroline (phendione) was fundamental to obtaining the desired compounds. Phendione could be combined with other diamine ligands such as 1,2-phenylene diamine and benzene tetramine, but there are limitations to the number of different combinations which could be synthesised. Once these synthons were obtained, further reactions using condensation methods could be used to construct the bridging compounds displayed in Scheme 4.2. The planarity of the constructed ligands unfortunately created significant solubility problems but metal centres such as palladium could still be coordinated to these ligands.



Scheme 4.2 Different synthetic strategies followed for the synthesis of various bridging ligands based on multiple phen framework structures.

The third pathway that was followed in the synthetic strategy, involved the design and synthesis of compounds that mimic the 1,10-phenanthroline coordination mode. Cyclohexane-1,2,3,4,5,6-hexanone was used as the starting material to which other compounds such as 1,2-phenylene diamine and 2,3-diaminomaleonitrile were used to make ligands that theoretically can coordinate to three or more metal centres. This concept is presented in Scheme 4.3



Scheme 4.3: Synthetic strategy for the synthesis of bridging ligands that further mimic the coordination mode of 1,10-phenanthroline.

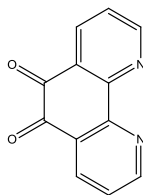
Theoretically, there should be minimal problems in the proposed synthetic pathways; however, there were some limitations in the synthesis of the shown ligands illustrated due to the formation of multiple species. Eventually, some of the desired compounds could however be isolated, although the resulting coordinating ability of the ligands were not always as expected. The proposed pathways were merely a guideline, as there are a large number of different combinations with the synthons that were chosen for this aspect of the project. It is important to note that not all of the compounds are completely planar and some of the ligands are also not proven bridging ligands. Certain compounds were chosen for simplicity and others were synthesised in an attempt to manipulate the electronic environment and solubility of the final complexes.

4.2 Chemicals and Apparatus

All reagents utilised for the synthesis of compounds were of analytical grade and were purchased from Sigma-Aldrich, South Africa. Reagents were used as received without further purification. All experiments were performed in air unless otherwise stated. Infrared spectra of the complexes were recorded on a Bruker Tensor 27 Standard System ATR spectrophotometer with a laser range of 4000 – 370 cm^{-1} . Data was collected at ambient temperatures in air and reported in cm^{-1} . The ^1H NMR data was obtained from a Bruker 300 MHz spectrometer using the mentioned deuterated solvent. ^{13}C NMR data was obtained from a Bruker 600 MHz. All chemical shifts, δ , are reported in ppm using ^1H -TMS as internal standard. Coupling constants, J , are reported in Hertz. The powder products that were collected from the reported synthetic procedures were air-dried with mild heating. The yields reported for products were reported under the assumption that all solvents were removed in the drying process. The crystal structures obtained are discussed in Chapter 5 and Chapter 6.

4.3 Synthesis of Organic Ligands

4.3.1 1,10-Phenanthroline- 5,6-dione (phendione)

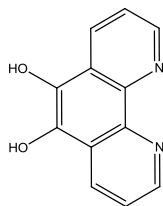


The title compound was synthesised according to the literature procedure¹. 1,10-Phenanthroline (4.0 g, 2.0×10^{-3} mol) and KBr (4.0 g, 3.36×10^{-3} mol) were mixed and slowly added to a mixture of HNO_3 (20 ml) and H_2SO_4 (40 ml) and was cooled to 0° C. The temperature was kept below 5 °C throughout the addition. The solution was then refluxed for four hours. The mixture was neutralised to pH 4.5 using a saturated KOH solution. The product was extracted with chloroform and crystallised. Yield: 3.2 g, 76 %. ^1H NMR (300 MHz, CDCl_3): 9.14 (s, 2H), 8.53

¹ J. Etteedgui, Y. Diskin-Posner, L. Weiner, and R. Neumann, *Journal of the American Chemical Society*, **2011**, 133, 188–190.

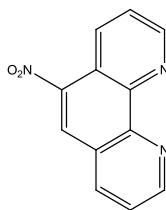
(dd, $J = 7.9, 1.8$ Hz, 2H), 7.61 (dd, $J = 7.9, 4.7$ Hz, 2H). IR (KBr): 1685 ($\nu_{\text{C=O}}$). MS (EI) m/z calcd for $[\text{M} + \text{H}]^+ \text{C}_{12}\text{H}_6\text{N}_2\text{O}_2$: 210.06; found: 210.04.

4.3.2 1,10-Phen-5,6-diol



The title compound was prepared according to the published procedure.¹ 5,6-Phendione (0.250 g, 1.19×10^{-3} mol) and hydrazine sulphate (0.550 g, 4.2×10^{-3} mol) were mixed in H_2O (20 ml) and placed in a boiling water bath for five minutes. The yellow solid was filtered and washed with water. Yield: 0.193 g, 77 %. ^1H NMR (600 MHz, DMSO): 9.12 (dd, $J = 4.8, 1.3$ Hz, 2H), 9.07 – 8.99 (m, 2H), 8.14 (dd, $J = 8.4, 4.8$ Hz, 2H). MS (EI) m/z calcd for $[\text{M} + \text{H}]^+ \text{C}_{12}\text{H}_8\text{N}_2\text{O}_2$: 212.06; found: 212.0.

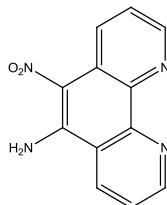
4.3.3 5-Nitro-1,10-phenanthroline



The title compound was prepared according to the published procedure.² 1,10-Phenanthroline (5.0 g, 27.7×10^{-3} mol) was dissolved in concentrated H_2SO_4 (7.5ml). A mixture of concentrated H_2SO_4 (15 ml) and concentrated HNO_3 (15 ml) was then slowly added to ensure that the temperature did not exceed 170 °C. The solution was then refluxed at 170° C for three hours. It is important to ensure that the solution itself reached and didn't exceed 170° C. The solution was then poured onto ice and neutralised to pH 6 using a 30% KOH solution. The precipitate was then filtered off and washed with cold water and dried to produce a pale yellow solid. Yield: 3.2g, 51 %. ^1H NMR (300 MHz, CDCl_3): 9.37 – 9.17 (m, 2H), 8.96 (d, $J = 8.6$ Hz, 1H).

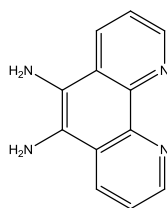
² K. Binnemans, P. Lenaerts, K. Driesen, and C. Gorller-Walrand, *Journal of Materials Chemistry*, **2004**, 14, 191.

4.3.4 5-Amino-6-nitro-1,10-phenanthroline



The title compound was prepared according to the published procedure.³ 5-Nitro-1,10-phen (3.5 g, 15.5×10^{-3} mol) was dissolved in 100 ml of ethanol/dioxane (3:2; v/v) mixture. The solution was heated to 60 °C until all the solids were dissolved. It was then rapidly cooled to 4 °C which resulted in a fine suspension. Powdered hydroxyl amine hydrochloride (6.83 g, 98.4×10^{-3} mol) was then added. This was followed by the dropwise addition of KOH (7.3 g, 129.5×10^{-3} mol) in methanol (100 ml). The solution was stirred at 4 °C for one hour and then heated to 60 °C for one hour. The solution was then poured onto ice which resulted in the formation of a yellow solid. The solid was filtered and washed with methanol and water. Yield: 1.85 g, 49%. ¹H NMR (300 MHz, DMSO): 9.18 (d, $J = 3.4$ Hz, 1H), 9.08 (d, $J = 8.4$ Hz, 1H), 8.78 (d, $J = 3.2$ Hz, 1H), 8.73 (d, $J = 8.6$ Hz, 1H), 8.65 (s, 2H), 7.86 (dd, $J = 8.1, 4.3$ Hz, 1H), 7.68 (dd, $J = 8.5, 4.2$ Hz, 1H). IR (KBr): 3144 ($\nu_{\text{N-H}}$), 1633 ($\nu_{\text{N-O}}$), 1590 ($\nu_{\text{C-N}}$, $\nu_{\text{C-C}}$). MS (EI) m/z calcd for $[\text{M} + \text{H}]^+$ C₁₂H₈N₄O₂: 240.06; found: 240.1.

4.3.5 1,10-Phenanthroline-5,6-diamine

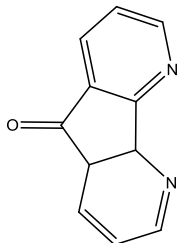


The title compound was prepared according to the published procedure.³ 5-Nitro-6-amino-1,10-phen (0.2 g, 0.83×10^{-3} mol) and Pd on carbon (10%) was placed in ethanol (200 ml) and brought to reflux. Hydrazine hydrate (1.0 ml, 17.2×10^{-3} mol) in ethanol (20 ml) was then added dropwise over fifteen minutes. The solution was then refluxed for two hours and filtered through a bed of Celite. 80% of the ethanol was removed under vacuum. The final product was

³ J. Bolger, A. Gourdon, E. Ishow, and J. P. Launay, *Inorganic Chemistry*, **1996**, 35, 2937–2944.

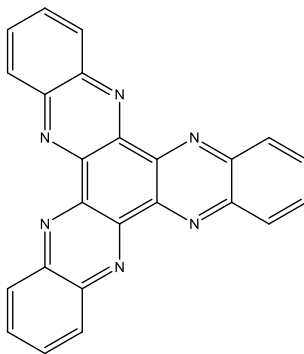
precipitated by the addition of excess pentane. Yield: 0.110g, 65 %. ^1H NMR (300 MHz, MeOH): 8.86 (d, $J = 3.0$ Hz, 1H), 8.56 (d, $J = 8.3$ Hz, 1H), 7.71 (dd, $J = 8.3, 4.2$ Hz, 1H). IR (KBr): 3422 ($\nu_{\text{N-H}}$), 2664, 1619, ($\nu_{\text{C-N}}$), 1550($\nu_{\text{C-C}}$). MS (EI) m/z calcd for $[\text{M} + \text{H}]^+$ $\text{C}_{12}\text{H}_{10}\text{N}_4$: 210.09; found: 210.10.

4.3.6 4,5-Diazafluoren-9-one (Dafone)



The title compound was prepared according to the published procedure.⁴ KMnO_4 (4.0 g, 0.0256mol) in H_2O (250 ml) was heated and added dropwise to a solution of 1,10-phenanthroline (1.6 g, 8.8×10^{-3} mol), KOH (8.0 g, 2.91×10^{-2} mol) and H_2O (250 ml). The solution was refluxed for three hours and the product extracted with chloroform and dried over anhydrous MgSO_4 . Yield: 0.673 g, 41 %. ^1H NMR (300 MHz, CDCl_3): 8.8 (d, $J = 4.4$ Hz, 2H), 8.0(d, $J = 7.5$ Hz, 2H), 7.4 (t, 2H, $J = 5.1$ Hz). IR (ATR): 1714 ($\nu_{\text{C-O}}$), 1258 ($\nu_{\text{C-N}}$), 838 ($\nu_{\text{Ar-H}}$). MS (EI) m/z calcd for $[\text{M} + \text{H}]^+$ $\text{C}_{11}\text{H}_8\text{N}_2\text{O}$: 184.06; found: 182.10.

4.3.7 Diquinoxalino[2,3-a:2',3'-c]phenazine

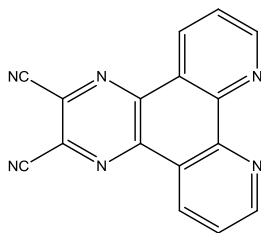


1,2-Phenylenediamine (0.520 g, 4.81×10^{-3} mol) and cyclohexane-1,2,3,4,5,6-hexaone (0.5 g, 2.98×10^{-3} mol) was stirred in ethanol for twenty four hours. The solution was then heated to 70 °C for one hour. The resulting green yellow precipitate was filtered and washed with diethyl

⁴ Q. Zhu, *Inorganica Chimica Acta*, **2003**, 351, 177-182.

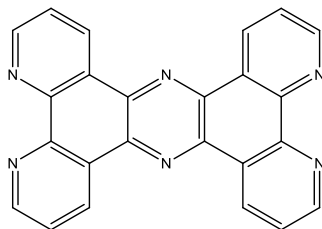
ether. Yellow crystals were obtained from chloroform in the fume hood after 30 minutes. The crystal structure of this compound is discussed in Paragraph 5.3.1. Yield: 0.321 g, 52 %. ^1H NMR (300 MHz, CDCl_3): 8.73 (dd, $J = 6.5, 3.4$ Hz, 6H), 8.08 (dd, $J = 6.5, 3.3$ Hz, 1H). ^{13}C NMR (150 MHz, CDCl_3): 143.55(s), 132.30(s), 130.66(s). MS (EI) m/z calcd for $[\text{M} + \text{H}]^+$ $\text{C}_{24}\text{H}_{12}\text{N}_6$: 384.1; found: 384.20.

4.3.8 Pyrazino[2,3-f][1,10]phenanthroline-2,3-dicarbonitrile



5,6-Phendione (0.250 g, 1.19×10^{-3} mol) and 2,3-diaminomaleonitrile (0.130 g, 1.20×10^{-3} mol) were mixed in DMF (20 ml) and heated to 120 °C for three hours. Water was added and the resulting off-white precipitate was filtered and washed with methanol and diethyl ether. Yield: 0.145 g, 43 %. ^1H NMR (300 MHz, DMSO): 9.41 (dd, $J = 8.2, 1.6$ Hz, 2H), 9.36 (dd, $J = 4.3, 1.6$ Hz, 2H), 8.05 (dd, $J = 8.2, 4.4$ Hz, 2H). ^{13}C NMR (150 MHz, CDCl_3): 154.75 (s), 148.47 (s), 141.40 (s), 134.25 (s), 132.00 (s), 125.73 (s), 125.04 (s), 114.97 (s). IR (KBr): 3144 ($\nu_{\text{N-H}}$), 1633 ($\nu_{\text{N-O}}$), 1590 ($\nu_{\text{C-N}}$, $\nu_{\text{C-C}}$). MS (EI) m/z calcd for $[\text{M} + \text{H}]^+$ $\text{C}_{16}\text{H}_6\text{N}_6$: 282.07; found: 282.10.

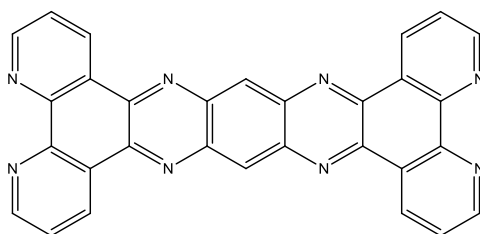
4.3.9 Tetrapyrido[3,2-a:2',3'-c:3'',2''-h:2''',3'''-j]phenazine



1,10-Phenanthroline-5,6-diamine (0.10 g, 0.476×10^{-3} mol) was added to a boiling solution of phendione (0.100 g, 0.476×10^{-3} mol) in methanol (20 ml). The solution was refluxed for twelve hours and the resulting suspension filtered while hot to recover a pale yellow powder that was washed with methanol and diethyl ether. Yield: 0.172 g, 60%. ^1H NMR (300 MHz, CDCl_3 /

trifluoroacetic acid): 10.25 (dd, $J = 8.3$ Hz, 1.6 Hz, 4H), 9.53 (dd, $J = 5.1$ Hz, 1.4 Hz, 4H), 8.46 (dd, $J = 8.3$ Hz, 5.1 Hz, 4H). MS (EI) m/z calcd for $[M + H]^+$ $C_{16}H_6N_6$: 385; found: 385.

4.3.10 9,11,20,22-Tetraazatetrapyrido[3,2-a:2'3'-c:3'',2''-l:2''',3'''-n]pentacene (tatpp)



A mixture of phendione (0.250 g, 1.2×10^{-3} mol), 1,2,4,5-benzenetetramine tetrahydrochloride (0.170 g, 0.60×10^{-3} mol) and potassium carbonate (0.165 g, 1.20×10^{-3} mol) was suspended in ethanol (15 ml) and refluxed for twelve hours. After cooling of the reaction to room temperature, the precipitate was filtered and washed with 15 ml of hot water and boiling ethanol. Yield: 0.1 g, 35 %. 1H NMR (300 MHz, $CDCl_3$ /trifluoroacetic acid): 10.20 (d, $J = 8.0$ Hz, 4H), 9.79 (s, 2H), 8.33 (d, $J = 4.0$ Hz, 4H), 8.36 (dd, $J = 7.3$ Hz, 4.5 Hz, 4H). EI MS: m/z 486.7.

4.4 Synthesis of Metal-ligand Complexes

4.4.1 Dichlorido-(2,2'-bipyridine)-palladium(II)

This compound was prepared by modifying the literature procedure.⁵ PdCl₂ (0.20 g, 1.13×10^{-3} mol) was dissolved in boiling acetonitrile (30.0 ml). 2,2'-Bipyridine (0.220 g, 1.13×10^{-3} mol) was added. Upon addition a yellow precipitate formed. The solvent was evaporated in the fume hood. Yield: 0.243 g, 64 %. ¹H NMR (300 MHz, DMSO): 9.1 (d, $J = 5.4$ Hz, 2H), 8.5 (d, $J = 7.8$ Hz, 2H), 8.3 (t, $J = 7.8$ Hz, 2H), 7.8 (t, $J = 6.7$ Hz, 2H). IR (ATR): 1599 (ν_{C-H}), 1162 (ν_{C-N}), 802 (ν_{Ar-H}).

4.4.2 Dichlorido-1,10-phenanthroline-palladium(II)

This compound was prepared by modifying the literature procedure.⁵ PdCl₂ (0.20 g, 1.13×10^{-3} mol) was dissolved in boiling acetonitrile (300 ml). 1,10-Phenanthroline monohydrate (0.176 g, 1.13×10^{-3} mol) was added and a yellow precipitate formed. The solvent was evaporated in the fume hood. Yield: 0.273 g, 68 %. ¹H NMR (300 MHz, DMSO): 9.3 (d, $J = 4.8$ Hz, 2H), 9.0 (d, $J = 8.3$ Hz, 2H), 8.3 (s, 2H), 8.1 (m, 2H). IR (ATR): 1599 (ν_{C-H}), 1153 (ν_{C-N}), 802 (ν_{Ar-H}).

4.4.3 Dichlorido-(1,10-phenanthroline)-palladium(II)

Pd(CH₃CN)₂Cl₂ (0.051 g, 1.92×10^{-4} mol) was dissolved in warm DCM. A solution of 1,10-phenanthroline (0.04 g, 1.92×10^{-4} mol) in DCM (15 ml) was then added, which resulted in the immediate formation of a yellow precipitate. The precipitate was washed with ether to give the final product. Yield: 0.060 g, 82%. ¹H NMR (300 MHz, DMSO): 9.24 (d, $J = 5.5$ Hz, 1H), 8.78 (d, $J = 7.7$ Hz, 1H), 8.05 (dd, $J = 7.7, 5.9$ Hz, 1H).

4.4.4 Dichlorido-(5-nitro-1,10-phenanthroline)-palladium(II)

Pd(CH₃CN)₂Cl₂ (0.050 g, 1.92×10^{-4} mol) was dissolved in DMF (5 ml), to which 5-nitro-1,10-phenanthroline (0.060 g, 1.92×10^{-4} mol) was added. The solution was stirred for thirty minutes at 40 °C. A small amount of DCM and excess pentane was then added to the solution which resulted in the formation of a pale yellow solid, which was filtered and dried. Yield: 0.044 g,

57 %. ^1H NMR (300 MHz, DMSO): 9.48 (s, 2H), 9.38 (s, 1H), 9.32 (d, $J = 8.9$ Hz, 1H), 9.19 (d, $J = 7.8$ Hz, 1H), 8.27 (dd, $J = 14.2, 5.9$ Hz, 2H).

4.4.5 6-Amino-5-nitro-1,10-phenthroline-dichlorido-palladium(II)

$\text{Pd}(\text{CH}_3\text{CN})_2\text{Cl}_2$ (0.050 g, 1.92×10^{-4} mol) was dissolved in DMF (5 ml), to which 5-nitro-6-amino-1,10-phenanthroline (0.070 g, 1.92×10^{-4} mol) was added. The solution was stirred for thirty minutes at 40 °C. A small amount of DCM and excess pentane was then added to the solution which resulted in the formation of a pale yellow solid, which was filtered and dried. Crystals were obtained after one week from a DMSO solution. The crystal structure of this compound is discussed in Paragraph 6.2.1 Yield: 0.042 g, 53 %. ^1H NMR (300 MHz, DMSO): 9.45 (s, 2H), 9.05 (m, 4H), 8.23 – 8.11 (m, 1H), 8.04 – 7.92 (m, 1H).

4.4.6 6-Amino-5-nitro-1,10-phenthroline-dichlorido-palladium(II)

K_2PtCl_4 (0.80 g, 1.925×10^{-4} mol) was dissolved in H_2O (10 ml). To this 6-amino-5-nitro-1,10-phenthroline (0.050 g, 2.0×10^{-4}) and 2 M HCl (2 ml) was added. The solution was boiled, which resulted in the formation of an orange precipitate, which was filtered and dried. Crystals were obtained after one week from a DMSO solution. The crystal structure of this compound is discussed in Paragraph 6.2.2. Yield: 0.41 g, 40 %. ^1H NMR (300 MHz, DMSO): 9.73 (s, 2H), 9.17 (m, 4H), 8.43 – 8.31 (m, 1H), 8.11 – 7.97 (m, 1H).

4.4.7 Dichlorido-(μ_2 -5,6-diamino-1,10-phenthroline)-palladium(II)

$\text{Pd}(\text{CH}_3\text{CN})_2\text{Cl}_2$ (0.050 g, 1.93×10^{-4} mol) dissolved in ethanol (15 ml) which was slowly added to a solution of 5,6-phendiamine (0.040 g, 1.92×10^{-4} mol). This was then dissolved in ethanol (20 ml) and a dark brown precipitate formed, which was filtered and washed with ether. Yield: 0.055 g, 61 %. ^1H NMR (300 MHz, DMSO): 8.98 (d, $J = 4.8$ Hz, 2H), 8.82 (d, $J = 8.3$ Hz, 2H), 7.87 (dd, $J = 8.6, 4.6$ Hz, 2H). IR (KBr): 3390, 3308 (ν_{NH_2}), 1635 ($\nu_{\text{C-c}}$), 1581 ($\nu_{\text{C-N}}$).

4.4.8 Tetrachlorido-(μ_2 -2,2'-Bipyrimidine)-palladium(II)⁵

This compound was prepared by modifying the published procedure.⁵ PdCl₂ (0.200 g, 1.13×10^{-3} mol) was dissolved in boiling acetonitrile (30 ml). 2,2'-Bipyridine (0.092 g, 5.71×10^{-4} mol) was then added to the solution and a yellow precipitate formed. The solvent was evaporated in the fume hood. Yield: 0.244 g, 85%. ¹H NMR (300 MHz, DMSO): 7.9 (t, $J = 5.2$ Hz, 2H), 9.3 (dd, $J = 5.1$ Hz, 4H). IR (ATR): 1589 (ν_{C-H}), 1137 (ν_{C-N}), 813 (ν_{Ar-H}).

4.4.9 Dichlorido-(2,2'-Bipyridine)-platinum(II)

The title compound was prepared according to the published procedure.⁶ K₂PtCl₄ (0.160 g, 3.855×10^{-4} mol) was dissolved in H₂O (10 ml). To this 2,2'-bipyridine (0.0624 g, 4.0×10^{-4} mol) and 2 M HCl (2 ml) was added. The solution was boiled, which resulted in the formation of a yellow precipitate, which was then filtered. Yield: 0.122 g, 75 %. ¹H NMR (300 MHz, DMSO): 9.52 (t, $J = 9.9$ Hz, 2H), 8.59 (d, $J = 8.0$ Hz, 2H), 8.42 (dd, $J = 11.1, 4.6$ Hz, 1H), 7.8 (dd, $J = 9.8, 3.7$ Hz, 2H). IR (ATR): 1604 (ν_{C-H}), 1163 (ν_{C-N}), 758 (ν_{Ar-H}).

4.4.10 Diacetonitrile-bis-dichlorido-palladium(II)⁶

Palladium chloride (0.2 g, 1.12×10^{-3} mol) was dissolved in boiling acetonitrile. The solution was filtered and the excess solvent was removed to give a bright yellow powder. Yield: 0.185 g, 65 %. ¹H NMR (300 MHz, CDCl₃): 2.40 (s, CH₃). IR (ATR): 2335, 2304.

4.4.11 Bis-(5-diazafluoren-9-one)-dichlorido-palladium(II)⁵

This compound was prepared by modifying the procedure used by Boyle. PdCl₂ (0.100 g, 5.64×10^{-4} mol) was dissolved in boiling acetonitrile (20 ml). 4,5-Diazafluoren-9-one (0.205 g, 1.12×10^{-3} mol) was added. Upon addition a yellow precipitate formed. The solvent was evaporated. Yield: 0.258 g, 85 %. ¹H NMR (300 MHz, DMSO): 9.1 - 9.3 (1H), 8.8 (1H), 8.3 (1H), 8.0 (1H), 7.7 (1H), 7.5 (1H). IR (ATR): 1737 ($\nu_{C=O}$), 1221 (ν_{C-N}), 827 (ν_{Ar-H}).

⁵ C. Young, A. Roodt, B. C. B. Bezuidenhout, *Acta Crystallographica Section E Structure Reports Online*, **2012**, 68, m1374–m1374.

⁶ G. Morgan, F. Burstall, *Journal of the Chemical Society*, **1934**, 965–971.

4.5 Discussion

In the previous paragraphs, all the different chemical properties of the 1,10-phenanthroline synthons were indicated. Some attention was also given to the possible planar bridging ligands that can be constructed using available processes. Finally, some bridged metal complexes were also described. Although a significant amount of information for some of these bridging ligands and complexes is available, it is important to focus on some of the challenges which were encountered when trying to construct these multi-metal centre housing ligands.

4.5.1 Synthetic Challenges

Unfortunately, not all the building blocks that were required for this project were commercially available. As a result, a significant amount of synthetic organic chemistry had to be performed in order to obtain all the components. This essentially meant that a considerable amount of project time was spent on the synthesis of these materials. One reaction which proved to be synthetically problematic was the synthesis of phendiamine. Published procedures were followed, but a final product could not be isolated. This was in part due to the insolubility of dioxime species, as well as the fact that it was poorly characterised in literature. It should also be mentioned that various techniques were employed. Different bases, different/new starting materials, dry conditions as well as multiple solvents were all used in an attempt to remove all the possible problems with this reaction. Finally, a different pathway was followed, which gave the desired phendiamine but in very low yields. Typically, only 600 mg was isolated from 5 g of phen starting material.

Not only was it time consuming to synthesise the desired synthons for the project, but the synthesis of the actual bridging ligands was not as simple as many of the published procedures suggested.^{4,7} Therefore a large amount of time was spent trying to optimise the synthetic procedures for the synthons and the bridging compounds, which resulted in far less time for evaluating the actual bridging ligands as potential catalysts on heterogeneous supports.

4.5.2 Solubility

Solubility of the ligands and metal complexes was again, as mentioned for the systems described in Chapter 3, one of the major problems which were encountered with this PhD study. It is therefore important to explore the possible reasons and define some solutions for the difficulties which were experienced. In order to create a network of bridged metal species it was decided to focus mainly on planar ligand systems. These planar bridging ligands combined with square planar coordinating metals, such as platinum, palladium and copper, could provide the desired effect as anticipated in Chapter 1. Unfortunately, by using these sheet-like compounds, an environment which favours π - π -stacking is created, *i.e.* the attractive, non-covalent interactions between aromatic rings. These forces influence the structures of, for example, proteins and DNA and they also play a role in the assembly of supramolecular architectures.⁸ It is also responsible for solubility problems. Further evidence that π - π -stacking is present in these systems was shown by Lind *et al.*⁹ who tried to exploit this phenomena for charge transfer purposes. One way in which π - π -stacking interactions can be completely elucidated is through the use of single crystal X-Ray diffraction studies. The interactions between molecules in the crystalline phase can be investigated using this technique. Ironically, systems where π - π -stacking is found to a greater extent, tend to be more difficult to crystallise. Furthermore, the properties of many compounds tend to vary greatly between the solid state and solution. This poses some limitations on the deductions that can be made from crystal structures. Even so, considerable attempts were made to crystallise some of the ligands that were synthesised and the crystallographic data is reported in Chapter 5 and Chapter 6.

Possible solutions for the solubility problems that were encountered entail using highly polar or strong coordinating solvents. Dimethyl sulfoxide and dimethylformamide are some of the common solvents which can be employed. However, these have high boiling points and are difficult to remove from final products. Other solvents like nitromethane, dioxane and THF were explored with little success. One could argue that the poor solubility of these compounds could be an asset in terms of heterogeneous catalysis, but it is a drawback when trying to build a knowledge base as well as gain insight and understanding of the mechanism present in the catalysis processes.

Although these solubility problems are present, there are some ways in which these could be minimised. One way would be to substitute phen with 2,9-dimethyl-1,10-phenanthroline (neocuproine). The methyl groups could minimise π - π -stacking and increase electron density on the conjugated system but these methyl groups introduce a steric parameter for coordination to the nitrogen atoms, and it is considerably more expensive than non-functionalized phen. Evidence that substituents of the phen ring can reduce solubility problems was shown by the isolation of crystals, for which the structure of 5-nitro-6-amino-1,10-phenanthroline complexes could be solved in Chapter 5. In those instances the nitro group increased the solubility. Other solvent systems such as ionic liquids may also be explored in future.

4.5.3 Characterisation

The problems that were encountered when trying to characterise these ligands, go hand in hand with the solubility problems. Due to the insolubility of many of the planar compounds, characterisation became a real problem. NMR could be used to an extent, but this meant that one had to make use of dimethyl sulfoxide (DMSO) as a deuterated solvent. DMSO introduces a range of new challenges and limitations, as it coordinates to metal centres such as palladium and platinum resulting in difficult to interpret NMR spectra for certain species. The growth of single crystals for many of these compounds was also impeded by the solubility problems. This virtually removed another very important analytical tool from the equation. Elemental analysis is widely used in published procedures; however, it is expensive, time consuming and does not always provide the correct information about coordination modes which limits its use for this project. Perhaps the easiest way to find solutions to these difficulties would be to overcome the solubility problems. Nevertheless, the single crystal structure determinations that were possible in this PhD study are described in the following chapters, which also highlights information of coordination and packing modes in these compounds.

5 SINGLE CRYSTAL X-RAY STUDY OF SELECTED MODEL LIGANDS

5.1 Introduction

A major part of this project focuses on the synthesis of planar bridging ligands that could be used to link various metal species in order to create a network of metal centres. Various planar bridging ligands were investigated through the use of single crystal X-ray crystallography to gain insight into the planarity and the electronic nature of the ligands. One major problem that was encountered throughout this project has been poor solubility. The poor solubility has limited the number of other techniques, such as NMR and Gas chromatography for the in-depth characterisation of many of the ligand systems. Limited information has been obtained regarding the planarity and geometry using the aforementioned techniques. As a result, a crystallographic investigation was launched to learn more about the properties of the ligands investigated in this PhD study. In this chapter the crystal structures of the following bridging ligands are discussed: 1,6,7,12,13,18-hexaazatrinaphthylene octa-chloroform solvate (I), benzo[1,2-c:4,5-c'] dipyrrole-1,3,5,7(2H,6H)-tetrone,2,6-dihydroxy-dihydrate (II), 2,7-di(pyridin-2-yl)benzo[lmn][3,8] phenanthroline- 1,3,6,8(2H,7H)-tetraone (III) and 2-Amino-4,6-dichloropyrimidine, acetic acid solvate (IV). Due to the poor solubility of these planar compounds only a few crystal structures of the bridging ligands were obtained.

5.2 Experimental

A Bruker X8 ApexII 4K diffractometer¹ using graphite monochromated Mo K α radiation with ω -and- ϕ -scans at 100K with an Oxford cooling unit was used to obtain reflection data. COSMO² was used for optimum collection of more than a hemisphere of reciprocal space. The first fifty frames were repeated periodically to ensure that no decomposition of the crystals took place. The crystals remained stable throughout the data collection. The cell refinement was performed with SAINT-Plus³ and data reduction with SAINT-Plus and XPREP.² Data corrections for absorption effects were performed using the multi-scan technique SADABS.⁴ The structures were solved by the direct method package SIR97⁵ and refined using the software package WinGX14,⁶ incorporating SHELXL.⁷ Graphical representations of crystal structures were created by DIAMOND.⁸ All structures are shown with thermal ellipsoids drawn at a 50% probability level and refined anisotropically, unless otherwise stated. Methyl and aromatic hydrogen atoms were placed in geometrically idealised positions (C-H = 0.95 – 0.98 Å) and constrained to ride on their parent atoms ($U_{\text{iso}}(\text{H}) = 1.5 U_{\text{eq}}(\text{C})$ and $1.2 U_{\text{eq}}(\text{C})$).

¹ Bruker, APEX2 (Version 1.0-27), Bruker AXS Inc., Madison, Wisconsin, USA, **2005**.

² Bruker, COSMO, (Version 1.48), Bruker AXS Inc., Madison, Wisconsin, USA, **2003**.

³ Bruker, SAINT-Plus (Version 7.12) (Including XPREP), Bruker AXS Inc., Madison, Wisconsin, USA, **2004**.

⁴ Bruker, SADABS, (Version 2004/1), Bruker AXS Inc., Madison, Wisconsin, USA, **1998**.

⁵ A. Altomare, M. C. Burla, M. Camalli, G. L. Cascarano, C. Giacovazzo, A. Guagliardi, A. G. Moliterni, G. Polidori, R. Spagna, *Journal of Applied Crystallography*, **1999**, 32, 115-119.

⁶ L. J. Farrugia, *Journal of Applied Crystallography*, **1999**, 32, 837-838.

⁷ G.M. Sheldrick, SHELXL97, Program for Solving Crystal Structures, University of Göttingen, Germany, **1997**.

⁸ K. Brandenburg, H. Putz, *DIAMOND, Release 3.0c, Crystal Impact GbR, Bonn, Germany*, **2005**.

5.3 Organic Bridging Ligands

Table 5.1: Crystal data parameters for [C₂₄H₁₂N₆]₂·8CHCl₃ (I), C₁₀H₄N₂O₆·2H₂O (II), C₁₂H₆N₂O₂ (III) and C₈H₁₁Cl₂N₃O₄ (IV).

Compound	(I)	(II)	(III)	(IV)
Empirical formula	C ₅₆ H ₃₂ Cl ₂₄ N ₁₂	C ₁₀ H ₈ N ₂ O ₈	C ₂₄ H ₁₂ N ₄ O ₄	C ₈ H ₁₁ Cl ₂ N ₃ O ₄
F.W.	1723.81	284.18	210.19	284.10
Temperature K	100 (2)	100 (2)	100 (2)	100 (2)
Crystal system, Space group	Triclinic, $P\bar{1}$	Monoclinic, $P2_1/c$	Monoclinic, $P2_1/c$	Triclinic $P\bar{1}$
a (Å)	11.582(1)	6.884(1)	9.802(5)	5.1370(2)
b (Å)	14.936(2)	10.160(7)	8.793(5)	10.7670(4)
c (Å)	19.893(2)	8.022(4)	11.737(10)	11.1620(4)
α (°)	78.044(5)	90	90	93.331(2)
β (°)	89.909(5)	107.13(1)	113.212(5)	96.056(2)
γ (°)	89.799(5)	90	90	95.870(2)
Volume (Å ³)	3366.7(6)	536.2	929.7(8)	609.22(4)
Z	4	2	2	2
ρ_{calc} (g cm ⁻³)	1.700	1.760	1.502	1.549
μ (mm ⁻¹)	1.02	0.16	0.106	0.540
F(000)	1720	292	432	292
Crystal Colour	Yellow	Yellow	Colourless	Light yellow
Morphology	Needle	Cuboid	Needle	Needle
Crystal size (mm)	0.31 x 0.18 x 0.12	0.083x0.121x0.13	0.065x0.115x0.57	0.81 x 0.31 x 0.22
Theta range (°)	1.05 to 28.48	3.10 to 27.99	2.26 to 28.28	1.91 to 28.29
Completeness %	97	99	99	99
Limiting indices	-15<= h <=15 -19<= k <=19 26<= l <=26	-8<= h <=9 -13<= k <=13 -10<= l <=9	-12<= h <=13 -11<= k <=11 -15<= l <=15	-6<= h <=5 -14<= k <=13 -14<= l <=14
Reflections collected	69165	9422	11246	10439
Unique reflections	16534	1299	2295	3007
R _{int}	0.0721	0.0274	0.0424	0.0196
Refinement method	Full-matrix least-squares on F ²	Full-matrix least-squares on F ²	Full-matrix least-squares on F ²	Full-matrix least-squares on F ²
Data / restraints / parameters	16546 / 0 / 832	1299 / 0 / 107	2295 / 0 / 145	3007 / 2 / 164
Goodness-of-fit on F ²	1.07	1.05	1.05	1.07
Final R indices [$I > 2\sigma(I)$]	R1 = 0.0616 wR2 = 0.1565	R1 = 0.0423 wR2 = 0.1121	R1 = 0.0461 wR2 = 0.1124	R1 = 0.0249 wR2 = 0.0660
R indices (all data)	R1 = 0.987 wR2 = 0.1998	R1 = 0.0495 wR2 = 0.1173	R1 = 0.0664 wR2 = 0.1243	R1 = 0.0272 wR2 = 0.0679
$\Delta\rho_{\text{min}}$; $\Delta\rho_{\text{max}}$ (e.Å ⁻³)	1.052 and -1.049	0.567 and -0.342	0.288 and -0.265	0.346 and -0.321

5.3.1 1,6,7,12,13,18-Hexaazatrinaphthylene octa-chloroform solvate (heprazine) (I)

Yellow crystals of the title compound (I) were obtained according to the procedure described in Paragraph 4.3.7. The compound crystallised in a triclinic $P\bar{1}$ space group with four heprazine units, accompanied by sixteen chloroform solvate molecules per unit cell. The graphical representation and the numbering system are illustrated in Figure 5.1. Selected bond lengths and angles are reported in Table 5.1. Atomic coordinates, anisotropic displacement parameters, all bond distances and angles are given in Appendix A.

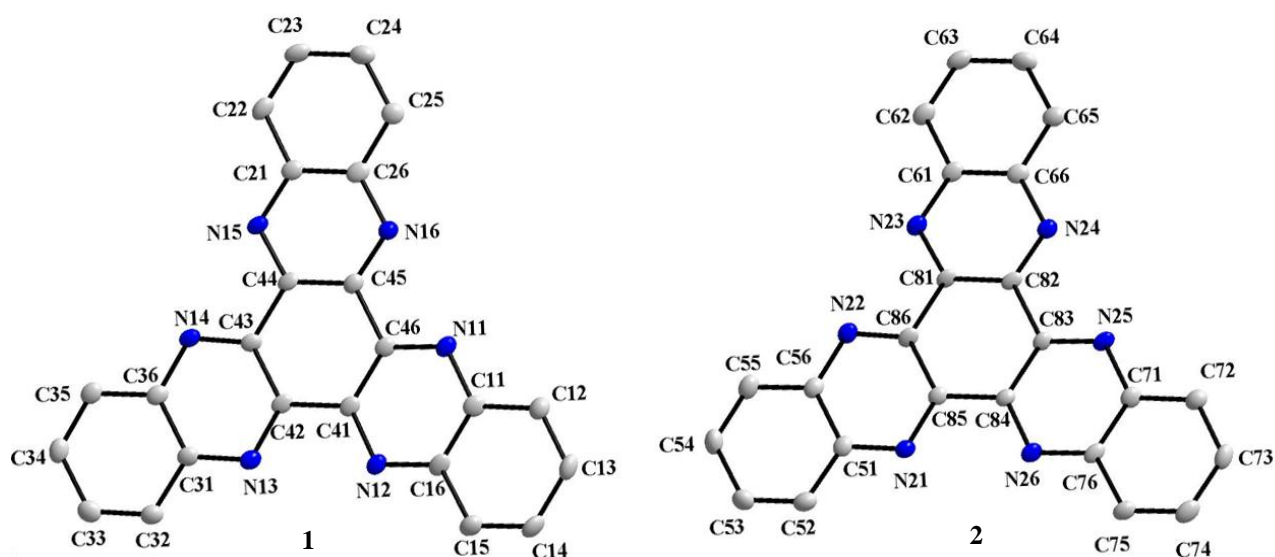


Figure 5.1: Diamond representation of heprazine (I) molecule 1 and molecule 2 at 50 % probability level, displaying the numbering scheme employed. The first digit represents the ring and the second digit the number of the atom in the ring. The chloroform solvate molecules and hydrogen atoms are omitted for clarity.

Table 5.2: Selected geometric parameters (Å, °) for heprazine.

Molecule 1		Selected bond lengths (Å)		Molecule 2	
C91—C113	1.757 (4)	C92—C122	1.758 (4)		
C11—N11	1.364 (4)	C71—N25	1.364 (4)		
C12—C13	1.362 (5)	C72—C73	1.380 (5)		
C15—C16	1.425 (5)	C75—C76	1.423 (5)		
Selected Bond angles (°)					
C113—C91—C111	110.7 (2)	C122—C92—C123	111.0 (2)		
N11—C11—C12	119.4 (3)	N26—C76—C75	119.2 (3)		
N11—C11—C16	120.7 (3)	N25—C71—C76	120.6 (3)		
N12—C16—C11	121.7 (3)	N26—C76—C71	122.0 (3)		

The molecular structure of heprazine (**I**) consists of three benzene units linked to a central benzene ring by three pyrazine moieties. This creates three 1,10-phenanthroline type coordination sites surrounding the central benzene ring. A plane was constructed through the six carbon atoms of the central benzene ring in Figure 5.2. This plane indicates that the heprazine molecule is almost completely planar, with the largest deviation from the plane being C13 (0.0823 Å). No major distortions appear to be evident from the hydrogen interactions between the terminal carbons and the chloroform molecules, which are found between respective heprazine units within the unit cell. There appears to be no significant differences between the two heprazine molecules within the unit cell.

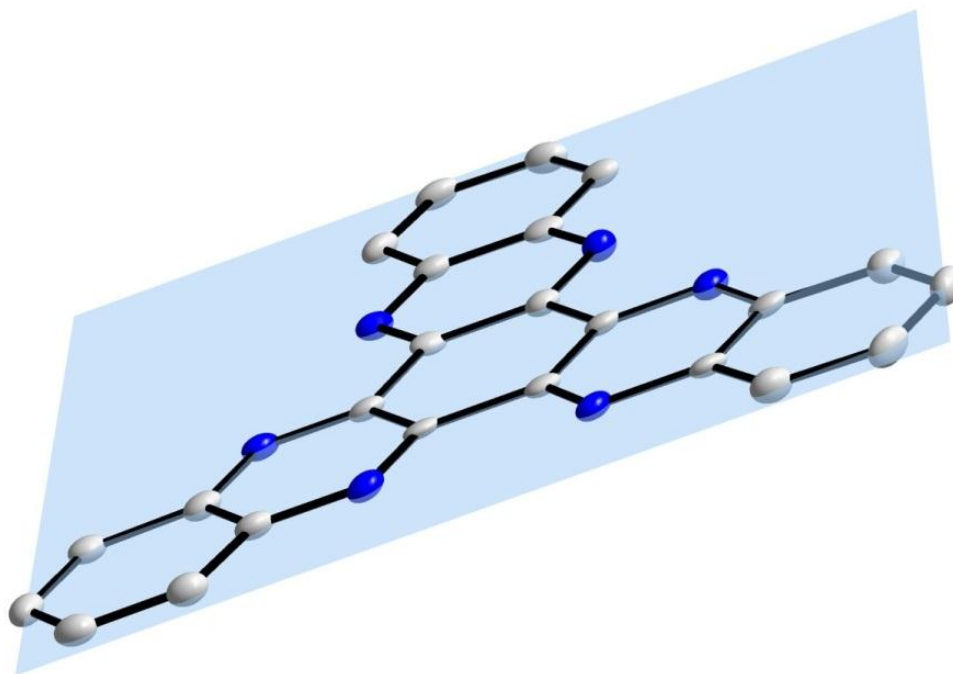


Figure 5.2: Diamond representation of heprazine (I) at 50 % probability level, displaying the inserted plane through the central benzene ring with no obvious distortion from the plane.

Intermolecular C—H...Cl and C—H...N hydrogen interactions exist between the heprazine and chloroform solvate molecules (see Figure 5.3). The bond distances and angles for the hydrogen bonding are reported in Table 5.3. The chloroform hydrogen molecule is situated half-way between, and has an interaction with both the nitrogens within the heprazine ring. As a result, each of the three heprazine cavities exhibits a chloroform solvent interaction. N24 and N25 have interactions with two chloroform molecules. The protons from carbons on the terminal rings also have interactions with the chlorine from the chloroform solvate. The bond lengths and angles compare well to the monoclinic polymorph⁹ which is almost completely planar, however there are differences in the hydrogen interactions. The monoclinic moiety does not display hydrogen interactions between the chloroform solvate hydrogens and the hydrogens of the terminal benzene rings.

⁹ M. Alfonso, H.Stoeckli-Evans, *Acta Crystallographica Section E Structure Reports Online*, **2001**, 57, o242–o244.

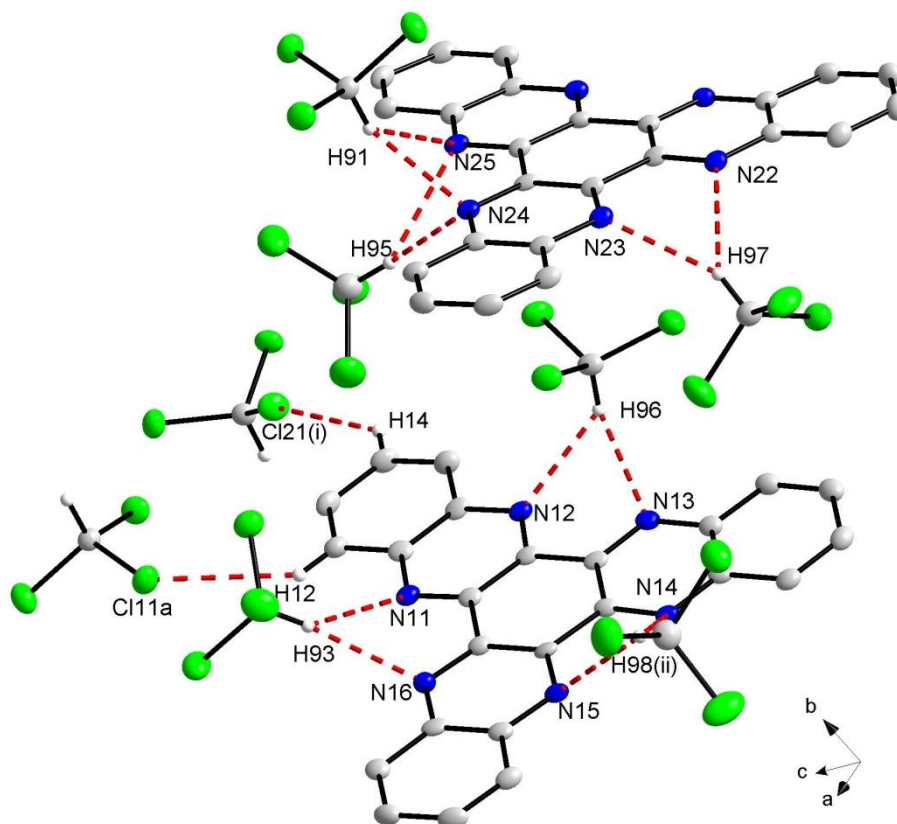


Figure 5.3: Diamond representation of the hydrogen interactions between heprazine and the chloroform solvate molecules. The red fragmented lines indicates the intermolecular hydrogen bonding between heprazine and the chloroform solvate molecules. Irrelevant hydrogen atoms and solvate molecules are omitted for clarity. Symmetry transformations used to generate equivalent atoms: (i) $1-x, -1-y, 1-z$, (ii) $1+x, y, z$.

Table 5.3: Hydrogen interactions (\AA , $^\circ$) for heprazine (I).

D—H \cdots A	D—H	H \cdots A	D \cdots A	D—H \cdots A
C12—H12 \cdots Cl11 ⁱ	0.93	2.96	3.713 (4)	139
C53—H53 \cdots Cl12 ⁱⁱ	0.93	2.74	3.458 (4)	134
C55—H55 \cdots Cl22 ⁱⁱⁱ	0.93	2.95	3.705 (4)	139
C14—H14 \cdots Cl21 ⁱ	0.93	2.73	3.450 (4)	135
C91—H91 \cdots N24	0.98	2.50	3.274 (5)	136
C91—H91 \cdots N25	0.98	2.52	3.279 (5)	134
C92—H92 \cdots N14 ^{iv}	0.98	2.50	3.262 (5)	135
C92—H92 \cdots N15 ^{iv}	0.98	2.50	3.275 (5)	136
C93—H93 \cdots N16	0.98	2.50	3.406 (5)	154
C94—H94 \cdots N21 ^v	0.98	2.48	3.201 (5)	130
C94—H94 \cdots N26 ^v	0.98	2.49	3.218 (5)	131
C95—H95 \cdots N24	0.98	2.55	3.459 (5)	154
C96—H96 \cdots N12	0.98	2.48	3.200 (5)	130
C96—H96 \cdots N13	0.98	2.49	3.218 (5)	131
C97—H97 \cdots N23	0.98	2.50	3.402 (5)	154

Symmetry codes: (i) $-x+1, -y+1, -z+1$; (ii) $-x, -y+1, -z$; (iii) $-x+1, -y+1, -z$; (iv) $x, y+1, z$; (v) $x+1, y, z$.

When viewed along the a -axis some interesting packing effects are visible (see Figure 5.4). Chloroform solvent molecules are found between terminal ends of the heprazine molecule and between the centre sections of the stacked heprazine molecules. The presence of the solvent molecule interactions probably diminishes the stacking effects which are present, as heprazine is not soluble in other common organic solvents and seems to play an important role in the packing. The packing in the monoclinic⁹ and triclinic polymorphs are similar to the chloroform atoms lying between the different heprazine molecules. The chloroform solvent molecules are found at different positions with regards to the hydrogen bonding as mentioned before.

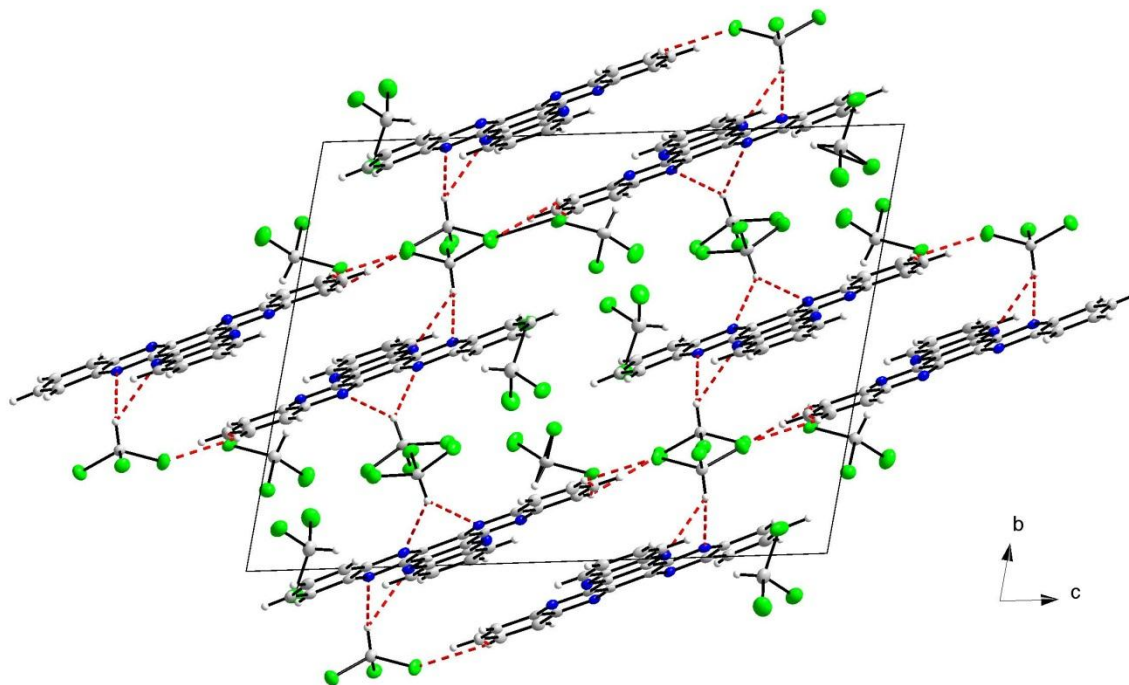


Figure 5.4: Packing of heprazine in the unit cell, viewed along the a-axis. Hydrogen interactions are also shown.

5.3.2 Benzo[1,2-c:4,5-c']dipyrrole-1,3,5,7(2H,6H)-tetrone, 2,6-dihydroxy-dihydrate (*N,N'*-dihydroxypyromellitic diimide)(II)

Yellow crystals of the title compound (II) were obtained according to the procedure described in Paragraph 3.3.5. The compound crystallised in a monoclinic $P2_1/c$ space group with two *N,N'*-dihydroxypyromellitic diimide molecules, accompanied by four water solvate molecules in the unit cell. The graphical representation and the numbering scheme are illustrated in Figure 5.5 and selected bond lengths and angles are reported in Table 5.4. Atomic coordinates, anisotropic displacement and parameters and all bond distances and angles are given in Appendix A.

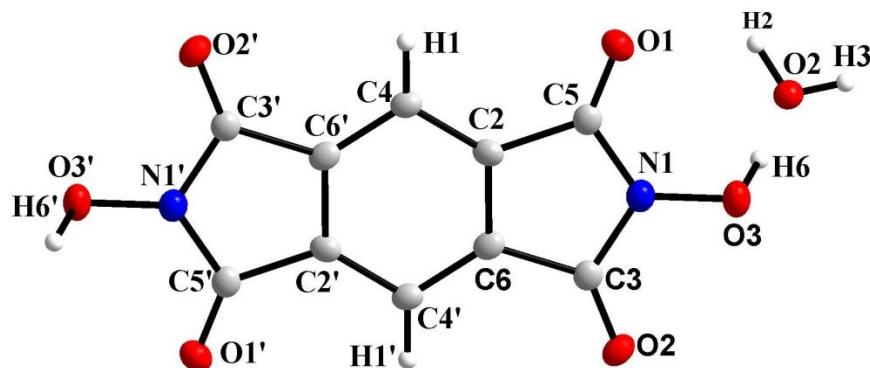


Figure 5.5: Diamond representation of *N,N'*-dihydroxypyromellitic (II) and the water solvent molecule at 50 % probability level, displaying the numbering scheme employed. Symmetry operations used '2-x, 1-y, 1-z.

Table 5.4: Selected geometric parameters (Å, °) for *N,N'*-dihydroxypyromellitic.

Selected bond lengths (Å)		Selected Bond angles (°)	
O1—C5	1.201 (2)	O3—N1—C3	121.7 (1)
O3—N1	1.370 (2)	C3—N1—C5	114.6 (1)
N1—C5	1.398 (2)	C4—C2—C5	128.8 (2)
C2—C6	1.395 (2)	O2—C3—N1	126.4 (2)
C2—C5	1.491 (2)	O1—C5—C2	129.9 (12)
		N1—C5—C2	104.0 (1)

The molecular structure of *N,N'*-dihydroxypyromellitic diimide consists of a central benzene ring with two *N*-hydroxy-succinimide units on opposite ends of the ring. This combination forms a planar compound with six terminal oxygens. There are O—H···O and C—H···O hydrogen interactions present between (II) and the water solvate molecule (see Figure 5.6). The bond distances and angles for the hydrogen bonding are reported in Table 5.5. The bond distances compare well to the mono *N*-hydroxy-succinimide variation.¹⁰ There are slight variations in the bond angles, but no major inconsistencies are present.

¹⁰ F. M. Miao, J. L. Wang, X. S. Miao, *Acta Crystallographica Section C Crystal Structure Communications* **1995**, *51*, 712-713.

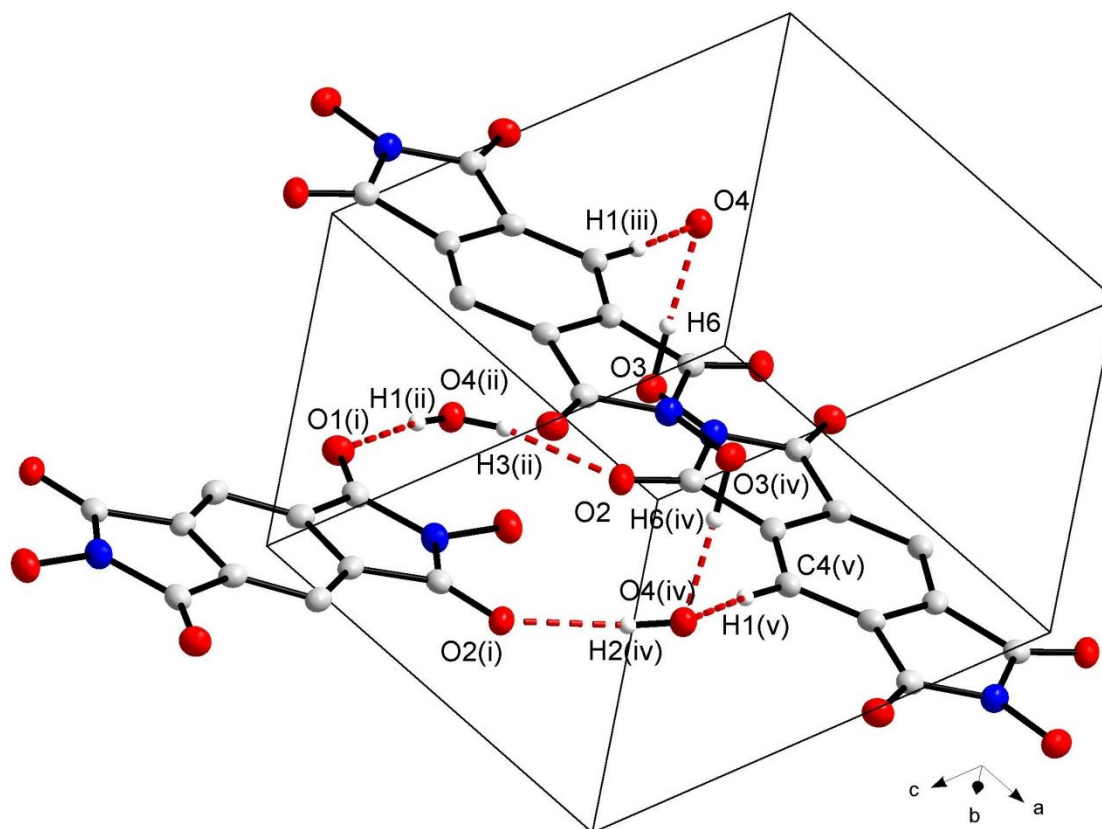


Figure 5.6: Graphical representation of the intermolecular H-bond interactions for *N,N'*-dihydroxypyromellitic. Only applicable H atoms with relevance to the H-bond interactions are indicated. The red fragmented lines indicate the intermolecular hydrogen bonding between the *N,N'*-dihydroxypyromellitic and water solvate molecules. (i) 1-*x*, 1/2+*y*, 1.5-*z*, (ii) *x*, 1/2-*y*, 1/2 +*z*, (iii) 1-*x*,*y*,*z*, (iv) 1-*x*,1-*y*,1-*z* and (v) 2-*x*,1-*y*,1-*z*.

Table 5.5: Hydrogen interactions (Å, °) for *N,N'*-Dihydroxypyromellitic (II).

D—H···A	D—H	H···A	D···A	D—H···A
O3—H6···O4	0.99 (3)	1.66 (3)	2.6445 (18)	175 (3)
C4—H1···O4 ⁱⁱ	0.94 (2)	2.38 (2)	3.282 (2)	159.1 (2)
O4—H3···O1 ⁱⁱⁱ	0.82 (3)	2.19 (3)	3.0071 (18)	172 (2)
O4—H2···O2 ^{iv}	0.86 (3)	2.02 (3)	2.8754 (17)	169 (3)

Symmetry codes: (ii) *x*+1, *y*, *z*; (iii) -*x*+1, -*y*, -*z*+1; (iv) *x*, -*y*+1/2, *z*-1/2.

The packing of the title compound is displayed in Figure 5.7. The *N,N'*-dihydroxypyromellitic molecules are arranged in a face-centred like manner, with four molecules on opposite corners, instead of eight. Two *N,N'*-dihydroxypyromellitic molecules are found on the *c* faces with half the molecule within the unit cell.

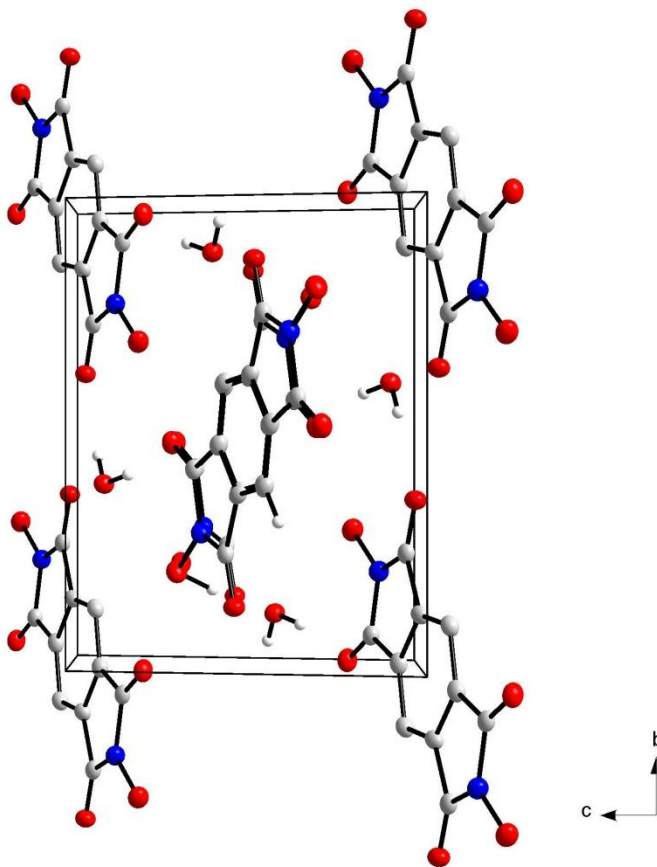


Figure 5.7: Diamond representation of *N,N'*-dihydroxypyromellitic, at 50 % probability level, displaying the packing in the unit cell along the *a* axis. Hydrogen atoms are omitted for clarity.

5.3.3 *N,N'*-Bis(2-pyridyl)naphthalene-3,4:7,8-di-carboximide (dpbpt) (III)

Yellow crystals of the title compound (III) were obtained according to the procedure described in Paragraph 3.3.10. The compound crystallised in a monoclinic $P2_1/c$ space group, with two dpbpt units per unit cell. The graphical representation and the numbering scheme are illustrated in Figure 5.8 and selected bond lengths and angles are reported in Table 5.6. Atomic coordinates, anisotropic displacement parameters and all bond distances and angles are given in Appendix A.

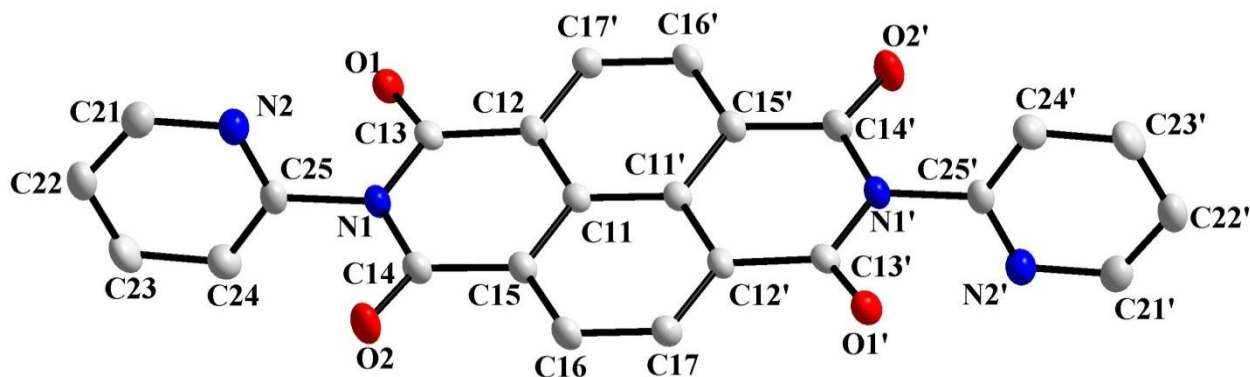


Figure 5.8: Diamond representation of dpbpt (III), at 50 % probability level, displaying the numbering scheme employed. The hydrogen atoms are omitted for clarity. Symmetry operations used: $-x, -y, 2-z$.

Table 5.6: Selected geometric parameters (\AA , $^\circ$) for dpbpt (III).

Selected bond lengths (\AA)		Selected Bond angles ($^\circ$)	
O2—C14	1.220 (2)	C25—N2—C21	116.21 (14)
N2—C25	1.333 (2)	C25—C24—C23	117.43 (17)
O1—C13	1.210 (2)	C14—N1—C13	125.66 (12)
C22—C23	1.381 (3)	C14—N1—C25	117.65 (13)
N1—C14	1.400 (2)	N2—C21—C22	123.41 (17)
N1—C25	1.455 (2)	C11—C12—C13	119.47 (13)
C15—C11	1.414 (2)	O1—C13—C12	123.44 (14)
C15—C14	1.481 (2)	N1—C13—C12	116.42 (14)

The title compound consists of a naphthalene imide skeleton with two 2-aminopyridine moieties attached to it, in an attempt to create a planar molecule. The backbone is approximately planar, as indicated by a small mean deviation of 0.006 \AA from the least-squares plane of the rings defined by atoms C11, C12, C15, C16 and C17. The pyridyl rings are twisted by $76.7 (2)^\circ$, in the opposite direction, out of the plane of the naphthalene imide skeleton (see Figure 5.9). The diformamide plane illustrates how O1 and O2 bend away from the plane in opposite directions by 0.2084 \AA and 0.1102 \AA respectively.

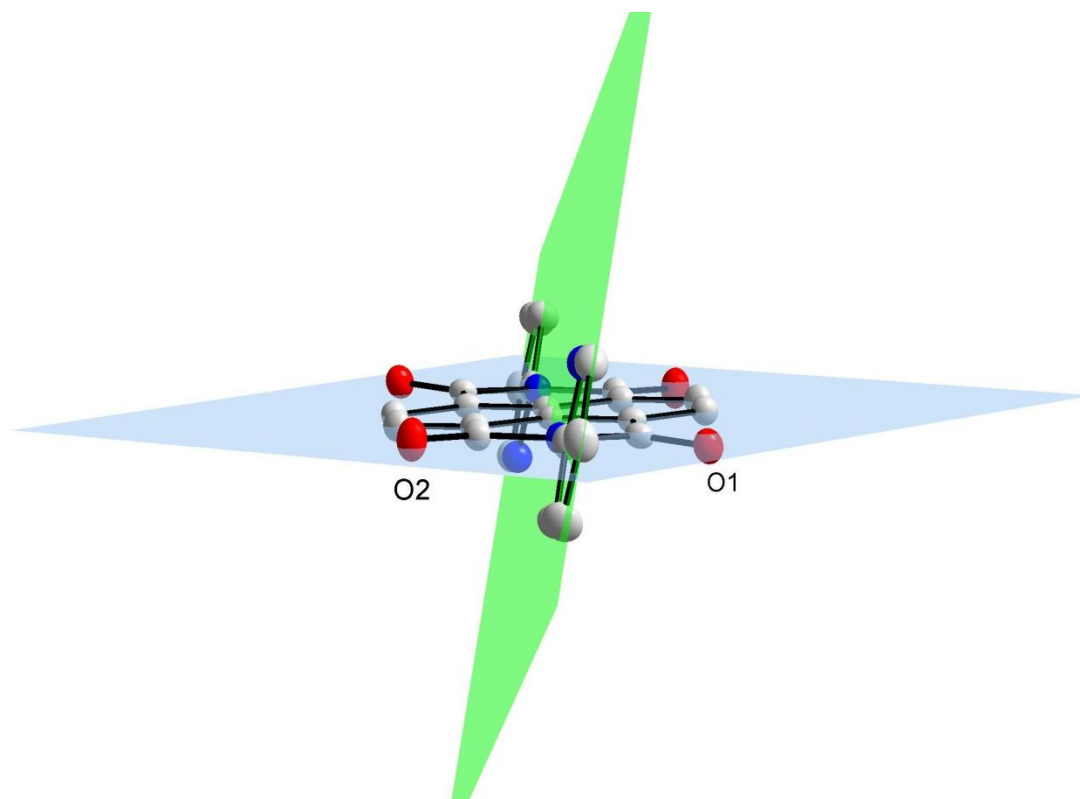


Figure 5.9: Diamond representation of dpbpt (III), displaying the inserted planes through the central carbon rings and the pyridine rings. O1 and O2 are visibly distorted from the blue plane. Hydrogen atoms have been omitted for clarity.

Intermolecular C—H \cdots O interactions are observed between the hydrogen atoms of the pyridine rings and oxygen atoms from neighboring molecules (see Figure 5.10). The bond distances and angles for the hydrogen interactions are reported in Table 5.7. These interactions could be responsible for the distortion of the two oxygen atoms from plane as discussed earlier. The bond distances compare well to the 4-amino counterpart¹¹ and no major differences can be seen in the bond angles. The pyridine rings in the structure reported by Mizuguchi *et al.* are only rotated at 69.2 ° in comparison to the 76.7 ° in the structure of (III). The oxygen atoms are distorted in a similar manner.

¹¹ J. Mizuguchi, T. Makino, Y. Imura, H. Takahashi, S. Suzuki, *Acta Crystallographica Section E Structure Reports Online*, **2005**, 61, o3044–o3046.

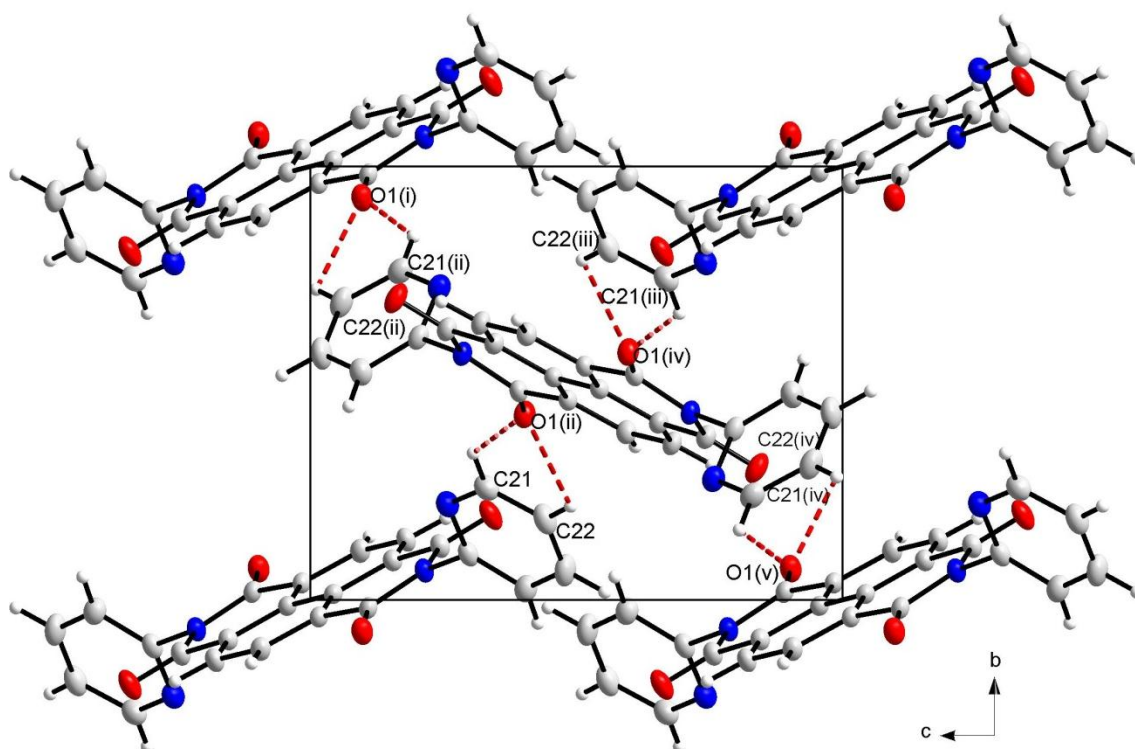


Figure 5.10: Graphical representation of the intermolecular H-bond interactions for dpbpt (III). The red fragmented lines indicate the intermolecular hydrogen bonding between the dpbpt (III) molecules. (i) $x, 1+y, z$, (ii) $1-x, \frac{1}{2}+y, 1\frac{1}{2}-z$, (iii) $1-x, 1-y, 1-z$, (iv) $1+x, \frac{1}{2}-y, \frac{1}{2}+z$ and (v) $1-x, -y, 1-z$.

Table 5.7: Hydrogen interactions (\AA , $^\circ$) for dpbpt (III).

D—H \cdots A	D—H	H \cdots A	D \cdots A	D—H \cdots A
C21—H21 \cdots O1 ⁱⁱ	0.93	2.45	3.114 (2)	128
C22—H22 \cdots O1 ⁱⁱ	0.93	2.63	3.187 (2)	119

Symmetry code: (ii) $-x+1, y+1/2, -z+3/2$.

The molecules pack in a zig-zag fashion across the ab plane (see Figure 5.11). The dpbpt molecules are arranged in a face-centred like manner with molecules on all but two of the unit cell corners. Two dpbpt molecules are found on the c faces with half the molecule within the unit cell.

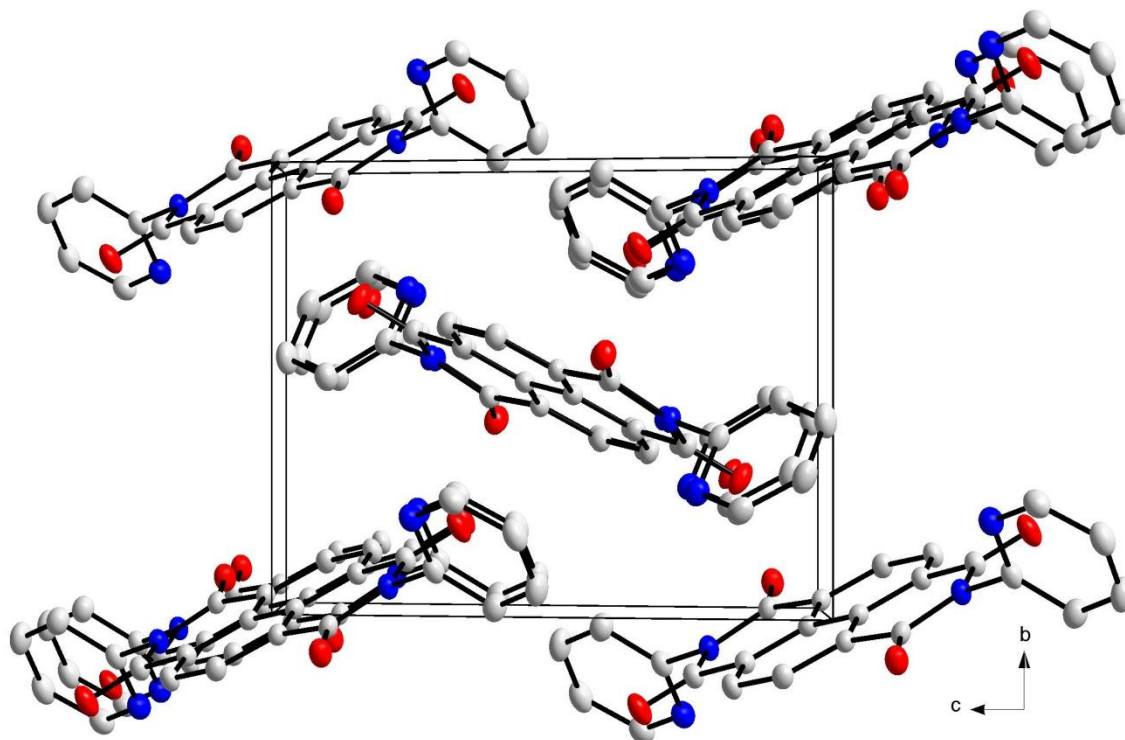


Figure 5.11: Diamond representation of *N,N'*-Dihydroxypyromellitic, at 50 % probability level, displaying the packing in the unit cell along the *a* axis. Hydrogen atoms are omitted for clarity.

5.3.4 2-Amino-4,6-dichloropyrimidine, acetic acid solvate (IV)

Light yellow crystals of the title compound (IV) were obtained from acetic acid, following solubility studies on the starting synthons for the construction of larger bridging ligands. The compound crystallised in a monoclinic triclinic $P\bar{1}$ space group with two pyrimidine units per unit cell. The graphical representation and the numbering scheme are illustrated in Figure 5.12 and selected bond lengths and angles are reported in Table 5.8. Atomic coordinates, anisotropic displacement parameters and all bond distances and angles are given in Appendix A.

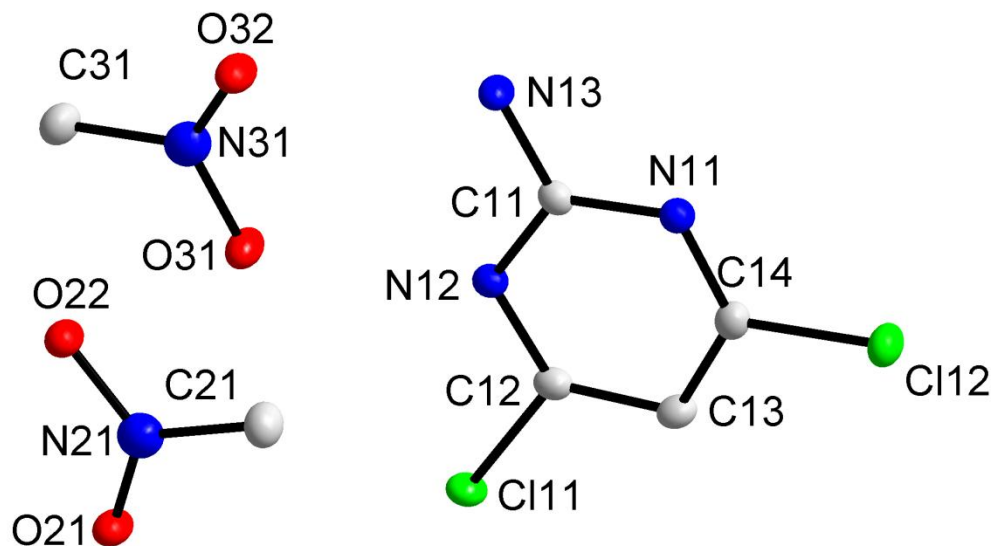


Figure 5.12: Diamond representation of 2-amino-4,6-dichloropyrimidine (IV) at 50 % probability level, displaying the numbering scheme employed. The first digit represents the ring and the second digit the number of the atom in the ring. The chloroform solvate molecules and hydrogen atoms are omitted for clarity.

Table 5.8: Selected geometric parameters (Å, °) for 2-amino-4,6-dichloropyrimidine (IV).

Selected bond lengths (Å)		Selected Bond angles (°)	
Cl12—C14	1.732 (1)	N12 —C12 —Cl11	115.0 (8)
N11—C14	1.317 (3)	N11—C14—C13	125.5 (4)
N13 —C11	1.329 (2)	C13—C14—Cl12	118.5 (2)
C12 —C13	1.382 (6)	N11—C11—N12	124.2 (9)

The crystal structure consists of the planar 2-amino-4,6-dichloropyrimidine and two acetic acid solvate molecules. The planarity of the pyrimidine molecule is confirmed by the plane constructed through C11-C14 and N11-N13 in Figure 5.13 (RMS error = 0.0078 Å). The two chlorine atoms Cl11 and Cl12 are essentially co-planar and deviate from the plane by 0.038 Å and 0.053 Å respectively. The amino hydrogens H12 and H13 are also co-planar and deviate from the plane by 0.040 Å and 0.043 Å respectively. The bond lengths and angles compare well to the two monoclinic polymorphs of 2-amino-4,6-dichloropyrimidine reported by Clews & Cochran¹² and Fun *et al.*¹³ A more comprehensive comparison is done in Paragraph 5.3.5.4.

¹² C. J. B. Clews, W. Cochran, *Acta Crystallographica*, **1948**, *1*, 4–11.

¹³ H. K. Fun, S. Chantrapromma, S. Jana, R. Chakrabarty, S. Goswami, *Acta Crystallographica*, **2008**, *E64*, o1659–o1660.

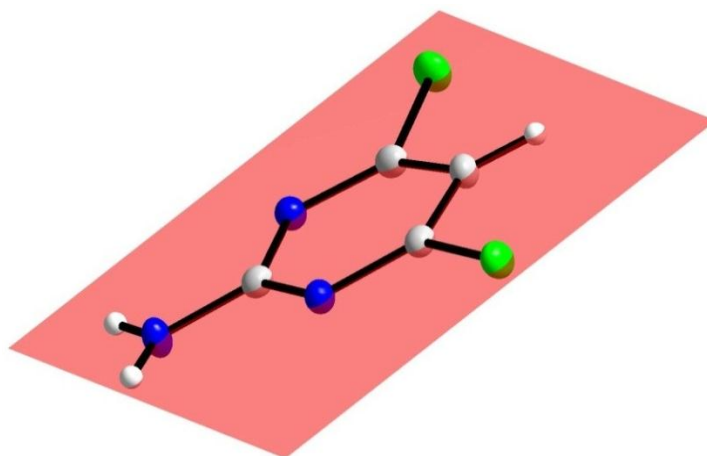


Figure 5.13: Diamond representation of 2-amino-4,6-dichloropyrimidine at 50 % probability level, displaying the inserted plane through C11-C14 and N11-N13.

Intermolecular C—H...O, N—H...N and O—H...N hydrogen interactions exist between adjacent pyrimidine molecules and the acetic acid molecules (see Figure 5.14). The bond distances and angles for the hydrogen bonding are reported in Table 5.9. The amino group acts as a double donor in N—H...N and N—H...O hydrogen bonds, while the two ring N atoms (N11 and N12) act as the acceptors. These intermolecular hydrogen interactions form R^2_1 (8) ring motifs. R^2_2 (8) ring motifs are formed between the adjacent pyrimidine molecules, adjacent acetic acid molecules and between the pyrimidine and acetic acid molecules. All the hydrogen interactions lie in a single plane that runs at an angle to the *bc*-axis (see Figure 5.15) although one of the hydrogen atoms on C21 deviates slightly from the plane.

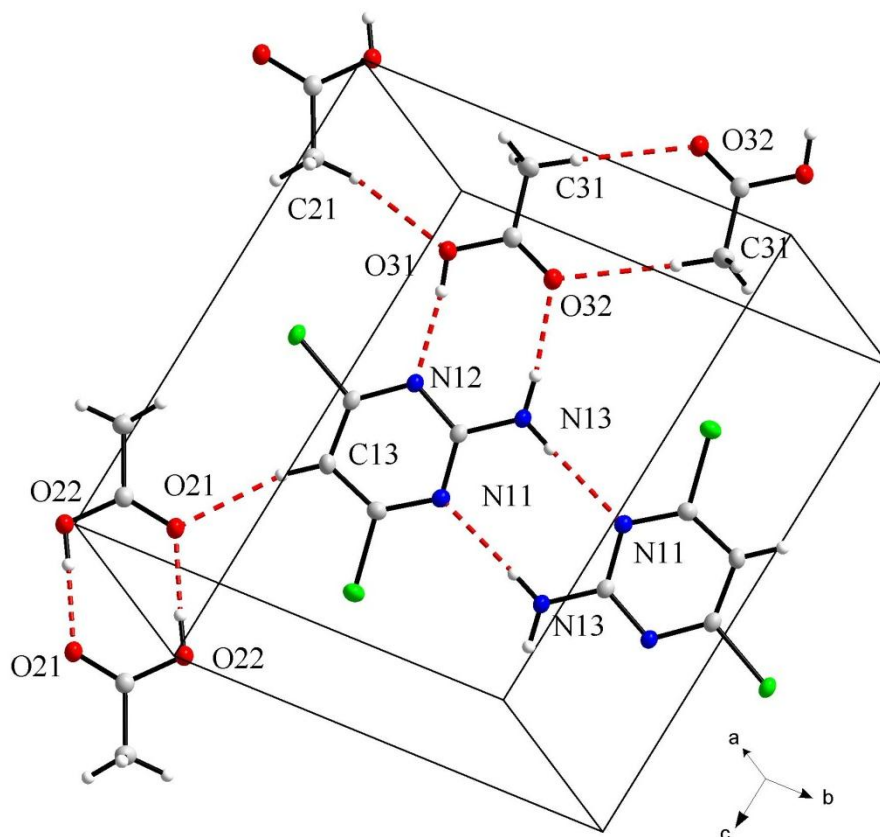


Figure 5.14: Diamond representation of the hydrogen interactions between 2-amino-4,6-dichloropyrimidine and the acetic acid solvate molecules. The red fragmented lines indicate the intermolecular hydrogen bonding.

Table 5.9: Hydrogen interactions (\AA , $^\circ$) for 2-amino-4,6-dichloropyrimidine (IV).

D—H \cdots A	D—H	H \cdots A	D \cdots A	D—H \cdots A
N13—H12 \cdots O32	0.897(1)	1.987(1)	2.879 (4)	173.3 (2)
N13—H13 \cdots N11 ⁱ	0.843(1)	2.157(2)	2.999 (3)	177.5 (2)
C13—H11 \cdots O21 ⁱⁱ	0.95	2.40	3.323 (6)	165.1
C21—H21B \cdots O31 ⁱⁱⁱ	0.98	2.50	3.322 (2)	141.3
O22—H22 \cdots O21 ^{iv}	0.84	1.81	2.645 (2)	177.8
O31—H31 \cdots N12	0.84	1.94	2.773 (3)	172.4

Symmetry transformations used to generate equivalent atoms: (i) $1-x, -y+1, -z+1$, (ii) $-x+1, -y, -z+1$, (iii) $x-1, y, z$ (iv) $-x+1, -y, -z$

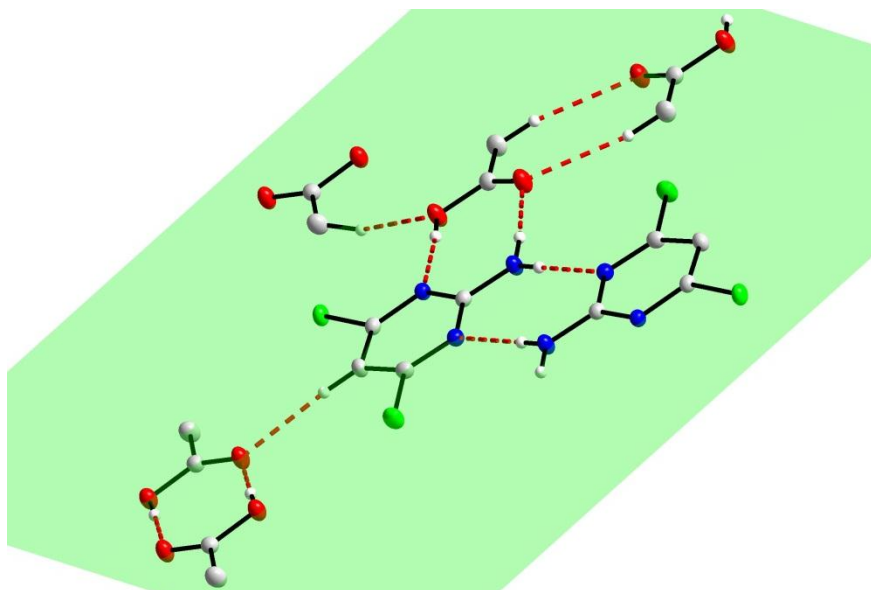


Figure 5.15: A plane constructed through the atoms involved in the hydrogen bonding between 2-amino-4,6-dichloropyrimidine and the acetic acid solvate molecules.

Hydrogen interactions seem to play a dominant role in the packing within the unit cell, but it would seem that the hydrogen interactions are restricted to a single plane. No interactions between the pyrimidine molecules or acetic acid molecules were found between the ‘interaction planes’.

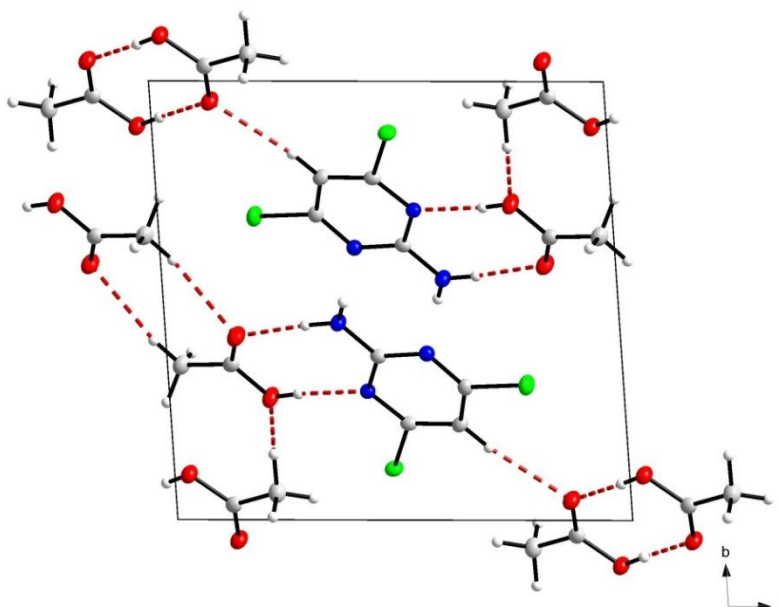


Figure 5.16: Packing between 2-amino-4,6-dichloropyrimidine in the unit cell, viewed along the a-axis. Hydrogen interactions are also shown.

5.3.5 Comparison of Organic Ligands

Various organic structures have been reported in the previous paragraphs. There are some polymorphs and similar structures that have previously been reported. In this section similarities and differences will be indicated and discussed.

5.3.5.1 1,6,7,12,13,18-Hexaazatrinaphthylene (heprazine)

The heprazine structure (I) reported in paragraph 5.3.1 crystallised in a triclinic $P\bar{1}$ space group. However, this is not the first reported structure for this compound. A monoclinic polymorph was reported by Alfonso⁹ (V) and Du¹⁴ (VI). Additionally, a structure where two chlorine atoms have been attached to terminal carbons was also reported by Barlow¹⁵ (VII) and a zinc complex was reported by Krahmer¹⁶ (VIII). These two structures are presented in Figure 5.17.

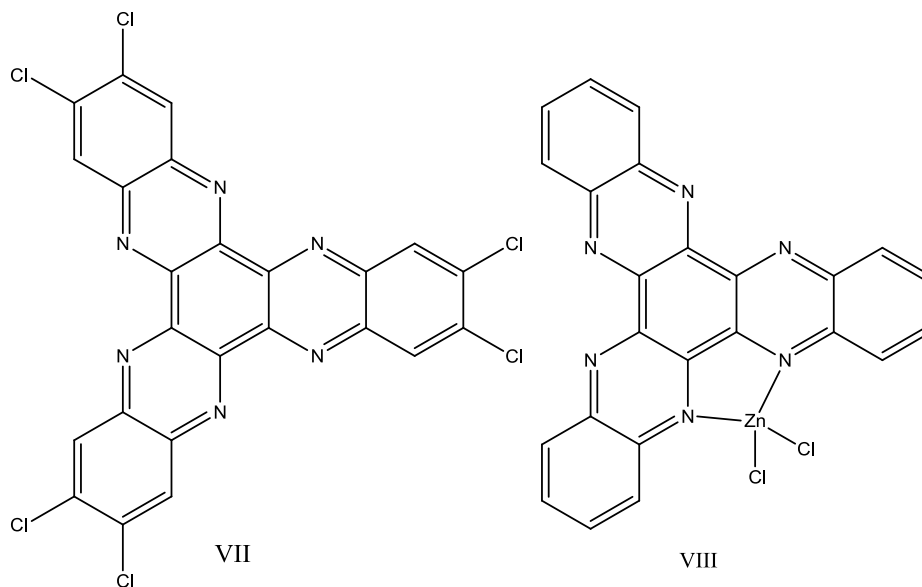


Figure 5.17: Structures of heprazine reported by Barlow¹⁵ (VII) and Krahmer¹⁶ (VIII).

¹⁴ M. Du, X. H. Bu, K. Biradha, *Acta Crystallographica Section C Crystal Structure Communications*, **2001**, 7, 199–200.

¹⁵ S. Barlow, *Chemistry - A European Journal*, **2007**, 13, 3537–3547.

¹⁶ J. Krahmer, R. Beckhaus, W. Saak, D. Haase, *Zeitschrift für anorganische und allgemeine Chemie*, **2008**, 634, 1696–1702.

A plane (green) was constructed through the central benzene ring of the monoclinic polymorph reported by Du¹⁴ in Figure 5.18. Two additional planes (orange and blue), which run through the terminal benzene rings are also indicated. A comparison between the crystallographic data, bond distances and the distortion of terminal benzene ring planes from the central plane was done in Table 5.10.

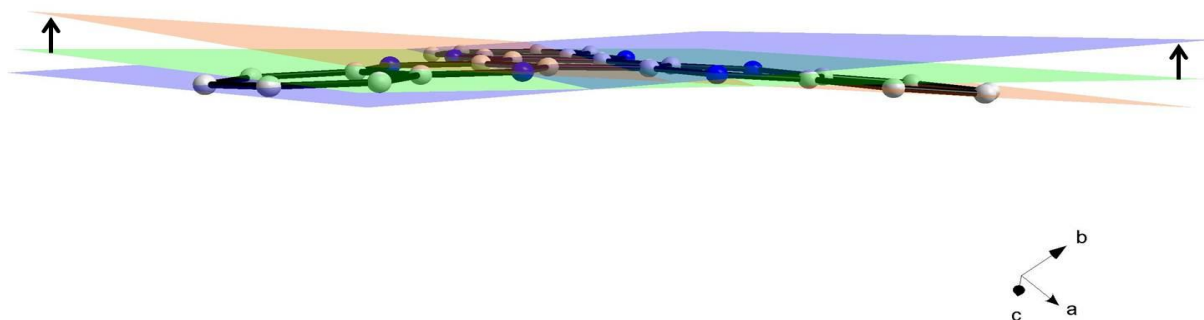


Figure 5.18: Diamond representation showing the plane constructed through the central heprazine benzene ring (green) and two other planes (orange and blue) constructed through the terminal benzene rings. The arrows show the deviation of the terminal planes from the central one.

The comparison of the three heprazine polymorphs, the chlorine substituted ligand and the zinc complex elucidated some interesting results. There are no major inconsistencies in the crystallographic data other than the subtle space group changes. Major differences were observed when looking at the planarity of these compounds. As a measure of the planarity, the deviation of the terminal carbons from a plane constructed through the central benzene ring was investigated. It was found that (I) and (V) show very subtle deviations in the order of 0.05 Å. The carbon atoms of (VI), (VII) and (VII) deviate from the plane substantially with 0.23 Å or more. There are no differences in bond lengths, which accounts for the change in geometry. Further investigation into the unit cell contents revealed that the major difference between a contorted heprazine molecule and a planar molecule is the electronic environment of the ligand surroundings. There are four chloroform molecules in the unit cell for (I), (V), one for (VI) and none for (VII) and (VIII). The high electron negative substituted chlorine atoms also reduce the electron density of (VII).

Table 5.10: Comparison of the crystal data, bond lengths (Å) and the deviation of the terminal carbons from the central ring plane.

Compound	(I)	(V)	(VI)	(VII)	(VIII)
Crystal system	Triclinic	Monoclinic	Monoclinic	Monoclinic	Monoclinic
Space group	$P\bar{1}$	$P2_1/n$	$P2_1/c$	$P2_1/c$	$P2_1/c$
a (Å)	11.582 (1)	15.117(1)	19.506 (2)	10.964 (1)	8.416 (2)
b (Å)	14.936 (2)	11.629(6)	5.382 (5)	26.634 (3)	20.698 (8)
c (Å)	19.893 (2)	19.974(2)	20.976 (2)	8.016 (1)	10.027 (9)
$\alpha(^{\circ})$	78.044 (5)	90	90	90	90
$\beta(^{\circ})$	89.909 (5)	101.62 (1)	103.90 (1)	108.90(8)	96.70 (7)
$\gamma(^{\circ})$	89.799 (5)	90	90	90	90
Volume (Å) ³	3366.7 (6)	3439.1(4)	2137.6(2)	2214.5(9)	2080.7 (1)
Z	4	4	4	4	4
ρ_{calc} (g cm ⁻³)	1.700	1.665	1.565	1.773	1.662
Selected bond lengths (Å)					
C(43)—C(44)	1.477 (3)	1.491 (6)	1.473 (4)	1.484 (3)	1.458 (3)
C(44)—C(45)	1.422 (1)	1.427 (8)	1.426 (4)	1.426 (4)	1.440 (4)
C(45)—N(16)	1.320 (1)	1.326 (6)	1.323 (3)	1.319 (3)	1.326 (3)
N(16)—C(26)	1.362 (2)	1.359 (7)	1.362 (4)	1.351 (3)	1.362 (3)
C(26)—C(21)	1.421 (2)	1.423 (8)	1.423 (4)	1.428 (4)	1.434 (4)
C(21)—C(22)	1.421 (3)	1.409 (8)	1.413 (4)	1.410 (3)	1.418 (4)
C(22)—C(23)	1.359 (5)	1.347 (6)	1.352 (4)	1.365 (3)	1.373 (3)
C(23)—C(24)	1.409 (8)	1.425 (8)	1.407 (5)	1.428 (3)	1.416 (4)
Distance of terminal carbon atoms from central ring plane (Å)					
C1	0.0392 (1)	0.0957 (5)	0.2509 (3)	0.0431 (2)	-0.4029 (3)
C2	0.0823 (2)	0.0413 (5)	0.2338 (4)	0.2108 (1)	0.2954 (3)
C3	0.0407 (1)	0.0469 (4)	0.0200 (3)	0.0731 (2)	0.0648 (3)

- Indicates that the atom is distorted in the opposite direction of the other atoms

(I) Structure reported in Paragraph 5.3.1, (V) Monoclinic polymorph reported by Alfonso.⁹

(VI) Monoclinic polymorph reported by Maio,¹⁰ (VII) Chlorine substituted structure by Barlow.¹⁵

(VIII) Zinc complex of heprazine by Krahmer.¹⁶

Since the chloroform solvate molecules create an electron rich environment, it can be concluded that the contortion of heprazine is proportional to the electron density of the nitrogen atoms. The six nitrogen atoms could become electron poor as a result of the two adjacent benzene rings. When this electron deficiency is accentuated by hydrogen interactions, the nitrogen atom can start to lose its double bond sp^2 geometry and tend towards the sp^3 bond configuration. This change could result in the observed contortion and loss of planarity. Heprazine is even more contorted when coordinated to metal centres such as palladium¹⁷ and zinc¹⁶ which reduces the electron density of the nitrogen atoms further. It is important to note that the coordination of one ‘soft’ metal species to heprazine, makes coordination of the next metal centre exponentially more difficult. The tri-coordinated ‘harder’ silver and titanium species are easily formed. This provides further evidence of the electron poor nature of the nitrogen atoms. It can therefore be concluded that by draining the electron density from the heprazine nitrogen atoms a ‘pseudo- sp^3 ’ configuration is created. Unfortunately, this loss of planarity and poor coordination ability of the nitrogen atoms destroys the bridging capability of this compound for softer metal species such as palladium.

5.3.5.2 Benzo[1,2-c:4,5-c']dipyrrole-1,3,5,7(2H,6H)-tetrone, 2,6-dihydroxy-dihydrate (*N,N'*-dihydroxypyromellitic diimide)

The *N,N'*-dihydroxypyromellitic diimide structure (II) that is reported is the first of its kind. There are two similar structures that were reported by Miao¹⁰ (IX) and Li¹⁸ (X). Both these structures consist of the central benzene ring with only one *N*-hydroxy-succinimide moieties attached to it. The structure reported by Li has four chlorido substituents on the remainder of the benzene ring. These two structures are presented in a comparison between the crystallographic data, bond distances and the distortion of terminal oxygen atoms from the benzene ring plane in Table 5.11.

¹⁷ V. J. Catalano, W. E. Larson, M. M. Olmstead, H. B. Gray, *Inorganic Chemistry*, **1994**, 33, 4502–4509.

¹⁸ J. Li, *Acta Crystallographica Section E Structure Reports Online*, **2007**, 63, o3333–o3333.

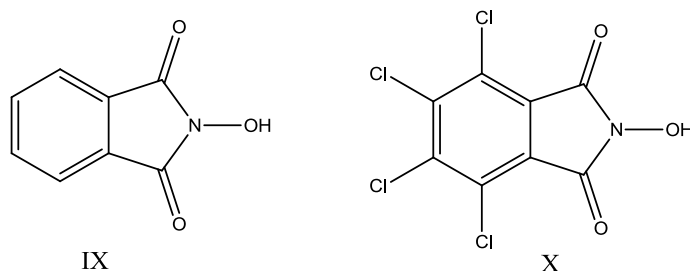


Figure 5.19: Representation of the structures reported by Miao¹⁰ and Li¹⁸.

Table 5.11 Comparison of the crystal data, bond lengths (Å) and the deviation of the terminal carbons from the central ring plane for (I), (IX) and (X).

Compound	(II)	(IX)	(X)
Crystal system	Monoclinic	Monoclinic	Orthorhombic
Space group	$P 2_1/c$	$P2_1/n$	$Pbca$
a (Å)	6.884	11.549 (3)	16.885 (2)
b (Å)	10.160	3.756 (1)	7.7823 (11)
c (Å)	8.022	16.442 (8)	21.974 (3)
$\alpha(^{\circ})$	90	90	90
$\beta(^{\circ})$	107.13	104.94 (3)	90
$\gamma(^{\circ})$	90	90	90
Volume (Å) ³	536.2	689.11	2887.47
Z	2	4	8
ρ_{calc} (g cm ⁻³)	1.760	1.572	1.721
Selected bond lengths (Å)			
O1—C5	1.201 (2)	1.213 (5)	1.203 (3)
O3—N1	1.370 (2)	1.374 (6)	1.372 (3)
N1—C5	1.398 (2)	1.384 (6)	1.379 (3)
C2—C6	1.395 (2)	1.399 (6)	1.396 (3)
C2—C5	1.491 (2)	1.467 (6)	1.491 (3)
Distance of terminal oxygen atoms from central ring plane (Å)			
O1	0.0142 (1)	-0.0090 (2)	0.0471 (4)
O2	0.0107 (1)	-0.0108 (2)	0.1610 (4)
O3	0.0977 (1)	0.0213 (2)	0.2231 (4)

- Indicates that the atom is distorted in the opposite direction of the other atoms

(II) Structure reported in Paragraph 5.3.2, (IX) Structure reported by Miao,¹⁰ (X) Structure reported by Li.¹⁸

The bond distances and angles of (II) compare well with the other two structures. The three terminal oxygens of all three compounds bend away from the plane constructed through the central benzene ring (see Figure 5.20). In the structures of (II) and (X) all three atoms bend in the same direction, but in that of (XI) the central atom bends away in the other direction than the diamide oxygens. The most bending is observed for the chlorine substituted compound and the least for the single *N*-hydroxy-succinimide moiety which suggests that this is an electronic effect. It is important to note the bending of the central oxygen atom for (X) could be magnified by the hydrogen bonding with the DMF solvate molecule. However, when looking at the overall electronic nature of these structures, it can be deduced that the more electron poor the central benzene ring is, the more bending is observed for the central oxygen atom.

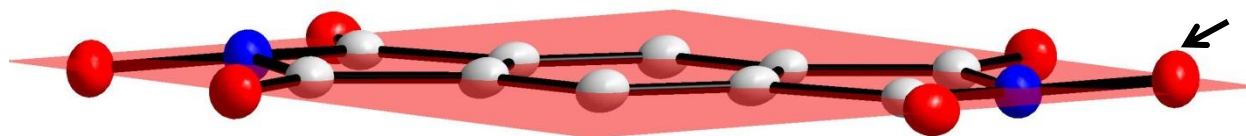


Figure 5.20: Diamond representation of *N,N'*-dihydroxypyromellitic diimide at 50 % probability level, displaying the inserted plane through the central benzene ring and the distortion of the terminal oxygen atoms from the plane. Hydrogen atoms and the water solvate molecules are omitted for clarity.

5.3.5.3 *N,N'*-Bis(2-pyridyl)naphthalene-3,4:7,8-di-carboximide

The title compound (III) is the first reported 2-pyridyl based compound, however two 4-pyridyl polymorphs have been reported by Mizuguchi¹¹ (XII), Trivedi¹⁹ (XIII) and a phenyl derivative by Ofir²⁰ (XIV). A comparison between the crystallographic data, bond distances, the rotation of terminal pyridyl/phenyl rings from the central plane and the distortion of the selected atoms from the naphthalene imide skeleton was done in Table 5.12. The distortion of the nitrogen and carbon is illustrated in Figure 5.21.

¹⁹ D. R. Trivedi, Y. Fujiki, N. Fujita, S. Shinkai, K. Sada, *Chemistry - An Asian Journal*, **2009**, 4, 254–261.

²⁰ Y. Ofir, A. Zelichenok, S. Yitzchaik, *Journal of Materials Chemistry*, **2006**, 16, 2142.

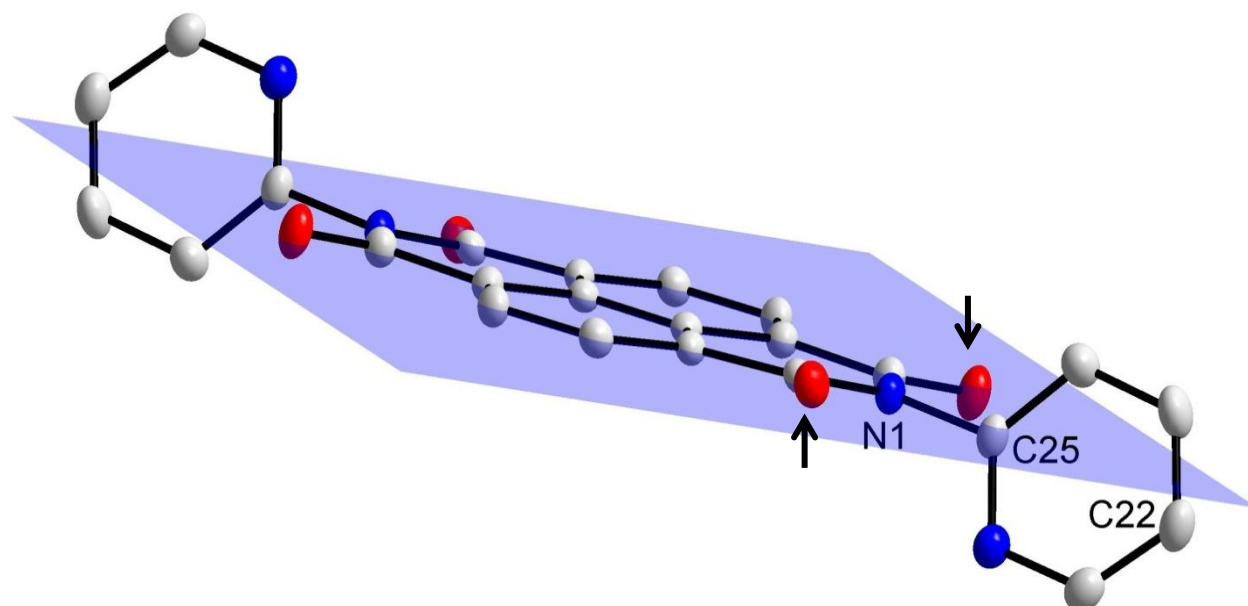


Figure 5.21: Diamond representation of (III) at 50 % probability level, displaying the inserted plane through the central backbone. The arrows indicate where certain atoms lie out of the plane.

Table 5.12: Comparison of the crystal data, bond lengths (Å) and the deviation selected atoms from the central ring plane.

Compound	(III)	(XII)	(XIII)	(XIV)
Crystal system	Monoclinic	Monoclinic	Triclinic	Monoclinic
Space group	P2 ₁ /c	P 2 ₁ /c	P $\bar{1}$	P2 ₁ /n
a (Å)	9.802 (5)	5.3890 (8) Å	7.7593 (6)	5.1360 (6)
b (Å)	8.793 (6)	12.201 (2) Å	9.1374 (7)	7.5227 (8)
c (Å)	11.737 (5)	19.998 (3) Å	9.8283 (8)	25.623 (3)
$\alpha(^{\circ})$	90	90	85.871 (2)	90
$\beta(^{\circ})$	113.212(5)	91.764 (1) $^{\circ}$	80.394 (2)	91.005 (2)
$\gamma(^{\circ})$	90	90	70.766 (2)	90
Volume (Å) ³	929.7	1314.29	648.60	989.83
Z	2	2	1	2
ρ_{calc} (g cm ⁻³)	1.502	1.432	1.486	1.404
Selected bond lengths (Å)				
C17—C16	1.412 (3)	1.404 (6)	1.400 (3)	1.395 (4)
C16—C15	1.379 (2)	1.366 (5)	1.373 (3)	1.376 (4)
C15—C14	1.481 (3)	1.474 (5)	1.479 (2)	1.474 (4)
C14—O2	1.220 (2)	1.247 (4)	1.207 (4)	1.212 (3)
C14—N1	1.400 (2)	1.413 (4)	1.407 (3)	1.409 (3)
N1—C25	1.456 (3)	1.454 (5)	1.446 (3)	1.447 (8)
Distance of terminal selected atoms from central ring plane (Å)				
N1	0.0216 (1)	0.0416 (3)	0.0727 (3)	0.0830 (2)
C25	0.1431 (2)	0.1036 (4)	0.2031 (2)	0.2246 (3)
C22/N2	0.4943 (2)	0.2498 (4)	0.5136 (2)	0.5168 (4)
O1	-0.2058 (1)	-0.0394 (2)	-0.0724 (2)	-0.0703 (1)
O2	0.1168 (1)	0.0593 (3)	0.1218 (1)	0.0127 (2)
Rotation of pyridine/phenyl rings away from planarity ($^{\circ}$)				
Rotation	76.7 (4)	69.2 (5)	59.7 (6)	79.1 (8)

- Indicates that the atom is distorted in the opposite direction of the other atoms

(III) Structure reported in Paragraph 5.3.3, (XII) 4-pyridyl polymorph reported by Mizuguchi,¹¹

(XIII) 4-pyridyl polymorph reported by Trivedi,¹⁹ (XIV) phenyl derivative by Ofir²⁰.

There are no significant differences in the bond lengths for the four compounds, however there are some variations in the rotation of the phenyl rings away from the planar configuration. The phenyl ring of (III) is almost perpendicular to the backbone (80°), while (XIII) is rotated the least (60°). Further investigation into the unit cell contents revealed that the degree of rotation could be linked to hydrogen interactions. The phenyl ring of (XIV) is not involved in any hydrogen interactions, which means it is free to rotate, whereas all the other ligands have interactions which could 'hold' the rings at a certain degree of rotation. These hydrogen interactions are also responsible for the distortion of the oxygen atoms from the planar plane. The biggest distortion from the plane is observed for O2 of (III). This could be due to the fact that O2 is involved in two hydrogen interactions, whereas the other atoms only have one hydrogen interaction. Another phenomenon which is present in these compounds is the upward and downward bending of the pyridyl rings on opposite sides of the compounds. C25 of (XII) is tilted away from the plane with $\sim 0.25 \text{ \AA}$, which is about half that of the other three compounds. The reason for this tilt is unknown, but could be the result of the strain on the five membered ring or the electronic effects of the two carbonyl species on either side of the nitrogen atom. There seems to be no link between the degree of rotation and the bending of the atoms from the plane.

5.3.5.4 2-Amino-4,6-dichloropyrimidine acetic acid solvate

The structure of 2-Amino-4,6-dichloropyrimidine (IV) reported in paragraph 5.3.4 crystallised in a triclinic $P\bar{1}$ space group. However, this is not the first reported structure for this compound. Two monoclinic polymorphs, without the acetic acid solvate molecules, have been reported by Clews & Cochran¹² (XV) and Fun *et al.*¹³ (XVI). Additionally the crystal structure of the unsubstituted pyrimidine was reported by Scheinbeim *et al.*²¹ (XVII). A comparison between the crystallographic data, bond distances and angles was done in Table 5.13. The comparison of the four different structures did not yield any major abnormalities.

²¹ J. Scheinbeim, E. Schempp, *Acta Crystallographica Section B Structural Crystallography and Crystal Chemistry* **1976**, 32, 607–609.

Table 5.13: Comparison of the crystal data, bond lengths (Å) and bond angles (°) for (IV), (XV), (XVI) and (XVII).

Compound	(IV)	(XV)	(XVI)	(XVII)
Crystal system	Triclinic	Monoclinic	Monoclinic	Orthorhombic
Space group	$P\bar{1}$	$P2_1/a$	$C2/c$	$Pcab$
a (Å)	5.1370 (2)	16.447 (5)	32.060 (4)	14.862 (2)
b (Å)	10.7670 (4)	3.845 (5)	3.8045 (6)	10.884 (2)
c (Å)	11.1620 (4)	10.283 (5)	21.302 (3)	5.633 (1)
α (°)	93.331 (2)	90	90	90
β (°)	96.056 (2)	107.97	102.193	90
γ (°)	95.870 (2)	90	90	90
Z	2	4	16	8
Selected bond lengths (Å)				
Cl12—C14	1.732 (1)	1.806 (4)	1.731 (2)	-----
N11—C14	1.317 (3)	1.336 (1)	1.357 (3)	1.352 (6)
N13—C11	1.329 (2)	1.267 (2)	1.317 (3)	1.354 (1)
C12—C13	1.382 (6)	1.396 (3)	1.376 (2)	1.389 (7)
Selected bond angles (°)				
N12—C12—Cl11	115.0 (8)	118.0 (3)	116.1 (2)	-----
N11—C14—C13	125.5 (4)	131.5 (1)	125.2 (2)	123.4 (4)
C13—C14—Cl12	118.5 (2)	110.0 (1)	114.3 (2)	-----
N11—C11—N12	124.2 (9)	126.8 (5)	125.2 (2)	126.8 (5)

(IV) Structure reported in Paragraph 5.3.4, (XV) Monoclinic polymorphs reported by Clews & Cochran,¹² (XVI) Monoclinic polymorphs reported Fub,¹³ (XVII) Unsubstituted pyrimidine was reported by Scheinbeim.²¹

There are some minor differences in the bond lengths, but the most unexpected difference is seen in the amino N-C bond for (XV) which is 0.060 Å shorter than the other counterparts. The reason for this is unclear, but could be due to the lesser degree of hydrogen interactions that are present in this structure. The same structure also shows some inconsistencies in bond angles. The C13—C14—Cl12 bond angle is substantially less than the other two polymorphs. This could be attributed to the change in electronic properties as a result of the shorter N-C bond that was just mentioned. Similar ring motifs were seen in all of the structures, although only the structures of (IV) and (XV) have the hydrogen interactions lying within a plane.

5.4 Conclusions

In this section, four new potential planar bridging ligands were investigated using single crystal X-ray diffraction. Some vital information with regards to the planarity and electronic nature of these ligands were obtained, which have been discussed in detail above.

Heprazine (I) was found to be a hard ligand as its nitrogen atoms are so electron poor that the nitrogen atoms form a pseudo-sp³ configuration. This directly impacts the planarity of the ligand, as it starts to contort into various positions. Interestingly, these contortions have no impact on the bond distances throughout the molecule and other polymorphs. *N,N'*-Dihydroxypyromellitic diimide (II) also displayed some interesting electronic effects when looking at the planarity of the compound. The degree of bending by the terminal oxygen could be attributed to the electronic environment of the benzene ring, which also suggested that this ligand is incredibly hard as there are three oxygen atoms and a nitrogen atom in close proximity. This bending of the oxygen atoms was accentuated further by hydrogen bonding in the unit cell.

The crystal structure of dpbpt (III) showed that the ligand is not completely planar and prefers to have its terminal pyridyl ring rotated away from the plane of the central backbone. No link between the degree of rotation and the electronic environment could be drawn, but hydrogen interactions seem to be the prevailing factor. Similar bending of the atom attached to the nitrogen atoms was observed for *N,N'*-dihydroxypyromellitic diimide (II) which suggests that all three ligands, as discussed here, have electron poor donor capabilities. Consequently, the coordination of harder metal species should yield the best coordination results.

Finally the crystal structure of the synthon 2-amino-4,6-dichloropyrimidine (IV) was reported to illustrate the interesting hydrogen interactions that are observed for this compound. The hydrogen interactions that all lie within a plane show the potential of having these types of derivatives as bridging ligands. By exploiting these properties, the compounds could be used to grow single crystalline layers on the surface of heterogeneous supports, although there are practical limitations that have not been considered. All the ligands displayed show very good planar geometries, which has been a pre-requisite for the ligand design. These ligand systems were utilised in further synthetic steps to produce the metal complexes which will be further investigated for catalytic activity in selected processes.

6 CRYSTALLOGRAPHIC STUDY OF PLATINUM(II) AND PALLADIUM(II) COMPLEXES

6.1 Introduction

In order to construct bridging ligands that can accommodate multiple metal centres, two different strategies were followed. The first involved the synthesis of diamide type ligands that have a fairly unfamiliar bonding mode and the second was centred around the functionalization of 1,10-phenanthroline (phen) of which the coordination chemistry is well known and understood. Difficulties were experienced in the characterisation of the diamide compounds due to solubility limitations. As a result no crystal structures of these types of compounds were isolated and investigated.

Phen type compounds have been extensively characterised by the use of single crystal X-ray diffractometry studies.¹ These studies have been limited to the unfunctionalized phen ligands. As a result, palladium and platinum were coordinated to ‘intermediate’ ligands that were eventually used to construct the larger bridging compounds. Although many of the palladium and platinum complexes were obtained and characterised through other analytical methods, only the crystal structures of *cis*-[Pd(C₁₂H₈N₄O₂)Cl₂].2DMSO (I) and *cis*-[Pt(C₁₂H₈N₄O₂)Cl₂].2DMSO (II) were obtained and are discussed here. These two crystal structures are complete isomorphs and a comparison between these compounds are also presented.

Unfortunately, the coordination of metal species to the larger planar bridging ligands, resulted in compounds with poor solubility. This drastically reduced the possibility of growing and obtaining suitable crystals, although numerous attempts were made.

¹ F.H. Allen, *Acta Crystallographica*, **2002**, B58, 380.

6.2 Crystallographic Study of Selected Metal Complexes

Table 6.1: Crystal Data parameters for PdCl₂(5-nitro-6-amino-phen).2DMSO (I) and [PtCl₂(5-nitro-6-amino-phen).2DMSO (II).

Compound	(I)	(II)
Empirical formula	C ₁₆ H ₂₀ Cl ₂ N ₄ O ₄ Pd S ₂	C ₁₆ H ₂₀ Cl ₂ N ₄ O ₄ Pt S ₂
F.W.	573.80	662.47
Temperature K	100	100
Crystal system, Space group	Triclinic, $P\bar{1}$	Triclinic, $P\bar{1}$
a (Å)	8.998(5)	9.028(2)
b (Å)	10.235(5)	10.253(2)
c (Å)	13.555(5)	13.410(2)
α (°)	101.706(5)	101.79(2)
β (°)	101.813(5)	101.55(1)
γ (°)	114.476(5)	114.03(3)
Volume (Å ³)	1052.5(9)	1052.6(6)
Z	2	2
ρ_{calc} (g cm ⁻³)	1.811	2.090
μ (mm ⁻¹)	1.365	7.149
F(000)	576	640
Crystal Colour	Yellow	Yellow
Morphology	Rhombohedral	Cuboid
Crystal size (mm)	0.147 x 0.081 x 0.078	0.035x0.062x0.198
Theta range (°)	2.31 to 28.39	2.30 to 28.29
Completeness %	98.9	98.8
Limiting indices	-12<= h <=11 -8<= k <=13 -18<= l <=17	-12<= h <=13 -11<= k <=11 -15<= l <=15
Reflections collected	21248	14202
Unique reflections	5200	5161
R_{int}	0.0327	0.0241
Refinement method	Full-matrix least- squares on F^2	Full-matrix least-squares on F^2
Data / restraints / parameters	5200 / 0 / 274	5161 / 0 / 270
Goodness-of-fit on F^2	1.031	1.029
Final R indices [$I > 2\sigma(I)$]	R1 = 0.0272 wR2 = 0.0545	R1 = 0.0200 wR2 = 0.0462
R indices (all data)	R1 = 0.0364 wR2 = 0.0583	R1 = 0.0225 wR2 = 0.0473
$\Delta\rho_{\text{min}}$; $\Delta\rho_{\text{max}}$ (e.Å ⁻³)	0.780 and -0.529	1.638 and -0.963

6.2.1 Crystal Structure of *cis*-[Pd(C₁₂H₈N₄O₂)Cl₂].2DMSO (I)

Yellow crystals of the title compound (I) were obtained according to the procedure described in Paragraph 4.4.5. The compound crystallised in the triclinic space group $P\bar{1}$, with a palladium complex molecule and two DMSO solvate molecules in the asymmetric unit. The graphical representation and the numbering scheme are illustrated in Figure 6.1 and selected bond lengths and angles are reported in Table 6.2. Torsion angles are given in Table 6.3. Atomic coordinates, anisotropic displacement parameters, all bond distances and angles are reported in Appendix A.

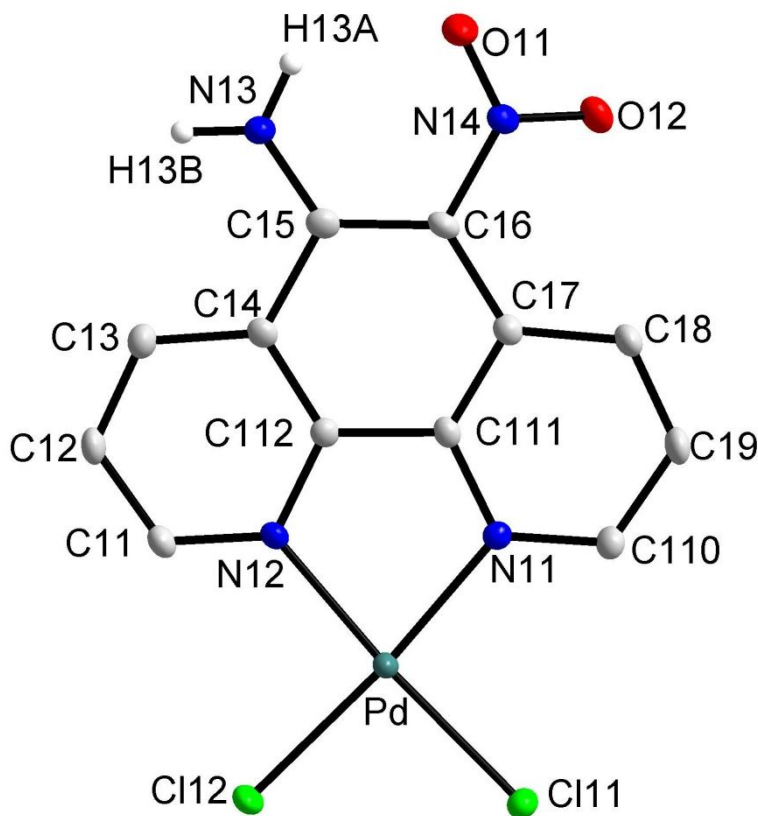


Figure 6.1: Diamond representation of [Pd(C₁₂H₈N₄O₂)Cl₂].2DMSO (I) at 50 % probability level, displaying the numbering scheme employed: the first digit represents the ring and the second digit the number of the atom in the ring. Solvent molecules and hydrogen atoms are omitted for clarity.

Table 6.2: Selected geometric parameters (Å, °) for [Pd(C₁₂H₈N₄O₂)Cl₂].2DMSO (I).

Selected bond lengths (Å)		Selected Bond angles (°)	
C11—N12	1.330 (3)	C111—N11—Pd01	113.6 (1)
C11—C12	1.387 (3)	C11—N12—Pt01	127.3 (2)
C111—C112	1.435 (3)	C11—N12—C112	118.9 (2)
N14—O11	1.243 (3)	O11—N14—O12	120.3 (2)
Cl11—Pd01	2.2920 (9)	N12—Pd01—N11	80.87 (7)
Cl12—Pd01	2.2861 (13)	N12—Pd01—Cl12	94.25 (5)
N11—Pd01	2.024 (2)	N11—Pd01—Cl12	175.04 (5)
N12—Pd01	2.0173 (19)	N12—Pd01—Cl11	174.73 (5)

The molecular structure of *cis*-[Pd(C₁₂H₈N₄O₂)Cl₂].2DMSO (I) consists of a palladium(II) centre that is coordinated to 5-nitro-6-amino-1,10-phenanthroline. The complex is neutral as the two chlorido ligands compensate for the 2+ charge on the metal. The complex molecule crystallised with two dimethylsulfoxide solvate molecules. The geometry of the palladium centre is distorted from the square planar geometry, which is illustrated by the N(12)—Pd(01)—N(11) angle of 80.9 °. The square planar nature of the palladium metal centre resulted in the formation of a planar complex molecule. One of the chlorido atoms deviates more significantly from the square planar configuration than the other, as shown by the torsion angles in Table 6.3.

Table 6.3: Selected torsion angles (°) for [Pd(C₁₂H₈N₄O₂)Cl₂].2DMSO (I).

Selected torsion angles (°)	
Cl11 – Pd – N11 – C110	5.1(2)
Cl12 – Pd – N12 – C11	0.5(2)

Intra- and intermolecular hydrogen interactions are illustrated in Figure 6.2 and presented in Table 6.4. Intramolecular hydrogen contacts are found between the protons on the phenanthroline ring, with the chlorido ligands found on the palladium(II) centre and with the oxygens from the nitro group. An interaction exists between the nitro group from one of the complex molecules with the carbon atoms from another phenanthroline ring. The amino group also has hydrogen interactions with DMSO solvent molecules.

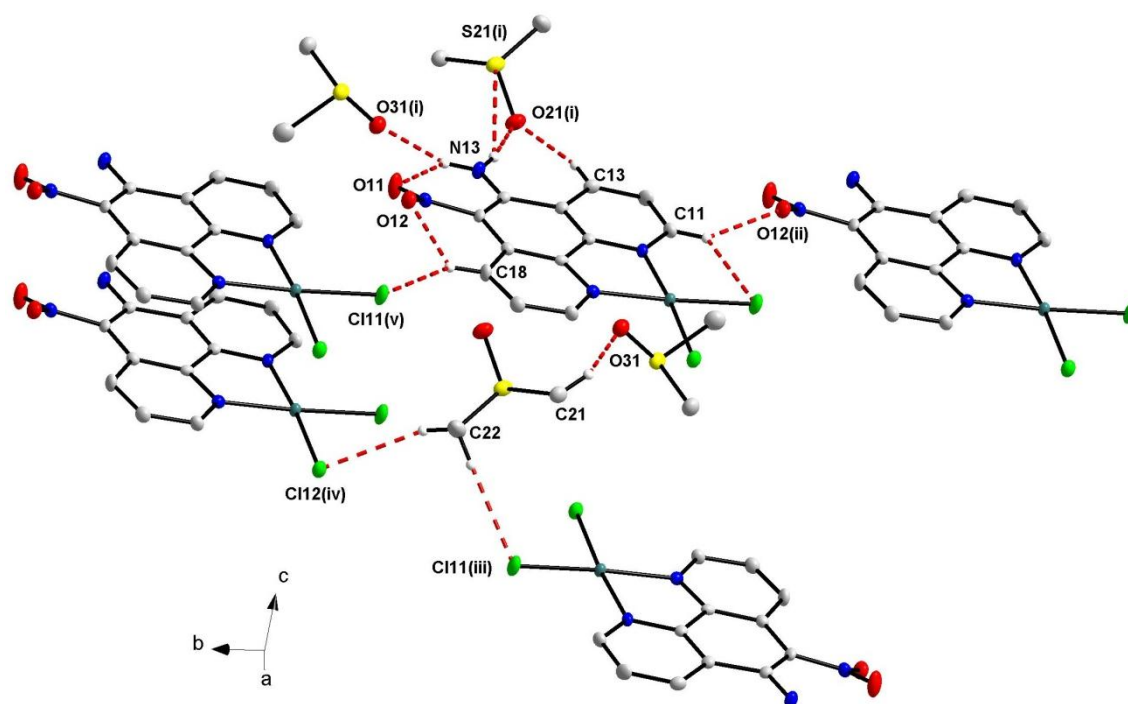


Figure 6.2: Graphical representation of the most important intermolecular H-bond interactions for $[\text{Pd}(\text{C}_{12}\text{H}_8\text{N}_4\text{O}_2)\text{Cl}_2]\cdot 2\text{DMSO}$ (I). The red fragmented lines indicate the intermolecular hydrogen interactions. Symmetry codes: (i) $-x+2, -y+2, -z+1$; (ii) $x, y-1, z$; (iii) $x, y+1, z$; (iv) $x+1, y+1, z$; (v) $-x+1, -y+1, -z$.

Table 6.4: Hydrogen interactions ($\text{\AA}, ^\circ$) for $[\text{Pd}(\text{C}_{12}\text{H}_8\text{N}_4\text{O}_2)\text{Cl}_2]\cdot 2\text{DMSO}$ (I).

D—H \cdots A	D—H	H \cdots A	D \cdots A	D—H \cdots A
N13—H13A \cdots O11	0.85 (3)	2.01 (3)	2.596 (3)	126 (2)
N13—H13A \cdots O31 ⁱ	0.85 (3)	2.20 (3)	2.930 (3)	145 (2)
N13—H13B \cdots S21 ⁱ	0.90 (3)	2.77 (3)	3.472 (2)	136 (2)
N13—H13B \cdots O21 ⁱ	0.90 (3)	1.96 (3)	2.841 (3)	166 (3)
C11—H11 \cdots Cl11	0.93	2.65	3.233 (3)	122
C11—H11 \cdots O12 ⁱⁱ	0.93	2.4	3.147 (3)	138
C13—H13 \cdots O21 ⁱ	0.93	2.34	3.248 (3)	167
C18—H18 \cdots Cl11 ⁱⁱⁱ	0.93	2.76	3.484 (2)	136
C18—H18 \cdots O12	0.93	2.15	2.709 (3)	118
C21—H21A \cdots O31	0.96	2.47	3.271 (3)	141
C22—H22C \cdots Cl12 ^{iv}	0.96	2.79	3.662 (3)	151
C22—H22B \cdots Cl11 ^v	0.96	2.76	3.715 (3)	172

Symmetry codes: (i) $-x+2, -y+2, -z+1$; (ii) $x, y-1, z$; (iii) $x, y+1, z$; (iv) $x+1, y+1, z$; (v) $-x+1, -y+1, -z$.

The H-bond intermolecular interactions appear to be the dominant factor in the packing pattern of the $[\text{Pd}(\text{C}_{12}\text{H}_8\text{N}_4\text{O}_2)\text{Cl}_2]\cdot 2\text{DMSO}$ complex as seen in Figure 6.3.

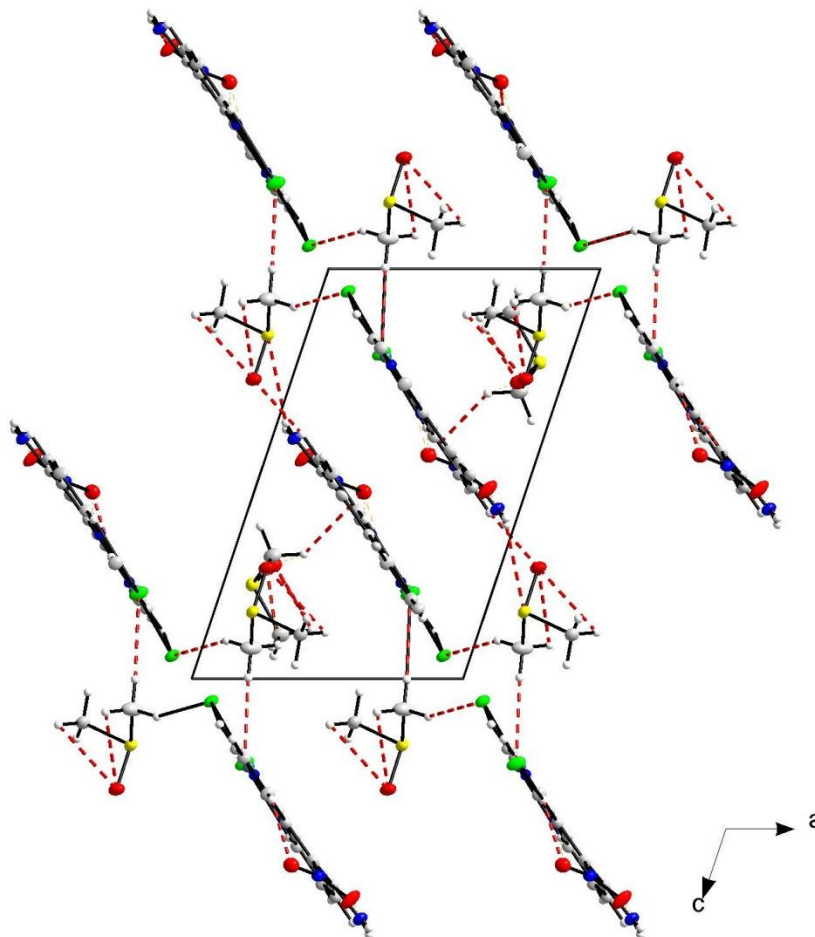


Figure 6.3: Graphical representation of the intermolecular H-bond interactions for $[\text{Pd}(\text{C}_{12}\text{H}_8\text{N}_4\text{O}_2)\text{Cl}_2]\cdot 2\text{DMSO}$ (I) along the b-axis. The red fragmented lines indicate the intermolecular hydrogen bonding between the $[\text{Pd}(\text{C}_{12}\text{H}_8\text{N}_4\text{O}_2)\text{Cl}_2]\cdot 2\text{DMSO}$ (I) molecules.

The packing of the $[\text{Pd}(\text{C}_{12}\text{H}_8\text{N}_4\text{O}_2)\text{Cl}_2]$ molecules within the unit cell, consists of layers perpendicular to the ac plane. The layers are made up of two rows of complex molecules, with the chlorine ends facing one another (see Figure 6.4). DMSO solvate molecules are found in-between the complex molecules, with the oxygen end interacting with the amino end and the methyl groups interacting with the chlorido side of another molecule. Interestingly, although all the DMSO molecules seem to be in a row, there is one molecule that ‘jumps out’ of the row (see Figure 6.4). This is because the molecule is rotated more than the other solvate molecules. This can possibly be attributed to the hydrogen interactions that are present. The platinum isomorph is almost identical to the palladium complex in terms of bond angles and lengths. A more

comprehensive comparison is discussed between the isomorphs and other complexes in Paragraph 6.2.3.

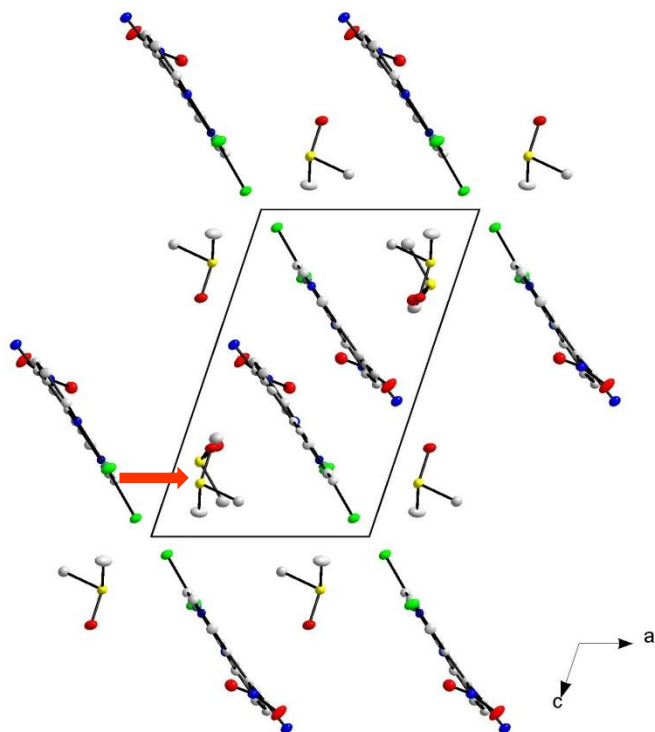


Figure 6.4: Diamond representation of [Pd(C₁₂H₈N₄O₂)Cl₂].2DMSO (I), at 50 % probability level, displaying the packing in the unit cell along the b-axis. Hydrogen atoms are omitted for clarity. The orange arrow shows one of the DMSO molecules that is rotated more than the other molecules.

6.2.2 Crystal Structure of *cis*-[Pt(C₁₂H₈N₄O₂)Cl₂].2DMSO (II)

Yellow crystals of the title compound (II) were obtained according to the procedure described in Paragraph 6.2.2. The compound crystallised in a triclinic $P\bar{1}$ space group, with a platinum complex molecule accompanied by two DMSO solvate molecules in the asymmetric unit. The graphical representation and the numbering are illustrated in Figure 6.5. Selected bond lengths and angles are represented in Table 6.5 and torsion angles are given in Table 6.6. Atomic coordinates, anisotropic displacement parameters, all bond distances and angles are given in Appendix A.

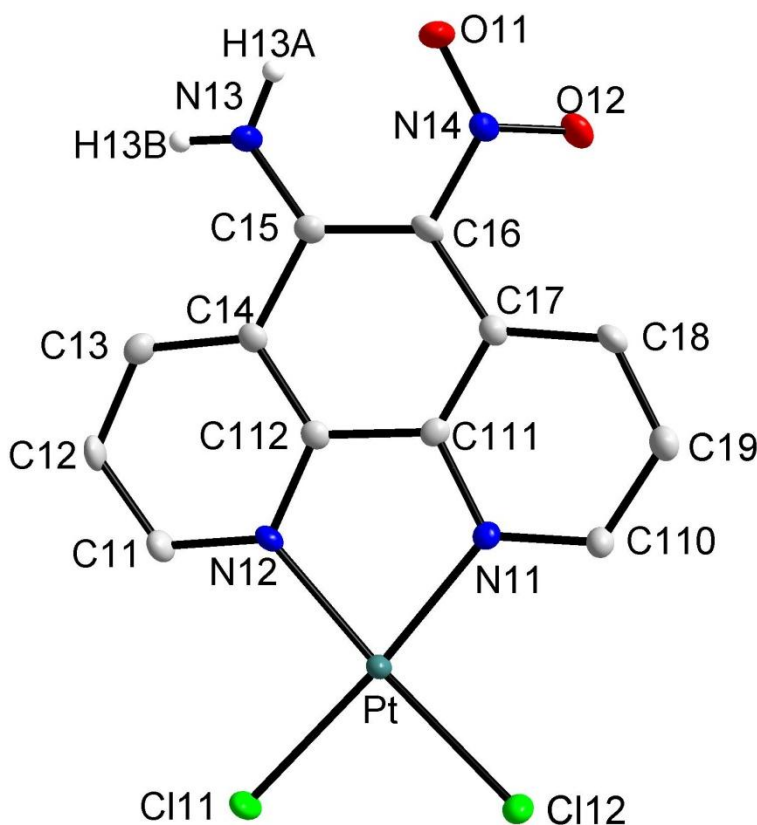


Figure 6.5: Diamond representation of [Pt(C₁₂H₈N₄O₂)Cl₂].2DMSO (II) at 50 % probability level, displaying the numbering scheme employed: the first digit represents the ring and the second digit the number of the atom in the ring. The DMSO solvate molecules and hydrogen atoms are omitted for clarity.

Table 6.5: Selected geometric parameters (Å, °) for [Pt(C₁₂H₈N₄O₂)Cl₂].2DMSO (II).

Selected bond lengths (Å)		Selected Bond angles (°)	
C11—N12	1.333 (3)	C111—N11—Pt01	114.05 (18)
C13—C14	1.401 (4)	C11—N12—Pt01	127.23 (18)
C111—C112	1.435 (4)	C11—N12—C112	118.5 (2)
C112—N12	1.363 (3)	O11—N14—O12	120.8 (2)
N14—O11	1.241 (3)	N12—Pt01—N11	80.81 (9)
N11—Pt1	2.013 (2)	N12—Pt01—Cl12	94.71 (7)
N12—Pt1	2.008 (2)	N11—Pt01—Cl12	175.20 (6)
Cl11—Pt1	2.2960 (7)	N12—Pt01—Cl11	94.98 (6)
Cl12—Pt1	2.3013 (7)	C111—N11—Pt01	175.48 (6)
		Cl(12) —Pt(01) —Cl(11)	89.52 (2)

The molecular structure of *cis*-[Pt(C₁₂H₈N₄O₂)Cl₂].2DMSO (II) consists of a platinum(II) centre that is coordinated to 5-nitro-6-amino-1,10-phenanthroline. The complex is neutral as the two chlorido ligands compensate for the 2+ charge on the metal centre. The complex molecule is accompanied by two dimethylsulfoxide solvate molecules. The geometry of the platinum centre is slightly distorted from the square planar geometry. This is illustrated by the N(12) —Pt(01) —N(11) and Cl(12) —Pt(01) —Cl(11) angles that are reported as 80.8 ° and 89.52 ° respectively. The square planar nature of the platinum metal centre results in the formation of an almost planar molecule. One of the chlorido atoms deviates slightly from this planarity as indicated by the torsion angles in Table 6.6.

Table 6.6: Selected torsion angles (°) for [Pt(C₁₂H₈N₄O₂)Cl₂].2DMSO (II).

Selected torsion angles (°)	
Cl11 – Pt – N11 – C110	4.4 (2)
Cl12 – Pt – N12 – C11	0.42(2)

Intra and intermolecular hydrogen interactions are illustrated in Figure 6.6 and presented in Table 6.7. Intramolecular hydrogen contacts are found between the protons on the phenanthroline ring with the chlorido ligands found on the platinum(II) center as well as with the oxygens from the nitro group. An interaction exists between the nitrogen from one of the complex molecules with the carbon atoms from another phenanthroline ring. The DMSO solvent molecules have hydrogen interactions with the amino group and the chlorido ligands.

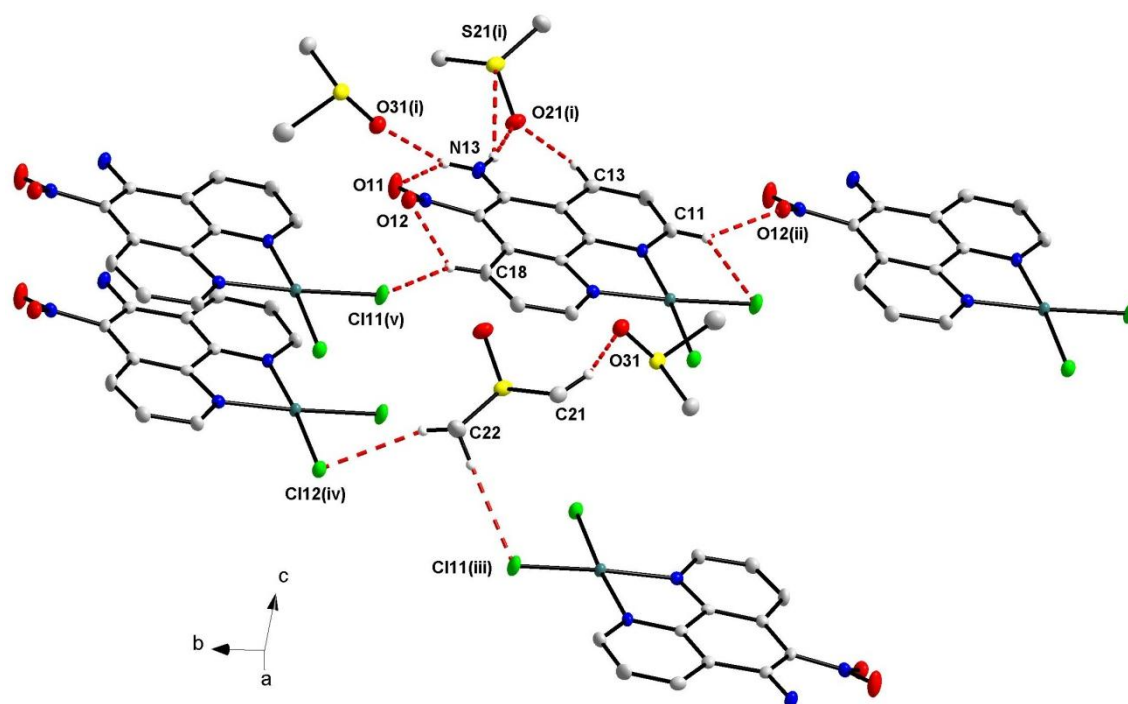


Figure 6.6: Graphical representation of the intermolecular H-bond interactions for $[\text{Pt}(\text{C}_{12}\text{H}_8\text{N}_4\text{O}_2)\text{Cl}_2]\cdot 2\text{DMSO}$ (II). The red fragmented lines indicate the intermolecular hydrogen interactions. Symmetry codes: (i) $-x+2, -y+2, -z+1$; (ii) $x, y-1, z$; (iii) $x, y+1, z$; (iv) $x+1, y+1, z$; (v) $-x+1, -y+1, -z$.

Table 6.7: Hydrogen interactions ($\text{\AA}, ^\circ$) for $[\text{Pt}(\text{C}_{12}\text{H}_8\text{N}_4\text{O}_2)\text{Cl}_2]\cdot 2\text{DMSO}$ (II).

D—H \cdots A	D—H	H \cdots A	D \cdots A	D—H \cdots A
N13—H13A \cdots O11	0.86 (3)	2.00 (3)	2.586 (4)	124 (3)
N13—H13A \cdots O31 ⁱ	0.86 (3)	2.17 (3)	2.923 (3)	146 (3)
N13—H13B \cdots S21 ⁱ	0.81 (4)	2.79 (3)	3.472 (3)	142 (3)
N13—H13B \cdots O21 ⁱ	0.81 (4)	2.04 (4)	2.834 (3)	167 (3)
C11—H11 \cdots Cl11	0.93	2.66	3.244 (3)	122
C11—H11 \cdots O12 ⁱⁱ	0.93	2.39	3.151 (3)	139
C13—H13 \cdots O21 ⁱ	0.93	2.34	3.254 (3)	166
C18—H18 \cdots Cl11 ⁱⁱⁱ	0.93	2.76	3.498 (3)	137
C18—H18 \cdots O12	0.93	2.15	2.714 (3)	118
C21—H21A \cdots O31	0.96	2.47	3.279 (4)	142
C22—H22A \cdots Cl12 ^{iv}	0.96	2.77	3.639 (3)	152
C22—H22C \cdots Cl11 ^v	0.96	2.75	3.705 (3)	177

Symmetry codes: (i) $-x+2, -y+2, -z+1$; (ii) $x, y-1, z$; (iii) $x, y+1, z$; (iv) $x+1, y+1, z$; (v) $-x+1, -y+1, -z$.

The H-bond intermolecular interactions appear to be the dominant factor in the packing pattern of $[\text{Pt}(\text{C}_{12}\text{H}_8\text{N}_4\text{O}_2)\text{Cl}_2]\cdot 2\text{DMSO}$ as seen in Figure 6.7.

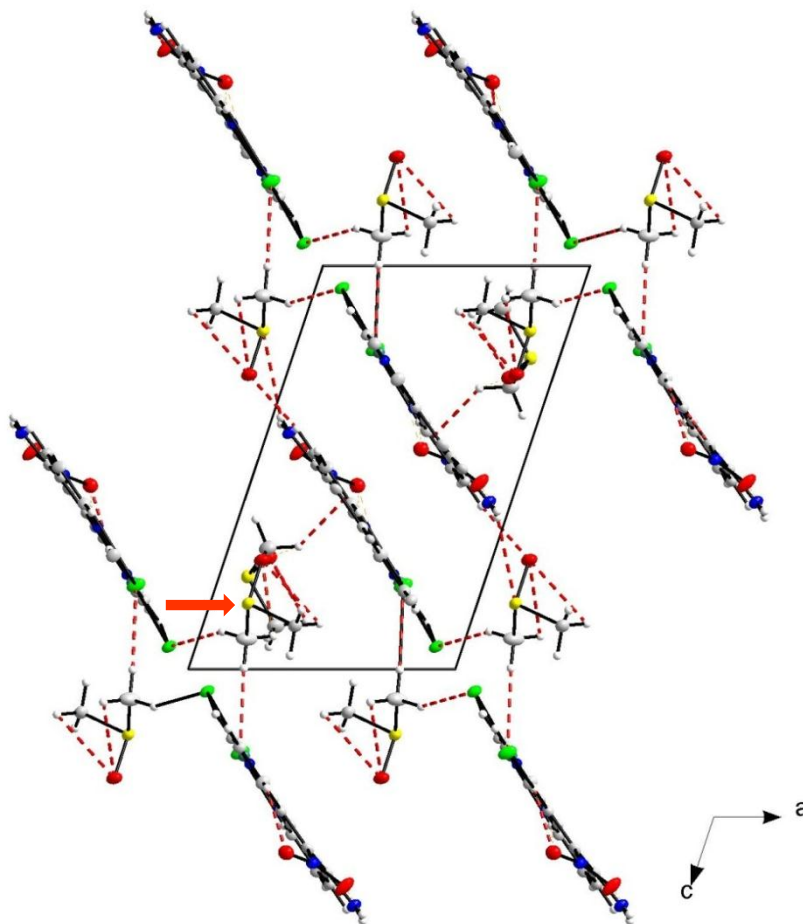


Figure 6.7: Graphical representation of the intermolecular H-bond interactions for $[\text{Pt}(\text{C}_{12}\text{H}_8\text{N}_4\text{O}_2)\text{Cl}_2]\cdot 2\text{DMSO}$ (II) along the b-axis. The red fragmented lines indicate the intermolecular hydrogen bonding between the $[\text{Pt}(\text{C}_{12}\text{H}_8\text{N}_4\text{O}_2)\text{Cl}_2]\cdot 2\text{DMSO}$ (II) molecules. The orange arrow shows one of the DMSO molecules that is rotated more than the other molecules.

The packing of the $[\text{Pt}(\text{C}_{12}\text{H}_8\text{N}_4\text{O}_2)\text{Cl}_2]$ molecules within the unit cell, consists of layers perpendicular to the ac plane. The layers are made up of two rows of complex molecules with the chlorine ends facing one another (see Figure 6.7). Between the complex molecules, DMSO solvent oxygen atoms interact with the amino end while the methyl part interacts with the chlorido side from the next molecule. In a similar fashion to the palladium isomorph, all the DMSO molecules lie in a row with one molecule that is rotated more than the other solvate molecules (see Figure 6.8). This can possibly be attributed to the hydrogen interactions which are present.

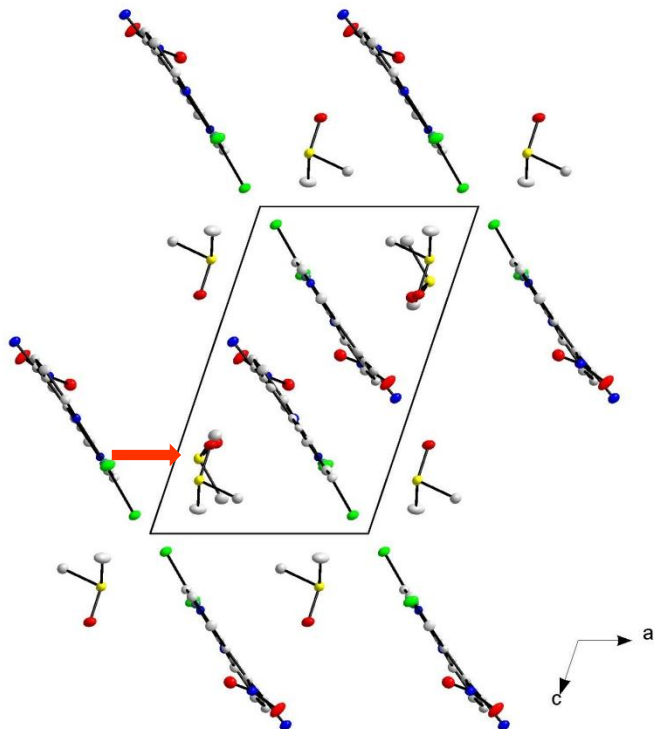


Figure 6.8: Diamond representation of $[\text{Pt}(\text{C}_{12}\text{H}_8\text{N}_4\text{O}_2)\text{Cl}_2]\cdot 2\text{DMSO}$ (2), at 50 % probability level, displaying the packing in the unit cell along the b-axis and the deviation of one of the DMSO solvate molecules. Hydrogen atoms are omitted for clarity. The orange arrow shows one of the DMSO molecules that is rotated more than the other molecules.

6.2.3 Comparison of Crystal Structures

In this chapter, two crystal structures, one of palladium (I) and one of platinum (II) coordinated to 5-nitro-6-amino-1,10-phenanthroline were reported. Unfortunately, no other crystal structures of this particular ligand are available on the Cambridge Structural Database. As a result, the reported structures were compared to the palladium and platinum 1,10-phenanthroline derivatives published by Ha² (III) and Grzesiak *et al.*³ (IV) respectively. A closer investigation into the crystallographic data and selected bond lengths, angles and torsion angles are reported in Table 6.8.

² K. Ha, *Acta Crystallographica Section E Structure Reports Online*, **2009**, 66, m38–m38.

³ A. L. Grzesiak, A. J. Matzger, *Inorganic Chemistry*, **2007**, 46, 453–457.

Table 6.8: Comparison of the crystal data, bond lengths (Å) and torsion angles for (I), (II), (III) and (IV).

Compound	(I)	(II)	(III)	(IV)
Crystal system	Triclinic	Triclinic	Monoclinic	Monoclinic
Space group	$P\bar{1}$	$P\bar{1}$	$P2_1/c$	$P2_1/c$
a (Å)	8.998 (5)	9.028 (2)	9.6170 (8)	9.602 (1)
b (Å)	10.235 (2)	10.253 (2)	17.1402 (14)	17.119 (5)
c (Å)	13.56 (6)	13.410 (3)	7.2529 (6)	7.339 (5)
$\alpha(^{\circ})$	101.71 (1)	101.79 (2)	90	90
$\beta(^{\circ})$	101.81 (3)	101.55 (1)	109.31 (4)	109.48 (2)
$\gamma(^{\circ})$	114.48 (1)	114.03 (3)	90	90
Volume (Å) ³	1052.5 (9)	1052.6 (6)	1128.26 (2)	1137.61 (5)
Z	2	2	4	4
ρ_{calc} (g cm ⁻³)	1.811	2.090	2.105	2.605
Selected bond lengths (Å)				
C11—N12	1.330 (3)	1.333 (3)	1.327 (9)	1.365 (7)
C11—C12	1.387 (3)	1.401 (4)	1.392 (1)	1.405 (3)
C111—C112	1.435 (3)	1.435 (4)	1.441(1)	1.417 (1)
N14—O11	1.243 (3)	1.241 (3)	-----	-----
N11—Pd/Pt	2.024 (2)	2.013 (2)	2.035 (6)	2.006 (6)
Cl11—Pd/Pt	2.292 (1)	2.301 (4)	2.283 (6)	2.292 (3)
Selected Bond angles (°)				
C111—N11—Pd/Pt	113.6 (1)	114.1 (2)	112.2 (4)	112.7 (2)
C11—N12—C112	118.9 (2)	118.5 (2)	118.4 (7)	117.3 (2)
O11—N14—O12	120.3 (2)	120.8 (2)	-----	-----
N12—Pd/Pt—N11	80.9 (2)	80.8 (9)	81.5 (2)	81.5 (3)
N12—Pd/Pt—Cl12	94.25 (5)	94.71 (7)	93.2 (2)	94.4 (2)
Cl12—Pd/Pt—Cl11	90.27 (3)	89.52 (2)	91.4 (3)	90.7 (3)
Selected torsion angles (°)				
Cl11 – Pd – N11 – C110	5.1 (2)	4.4 (2)	4.4 (7)	4.05 (7)
Cl12 – Pd – N12 – C11	0.5 (2)	0.42 (2)	1.4 (6)	1.2 (3)

(I) PdCl₂(5-nitro-6-amino-phen), (II) PtCl₂(5-nitro-6-amino-phen), (III) PdCl₂(phen), (IV) PtCl₂(phen)

The crystallographic data, bond lengths and angles compare well with no major abnormalities. In fact, it would seem that in both cases the platinum and palladium complexes of 5-nitro-6-amino-1,10-phenanthroline and 1,10-phenanthroline are complete isomorphs. There are one or two minor differences in the unit cell parameters that prevent completely identical values. This could be attributed to the difference in size between the platinum and palladium metal centres. An overlay of the asymmetric unit contents for palladium (I) (red) and the platinum (II) (blue) complexes of 5-nitro-6-amino-1,10-phenanthroline was performed. This overlay, without the solvent molecules of the complex molecules, is presented in Figure 6.9. The overlay confirms the isomorphism of these two structures (RMS error = 0.041). It is clear that on the complex molecule itself there are virtually no differences, while the only minor difference is found between the DMSO solvent molecules.

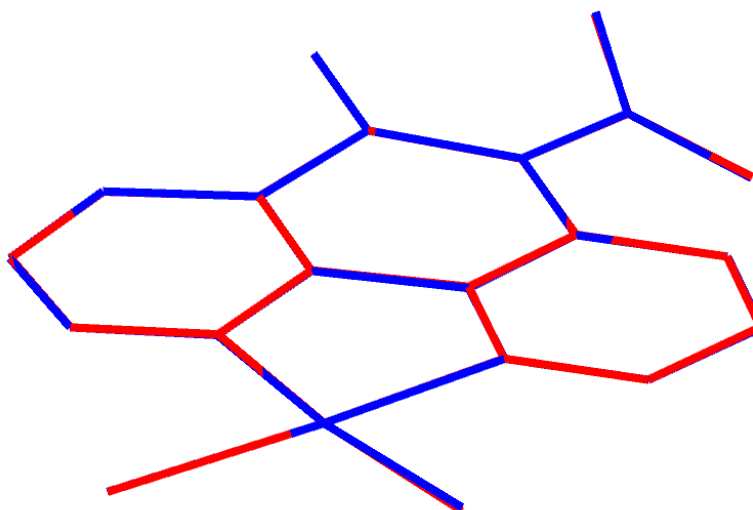


Figure 6.9: Overlay of the asymmetric units of palladium and platinum nitro-6-amino-1,10-phenanthroline DMSO solvate crystal structures.

In order to display the slight curvature in the 5-nitro-6-amino-1,10-phenanthroline ligand an overlay was done between the 5-nitro-6-amino-1,10-phenanthroline and 1,10-phenanthroline structures in Figure 6.10. The red and blue overlay between (I) and (II) shows that the platinum and palladium structures are virtually identical (RMS error = 0.013). The same is found for the 1,10-phenanthroline complexes, which are indicated in the black and yellow (III) and (IV) comparison (RMS error = 0.035). There are differences in the planarity and angles of (I) and (III) as seen in the red and black overlay (RMS error = 0.11).

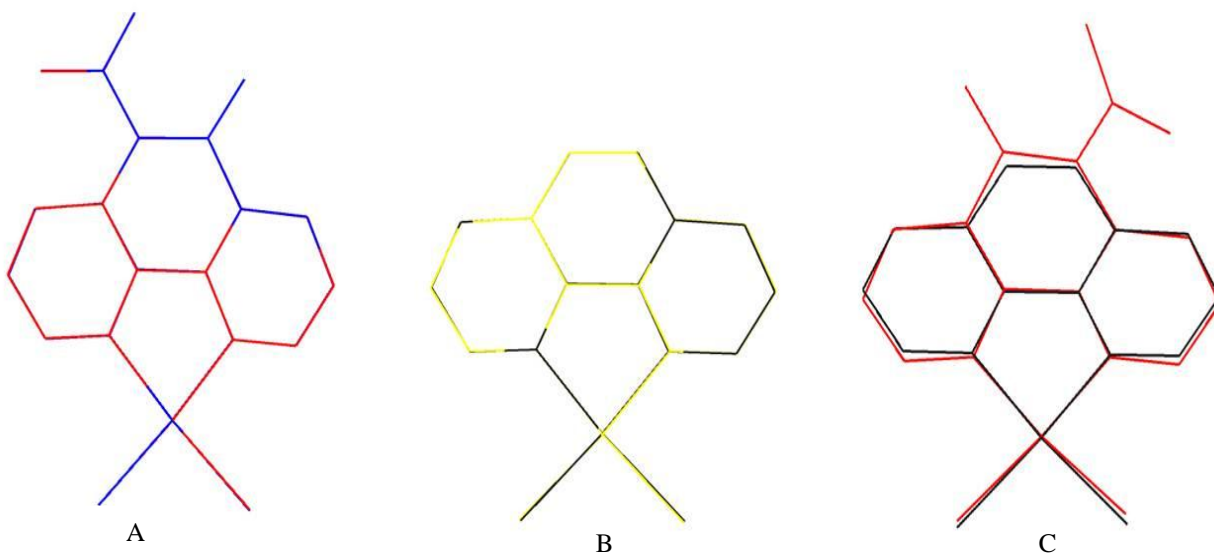


Figure 6.10: Overlay of the palladium and platinum complexes of 5-nitro-6-amino-1,10-phenanthroline, 1,10-phenanthroline and an overlay between the two different ligands. A presents the overlay between (I) and (II), B between (III) and (IV) and C between (I) and (III).

The comparison between the reported crystals and those found in literature confirmed that there are no major influences of the functionalization of the phen ligand and that the coordination mode remains unchanged for these types of compounds. A slight curvature was observed in the 5-nitro-6-amino-1,10-phenanthroline ligand, but this anomaly had no influence on the coordination of the square planar metal species. Unfortunately none of the crystal structures of the larger molecules could be obtained to gain further insight into these compounds.

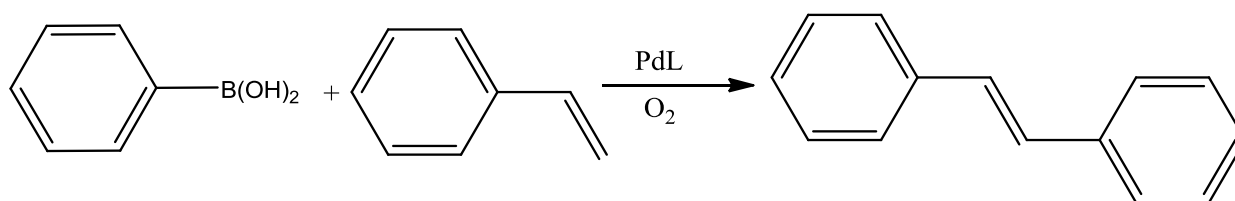
6.3 Conclusions

Single crystal X-Ray Diffractometry was utilised for this PhD project to obtain detailed information about the geometries of the ligands and metal complexes. Although the isolation of crystals, for most of the complexes, remains a massive challenge some valuable insight was gained. The identical crystal structures of 6-amino-5-nitro-1,10-phenanthroline using platinum were obtained, which provides evidence that the phenanthroline based synthons can find application as a dispersion catalyst used for different metal centres. By investigating the planarity of the phen backbone, it has become clear that functionalization on the fifth and sixth positions influence curvature of the ligand. The catalytic properties of the 1,10-phenanthroline type ligands, presented in Chapter 7, have shown that the electronic nature of the nitrogen atoms coordinated to the palladium(II) metal centers plays a significant role in the reactivity of the compounds. Although not performed in this study due to time constraints, an in-depth crystallographic investigation into the palladium nitrogen bond lengths for the various synthons could provide valuable information to further understand the mechanism of the Heck coupling and other catalytic processes. Solubility is one of the issues that have been encountered throughout this project. This has limited the characterisation techniques such as NMR and mass spectrometry. Also, heterogeneous catalysis has always been plagued by poor selectivity, but due to recent developments, tuning these catalysts in a similar fashion to homogeneous catalysts is becoming a real possibility. The heterogenisation of homogeneous systems has been mentioned and in order to develop greater insight and understanding, investigations using X-Ray diffraction will remain an important tool in the arsenal of the modern Chemist.

7 CATALYTIC EVALUATION OF PALLADIUM AND BRIDGED PALLADIUM COMPLEXES

7.1 Introduction

One of the principle aims of this study was the design and synthesis of planar bridging ligands that could possibly be used to disperse active catalytic species onto heterogeneous supports at optimum levels. In Chapter 2, the heterogenisation of homogeneous systems has already been discussed. In order to attempt in exploiting these methodologies, it was decided to first investigate the homogeneous properties of the constructed bridging ligands and the synthons used to construct the larger ligands. The Heck coupling has been investigated since the early 70's and various palladium compounds have found applications in this arena. The general and mechanistic aspects of the Heck coupling have already been discussed in detail in Chapter 2. However a slight modification was made to the Heck reaction before investigating the catalytic capabilities of the 1,10-phenanthroline and diamide type ligands. The modified Heck reaction is present in Scheme 7.1.



Scheme 7.1: Modified Heck coupling used to investigate the catalytic activity of the 1,10-phenanthroline and diamide type ligands.

In the scheme the aryl halide used in the classical Heck reaction has been replaced by a boronic acid species. Boronic acids are cheap and more environmentally friendly than the halogenated compounds. Mechanistically the coupling remains the same except for the addition of a transmetallation step that replaces the insertion of the Pd(0) species into the aryl halide bond. Once this reaction was identified, the optimal conditions were developed using 1,10-phenanthroline and a range of compounds that were evaluated to investigate the catalytic

properties of these systems. Ideally, the catalysts should have been added to a support in order to investigate whether or not there is potential in the original assumption that these compounds would improve catalyst dispersion. Due to the time frame of this project, this became impossible as difficulties were encountered with synthesis and characterisation. However, this could still be a future prospect. Nevertheless, the catalytic activity of the designed systems have been done, at least on a preliminary base, and are reported on in this chapter.

The ability of the planar ligands that were constructed in Chapter 3 and Chapter 4 to act as dispersion spacers, could be investigated and in doing so, see whether it is possible to exploit all the benefits of heterogeneous catalysis. Again, time constraints made this somewhat ambitious goal impossible to complete. Even so, it was decided to evaluate some of the synthons and bridging compounds that were synthesised to investigate whether or not these compounds performed any catalysis at all. Furthermore, the range of different phenanthroline compounds could provide some insight into mechanistic workings of the Heck coupling. Finally, many of the metal complexes that were synthesised in Chapter 3, using the diamide type compounds, could not be characterised in such a way to fully confirm the coordination mode of the palladium to the ligands. By placing these ligands into an optimised catalytic system, the coordination of the palladium to the compounds could be confirmed, as the palladium salt without any ligands present is inactive. The product distribution of the Heck coupling could also be compared to similar systems to shed some light on the coordination mode of the diamide moieties.

7.2 Experimental Section

All the chemicals and solvents were purchased from Sigma-Aldrich. GC grade solvents were used for the catalytic processes without further purification. The synthesis of the ligands and complexes are reported in Chapter 3 and Chapter 4. It is assumed that the ligands are coordinated to the palladium species for the complexes that are not fully characterised. The percentage yields were determined using GC measurements and were done on a Shimadzu 2010 Chromatograph equipped with an FID detector and a J&W HP-1 capillary column (30 m x 0.25 mm x 0.25 μ m). Hydrogen gas was used as the carrier gas. The temperature programme used was as follows: start at 50.0 °C for four minutes, ramp at 17.0 °C per minute up to 250.0°C and kept constant for two minutes. The GC traces, using the internal standard addition method, was used

to determine the RF factors of the different products, namely; biphenyl (4), diphenylethylene (5) and *trans*-stilbene (6). These were relative to the internal dodecane standard peak (3) and are presented in Figure 7.1. All other yields were calculated using the RF factors. All products were confirmed by GCMS using the same parameters as for the GC runs. Data analysis was conducted by means of Microsoft Office Excel 2010.¹

7.2.1 Typical Procedure for the Heck Coupling Reactions

In a typical experiment Pd(OAc)₂ (0.0125 g, 5.56 x 10⁻⁵ mol) and the ligand (5.56 x 10⁻⁵ mol) were placed in dimethylacetamide (DMA) (2 ml) and stirred at the reaction temperature for twenty minutes, after which 4-methyl morpholine (0.75 ml) was added. When evaluating the bridging ligands, half the amount of ligand were added to the solution. In a different vessel, dodecane, styrene and phenyl boronic acid were mixed in DMA (3 ml). This mixture was then added to the palladium acetate mixture. The vessel was fitted with a balloon filled with molecular oxygen. Samples (0.25 ml) were taken every forty minutes for four hours and diluted to 0.75 ml. The general appearances of the GC traces are presented in Figure 7.1. A range of different ligands were tested at 90 °C using a 1:1 molar ratio of styrene: phenylboronic acid. The optimum conditions for the coupling were evaluated using 1,10-phenanthroline as a stabilising ligand.² Reactions were performed at 50 °C, 70 °C and 90 °C to evaluate at which temperature the best yields were obtained. Different molar concentrations of starting materials were also tested, with the best reactivity found for a 1:3 ratio of styrene: phenylboronic acid. The most promising and relevant ligands synthesised in this study, reported on in Chapter 3 and Chapter 4, were then tested under these conditions. It is important to note that the phenylboronic acid starting material is not visible on the GC trace. As a result of this, all the selectivities for the *trans*-stilbene product are reported relative to the styrene peak (2). Furthermore when the biphenyl selectivity is reported, it is reported relative to the amount of starting phenyl boronic acid used at the start of the reaction and not to the amount of phenylboronic acid present at the time that the sample is taken. This could lead to selectivities which are not entirely as expected but these values can still provide valuable information.

¹ Microsoft Office Professional Edition 2010 Copyright© 1985-2010 Microsoft Corporation.

² K. S. Yoo, C. H. Yoon, K. W. Jung, *Journal of the American Chemical Society*, **2006**, 128, 16384–16393.

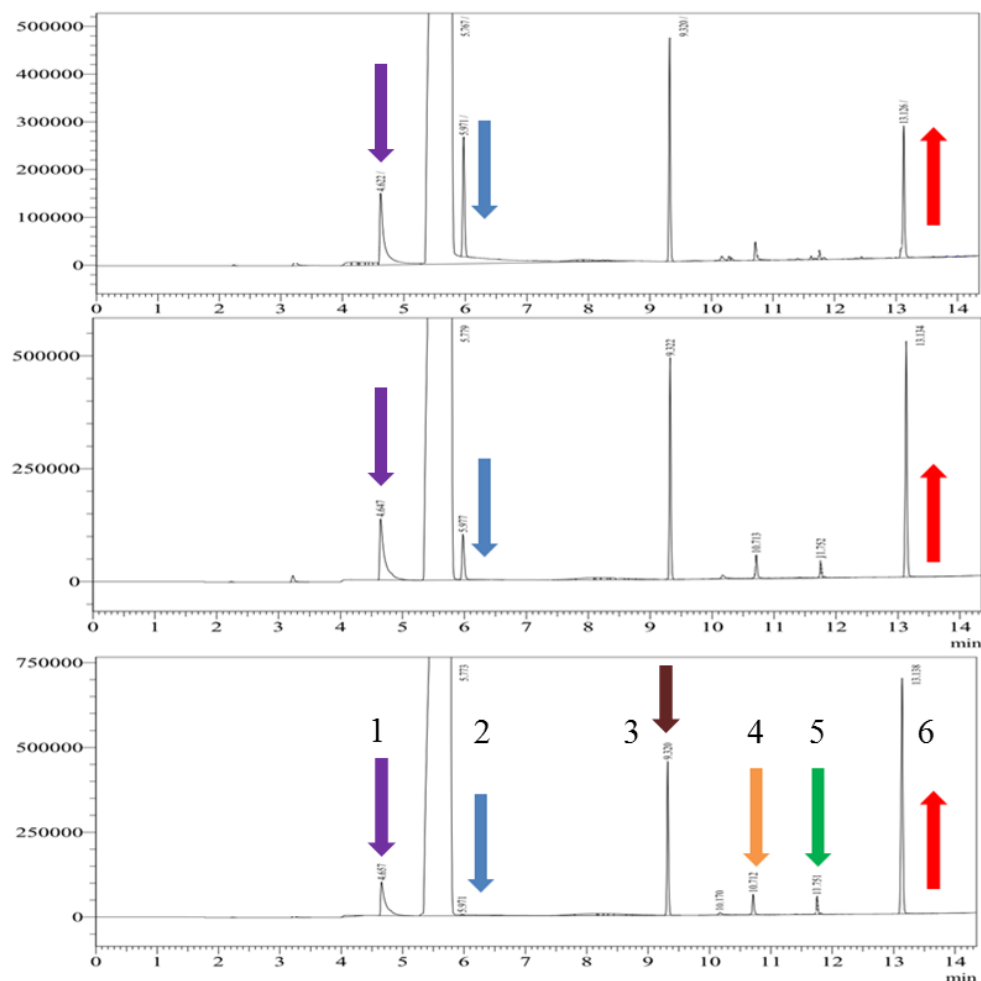


Figure 7.1: Typical GC spectrum seen for the Heck coupling reaction. The blue arrow indicates the decrease of the starting styrene, the red shows the growth of the *trans*-stilbene product. (1) 4-Methylmorpholine, (2) Styrene, (3) Dodecane, (4) Biphenyl, (5) Diphenylethylene, (6) *trans*-Stilbene.

7.2.2 Results and Discussion

7.2.2.1 Optimisation of reactions conditions using 1,10-phenanthroline as reference benchmarking ligands

Initially the optimum conditions were investigated using 1,10-phenanthroline as a ligand. As previously mentioned, different temperatures and concentrations were evaluated for this catalytic system. The different temperatures and mol ratios that were tested for 1,10-phenanthroline are presented in Table 7.1.

Table 7.1: Different reaction conditions tested for the Heck coupling using 1,10-phenanthroline.

Entry	Ratio	T/ °C	Time/ min	% <i>E</i> -stilbene	Selectivity
1	1:1	90	200	54	92
2	1:1	70	200	62	99
3	1:1	50	240	37	87
4*	1:1	70	240	66	99
5	2:1	70	240	30	51
6	3:1	70	240	28	40
7	1:2	70	120	64	95
8	1:3	70	120	82	96

* Twice the amount of catalyst

The results for the optimisation reactions of 1,10-phenanthroline in terms of temperature are presented in Figure 7.2.

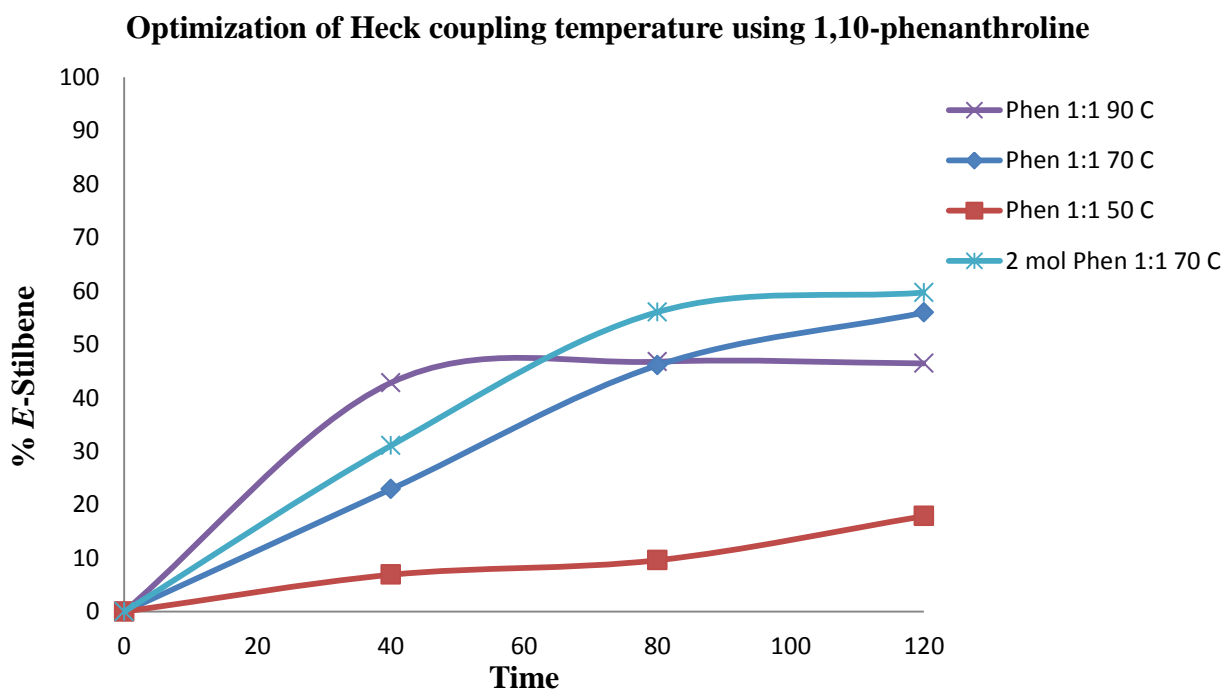






Figure 7.2: Graph showing the optimization of the temperature for the Heck coupling reaction using, Pd(OAc)₂ (0.0125 g, 5.56 x 10⁻⁵ mol), 1,10-phenanthroline (0.0125 g, 5.56 x 10⁻⁵ mol) and 4-methylmorpholine (0.75 ml) at different temperatures using a mol ratio 1:1 of styrene: phenylboronic acid. The light blue line indicates the use of double the mol amount of catalyst and ligand.

From Figure 7.2 the following key elements are visible:

-  The effect of temperature on the reaction rate: As expected, the fastest initial rate is observed for the reaction performed at 90 °C and the slowest rate is observed for the reaction done at 50 °C.
-  The reaction done at 90 °C reaches a plateau: The same decrease in reaction rate is observed for the reaction done at 70 °C but to a lesser extent with the final yield of the reaction being more than the reaction done at 90 °C.
-  These results strongly suggest that at 90 °C the catalyst deactivates much quicker than at 70 °C. This is further substantiated by the visibly black formation of Pd(0) at 90° C.
-  The highest yields were seen for the reaction done at 70 °C using double the amount of catalyst. However, all the reactions were flawed by having good activity initially and then considerable drops after roughly a 50 % conversion.

This suggests that after either the styrene or phenyl boronic acid start to decline in concentration, the reaction rate significantly decreases. In order to investigate this further, reactions using different ratios of styrene:phenylboronic acid was performed. The results are presented in Figure 7.3.

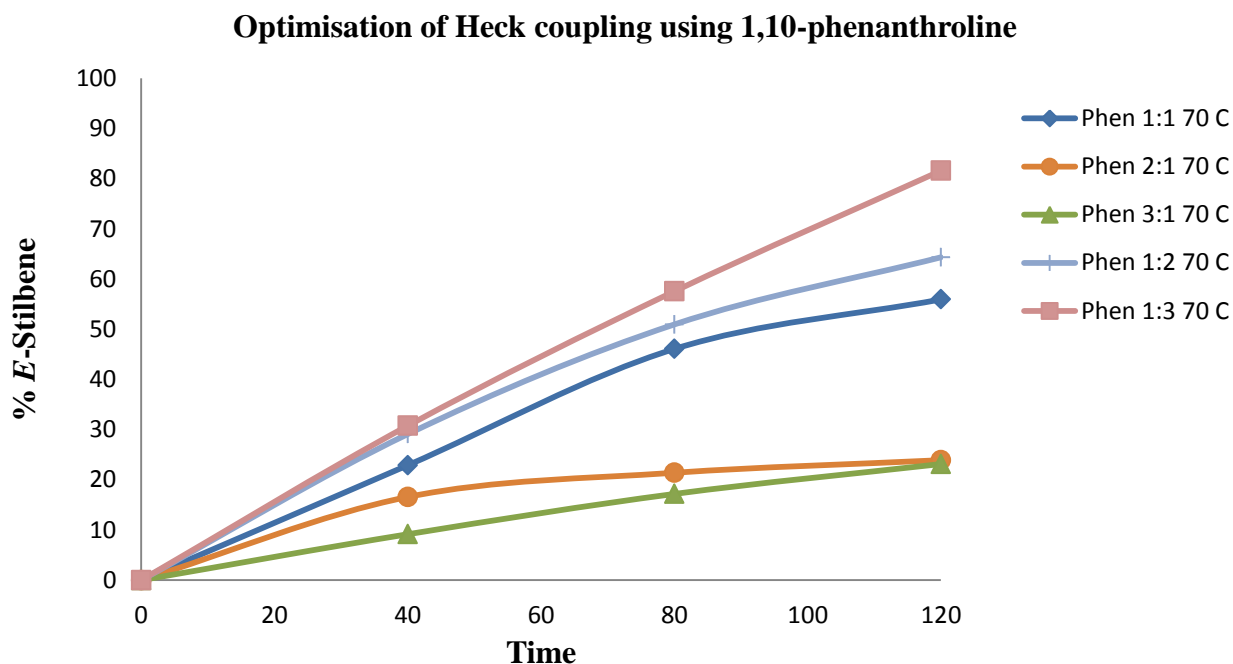


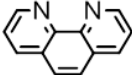
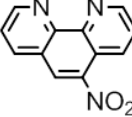
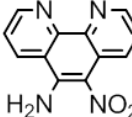
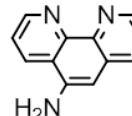
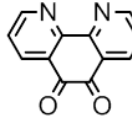
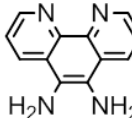
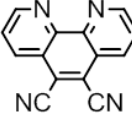
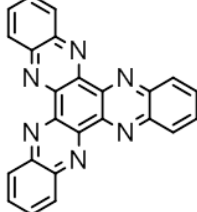
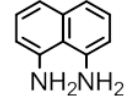
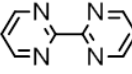
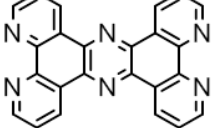
Figure 7.3: Graph showing the reaction yields for the Heck coupling performed at 70° using, Pd(OAc)₂ (0.0125 g, 5.56 x 10⁻⁵ mol), 1,10-phenanthroline (0.0125 g, 5.56 x 10⁻⁵ mol), 4-methylmorpholine (0.75 ml) and different mol ratios of styrene: phenylboronic acid.

The graph clearly indicates that the Heck coupling is dependent on the concentration of the phenylboronic acid. Increasing the concentration of the styrene drastically reduces the reactivity of the system. This suggests that the reaction is limited by the transmetallation step in which the phenyl gets transferred from the boron to the palladium. It could be that the increase in concentration of styrene creates a scenario where the ethene competes for coordination to the palladium centre with the boronic acid. This problem is clearly prevented by increasing the concentration of the phenyl boronic acid and 80 % conversion is observed after just two hours.

7.2.2.2 Heck coupling for phenanthroline type ligands at 90° C









Initially, a range of different ligands were tested at 90 °C using a 1:1 molar ratio of styrene: phenylboronic acid and 0.5 ml 4-methylmorpholine. The yields and selectivities are presented in Table 7.2. The use of 4-methylmorpholine (0.75 ml) as a base remained constant throughout the experiments.

Table 7.2: Heck coupling results for phenanthroline type ligands at 90 °C using a 1:1 styrene: phenylboronic acid ratio. The table displays the yields for the desired trans-stilbene product, homo-coupled and diphenylethene side products as well as the selectivity towards the trans-stilbene product.

Entry	Ligand	Time /min	% <i>E</i> -stilbene	% Diphenyl	% Homo-coupled	Selectivity
1		200	54	8	-	92
2		180	57	3	-	74
3		240	33	7	-	83
4		240	22	-	26	73
5		240	2	-	-	18
6		240	6	-	-	-
7		240	8	-	-	71
8		240	32	6	11	28
9		120	59	-	-	70
10		240	14	-	-	70
11		240	27	-	-	99

For entries 1, 2 and 9 the yields were reported at the time where the yields remained constant.

The following deductions can be made from Table 7.2:

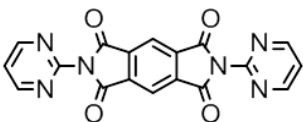
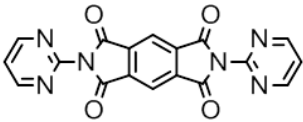
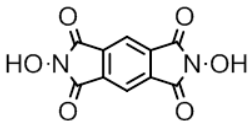
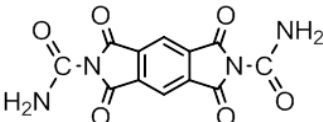
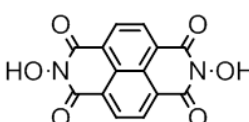
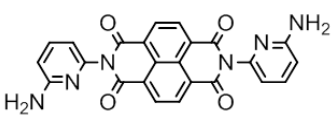
-  The most promising ligands that were investigated were 1,10-phenanthroline (1), 5-nitro-1,10-phenanthroline (2) and naphthalene-1,8-diamine (9) which gave yields of 54 % , 57 % and 59 % respectively.
-  It is however important to note that these yields were not obtained after the same time frames. The naphthalene-1,8-diamine was by far the quickest giving the reported yield after two hours while the 5-nitro-1,10-phenanthroline and 1,10-phenanthroline took three and four hours respectively.
-  The first trend observed is the drastic decline in reactivity from the 5-nitro-1,10-phenanthroline (2) species to the 5,6-dicarbonitrile-1,10-phenanthroline (7). Effectively there is a 45 % drop in yield that could be attributed to the change in electronic properties of the phenanthroline backbone.
-  The electron withdrawing nitro group shows the fastest reactivity while the electron donating substituents on the fifth and sixth positions, such as the 5,6-phenyldiamine and 5,6-dicarbonitrile-1,10-phenanthroline, show very poor yields. This notion is further supported by the 25 % drop in activity from the 5-nitro to the 5-nitro-6-amino species.
-  It has previously been mentioned that the rate determining step of the Heck coupling for bidentate nitrogen ligands is determined by the ability of the ligand to momentarily coordinate in a monodentate fashion. It could be that the 5-nitro species' asymmetric substitution could aid this process. However it would seem that the electronic effects have the most significant influence, as the 5-amino species are also considerably slower.
-  Heprazine (8), which has poor electron donating abilities as described in Paragraph 5.3.5.1, does not show very promising reactivity.
-  The reactivity of the phenazine (11) is very similar to that of the heprazine (8) and these complexes showed poor solubility. This could be a possible reason for the poor yields displayed by these compounds.
-  Most of the ligands displayed good selectivity, except for the phendione (5), heprazine (8) and the 5-amino-phenanthroline (4). The phendione (5) ligand is essentially inadequate under these reaction conditions, while the other two ligands did form the

homo-coupled product. The reason for this is unclear and further investigations will be needed in order to clarify this.

7.2.2.3 Heck coupling for Diamide type ligands at 90 °C

It was decided to test some of the diamide type ligands that were synthesised in Chapter 3 under the same reaction conditions as the 1,10-phenanthroline ligands. The results and different mol ratios of palladium to ligand are presented in Table 7.3. The use of 4-methylmorpholine (0.75 ml) as a base remained constant throughout the experiments. The characterisation and determination of the coordination mode of these ligands was problematic, and by using the Heck coupling reaction some similarities with bidentate ligands could be identified. The ligands were evaluated at 90 °C using a 1:1 ratio of styrene: phenyl boronic acid. Different ratios of palladium to ligands were also evaluated. The results for the range of ligands varied greatly and are presented in Table 7.3



Table 7.3: Heck coupling results for diamide type ligands at 90 °C using a 1:1 styrene: phenylboronic acid ratio.

Entry	Ligand	Pd:L	Time /min	% <i>E</i> -stilbene	% Homo-coupled	Selectivity
1		1:1	240	33	11	83
2		2:1	240	33	23	68
3		1:1	240	-	-	-
4		2:1	240	13	11	24
5		2:1	240	-	-	-
6		2:1	240	5	-	9

The synthesis and properties of these ligands are reported in Chapter 3

The following deductions can be made from Table 7.3:

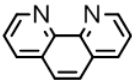
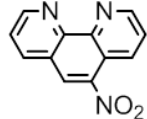
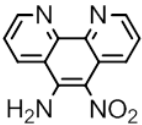
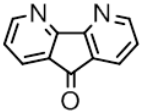
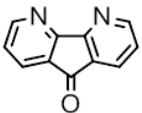
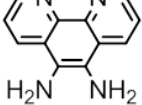
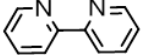
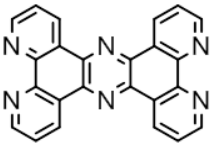
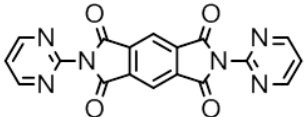
- 🧪 Ultimately, most of the diamide ligands that were tested performed poorly. The only ligand that displayed some sort of potential was the pyro-pyrimidine (1) type ligand that gave a yield of 33 % of the *trans*-stilbene product.
- 🧪 Another interesting feature of the above-mentioned ligand can be seen in the doubling of the homo-coupled product with the doubling of the mol ratio of palladium, without any increase in the formation of the desired product. The reason for this is unclear.
- 🧪 The poor performance of the other ligands could be attributed to the basic environment in which the reactions were performed. All the ligands that gave little to no yields can form monoionic molecules.

-  It has been shown that after the coordination of the ligand and one acetate molecule to the palladium, it could halt the transmetallation process and in so doing prevent the catalytic cycle from continuing. This could be supported by the pyro-urea (4) ligand that gives a 13 % yield with two mol of palladium.
-  Some of the palladium atoms could have coordinated to the oxo end of the molecule and the rest to the amino side. In such a scenario, the palladium on the oxo end could still do the Heck coupling, while the palladium on the amino end would be de-activated as mentioned. This is however just theoretical and further evidence is needed to make this observation a proven fact.

7.2.2.4 Heck coupling for Phenanthroline type ligands at 70 °C


After the optimisation of reaction conditions using 1,10-phenanthroline, the ligands with the most potential were identified and tested at 70° C using a molar ratio of 1:3 of styrene: phenylboronic acid. The use of 4-methylmorpholine (0.75 ml) as a base remained constant throughout the experiments. The optimal reaction conditions that were developed using 1,10-phenanthroline have already been discussed in Paragraph 7.2.2.1. Three bridging ligands were also tested at these conditions by using more than a 1:1 palladium: ligand mol ratio. The results for these ligands are presented in Table 7.4.








Table 7.4: Heck coupling results for ligands at optimised reaction conditions: 70 °C using a 1:3 styrene: phenylboronic acid ratio.

Entry	Ligand	Pd:L	Time /min	% <i>E</i> -stilbene	% Homo-coupled	Selectivity
1		1:1	120	82	-	96
2		1:1	120	100	-	99
3		1:1	240	34	-	80
4		1:1	240	65	23	78
5		1:2	240	36	6	88
6		2:1	240	25	28	88
7		1:1	240	100	-	98
8		2:1	240	16		76
9		2:1	240	36	56	82


For entries 1 and 2 the yields were reported after 2 hours as these reactions proceeded much quicker.


The following deductions can be made from Table 7.4

-  The results are very similar to the reactions that were carried out at 90 °C, although there are some differences. The same general trend is seen with regards to electron withdrawing and electron donating groups on the fifth and sixth positions of the phenanthroline backbone.

-  The 5-nitro species (2) performed very well under the optimised conditions and the reaction was complete within two hours. The only ligand that gave similar reaction rates was 1,10-phenanthroline (1) with which the reaction conditions were optimised.
-  2,2-Bipyridine (7) was the only other ligand that displayed some potential, although the 100% yield was only obtained after four hours.
-  The bimetallic 5,6-phendiamine (6) complex performed considerably better under these condition, however, this is probably not the only factor that resulted in better yields. The coordination of palladium to the NH_2 of the molecule will decrease the electron donating abilities of the amines into the conjugated phen backbone. This could have resulted in an increase of the *trans*-stilbene yield.
-  Another interesting feature of the phendiamine ligand (6) is the poor selectivity that resulted in the formation of 28 % of the homo-coupled product. One could argue that the palladium that coordinated to the phenanthroline end of the molecule, is responsible for the *trans*-stilbene yield, while the palladium which coordinated to the amine side of the molecule is responsible for the homo-coupled product. The yields of these products are virtually the same which further supports this theory.
-  For the phendiamine ligand (6) reaction performed at 90 °C using equal mol amounts, no homo-coupled products were observed. This suggests that the palladium prefers to bind to the phenanthroline end of the molecule.
-  The dafone ligand (4,5) which sports a larger bite angle than the conventional phenanthroline was also investigated at optimal conditions. In Paragraph 2.11.1.2 its bi- and monodentate abilities were mentioned. One and two mol ratios were evaluated to see which coordination mode is preferred under these reaction conditions. This could also give further insight into the coordination mode of the pyropyrmidine (9) type compounds. The results show that the bidentate mode is possibly favoured under these reaction conditions, as the addition of a second mol of the ligand resulted in the loss of approximately 50 % of the reactivity. This could be due to two ligands coordinating to some of the palladium atoms. This would block the access of the substrates to the palladium centre.
-  The 1:1 mol ratio for the dafone ligand suffered from poor selectivity forming 23 % of the homo-coupled product. This contradicts the notion that a purely bidentate

system is present, as the homo-coupled product is a characteristic of monodentate systems. Perhaps a mixture of coordinating modes is present. It is important to note that this reaction resulted in the formation of palladium black. This suggests that this ligand is not as effective in the stabilising of the palladium centre as the phenanthroline counterparts. The formation of palladium black was considerably less for the two mol system.

 The pyro-pyrimidine ligand (9) was also evaluated and gave somewhat unexpected results. At 90 °C, 33 % of the trans-stilbene product was accompanied by 11 % of the homo-coupled product. At the optimal conditions, the trans-stilbene yield remained virtually the same, but a dramatic increase from 23 % to 56 % was observed for the homo-coupled product. This increase in yield can be attributed to the increased concentration of phenyl boronic acid from one mol ratio to three as the yield almost increased by a factor of three.

 The yield of the phenazine (9) reaction is considerably less than the reaction at 90 °C. Theoretically, this can be due to the decrease in solubility of the compound at lower temperatures.

7.3 Conclusions

It has been shown that the phenanthroline type ligands can successfully stabilise a palladium center during the Heck coupling reaction. The electronic environment of the conjugated phenanthroline is vital to the reactivity of the ligand with electron withdrawing groups on the five and six position showing the most potential. Electron rich systems generally give much poorer results however it is important to note that the use of bis palladium compounds did increase the activity of 5,6-diamino-1,10-phenanthroline due to the electron withdrawing characteristics of the soft metal center. Finally the diamide compounds that form mono-negative charges are essentially useless for the Heck coupling while the pyro-pyrimidine compound favours the formation of the homo-coupled product.

8

CRITICAL EVALUATION OF THE STUDY

8.1 Introduction

One of the major aims of the project was the synthesis of planar bridging ligands that could be exploited as heterogeneous support dispersion spacers, while activating the metal centre to maintain or increase its catalytic ability. Two different pathways were followed to synthesise compounds that could be used for this purpose. Firstly 1,10-phenanthroline was functionalised on the fifth and sixth positions using oxo and amino groups to create synthons that could be combined to form various planar bridging ligands using a range of different synthons. This could be achieved by doing simple Schiff base reactions. Secondly, robust planar diamide backbones were identified and modified, using pyridines and pyrimidines, to form planar ligands that could coordinate to from one to four metal species using different coordination modes. All the compounds were characterised using spectroscopy and single crystal X-Ray diffraction techniques to investigate the planarity and electronic properties. Finally, the evaluation of the coordination of square planar metal centres, such as platinum and palladium bonded to these ligands, followed by the catalytic evaluation of the complexes before and after the addition to heterogeneous supports using the Heck coupling as a test reaction was investigated. Unfortunately the catalyst could not be tested on supports due to time limitations, however the homogeneous properties were investigated and confirmed.

8.2 Scientific Relevance of the Results Obtained

8.2.1 Diamide Type Building Blocks

The 1,4,5,8-naphthalenetetracarboxylic dianhydride and pyromellitic diamide backbones used to synthesise this range of compounds, were identified as planar, robust, relatively cost-effective and easy to modify moieties. Six diamide type ligands were synthesised using pyridines and pyrimidines by means of a dehydration reaction. The ligands were characterised using NMR, IR

and single crystal X-Ray diffraction. The crystal structures of *N,N'*-dihydroxypyromellitic diimide and *N,N'*-bis(2-pyridyl)naphthalene-3,4,7,8-di-carboximide provided valuable information about the planarity and configuration of these ligands. These ligands can in theory coordinate to up to four metal centres, although this coordination mode is uncommon. The coordination of palladium to these compounds was attempted, but some issues were encountered with regards to the characterisation and particularly the stability of these complexes. The palladium complexes of the ligands, with different molecular ratios of metal were characterised using elemental analysis and NMR. Differences between the various complexes could be identified, but complete structural elucidation was not possible. In order to see if these ligands coordinate to metals such as palladium the complexes were placed in the Heck coupling reaction. Palladium without a ligand present is inactive in this process and a ligand is required to stabilise the active species. Although most of the ligands were inactive for this process, the pyro-pyrimidine ligand did give some positive results. The pyro-pyrimidine ligand did however favour the formation of the homo-coupled product which is of lesser importance. The inactiveness of the other diamide species can be attributed to the formation of mono anionic ligands within the basic reaction conditions. Therefore this does not necessarily provide evidence that these compounds do not coordinate to metal centres and palladium in particular.

8.2.2 1,10-Phenanthroline Based Bridging Ligands

A ketone and an amine are required to utilise the Schiff base reaction as the construction mechanism for larger molecules. To achieve this, 1,10-phenanthroline was first oxidised to produce the diketone, but the synthesis of the diamine was much more challenging. Eventually it was synthesised but with poor yields. One major advantage of using these two ligands as synthons, is the ability to use them as bridging moieties in addition to their synthon role. The bridging ligands diquinoxalino[2,3-a:2',3'-c]phenazine (heprazine) and tetrapyrido[3,2-a:2',3'-c:3'',2''-h:2''',3'''-j]phenazine (phenazine) were synthesised using these synthons and other building blocks like cyclohexane-1,2,3,4,5,6-hexaone, phenylene diamine and benzenetetramine. Various other synthons such as 4,5-diazafluoren-9-one were also successfully synthesised and characterised. Two new crystal structures of 5-amino-6-nitro-1,10-phenanthroline were obtained by coordinating this ligand to palladium and platinum. The data from these two complexes was used to investigate the geometric and electronic properties.

8.2.3 Catalytic Evaluation of Phenanthroline and Diamide Ligands










A range of the 1,10-phenanthroline type ligands, along with the other planar bridging compounds, were tested using the Heck coupling reaction. After the reaction conditions were optimised, it was found that by adding electron withdrawing groups on the fifth and sixth positions the catalytic activity of the phenanthroline type complexes can be significantly improved. The addition of electron donating groups, such as amino and cyano, however drastically decreases the reactivity of the species. This was determined to be an electronic effect rather than a steric one. Most of these phenanthroline ligands displayed good selectivity for the desired *trans*-product. The larger heprazine and phenazine bridging ligands showed some reactivity towards the Heck coupling, but did not perform nearly as well as the smaller phenanthroline synthons. This is probably due to the poor solubility of these compounds under these reaction conditions.

The activity of the diamide type systems was also tested for the Heck coupling under the same conditions as the phenanthroline ligands. Most of the ligands were inactive, except for the pyro-pyrimidine complex. The inactiveness of the other species may be attributed, as mentioned before, to the formation of mono anionic ligands within the basic reaction conditions and therefore does not necessarily provide evidence that these compounds do not coordinate to metal centres. This conclusion is further supported by the activity of the pyro-pyrimidine complex which cannot form these charged species.

8.3 Future Research

The original idea of this project was to make new planar bridging ligands, investigate the coordination properties, attach these ligands to supports and to evaluate the catalytic properties before and after the deposition process. This was perhaps too optimistic. Nevertheless, excellent progress has been made in the synthetic optimisation for the synthesis of the bridging ligands and the catalytic ability of these ligands was also gauged. The poor solubility of most of the ligands and metal complexes also provided further challenges in the characterisation processes. However, these insolubilities probably also linked to π - π stacking interactions may specifically be exploited in future to reduce catalyst leaching in some systems.

Particular future aspects which need to be investigated further are the following:

-  Perform the functionalization and subsequent construction of larger bridging ligands using 2,9-dimethyl-1,10-phenanthroline.
-  The addition of long alkyl chains to the backbone of the 1,10-phenanthroline type ligands to increase the solubility of these molecules.
-  Perform reaction optimisation for the Schiff base reactions that are used in the construction of the larger bridging ligands.
-  Investigate methodologies for the crystallisation of planar ligands and metal complexes to exploit the valuable information obtained from single crystal X-Ray diffraction studies.
-  Extend the characterisation methods to completely characterise the insoluble species, such as the diamide type complexes that were investigated in this study.
-  Identification of planar backbones that can be exploited in a similar fashion as the 1,10-phenanthroline synthons. These backbones should display better solubility than the compounds investigated in this study.
-  Deposit some of the simpler bridging ligands onto supports and investigate the degree of dispersion using powder X-ray diffraction and surface techniques.
-  Evaluate the heterogeneous catalytic activity of the complexes that have been deposited onto the supports.
-  Develop optimum conditions for heterogenisation of homogeneous systems using insoluble planar networks.

Appendix A

Table A1: Atomic coordinates ($\times 10^4$) and equivalent isotropic displacement parameters ($\text{\AA}^2 \times 10^3$) for 1,6,7,12,13,18-Hexaazatrinaphthylene. $U(\text{eq})$ is defined as one third of the trace of the orthogonalized U^{ij} tensor.

Atoms	x	y	z	U(eq)
C(91)	3357(3)	7072(3)	2570(2)	19(1)
C(92)	8351(3)	7930(3)	2427(2)	20(1)
Cl(11)	2654(1)	7565(1)	3190(1)	28(1)
Cl(12)	2626(1)	7374(1)	1776(1)	30(1)
Cl(13)	4802(1)	7429(1)	2474(1)	26(1)
Cl(21)	7625(1)	7628(1)	3223(1)	30(1)
Cl(22)	7653(1)	7437(1)	1809(1)	28(1)
Cl(23)	9802(1)	7570(1)	2527(1)	26(1)
C(94)	8221(3)	2847(3)	2328(2)	20(1)
Cl(41)	7437(1)	2871(1)	3085(1)	29(1)
Cl(42)	9563(1)	2308(1)	2528(1)	26(1)
Cl(43)	7418(1)	2261(1)	1794(1)	30(1)
C(96)	3220(3)	2155(3)	2670(2)	20(1)
C(97)	4089(3)	2662(3)	137(2)	23(1)
C(98)	-954(4)	487(3)	1030(2)	29(1)
Cl(61)	4562(1)	2690(1)	2475(1)	27(1)
Cl(62)	2436(1)	2130(1)	1915(1)	28(1)
Cl(63)	2418(1)	2742(1)	3206(1)	30(1)
Cl(71)	5123(1)	2165(1)	750(1)	39(1)
Cl(72)	2951(1)	1887(1)	112(1)	29(1)
Cl(73)	4736(1)	2972(1)	-679(1)	35(1)
Cl(81)	269(1)	1202(1)	953(1)	44(1)
Cl(82)	-580(1)	-610(1)	905(1)	47(1)
Cl(83)	-2013(1)	977(1)	435(1)	38(1)
C(11)	5744(3)	1232(3)	4855(2)	18(1)
C(12)	5731(3)	1519(3)	5490(2)	20(1)
C(13)	4715(3)	1753(3)	5755(2)	22(1)
C(14)	3664(3)	1718(3)	5389(2)	23(1)
C(15)	3649(3)	1454(3)	4777(2)	21(1)
C(16)	4698(3)	1193(2)	4493(2)	17(1)
C(21)	9783(3)	8(2)	3150(2)	17(1)
C(22)	10848(3)	-227(3)	2876(2)	20(1)

Appendix A

C(23)	11838(3)	-171(3)	3231(2)	22(1)
C(24)	11836(3)	111(3)	3864(2)	21(1)
C(25)	10826(3)	355(3)	4140(2)	19(1)
C(26)	9781(3)	307(2)	3783(2)	18(1)
C(31)	4707(3)	18(2)	2069(2)	17(1)
C(32)	3671(3)	-29(3)	1697(2)	20(1)
C(33)	3691(3)	-339(3)	1102(2)	21(1)
C(34)	4732(3)	-622(3)	842(2)	20(1)
C(35)	5749(3)	-583(3)	1177(2)	19(1)
C(36)	5760(3)	-257(2)	1803(2)	18(1)
C(41)	5675(3)	674(2)	3646(2)	15(1)
C(42)	5676(3)	354(2)	2994(2)	15(1)
C(43)	6730(3)	91(2)	2719(2)	15(1)
C(44)	7823(3)	167(2)	3084(2)	15(1)
C(45)	7826(3)	472(2)	3715(2)	16(1)
C(46)	6727(3)	730(2)	4004(2)	15(1)
C(93)	9089(3)	2342(3)	4860(2)	23(1)
C(95)	4047(4)	4516(3)	3967(2)	31(1)
N(11)	6769(3)	1001(2)	4596(2)	17(1)
N(12)	4672(2)	910(2)	3883(2)	16(1)
N(13)	4683(2)	321(2)	2667(2)	17(1)
N(14)	6773(2)	-217(2)	2136(2)	16(1)
N(15)	8798(2)	-66(2)	2803(2)	17(1)
N(16)	8780(2)	550(2)	4060(2)	17(1)
CI(31)	10122(1)	2838(1)	4250(1)	39(1)
CI(32)	7950(1)	3116(1)	4888(1)	29(1)
CI(33)	9734(1)	2028(1)	5679(1)	35(1)
CI(51)	5269(1)	3799(1)	4046(1)	44(1)
CI(52)	2989(1)	4022(1)	4566(1)	38(1)
CI(53)	4418(1)	5609(1)	4095(1)	47(1)
C(51)	-308(3)	3811(2)	509(2)	17(1)
C(52)	-1348(3)	3548(3)	221(2)	21(1)
C(53)	-1341(3)	3287(3)	-389(2)	22(1)
C(54)	-288(3)	3246(3)	-755(2)	23(1)
C(55)	733(3)	3482(3)	-490(2)	22(1)
C(56)	751(3)	3768(3)	146(2)	17(1)
C(61)	4777(3)	4687(2)	1220(2)	17(1)
C(62)	5827(3)	4644(3)	862(2)	20(1)
C(63)	6835(3)	4891(3)	1131(2)	21(1)
C(64)	6842(3)	5173(3)	1766(2)	20(1)
C(65)	5843(3)	5224(3)	2127(2)	19(1)
C(66)	4782(3)	4989(2)	1850(2)	17(1)
C(71)	755(3)	5254(3)	3201(2)	17(1)

Appendix A

C(72)	756(3)	5584(3)	3818(2)	20(1)
C(73)	-274(3)	5626(3)	4159(2)	20(1)
C(74)	-1310(3)	5335(3)	3905(2)	22(1)
C(75)	-1332(3)	5027(3)	3304(2)	19(1)
C(76)	-290(3)	4984(2)	2932(2)	16(1)
C(81)	2826(3)	4525(2)	1288(2)	14(1)
C(82)	2822(3)	4838(2)	1915(2)	14(1)
C(83)	1732(3)	4908(2)	2280(2)	14(1)
C(84)	677(3)	4647(2)	2005(2)	15(1)
C(85)	670(3)	4328(2)	1355(2)	15(1)
C(86)	1727(3)	4274(2)	994(2)	15(1)
N(21)	-326(2)	4089(2)	1116(2)	16(1)
N(22)	1769(2)	3993(2)	406(2)	16(1)
N(23)	3780(2)	4454(2)	937(2)	17(1)
N(24)	3791(2)	5063(2)	2196(2)	16(1)
N(25)	1773(2)	5216(2)	2862(2)	16(1)
N(26)	-322(2)	4675(2)	2336(2)	16(1)

Table A2: Bond lengths [Å] and angles [°] for 1,6,7,12,13,18-Hexaazatrinaphthylene.

Atoms	Bond length (Å)	Atoms	Bond angle (°)
C(91)-Cl(13)	1.757(4)	Cl(13)-C(91)-Cl(11)	110.7(2)
C(91)-Cl(11)	1.760(4)	Cl(13)-C(91)-Cl(12)	110.2(2)
C(91)-Cl(12)	1.767(4)	Cl(11)-C(91)-Cl(12)	109.9(2)
C(91)-H(91)	0.98	Cl(13)-C(91)-H(91)	108.7
C(92)-Cl(22)	1.758(4)	Cl(11)-C(91)-H(91)	108.7
C(92)-Cl(23)	1.762(4)	Cl(12)-C(91)-H(91)	108.7
C(92)-Cl(21)	1.766(4)	Cl(22)-C(92)-Cl(23)	111.0(2)
C(92)-H(92)	0.98	Cl(22)-C(92)-Cl(21)	110.0(2)
C(94)-Cl(42)	1.755(4)	Cl(23)-C(92)-Cl(21)	109.7(2)
C(94)-Cl(41)	1.763(4)	Cl(22)-C(92)-H(92)	108.7
C(94)-Cl(43)	1.776(4)	Cl(23)-C(92)-H(92)	108.7
C(94)-H(94)	0.98	Cl(21)-C(92)-H(92)	108.7
C(96)-Cl(61)	1.756(4)	Cl(42)-C(94)-Cl(41)	110.5(2)
C(96)-Cl(62)	1.764(4)	Cl(42)-C(94)-Cl(43)	109.9(2)
C(96)-Cl(63)	1.773(4)	Cl(41)-C(94)-Cl(43)	109.89(19)
C(96)-H(96)	0.98	Cl(42)-C(94)-H(94)	108.8
C(97)-Cl(71)	1.759(4)	Cl(41)-C(94)-H(94)	108.8
C(97)-Cl(73)	1.760(4)	Cl(43)-C(94)-H(94)	108.8
C(97)-Cl(72)	1.766(4)	Cl(61)-C(96)-Cl(62)	111.0(2)
C(97)-H(97)	0.98	Cl(61)-C(96)-Cl(63)	109.6(2)
C(98)-Cl(83)	1.754(4)	Cl(62)-C(96)-Cl(63)	110.1(2)
C(98)-Cl(82)	1.760(5)	Cl(61)-C(96)-H(96)	108.7
C(98)-Cl(81)	1.764(4)	Cl(62)-C(96)-H(96)	108.7

Appendix A

C(98)-H(98)	0.98	Cl(63)-C(96)-H(96)	108.7
C(11)-N(11)	1.364(4)	Cl(71)-C(97)-Cl(73)	110.0(2)
C(11)-C(12)	1.416(5)	Cl(71)-C(97)-Cl(72)	110.1(2)
C(11)-C(16)	1.418(5)	Cl(73)-C(97)-Cl(72)	109.9(2)
C(12)-C(13)	1.362(5)	Cl(71)-C(97)-H(97)	108.9
C(12)-H(12)	0.93	Cl(73)-C(97)-H(97)	108.9
C(13)-C(14)	1.426(5)	Cl(72)-C(97)-H(97)	108.9
C(13)-H(13)	0.93	Cl(83)-C(98)-Cl(82)	110.2(2)
C(14)-C(15)	1.355(5)	Cl(83)-C(98)-Cl(81)	110.1(2)
C(14)-H(14)	0.93	Cl(82)-C(98)-Cl(81)	110.9(2)
C(15)-C(16)	1.425(5)	Cl(83)-C(98)-H(98)	108.6
C(15)-H(15)	0.93	Cl(82)-C(98)-H(98)	108.6
C(16)-N(12)	1.366(5)	Cl(81)-C(98)-H(98)	108.6
C(21)-N(15)	1.351(5)	N(11)-C(11)-C(12)	119.4(3)
C(21)-C(26)	1.420(5)	N(11)-C(11)-C(16)	120.7(3)
C(21)-C(22)	1.421(5)	C(12)-C(11)-C(16)	119.9(3)
C(22)-C(23)	1.360(5)	C(13)-C(12)-C(11)	120.1(4)
C(22)-H(22)	0.93	C(13)-C(12)-H(12)	120
C(23)-C(24)	1.409(6)	C(11)-C(12)-H(12)	120
C(23)-H(23)	0.93	C(12)-C(13)-C(14)	120.0(4)
C(24)-C(25)	1.371(5)	C(12)-C(13)-H(13)	120
C(24)-H(24)	0.93	C(14)-C(13)-H(13)	120
C(25)-C(26)	1.413(5)	C(15)-C(14)-C(13)	121.3(3)
C(25)-H(25)	0.93	C(15)-C(14)-H(14)	119.4
C(26)-N(16)	1.362(4)	C(13)-C(14)-H(14)	119.4
C(31)-N(13)	1.358(5)	C(14)-C(15)-C(16)	119.8(3)
C(31)-C(32)	1.420(5)	C(14)-C(15)-H(15)	120.1
C(31)-C(36)	1.421(5)	C(16)-C(15)-H(15)	120.1
C(32)-C(33)	1.358(5)	N(12)-C(16)-C(11)	121.7(3)
C(32)-H(32)	0.93	N(12)-C(16)-C(15)	119.4(3)
C(33)-C(34)	1.409(5)	C(11)-C(16)-C(15)	118.9(3)
C(33)-H(33)	0.93	N(15)-C(21)-C(26)	121.9(3)
C(34)-C(35)	1.362(5)	N(15)-C(21)-C(22)	118.9(3)
C(34)-H(34)	0.93	C(26)-C(21)-C(22)	119.2(3)
C(35)-C(36)	1.429(5)	C(23)-C(22)-C(21)	119.0(4)
C(35)-H(35)	0.93	C(23)-C(22)-H(22)	120.5
C(36)-N(14)	1.356(5)	C(21)-C(22)-H(22)	120.5
C(41)-N(12)	1.326(4)	C(22)-C(23)-C(24)	121.9(3)
C(41)-C(46)	1.425(5)	C(22)-C(23)-H(23)	119.1
C(41)-C(42)	1.473(5)	C(24)-C(23)-H(23)	119.1
C(42)-N(13)	1.327(4)	C(25)-C(24)-C(23)	120.6(3)
C(42)-C(43)	1.424(5)	C(25)-C(24)-H(24)	119.7
C(43)-N(14)	1.334(5)	C(23)-C(24)-H(24)	119.7

Appendix A

C(43)-C(44)	1.476(5)	C(24)-C(25)-C(26)	119.0(4)
C(44)-N(15)	1.336(4)	C(24)-C(25)-H(25)	120.5
C(44)-C(45)	1.421(5)	C(26)-C(25)-H(25)	120.5
C(45)-N(16)	1.320(4)	N(16)-C(26)-C(25)	118.7(3)
C(45)-C(46)	1.479(5)	N(16)-C(26)-C(21)	121.1(3)
C(46)-N(11)	1.323(5)	C(25)-C(26)-C(21)	120.2(3)
C(93)-Cl(31)	1.755(4)	N(13)-C(31)-C(32)	120.2(3)
C(93)-Cl(32)	1.760(4)	N(13)-C(31)-C(36)	121.0(3)
C(93)-Cl(33)	1.764(4)	C(32)-C(31)-C(36)	118.8(3)
C(93)-H(93)	0.98	C(33)-C(32)-C(31)	120.2(3)
C(95)-Cl(51)	1.759(4)	C(33)-C(32)-H(32)	119.9
C(95)-Cl(53)	1.759(5)	C(31)-C(32)-H(32)	119.9
C(95)-Cl(52)	1.762(5)	C(32)-C(33)-C(34)	121.0(3)
C(95)-H(95)	0.98	C(32)-C(33)-H(33)	119.5
C(51)-N(21)	1.356(5)	C(34)-C(33)-H(33)	119.5
C(51)-C(52)	1.425(5)	C(35)-C(34)-C(33)	120.9(4)
C(51)-C(56)	1.430(5)	C(35)-C(34)-H(34)	119.6
C(52)-C(53)	1.348(5)	C(33)-C(34)-H(34)	119.6
C(52)-H(52)	0.93	C(34)-C(35)-C(36)	119.6(3)
C(53)-C(54)	1.427(5)	C(34)-C(35)-H(35)	120.2
C(53)-H(53)	0.93	C(36)-C(35)-H(35)	120.2
C(54)-C(55)	1.372(5)	N(14)-C(36)-C(31)	121.0(3)
C(54)-H(54)	0.93	N(14)-C(36)-C(35)	119.5(3)
C(55)-C(56)	1.417(5)	C(31)-C(36)-C(35)	119.4(3)
C(55)-H(55)	0.93	N(12)-C(41)-C(46)	121.5(3)
C(56)-N(22)	1.360(5)	N(12)-C(41)-C(42)	118.1(3)
C(61)-N(23)	1.362(5)	C(46)-C(41)-C(42)	120.4(3)
C(61)-C(62)	1.417(5)	N(13)-C(42)-C(43)	120.9(3)
C(61)-C(66)	1.418(5)	N(13)-C(42)-C(41)	119.0(3)
C(62)-C(63)	1.368(5)	C(43)-C(42)-C(41)	120.1(3)
C(62)-H(62)	0.93	N(14)-C(43)-C(42)	122.3(3)
C(63)-C(64)	1.412(5)	N(14)-C(43)-C(44)	118.2(3)
C(63)-H(63)	0.93	C(42)-C(43)-C(44)	119.4(3)
C(64)-C(65)	1.372(5)	N(15)-C(44)-C(45)	121.6(3)
C(64)-H(64)	0.93	N(15)-C(44)-C(43)	117.8(3)
C(65)-C(66)	1.422(5)	C(45)-C(44)-C(43)	120.6(3)
C(65)-H(65)	0.93	N(16)-C(45)-C(44)	122.9(3)
C(66)-N(24)	1.354(4)	N(16)-C(45)-C(46)	117.4(3)
C(71)-N(25)	1.364(4)	C(44)-C(45)-C(46)	119.8(3)
C(71)-C(72)	1.414(5)	N(11)-C(46)-C(41)	122.7(3)
C(71)-C(76)	1.416(5)	N(11)-C(46)-C(45)	117.7(3)
C(72)-C(73)	1.380(5)	C(41)-C(46)-C(45)	119.6(3)
C(72)-H(72)	0.93	Cl(31)-C(93)-Cl(32)	110.2(2)

Appendix A

C(73)-C(74)	1.407(5)	Cl(31)-C(93)-Cl(33)	110.0(2)
C(73)-H(73)	0.93	Cl(32)-C(93)-Cl(33)	109.8(2)
C(74)-C(75)	1.367(5)	Cl(31)-C(93)-H(93)	108.9
C(74)-H(74)	0.93	Cl(32)-C(93)-H(93)	108.9
C(75)-C(76)	1.423(5)	Cl(33)-C(93)-H(93)	108.9
C(75)-H(75)	0.93	Cl(51)-C(95)-Cl(53)	110.7(2)
C(76)-N(26)	1.360(5)	Cl(51)-C(95)-Cl(52)	109.6(3)
C(81)-N(23)	1.321(4)	Cl(53)-C(95)-Cl(52)	110.2(2)
C(81)-C(82)	1.419(5)	Cl(51)-C(95)-H(95)	108.8
C(81)-C(86)	1.484(5)	Cl(53)-C(95)-H(95)	108.8
C(82)-N(24)	1.330(4)	Cl(52)-C(95)-H(95)	108.8
C(82)-C(83)	1.470(4)	C(46)-N(11)-C(11)	116.7(3)
C(83)-N(25)	1.332(5)	C(41)-N(12)-C(16)	116.6(3)
C(83)-C(84)	1.428(5)	C(42)-N(13)-C(31)	117.8(3)
C(84)-N(26)	1.335(4)	C(43)-N(14)-C(36)	116.9(3)
C(84)-C(85)	1.469(5)	C(44)-N(15)-C(21)	116.4(3)
C(85)-N(21)	1.326(4)	C(45)-N(16)-C(26)	116.2(3)
C(85)-C(86)	1.429(4)	N(21)-C(51)-C(52)	120.5(3)
C(86)-N(22)	1.321(5)	N(21)-C(51)-C(56)	120.9(3)
		C(52)-C(51)-C(56)	118.6(3)
		C(53)-C(52)-C(51)	120.9(3)
		C(53)-C(52)-H(52)	119.6
		C(51)-C(52)-H(52)	119.6
		C(52)-C(53)-C(54)	120.9(3)
		C(52)-C(53)-H(53)	119.6
		C(54)-C(53)-H(53)	119.6
		C(55)-C(54)-C(53)	120.0(4)
		C(55)-C(54)-H(54)	120
		C(53)-C(54)-H(54)	120
		C(54)-C(55)-C(56)	120.5(3)
		C(54)-C(55)-H(55)	119.8
		C(56)-C(55)-H(55)	119.8
		N(22)-C(56)-C(55)	119.9(3)
		N(22)-C(56)-C(51)	120.8(3)
		C(55)-C(56)-C(51)	119.2(3)
		N(23)-C(61)-C(62)	118.6(3)
		N(23)-C(61)-C(66)	121.8(3)
		C(62)-C(61)-C(66)	119.6(3)
		C(63)-C(62)-C(61)	119.5(4)
		C(63)-C(62)-H(62)	120.2
		C(61)-C(62)-H(62)	120.2
		C(62)-C(63)-C(64)	120.8(3)
		C(62)-C(63)-H(63)	119.6

Appendix A

C(64)-C(63)-H(63)	119.6
C(65)-C(64)-C(63)	121.3(3)
C(65)-C(64)-H(64)	119.3
C(63)-C(64)-H(64)	119.3
C(64)-C(65)-C(66)	118.8(4)
C(64)-C(65)-H(65)	120.6
C(66)-C(65)-H(65)	120.6
N(24)-C(66)-C(61)	121.2(3)
N(24)-C(66)-C(65)	119.0(3)
C(61)-C(66)-C(65)	119.9(3)
N(25)-C(71)-C(72)	118.9(3)
N(25)-C(71)-C(76)	120.6(3)
C(72)-C(71)-C(76)	120.5(3)
C(73)-C(72)-C(71)	118.9(3)
C(73)-C(72)-H(72)	120.5
C(71)-C(72)-H(72)	120.5
C(72)-C(73)-C(74)	120.8(4)
C(72)-C(73)-H(73)	119.6
C(74)-C(73)-H(73)	119.6
C(75)-C(74)-C(73)	121.1(3)
C(75)-C(74)-H(74)	119.4
C(73)-C(74)-H(74)	119.4
C(74)-C(75)-C(76)	119.8(3)
C(74)-C(75)-H(75)	120.1
C(76)-C(75)-H(75)	120.1
N(26)-C(76)-C(71)	122.0(3)
N(26)-C(76)-C(75)	119.2(3)
C(71)-C(76)-C(75)	118.8(3)
N(23)-C(81)-C(82)	122.8(3)
N(23)-C(81)-C(86)	117.0(3)
C(82)-C(81)-C(86)	120.1(3)
N(24)-C(82)-C(81)	121.8(3)
N(24)-C(82)-C(83)	117.8(3)
C(81)-C(82)-C(83)	120.4(3)
N(25)-C(83)-C(84)	122.5(3)
N(25)-C(83)-C(82)	118.0(3)
C(84)-C(83)-C(82)	119.5(3)
N(26)-C(84)-C(83)	121.0(3)
N(26)-C(84)-C(85)	118.5(3)
C(83)-C(84)-C(85)	120.6(3)
N(21)-C(85)-C(86)	121.2(3)
N(21)-C(85)-C(84)	118.9(3)
C(86)-C(85)-C(84)	119.9(3)

Appendix A

N(22)-C(86)-C(85)	122.4(3)
N(22)-C(86)-C(81)	118.1(3)
C(85)-C(86)-C(81)	119.5(3)
C(85)-N(21)-C(51)	117.6(3)
C(86)-N(22)-C(56)	117.1(3)
C(81)-N(23)-C(61)	115.8(3)
C(82)-N(24)-C(66)	116.6(3)
C(83)-N(25)-C(71)	116.9(3)
C(84)-N(26)-C(76)	117.1(3)

Table A3. Anisotropic displacement parameters ($\text{\AA}^2 \times 10^3$) for 1,6,7,12,13,18-Hexaazatrinaphthylene. The anisotropic displacement factor exponent takes the form: $-2 \pi [h^2 a^{*2} U_{11} + \dots + 2 h k a^* b^* U_{12}]$

	U11	U22	U33	U23	U13	U12
C(91)	20(2)	18(2)	18(2)	-2(2)	4(1)	-2(1)
C(92)	19(2)	22(2)	20(2)	-2(2)	3(1)	0(1)
Cl(11)	26(1)	32(1)	28(1)	-12(1)	8(1)	-1(1)
Cl(12)	30(1)	36(1)	22(1)	-2(1)	-2(1)	-7(1)
Cl(13)	19(1)	28(1)	31(1)	-2(1)	7(1)	-7(1)
Cl(21)	30(1)	35(1)	22(1)	-2(1)	12(1)	1(1)
Cl(22)	25(1)	31(1)	28(1)	-12(1)	2(1)	-5(1)
Cl(23)	18(1)	28(1)	30(1)	-2(1)	3(1)	2(1)
C(94)	19(2)	16(2)	22(2)	3(2)	4(1)	-4(1)
Cl(41)	28(1)	27(1)	29(1)	-2(1)	13(1)	-5(1)
Cl(42)	21(1)	22(1)	33(1)	3(1)	3(1)	1(1)
Cl(43)	30(1)	30(1)	29(1)	-4(1)	0(1)	-10(1)
C(96)	17(2)	18(2)	23(2)	1(2)	5(1)	-2(1)
C(97)	23(2)	23(2)	23(2)	-4(2)	5(1)	-1(2)
C(98)	30(2)	32(3)	24(2)	-2(2)	7(2)	-5(2)
Cl(61)	21(1)	23(1)	33(1)	2(1)	7(1)	-6(1)
Cl(62)	28(1)	27(1)	29(1)	-2(1)	-3(1)	-1(1)
Cl(63)	30(1)	30(1)	29(1)	-4(1)	11(1)	6(1)
Cl(71)	29(1)	51(1)	32(1)	2(1)	-5(1)	-3(1)
Cl(72)	26(1)	28(1)	33(1)	-5(1)	2(1)	-3(1)
Cl(73)	54(1)	22(1)	27(1)	3(1)	16(1)	-2(1)
Cl(81)	36(1)	50(1)	48(1)	-13(1)	6(1)	-16(1)
Cl(82)	66(1)	28(1)	44(1)	3(1)	27(1)	-2(1)
Cl(83)	41(1)	35(1)	36(1)	0(1)	-2(1)	-10(1)
C(11)	20(2)	13(2)	19(2)	4(2)	6(1)	-4(1)
C(12)	22(2)	16(2)	20(2)	-2(2)	4(1)	0(1)
C(13)	29(2)	20(2)	16(2)	-4(2)	8(1)	-1(2)
C(14)	22(2)	23(2)	22(2)	-2(2)	12(1)	0(2)
C(15)	18(2)	20(2)	25(2)	-3(2)	7(1)	-3(1)
C(16)	20(2)	12(2)	20(2)	0(2)	9(1)	-6(1)
C(21)	18(2)	11(2)	20(2)	3(1)	5(1)	-2(1)
C(22)	23(2)	15(2)	20(2)	0(2)	10(1)	-1(1)
C(23)	16(2)	18(2)	29(2)	3(2)	9(1)	-1(1)
C(24)	16(2)	17(2)	29(2)	1(2)	1(1)	-2(1)
C(25)	20(2)	14(2)	20(2)	3(2)	2(1)	-3(1)
C(26)	20(2)	9(2)	23(2)	4(1)	5(1)	0(1)
C(31)	16(2)	14(2)	20(2)	1(2)	4(1)	-3(1)
C(32)	17(2)	18(2)	22(2)	0(2)	3(1)	-2(1)
C(33)	20(2)	18(2)	24(2)	1(2)	0(1)	-5(1)

Appendix A

C(34)	27(2)	16(2)	17(2)	-1(2)	5(1)	-4(1)
C(35)	20(2)	13(2)	21(2)	0(2)	6(1)	-3(1)
C(36)	19(2)	12(2)	19(2)	2(1)	5(1)	-1(1)
C(41)	18(2)	8(2)	18(2)	2(1)	6(1)	-3(1)
C(42)	16(2)	8(2)	18(2)	3(1)	7(1)	-3(1)
C(43)	14(2)	11(2)	17(2)	3(1)	4(1)	-3(1)
C(44)	16(2)	7(2)	21(2)	0(1)	4(1)	0(1)
C(45)	17(2)	11(2)	17(2)	1(1)	5(1)	-2(1)
C(46)	16(2)	11(2)	17(2)	3(1)	5(1)	-3(1)
C(93)	26(2)	17(2)	27(2)	-5(2)	5(2)	-3(2)
C(95)	30(2)	32(3)	29(2)	-4(2)	2(2)	2(2)
N(11)	19(2)	14(2)	18(2)	0(1)	6(1)	-1(1)
N(12)	18(1)	12(2)	17(2)	1(1)	6(1)	-2(1)
N(13)	17(1)	14(2)	17(2)	2(1)	5(1)	-1(1)
N(14)	14(1)	12(2)	20(2)	0(1)	5(1)	-2(1)
N(15)	15(1)	13(2)	21(2)	-1(1)	5(1)	-1(1)
N(16)	15(1)	17(2)	18(2)	-2(1)	3(1)	-1(1)
Cl(31)	30(1)	50(1)	32(1)	2(1)	15(1)	-2(1)
Cl(32)	28(1)	27(1)	31(1)	-4(1)	9(1)	-2(1)
Cl(33)	52(1)	22(1)	28(1)	3(1)	-5(1)	-4(1)
Cl(51)	34(1)	52(1)	48(1)	-14(1)	5(1)	11(1)
Cl(52)	41(1)	35(1)	35(1)	0(1)	13(1)	4(1)
Cl(53)	65(1)	28(1)	44(1)	3(1)	-14(1)	-6(1)
C(51)	20(2)	13(2)	17(2)	0(1)	3(1)	0(1)
C(52)	17(2)	19(2)	27(2)	-2(2)	4(1)	1(1)
C(53)	18(2)	24(2)	25(2)	-5(2)	0(1)	-3(1)
C(54)	28(2)	23(2)	18(2)	-6(2)	3(1)	-5(2)
C(55)	25(2)	19(2)	20(2)	-3(2)	8(1)	-4(1)
C(56)	20(2)	14(2)	16(2)	1(1)	4(1)	0(1)
C(61)	18(2)	10(2)	19(2)	3(1)	7(1)	-2(1)
C(62)	21(2)	14(2)	22(2)	1(2)	9(1)	-3(1)
C(63)	17(2)	17(2)	27(2)	1(2)	9(1)	0(1)
C(64)	15(2)	17(2)	27(2)	2(2)	2(1)	-5(1)
C(65)	18(2)	14(2)	24(2)	0(2)	4(1)	-1(1)
C(66)	17(2)	11(2)	19(2)	4(1)	4(1)	-2(1)
C(71)	19(2)	15(2)	16(2)	1(1)	6(1)	-3(1)
C(72)	18(2)	17(2)	23(2)	-2(2)	5(1)	-1(1)
C(73)	28(2)	17(2)	15(2)	-2(2)	8(1)	-2(1)
C(74)	23(2)	16(2)	24(2)	2(2)	12(2)	-1(1)
C(75)	16(2)	16(2)	22(2)	1(2)	6(1)	-2(1)
C(76)	18(2)	10(2)	17(2)	2(1)	8(1)	0(1)
C(81)	14(2)	11(2)	16(2)	1(1)	7(1)	-4(1)
C(82)	14(2)	7(2)	19(2)	3(1)	7(1)	-2(1)
C(83)	15(2)	11(2)	15(2)	1(1)	6(1)	-3(1)
C(84)	14(2)	11(2)	17(2)	0(1)	3(1)	1(1)
C(85)	16(2)	10(2)	16(2)	1(1)	4(1)	-2(1)
C(86)	16(2)	11(2)	18(2)	1(1)	7(1)	-4(1)
N(21)	14(1)	15(2)	17(2)	0(1)	4(1)	-1(1)
N(22)	18(1)	13(2)	17(2)	0(1)	6(1)	-4(1)
N(23)	17(1)	14(2)	18(2)	0(1)	7(1)	-4(1)
N(24)	16(1)	12(2)	17(2)	1(1)	5(1)	-2(1)
N(25)	15(1)	12(2)	19(2)	2(1)	8(1)	-3(1)
N(26)	16(1)	14(2)	16(2)	2(1)	6(1)	-2(1)

Appendix A

Table A4: Atomic coordinates ($\times 10^4$) and equivalent isotropic displacement parameters ($\text{\AA}^2 \times 10^3$) for *N,N'*-dihydroxypyromellitic diimide. $U(\text{eq})$ is defined as one third of the trace of the orthogonalized U^{ij} tensor.

Atoms	x	y	z	U(eq)
O(1)	8917(2)	1364(1)	5273(2)	23(1)
O(4)	3205(2)	1095(1)	4111(2)	21(1)
O(3)	5899(2)	2037(1)	6927(2)	25(1)
O(2)	5737(2)	4825(1)	7072(2)	22(1)
N(1)	6978(2)	2893(2)	6222(2)	21(1)
C(2)	9450(2)	3735(2)	5169(2)	17(1)
C(3)	6881(2)	4249(2)	6439(2)	17(1)
C(4)	11009(2)	3912(2)	4430(2)	18(1)
C(5)	8508(2)	2482(2)	5518(2)	18(1)
C(6)	8481(2)	4781(2)	5722(2)	18(1)

Table A5: Bond lengths [\AA] and angles [$^\circ$] for *N,N'*-dihydroxypyromellitic diimide.

Atoms	Bond length (\AA)	Atoms	Bond angle ($^\circ$)
O(1)-C(5)	1.201(2)	H(2)-O(4)-H(3)	111(3)
O(4)-H(2)	0.86(3)	N(1)-O(3)-H(6)	104.8(16)
O(4)-H(3)	0.82(3)	O(3)-N(1)-C(3)	121.65(14)
O(3)-N(1)	1.3697(18)	O(3)-N(1)-C(5)	122.82(14)
O(3)-H(6)	0.99(3)	C(3)-N(1)-C(5)	114.57(14)
O(2)-C(3)	1.206(2)	C(4)-C(2)-C(6)	122.76(15)
N(1)-C(3)	1.393(2)	C(4)-C(2)-C(5)	128.84(15)
N(1)-C(5)	1.398(2)	C(6)-C(2)-C(5)	108.40(15)
C(2)-C(4)	1.382(2)	O(2)-C(3)-N(1)	126.42(16)
C(2)-C(6)	1.395(2)	O(2)-C(3)-C(6)	129.54(16)
C(2)-C(5)	1.491(2)	N(1)-C(3)-C(6)	104.03(13)
C(3)-C(6)	1.487(2)	C(2)-C(4)-C(6)#1	114.27(15)
C(4)-C(6)#1	1.388(2)	C(2)-C(4)-H(1)	122.3(12)
C(4)-H(1)	0.94(2)	C(6)#1-C(4)-H(1)	123.4(12)
C(6)-C(4)#1	1.388(2)	O(1)-C(5)-N(1)	126.13(16)
		O(1)-C(5)-C(2)	129.87(16)
		N(1)-C(5)-C(2)	104.00(14)
		C(4)#1-C(6)-C(2)	122.97(15)
		C(4)#1-C(6)-C(3)	128.10(15)
		C(2)-C(6)-C(3)	108.93(14)

Symmetry transformations used to generate equivalent atoms: #1 -x+2,-y+1,-z

Appendix A

Table A6. Anisotropic displacement parameters ($\text{\AA}^2 \times 10^3$) for *N,N'*-dihydroxypyromellitic diimide. The anisotropic displacement factor exponent takes the form: $-2\pi [h^2 a^{*2} U_{11} + \dots + 2hka^*b^*U_{12}]$.

	U11	U22	U33	U23	U13	U12
O(1)	25(1)	18(1)	24(1)	-1(1)	6(1)	-1(1)
O(4)	22(1)	20(1)	22(1)	-1(1)	9(1)	0(1)
O(3)	25(1)	26(1)	23(1)	1(1)	8(1)	-7(1)
O(2)	19(1)	28(1)	20(1)	1(1)	8(1)	2(1)
N(1)	22(1)	22(1)	21(1)	1(1)	7(1)	-2(1)
C(2)	15(1)	17(1)	16(1)	-2(1)	1(1)	0(1)
C(3)	16(1)	21(1)	14(1)	1(1)	2(1)	-1(1)
C(4)	15(1)	21(1)	16(1)	-2(1)	3(1)	2(1)
C(5)	18(1)	21(1)	14(1)	0(1)	2(1)	-2(1)
C(6)	13(1)	23(1)	15(1)	-1(1)	2(1)	1(1)

Table A7: Atomic coordinates ($\times 10^4$) and equivalent isotropic displacement parameters ($\text{\AA}^2 \times 10^3$) for *N,N'*-Bis(2-pyridyl)naphthalene-3,4:7,8-di-carboximide. $U(\text{eq})$ is defined as one third of the trace of the orthogonalized U^{ij} tensor.

Atoms	x	y	z	U(eq)
O(2)	-436(1)	1958(1)	6609(1)	31(1)
N(2)	3315(2)	2209(2)	7422(1)	26(1)
O(3)	3634(1)	-721(1)	9027(1)	25(1)
C(004)	2044(2)	260(2)	5950(2)	28(1)
C(005)	3796(2)	1865(2)	5589(2)	31(1)
N(32)	1624(2)	678(2)	7858(1)	21(1)
C(007)	4024(2)	2590(2)	6689(2)	28(1)
C(008)	2787(2)	684(2)	5209(2)	34(1)
C(009)	-501(2)	911(2)	8455(1)	20(1)
C(010)	-2581(2)	1131(2)	9064(1)	21(1)
C(011)	1785(2)	-391(2)	9840(1)	19(1)
C(012)	2450(2)	-185(2)	8913(1)	20(1)
C(013)	2355(2)	1060(2)	7031(1)	22(1)
C(014)	329(2)	136(2)	9569(1)	18(1)
C(015)	190(2)	1243(2)	7564(1)	22(1)
C(016)	-1931(2)	1389(2)	8201(1)	23(1)

Table A8: Bond lengths [\AA] and angles [$^\circ$] for *N,N'*-Bis(2-pyridyl)naphthalene-3,4:7,8-di-carboximide .

Atoms	Bond length (\AA)	Atoms	Bond angle ($^\circ$)
O(2)-C(015)	1.2195(19)	C(013)-N(2)-C(007)	116.21(14)
N(2)-C(013)	1.333(2)	C(013)-C(004)-C(008)	117.43(17)
N(2)-C(007)	1.345(2)	C(007)-C(005)-C(008)	118.82(16)
O(3)-C(012)	1.210(2)	C(015)-N(32)-C(012)	125.66(12)
C(004)-C(013)	1.375(2)	C(015)-N(32)-C(013)	117.65(13)

Appendix A

C(004)-C(008)	1.388(2)	C(012)-N(32)-C(013)	116.64(13)
C(005)-C(007)	1.377(2)	N(2)-C(007)-C(005)	123.41(17)
C(005)-C(008)	1.381(3)	C(005)-C(008)-C(004)	119.04(16)
N(32)-C(015)	1.400(2)	C(016)-C(009)-C(014)	120.81(13)
N(32)-C(012)	1.405(2)	C(016)-C(009)-C(015)	119.76(14)
N(32)-C(013)	1.4550(19)	C(014)-C(009)-C(015)	119.41(14)
C(009)-C(016)	1.379(2)	C(011)#1-C(010)-C(016)	119.82(15)
C(009)-C(014)	1.414(2)	C(010)#1-C(011)-C(014)	121.00(13)
C(009)-C(015)	1.481(2)	C(010)#1-C(011)-C(012)	119.51(14)
C(010)-C(011)#1	1.377(2)	C(014)-C(011)-C(012)	119.47(13)
C(010)-C(016)	1.412(2)	O(3)-C(012)-N(32)	120.13(13)
C(011)-C(010)#1	1.377(2)	O(3)-C(012)-C(011)	123.44(14)
C(011)-C(014)	1.413(2)	N(32)-C(012)-C(011)	116.42(14)
C(011)-C(012)	1.483(2)	N(2)-C(013)-C(004)	125.09(14)
C(014)-C(014)#1	1.419(3)	N(2)-C(013)-N(32)	114.32(13)
		C(004)-C(013)-N(32)	120.59(15)
		C(011)-C(014)-C(009)	121.92(13)
		C(011)-C(014)-C(014)#1	119.17(17)
		C(009)-C(014)-C(014)#1	118.91(17)
		O(2)-C(015)-N(32)	120.15(14)
		O(2)-C(015)-C(009)	123.09(15)
		N(32)-C(015)-C(009)	116.75(13)
		C(009)-C(016)-C(010)	120.26(14)

Symmetry transformations used to generate equivalent atoms: #1 -x,-y,-z+2

Table A9. Anisotropic displacement parameters ($\text{\AA}^2 \times 10^3$) for *N,N'*-Bis(2-pyridyl)naphthalene-3,4:7,8-dicarboximide . The anisotropic displacement factor exponent takes the form: $-2 \pi [h^2 a^{*2} U_{11} + \dots + 2 h k a^* b^* U_{12}]$.

	U11	U22	U33	U23	U13	U12
O(2)	31(1)	40(1)	24(1)	14(1)	14(1)	9(1)
N(2)	27(1)	30(1)	24(1)	3(1)	13(1)	0(1)
O(3)	24(1)	33(1)	21(1)	2(1)	10(1)	4(1)
C(004)	29(1)	33(1)	23(1)	-2(1)	11(1)	-2(1)
C(005)	29(1)	42(1)	24(1)	9(1)	13(1)	2(1)
N(32)	23(1)	26(1)	16(1)	3(1)	10(1)	1(1)
C(007)	26(1)	30(1)	28(1)	5(1)	12(1)	-1(1)
C(008)	37(1)	47(1)	20(1)	-3(1)	15(1)	0(1)
C(009)	23(1)	21(1)	17(1)	1(1)	9(1)	0(1)
C(010)	21(1)	25(1)	18(1)	0(1)	8(1)	2(1)
C(011)	23(1)	20(1)	15(1)	-1(1)	9(1)	-1(1)
C(012)	23(1)	22(1)	15(1)	-2(1)	7(1)	-1(1)
C(013)	22(1)	28(1)	19(1)	6(1)	11(1)	4(1)

Appendix A

C(014)	21(1)	18(1)	16(1)	-1(1)	7(1)	-1(1)
C(015)	23(1)	25(1)	17(1)	3(1)	8(1)	2(1)
C(016)	25(1)	25(1)	16(1)	4(1)	7(1)	3(1)

Table A10: Atomic coordinates ($\times 10^4$) and equivalent isotropic displacement parameters ($\text{\AA}^2 \times 10^3$) for 2-Amino-4,6-dichloropyrimidine, acetic acid solvate. U(eq) is defined as one third of the trace of the orthogonalize U^{ij} tensor.

Atoms	x	y	z	U(eq)
Cl(12)	1384(1)	3083(1)	7868(1)	22(1)
Cl(11)	7670(1)	1174(1)	4830(1)	19(1)
O(31)	6981(2)	2790(1)	2220(1)	23(1)
O(22)	2516(2)	1033(1)	318(1)	20(1)
N(11)	1915(2)	3796(1)	5718(1)	16(1)
O(21)	4346(2)	-459(1)	1315(1)	22(1)
O(32)	4332(2)	4177(1)	1552(1)	24(1)
N(12)	4712(2)	2935(1)	4364(1)	15(1)
N(13)	2185(2)	4497(1)	3817(1)	18(1)
C(12)	5455(2)	2203(1)	5219(1)	15(1)
C(13)	4582(2)	2189(1)	6348(1)	17(1)
C(32)	6110(2)	3544(1)	1402(1)	17(1)
C(14)	2758(2)	3032(1)	6517(1)	16(1)
C(11)	2942(2)	3732(1)	4647(1)	15(1)
C(31)	7560(2)	3523(1)	309(1)	22(1)
C(22)	2819(2)	342(1)	1251(1)	17(1)
C(21)	1141(2)	622(1)	2224(1)	23(1)

Table A11: Bond lengths [\AA] and angles [$^\circ$] for 2-Amino-4,6-dichloropyrimidine, acetic acid solvate.

Atoms	Bond length (\AA)	Atoms	Bond angle ($^\circ$)
Cl(12)-C(14)	1.7319(11)	C(32)-O(31)-H(31)	109.5
Cl(11)-C(12)	1.7368(11)	C(22)-O(22)-H(22)	109.5
O(31)-C(32)	1.3293(14)	C(14)-N(11)-C(11)	115.88(10)
O(31)-H(31)	0.84	C(12)-N(12)-C(11)	115.77(9)
O(22)-C(22)	1.3191(14)	C(11)-N(13)-H(12)	119.7(11)
O(22)-H(22)	0.84	C(11)-N(13)-H(13)	118.7(11)
N(11)-C(14)	1.3173(14)	H(12)-N(13)-H(13)	121.0(15)
N(11)-C(11)	1.3586(14)	N(12)-C(12)-C(13)	125.50(10)
O(21)-C(22)	1.2240(14)	N(12)-C(12)-Cl(11)	115.00(8)
O(32)-C(32)	1.2142(15)	C(13)-C(12)-Cl(11)	119.49(9)
N(12)-C(12)	1.3235(14)	C(12)-C(13)-C(14)	113.01(10)
N(12)-C(11)	1.3602(14)	C(12)-C(13)-H(11)	123.5
N(13)-C(11)	1.3290(15)	C(14)-C(13)-H(11)	123.5

Appendix A

N(13)-H(12)	0.897(13)	O(32)-C(32)-O(31)	122.37(11)
N(13)-H(13)	0.843(13)	O(32)-C(32)-C(31)	124.81(11)
C(12)-C(13)	1.3816(15)	O(31)-C(32)-C(31)	112.82(10)
C(13)-C(14)	1.3888(15)	N(11)-C(14)-C(13)	125.54(10)
C(13)-H(11)	0.95	N(11)-C(14)-Cl(12)	115.94(8)
C(32)-C(31)	1.4946(16)	C(13)-C(14)-Cl(12)	118.51(9)
C(31)-H(31A)	0.98	N(13)-C(11)-N(11)	118.26(10)
C(31)-H(31B)	0.98	N(13)-C(11)-N(12)	117.45(10)
C(31)-H(31C)	0.98	N(11)-C(11)-N(12)	124.29(10)
C(22)-C(21)	1.4922(16)	C(32)-C(31)-H(31A)	109.5
C(21)-H(21A)	0.98	C(32)-C(31)-H(31B)	109.5
C(21)-H(21B)	0.98	H(31A)-C(31)-H(31B)	109.5
C(21)-H(21C)	0.98	C(32)-C(31)-H(31C)	109.5
		H(31A)-C(31)-H(31C)	109.5
		H(31B)-C(31)-H(31C)	109.5
		O(21)-C(22)-O(22)	122.98(10)
		O(21)-C(22)-C(21)	122.78(11)
		O(22)-C(22)-C(21)	114.25(10)
		C(22)-C(21)-H(21A)	109.5
		C(22)-C(21)-H(21B)	109.5
		H(21A)-C(21)-H(21B)	109.5
		C(22)-C(21)-H(21C)	109.5
		H(21A)-C(21)-H(21C)	109.5
		H(21B)-C(21)-H(21C)	109.5

Table A12: Anisotropic displacement parameters ($\text{\AA}^2 \times 10^3$) for 2-Amino-4,6-dichloropyrimidine, acetic acid solvate. The anisotropic displacement factor exponent takes the form: $-2\pi [h^2 a^{*2} U_{11} + \dots + 2hk a^* b^* U_{12}]$.

	U11	U22	U33	U23	U13	U12
Cl(12)	24(1)	27(1)	17(1)	5(1)	7(1)	8(1)
Cl(11)	18(1)	17(1)	23(1)	4(1)	4(1)	8(1)
O(31)	26(1)	28(1)	19(1)	8(1)	7(1)	14(1)
O(22)	23(1)	22(1)	19(1)	5(1)	5(1)	9(1)
N(11)	15(1)	16(1)	16(1)	1(1)	2(1)	3(1)
O(21)	24(1)	23(1)	21(1)	7(1)	6(1)	11(1)
O(32)	27(1)	27(1)	22(1)	8(1)	7(1)	14(1)
N(12)	15(1)	15(1)	16(1)	1(1)	2(1)	4(1)
N(13)	20(1)	20(1)	17(1)	4(1)	4(1)	10(1)
C(12)	14(1)	14(1)	19(1)	1(1)	1(1)	3(1)
C(13)	17(1)	17(1)	18(1)	4(1)	1(1)	5(1)
C(32)	17(1)	17(1)	18(1)	2(1)	2(1)	1(1)

Appendix A

C(14)	15(1)	18(1)	16(1)	1(1)	2(1)	1(1)
C(11)	14(1)	14(1)	17(1)	0(1)	1(1)	2(1)
C(31)	23(1)	24(1)	20(1)	5(1)	7(1)	5(1)
C(22)	17(1)	17(1)	18(1)	1(1)	0(1)	2(1)
C(21)	23(1)	27(1)	20(1)	3(1)	5(1)	8(1)

Table A13: Atomic coordinates ($\times 10^4$) and equivalent isotropic displacement parameters ($\text{\AA}^2 \times 10^3$) for *cis*-[Pd(C₁₂H₈N₄O₂)Cl₂].2DMSO. U(eq) is defined as one third of the trace of the orthogonalized U^{ij} tensor.

Atoms	x	y	z	U(eq)
C(11)	10968(3)	5191(2)	9097(2)	15(1)
C(12)	12373(3)	6093(2)	10015(2)	16(1)
C(13)	13012(3)	7639(2)	10347(2)	16(1)
C(14)	12201(3)	8283(2)	9753(2)	13(1)
C(15)	12773(3)	9922(2)	10056(2)	14(1)
C(16)	11731(3)	10403(2)	9464(2)	14(1)
C(17)	10253(3)	9381(2)	8527(2)	13(1)
C(18)	9229(3)	9780(2)	7834(2)	17(1)
C(19)	7894(3)	8687(2)	6952(2)	18(1)
C(21)	3180(4)	9918(3)	5744(2)	32(1)
C(22)	1521(3)	7279(3)	6077(2)	23(1)
C(31)	2282(3)	3740(3)	6057(2)	26(1)
C(32)	3439(4)	3599(3)	7991(2)	28(1)
C(110)	7521(3)	7176(2)	6722(2)	15(1)
C(111)	9816(3)	7842(2)	8228(2)	12(1)
C(112)	10775(3)	7304(2)	8858(2)	12(1)
N(11)	8484(2)	6772(2)	7352(1)	12(1)
N(12)	10172(2)	5773(2)	8532(1)	12(1)
N(13)	14189(3)	10822(2)	10879(2)	17(1)
N(14)	12123(3)	11949(2)	9826(2)	17(1)
O(11)	13602(2)	12936(2)	10407(2)	28(1)
O(12)	10962(2)	12304(2)	9572(1)	20(1)
O(21)	3588(2)	9779(2)	7687(1)	24(1)
O(31)	3342(2)	6064(2)	7753(1)	24(1)
Cl(11)	6024(1)	3581(1)	5547(1)	18(1)
Cl(12)	8004(1)	2338(1)	7078(1)	24(1)
Pd(01)	8183(1)	4653(1)	7154(1)	13(1)
S(21)	3570(1)	8942(1)	6624(1)	21(1)
S(31)	3920(1)	4960(1)	7305(1)	21(1)
S(31)	3920(1)	4960(1)	7305(1)	21(1)

Table A14: Bond lengths [Å] and angles [°] for *cis*-[Pd(C₁₂H₈N₄O₂)Cl₂].2DMSO.

Atoms	Bond length (Å)	Atoms	Bond angle (°)
C(11)-N(12)	1.330(3)	N(12)-C(11)-C(12)	121.83(19)
C(11)-C(12)	1.387(3)	N(12)-C(11)-H(11)	119.1
C(11)-H(11)	0.93	C(12)-C(11)-H(11)	119.1
C(12)-C(13)	1.374(3)	C(13)-C(12)-C(11)	120.0(2)
C(12)-H(12)	0.93	C(13)-C(12)-H(12)	120
C(13)-C(14)	1.410(3)	C(11)-C(12)-H(12)	120
C(13)-H(13)	0.93	C(12)-C(13)-C(14)	119.1(2)
C(14)-C(112)	1.388(3)	C(12)-C(13)-H(13)	120.4
C(14)-C(15)	1.472(3)	C(14)-C(13)-H(13)	120.4
C(15)-N(13)	1.321(3)	C(112)-C(14)-C(13)	117.59(19)
C(15)-C(16)	1.414(3)	C(112)-C(14)-C(15)	119.39(19)
C(16)-N(14)	1.422(3)	C(13)-C(14)-C(15)	123.0(2)
C(16)-C(17)	1.446(3)	N(13)-C(15)-C(16)	125.2(2)
C(17)-C(111)	1.401(3)	N(13)-C(15)-C(14)	117.47(19)
C(17)-C(18)	1.419(3)	C(16)-C(15)-C(14)	117.3(2)
C(18)-C(19)	1.371(3)	C(15)-C(16)-N(14)	118.5(2)
C(18)-H(18)	0.93	C(15)-C(16)-C(17)	122.87(19)
C(19)-C(110)	1.390(3)	N(14)-C(16)-C(17)	118.65(18)
C(19)-H(19)	0.93	C(111)-C(17)-C(18)	115.5(2)
C(21)-S(21)	1.774(3)	C(111)-C(17)-C(16)	117.72(19)
C(21)-H(21A)	0.96	C(18)-C(17)-C(16)	126.73(19)
C(21)-H(21B)	0.96	C(19)-C(18)-C(17)	120.2(2)
C(21)-H(21C)	0.96	C(19)-C(18)-H(18)	119.9
C(22)-S(21)	1.781(3)	C(17)-C(18)-H(18)	119.9
C(22)-H(22A)	0.96	C(18)-C(19)-C(110)	120.8(2)
C(22)-H(22B)	0.96	C(18)-C(19)-H(19)	119.6
C(22)-H(22C)	0.96	C(110)-C(19)-H(19)	119.6
C(31)-S(31)	1.786(3)	S(21)-C(21)-H(21A)	109.5
C(31)-H(31A)	0.96	S(21)-C(21)-H(21B)	109.5
C(31)-H(31B)	0.96	H(21A)-C(21)-H(21B)	109.5
C(31)-H(31C)	0.96	S(21)-C(21)-H(21C)	109.5
C(32)-S(31)	1.784(3)	H(21A)-C(21)-H(21C)	109.5
C(32)-H(32A)	0.96	H(21B)-C(21)-H(21C)	109.5
C(32)-H(32B)	0.96	S(21)-C(22)-H(22A)	109.5
C(32)-H(32C)	0.96	S(21)-C(22)-H(22B)	109.5
C(110)-N(11)	1.337(3)	H(22A)-C(22)-H(22B)	109.5
C(110)-H(110)	0.93	S(21)-C(22)-H(22C)	109.5
C(111)-N(11)	1.360(3)	H(22A)-C(22)-H(22C)	109.5
C(111)-C(112)	1.435(3)	H(22B)-C(22)-H(22C)	109.5
C(112)-N(12)	1.364(3)	S(31)-C(31)-H(31A)	109.5
N(11)-Pd(01)	2.024(2)	S(31)-C(31)-H(31B)	109.5

Appendix A

N(12)-Pd(01)	2.0173(19)	H(31A)-C(31)-H(31B)	109.5
N(13)-H(111)	0.90(3)	S(31)-C(31)-H(31C)	109.5
N(13)-H(112)	0.85(3)	H(31A)-C(31)-H(31C)	109.5
N(14)-O(11)	1.243(3)	H(31B)-C(31)-H(31C)	109.5
N(14)-O(12)	1.249(2)	S(31)-C(32)-H(32A)	109.5
O(21)-S(21)	1.5129(18)	S(31)-C(32)-H(32B)	109.5
O(31)-S(31)	1.5003(18)	H(32A)-C(32)-H(32B)	109.5
Cl(11)-Pd(01)	2.2920(9)	S(31)-C(32)-H(32C)	109.5
Cl(12)-Pd(01)	2.2861(13)	H(32A)-C(32)-H(32C)	109.5
		H(32B)-C(32)-H(32C)	109.5
		N(11)-C(110)-C(19)	120.2(2)
		N(11)-C(110)-H(110)	119.9
		C(19)-C(110)-H(110)	119.9
		N(11)-C(111)-C(17)	123.50(19)
		N(11)-C(111)-C(112)	115.90(18)
		C(17)-C(111)-C(112)	120.6(2)
		N(12)-C(112)-C(14)	122.51(19)
		N(12)-C(112)-C(111)	115.69(19)
		C(14)-C(112)-C(111)	121.78(19)
		C(110)-N(11)-C(111)	119.78(18)
		C(110)-N(11)-Pd(01)	126.60(15)
		C(111)-N(11)-Pd(01)	113.61(13)
		C(11)-N(12)-C(112)	118.93(19)
		C(11)-N(12)-Pd(01)	127.28(15)
		C(112)-N(12)-Pd(01)	113.70(14)
		C(15)-N(13)-H(111)	122.6(18)
		C(15)-N(13)-H(112)	121.5(17)
		H(111)-N(13)-H(112)	116(3)
		O(11)-N(14)-O(12)	120.32(18)
		O(11)-N(14)-C(16)	120.22(19)
		O(12)-N(14)-C(16)	119.45(19)
		N(12)-Pd(01)-N(11)	80.87(7)
		N(12)-Pd(01)-Cl(12)	94.25(5)
		N(11)-Pd(01)-Cl(12)	175.04(5)
		N(12)-Pd(01)-Cl(11)	174.73(5)
		N(11)-Pd(01)-Cl(11)	94.64(5)
		Cl(12)-Pd(01)-Cl(11)	90.27(3)
		O(21)-S(21)-C(21)	105.77(12)
		O(21)-S(21)-C(22)	105.44(12)
		C(21)-S(21)-C(22)	97.64(13)
		O(31)-S(31)-C(32)	106.75(12)
		O(31)-S(31)-C(31)	105.30(12)
		C(32)-S(31)-C(31)	96.86(13)

Appendix A

Table A15: Anisotropic displacement parameters ($\text{\AA}^2 \times 10^3$) for *cis*-[Pd(C₁₂H₈N₄O₂)Cl₂].2DMSO. The anisotropic displacement factor exponent takes the form: $-2\pi [h^2 a^{*2} U_{11} + \dots + 2hka^*b^*U_{12}]$.

	U11	U22	U33	U23	U13	U12
C(11)	18(1)	13(1)	18(1)	7(1)	6(1)	10(1)
C(12)	19(1)	19(1)	17(1)	9(1)	5(1)	12(1)
C(13)	16(1)	18(1)	16(1)	7(1)	4(1)	9(1)
C(14)	14(1)	13(1)	14(1)	4(1)	6(1)	8(1)
C(15)	16(1)	14(1)	13(1)	4(1)	7(1)	7(1)
C(16)	16(1)	9(1)	16(1)	4(1)	6(1)	6(1)
C(17)	14(1)	13(1)	15(1)	6(1)	6(1)	7(1)
C(18)	19(1)	13(1)	20(1)	6(1)	4(1)	10(1)
C(19)	20(1)	19(1)	21(1)	10(1)	4(1)	13(1)
C(21)	40(2)	24(1)	20(1)	7(1)	5(1)	8(1)
C(22)	20(1)	23(1)	22(1)	6(1)	6(1)	8(1)
C(31)	28(2)	25(1)	20(1)	5(1)	5(1)	9(1)
C(32)	32(2)	30(1)	23(1)	10(1)	5(1)	16(1)
C(110)	14(1)	16(1)	16(1)	6(1)	3(1)	8(1)
C(111)	13(1)	13(1)	14(1)	6(1)	6(1)	8(1)
C(112)	14(1)	13(1)	11(1)	4(1)	5(1)	7(1)
N(11)	13(1)	13(1)	11(1)	4(1)	4(1)	6(1)
N(12)	14(1)	11(1)	13(1)	3(1)	5(1)	7(1)
N(13)	17(1)	12(1)	17(1)	2(1)	0(1)	6(1)
N(14)	20(1)	12(1)	16(1)	5(1)	4(1)	7(1)
O(11)	26(1)	14(1)	31(1)	4(1)	-6(1)	6(1)
O(12)	25(1)	18(1)	22(1)	7(1)	8(1)	14(1)
O(21)	24(1)	27(1)	16(1)	2(1)	2(1)	14(1)
O(31)	26(1)	21(1)	22(1)	6(1)	6(1)	11(1)
Cl(11)	19(1)	15(1)	15(1)	3(1)	-1(1)	7(1)
Cl(12)	30(1)	12(1)	22(1)	2(1)	-3(1)	11(1)
Pd(01)	14(1)	10(1)	12(1)	3(1)	1(1)	6(1)
S(21)	17(1)	24(1)	16(1)	3(1)	2(1)	8(1)
S(31)	19(1)	19(1)	20(1)	4(1)	5(1)	6(1)

Table A16: Atomic coordinates ($\times 10^4$) and equivalent isotropic displacement parameters ($\text{\AA}^2 \times 10^3$) for *cis*-[Pt(C₁₂H₈N₄O₂)Cl₂].2DMSO. U(eq) is defined as one third of the trace of the orthogonalized U^{ij} tensor.

Atoms	x	y	z	U(eq)
C(11)	5958(3)	5190(3)	4097(2)	15(1)
C(12)	7361(4)	6087(3)	5011(2)	16(1)
C(13)	7994(3)	7627(3)	5346(2)	15(1)
C(14)	7193(3)	8267(3)	4749(2)	12(1)
C(15)	7754(3)	9895(3)	5041(2)	13(1)
C(16)	6717(3)	10383(3)	4454(2)	13(1)

Appendix A

C(17)	5247(3)	9373(3)	3513(2)	13(1)
C(18)	4221(4)	9762(3)	2818(2)	17(1)
C(19)	2897(4)	8671(3)	1935(2)	17(1)
C(21)	6537(4)	7340(3)	1073(2)	21(1)
C(22)	8190(5)	9961(4)	748(3)	32(1)
C(31)	8536(4)	3690(4)	2999(3)	28(1)
C(32)	7258(4)	3799(3)	1063(2)	25(1)
C(110)	2518(3)	7167(3)	1710(2)	15(1)
C(111)	4825(3)	7846(3)	3222(2)	11(1)
C(112)	5773(3)	7298(3)	3852(2)	12(1)
N(11)	3485(3)	6768(2)	2346(2)	12(1)
N(12)	5168(3)	5775(2)	3524(2)	12(1)
N(13)	9167(3)	10790(3)	5864(2)	17(1)
N(14)	7106(3)	11929(3)	4812(2)	15(1)
O(11)	8570(3)	12890(2)	5393(2)	29(1)
O(12)	5963(3)	12295(2)	4551(2)	20(1)
O(21)	8601(3)	9803(2)	2707(2)	23(1)
O(31)	8364(3)	6133(2)	2772(2)	21(1)
S(2)	8574(1)	8971(1)	1626(1)	20(1)
S(3)	8928(1)	5029(1)	2294(1)	19(1)
Cl(11)	2998(1)	2343(1)	2075(1)	22(1)
Cl(12)	994(1)	3579(1)	556(1)	17(1)
Pt(1)	3185(1)	4667(1)	2158(1)	11(1)

Table A17: Bond lengths [Å] and angles [°] for *cis*-[Pt(C₁₂H₈N₄O₂)Cl₂].2DMSO..

Atoms	Bond length (Å)	Atoms	Bond angle (°)
C(11)-N(12)	1.333(3)	N(12)-C(11)-C(12)	121.7(3)
C(11)-C(12)	1.387(4)	N(12)-C(11)-H(11)	119.1
C(11)-H(11)	0.93	C(12)-C(11)-H(11)	119.1
C(12)-C(13)	1.376(4)	C(13)-C(12)-C(11)	120.3(3)
C(12)-H(12)	0.93	C(13)-C(12)-H(12)	119.8
C(13)-C(14)	1.401(4)	C(11)-C(12)-H(12)	119.8
C(13)-H(13)	0.93	C(12)-C(13)-C(14)	118.9(2)
C(14)-C(112)	1.391(4)	C(12)-C(13)-H(13)	120.6
C(14)-C(15)	1.470(4)	C(14)-C(13)-H(13)	120.6
C(15)-N(13)	1.325(3)	C(112)-C(14)-C(13)	117.7(2)
C(15)-C(16)	1.413(4)	C(112)-C(14)-C(15)	119.0(2)
C(16)-N(14)	1.426(3)	C(13)-C(14)-C(15)	123.2(2)
C(16)-C(17)	1.450(4)	N(13)-C(15)-C(16)	124.9(3)
C(17)-C(111)	1.398(4)	N(13)-C(15)-C(14)	117.3(2)
C(17)-C(18)	1.411(4)	C(16)-C(15)-C(14)	117.7(2)
C(18)-C(19)	1.373(4)	C(15)-C(16)-N(14)	118.8(2)

Appendix A

C(18)-H(18)	0.93	C(15)-C(16)-C(17)	122.9(2)
C(19)-C(110)	1.387(4)	N(14)-C(16)-C(17)	118.3(2)
C(19)-H(19)	0.93	C(111)-C(17)-C(18)	115.4(2)
C(21)-S(2)	1.781(3)	C(111)-C(17)-C(16)	117.2(2)
C(21)-H(21A)	0.96	C(18)-C(17)-C(16)	127.4(2)
C(21)-H(21B)	0.96	C(19)-C(18)-C(17)	120.3(3)
C(21)-H(21C)	0.96	C(19)-C(18)-H(18)	119.9
C(22)-S(2)	1.773(3)	C(17)-C(18)-H(18)	119.9
C(22)-H(22A)	0.96	C(18)-C(19)-C(110)	121.3(3)
C(22)-H(22B)	0.96	C(18)-C(19)-H(19)	119.3
C(22)-H(22C)	0.96	C(110)-C(19)-H(19)	119.3
C(31)-S(3)	1.781(3)	S(2)-C(21)-H(21A)	109.5
C(31)-H(31A)	0.96	S(2)-C(21)-H(21B)	109.5
C(31)-H(31B)	0.96	H(21A)-C(21)-H(21B)	109.5
C(31)-H(31C)	0.96	S(2)-C(21)-H(21C)	109.5
C(32)-S(3)	1.787(3)	H(21A)-C(21)-H(21C)	109.5
C(32)-H(32A)	0.96	H(21B)-C(21)-H(21C)	109.5
C(32)-H(32B)	0.96	S(2)-C(22)-H(22A)	109.5
C(32)-H(32C)	0.96	S(2)-C(22)-H(22B)	109.5
C(110)-N(11)	1.339(3)	H(22A)-C(22)-H(22B)	109.5
C(110)-H(110)	0.93	S(2)-C(22)-H(22C)	109.5
C(111)-N(11)	1.369(3)	H(22A)-C(22)-H(22C)	109.5
C(111)-C(112)	1.435(4)	H(22B)-C(22)-H(22C)	109.5
C(112)-N(12)	1.363(3)	S(3)-C(31)-H(31A)	109.5
N(11)-Pt(1)	2.013(2)	S(3)-C(31)-H(31B)	109.5
N(12)-Pt(1)	2.008(2)	H(31A)-C(31)-H(31B)	109.5
N(13)-H(13A)	0.86(3)	S(3)-C(31)-H(31C)	109.5
N(13)-H(13B)	0.81(4)	H(31A)-C(31)-H(31C)	109.5
N(14)-O(11)	1.241(3)	H(31B)-C(31)-H(31C)	109.5
N(14)-O(12)	1.246(3)	S(3)-C(32)-H(32A)	109.5
O(21)-S(2)	1.514(2)	S(3)-C(32)-H(32B)	109.5
O(31)-S(3)	1.503(2)	H(32A)-C(32)-H(32B)	109.5
Cl(11)-Pt(1)	2.2960(7)	S(3)-C(32)-H(32C)	109.5
Cl(12)-Pt(1)	2.3013(7)	H(32A)-C(32)-H(32C)	109.5
		H(32B)-C(32)-H(32C)	109.5
		N(11)-C(110)-C(19)	119.7(2)
		N(11)-C(110)-H(110)	120.2
		C(19)-C(110)-H(110)	120.2
		N(11)-C(111)-C(17)	123.6(2)
		N(11)-C(111)-C(112)	115.2(2)
		C(17)-C(111)-C(112)	121.2(2)
		N(12)-C(112)-C(14)	122.8(2)
		N(12)-C(112)-C(111)	115.6(2)

Appendix A

C(14)-C(112)-C(111)	121.6(2)
C(110)-N(11)-C(111)	119.7(2)
C(110)-N(11)-Pt(1)	126.26(18)
C(111)-N(11)-Pt(1)	114.05(18)
C(11)-N(12)-C(112)	118.5(2)
C(11)-N(12)-Pt(1)	127.23(18)
C(112)-N(12)-Pt(1)	114.22(18)
C(15)-N(13)-H(13A)	123(2)
C(15)-N(13)-H(13B)	124(2)
H(13A)-N(13)-H(13B)	113(3)
O(11)-N(14)-O(12)	120.8(2)
O(11)-N(14)-C(16)	119.6(2)
O(12)-N(14)-C(16)	119.6(2)
O(21)-S(2)-C(22)	105.69(14)
O(21)-S(2)-C(21)	105.66(13)
C(22)-S(2)-C(21)	97.23(16)
O(31)-S(3)-C(31)	107.06(15)
O(31)-S(3)-C(32)	105.39(14)
C(31)-S(3)-C(32)	96.68(15)
N(12)-Pt(1)-N(11)	80.81(9)
N(12)-Pt(1)-Cl(11)	94.71(7)
N(11)-Pt(1)-Cl(11)	175.48(6)
N(12)-Pt(1)-Cl(12)	175.20(6)
N(11)-Pt(1)-Cl(12)	94.98(6)
Cl(11)-Pt(1)-Cl(12)	89.52(2)

Table A18: Anisotropic displacement parameters ($\text{\AA}^2 \times 10^3$) for *cis*-[Pt(C₁₂H₈N₄O₂)Cl₂].2DMSO. The anisotropic displacement factor exponent takes the form: $-2 \pi [h^2 a^{*2} U_{11} + \dots + 2 h k a^* b^* U_{12}]$.

	U11	U22	U33	U23	U13	U12
C(11)	19(1)	14(1)	16(1)	8(1)	6(1)	9(1)
C(12)	20(1)	18(1)	16(1)	9(1)	4(1)	14(1)
C(13)	15(1)	18(1)	12(1)	4(1)	3(1)	7(1)
C(14)	14(1)	13(1)	13(1)	4(1)	6(1)	8(1)
C(15)	15(1)	12(1)	12(1)	3(1)	6(1)	7(1)
C(16)	19(1)	9(1)	14(1)	4(1)	9(1)	8(1)
C(17)	14(1)	13(1)	13(1)	6(1)	6(1)	7(1)
C(18)	20(1)	10(1)	19(1)	5(1)	4(1)	8(1)
C(19)	18(1)	17(1)	18(1)	8(1)	5(1)	10(1)
C(21)	19(1)	20(1)	18(1)	4(1)	4(1)	6(1)
C(22)	45(2)	24(2)	19(2)	9(1)	7(2)	8(2)
C(31)	28(2)	31(2)	22(2)	7(1)	3(1)	14(1)
C(32)	29(2)	19(2)	20(2)	3(1)	5(1)	8(1)

Appendix A

C(110)	16(1)	14(1)	14(1)	6(1)	3(1)	6(1)
C(111)	12(1)	14(1)	9(1)	4(1)	5(1)	5(1)
C(112)	14(1)	12(1)	11(1)	4(1)	6(1)	7(1)
N(11)	11(1)	12(1)	12(1)	4(1)	3(1)	5(1)
N(12)	14(1)	9(1)	14(1)	4(1)	6(1)	6(1)
N(13)	17(1)	11(1)	17(1)	2(1)	1(1)	5(1)
N(14)	19(1)	12(1)	13(1)	5(1)	3(1)	6(1)
O(11)	24(1)	12(1)	33(1)	2(1)	-9(1)	3(1)
O(12)	25(1)	16(1)	23(1)	7(1)	8(1)	13(1)
O(21)	24(1)	26(1)	15(1)	1(1)	2(1)	13(1)
O(31)	23(1)	18(1)	20(1)	4(1)	5(1)	9(1)
S(2)	15(1)	22(1)	16(1)	2(1)	2(1)	7(1)
S(3)	17(1)	17(1)	19(1)	3(1)	5(1)	5(1)
Cl(11)	29(1)	11(1)	20(1)	2(1)	-2(1)	10(1)
Cl(12)	18(1)	13(1)	15(1)	2(1)	-1(1)	6(1)
Pt(1)	13(1)	9(1)	11(1)	2(1)	2(1)	5(1)